Tracking the effect of pollution deposition from coal-fired power stations over the past 200 years on southern African lakes, using diatoms as a proxy.

Kestrel Raik

June 2022

Coal-fired power station within the Mpumalanga Highveld, South Africa.

A dissertation submitted to the Faculty of Science in fulfilment of the academic requirements for the degree of Master of Science.

School of Geography, Archaeology and Environmental Studies.

University of the Witwatersrand.

DECLARATION

I hereby declare that this dissertation is my own work, unless stated otherwise. It is submitted for the degree of Master of Science at the University of the Witwatersrand, Johannesburg, and has not been submitted in part, or in full towards any other degrees at this or any other university.

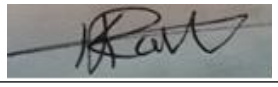

SIGNATURE

27-06-2022

DATE

ABSTRACT

Coal-fired power stations are sources of potentially harmful atmospheric emissions and deposition within both local and distal environments, on land and water surfaces. Sediment cores were obtained from Lake Chrissie in the Mpumalanga Province in relative proximity to these pollution sources and from Letšeng-la Letsie, a remote mountain lake in Lesotho, where deposited pollutants are solely atmospherically derived. This study is uses diatoms as they display sensitivities to pollutant loads and can provide the baseline information necessary to determine both the nature and extent of pollutant loading over time. This study investigated evidence for a diatom-based response, comparing findings for the sites. Both lake systems were characterised as nutrient enriched for ~80-years between the ~1930-2010s, with a more enriched environment and polluted conditions indicative from ~1960-1980s and within the ~2010s. *Fragilaria famelica* which signifies nutrient enrichment was found abundant in both lake systems. Lake Chrissie is described with increased levels of industrial pollution for ~60-years, during the ~1950s and between the ~1970-2010s. Letšeng-la Letsie is described as industrially polluted for ~50-years between the ~1940-1950s, ~1970-1980s and during the ~2010s. This is consistent with previous studies exploring pollution from coal-fired power stations on Letšeng-la Letsie, but these pollutant trends were found inconsistent with emissions over the same periods that increased continuously until the last ~20-years. Results show that diatom responses to increasing deposition do not follow the same unidirectional trend but are rather impacted by climatic variations which may have greater impact on diatom assemblages than the pollution load. The implication of this study highlights the importance of southern African aquatic systems, the effects pollution has on human health and potential mitigation action.

ACKNOWLEDGEMENTS

I would like to thank my two supervisors, Prof Jennifer M. Fitchett and Prof Chris J. Curtis for their guidance and help in developing both my academic writing and critical thinking throughout this degree. A specific thank you Prof Jennifer Fitchett, who has been beyond patient and supportive throughout this degree and through many difficult times I faced, for the endless encouragement and dedication to mentoring, I am eternally grateful. I would like to thank the National Research Foundation for my NRF Scarce Skills MSc. Scholarship, grant number 122932, which funded this research and to my supervisor, Prof Fitchett, who funded my attendance at the Society for South African Association of Geomorphologists (SAAG) conference in September of 2021. I further gratefully acknowledge National Geographic for funding the fieldwork which preceded this degree. A huge thank you to Profs Neil Rose, Jennifer Fitchett, Chris Curtis and Alice Milner for collecting the sediment cores and the Royal Holloway University, London (RHUL) laboratory for prepping the samples, and the University College London (UCL) laboratory for doing the ^{210}Pb dating. Thank you to Louise Pavid for the trip to Lake Chrissie and for providing photos used within this project.

A huge thank you to my mother, Lorraine and partner, Louise, whom without your love and support I would not be where and who I am today; thank you for many hours of listening to my work with keen interest, unending encouragement and enthusiasm which has made this degree possible; with particular thanks to my brother, Rustin and sister-in-law, Faye who often called me and provided all this from their home base in Italy. A further thanks to my brother, Terick and sister-in-law Sivan and their two children, Kiara and Kai, for providing a wonderful distraction when work became overwhelming, of which I am incredibly grateful. Last, but not least, a thanks to my step-father, Yossi, for continued interest in my work and for fuelling stimulating conversations; a huge thanks to Dr. Kim Laxton for her invaluable support and to my friend Lilly, for hours of listening and endlessly making cups of coffee during the final steps!

TABLE OF CONTENTS

LIST OF FIGURES

LIST OF TABLES

LIST OF ACRONYMS

AMD: Acid Mine Drainage.

CONISS: Constrained Incremental Sum of Squares.

CO_2: Carbon dioxide.

DAZ: Diatom Assembly Zones.

DEA: Department of Environmental Affairs.

ENSO: El Niño Southern Oscillation.

Fe: Iron.

GAES: Geography, Archaeology and Environmental Studies.

H_2O_2: Hydrogen peroxide.

HCl: Hydrochloric acid.

Hg: Mercury.

IASs: Inorganic Ash Spheres.

IOD: Indian Ocean Dipole.

LM: Light Microscope.

m.asl: Meters above sea level.

MeHg: Methyl mercury.

N: Nitrogen.

NO_x: Nitrogen oxides.

P: Phosphorous.

Pb: Lead.

PC: Principal Component.

PCA: Principal Component Analysis.

PM: Particulate Matter.

PCB: Polychlorinated biphenyl.

RHUL: Royal Holloway University, London.

SADI: South African Diatom Index.

SAM: Southern Annular Mode.

SANDC: South African National Diatom Collection.

SCPs: Spheroidal Carbonaceous Particle's.

SO_2: Sulphur dioxide.

SPI: Specific Pollution Sensitivity Index.

UCL: University College London.

CHAPTER 1: INTRODUCTION

1.1. Background

South Africa has 19 official coal fields distributed across five provinces, with 12 coal-fired power stations situated within the Mpumalanga Province; three of which are amongst the largest in the southern Hemisphere (Edenebe *et al*., 2017; Panichev *et al*., 2019). This burgeoning energy sector and heavy dependence on coal has qualified the country as the largest atmospheric polluter in Africa (Dunnink *et al*., 2016). The Mpumalanga Province experiences toxic deposition from these industrial sources; however, some is transported to more distal locations, including Lesotho (e.g. Rose *et al*., 2020) and understanding this transport is important. Coal-fired power stations are large sources of anthropogenic particulate matter (PM), sulphur dioxide (SO_2), nitrogen oxides (NO_x) and carbon dioxide (CO_2) emissions (Dalton *et al*., 2018; Langerman and Pauw, 2018). Coal releases heavy and trace metal, such as mercury (Hg) and lead (Pb) which are deposited on both land and water surfaces, posing adverse ecological impacts (Garnham and Langerman, 2016). Spheroidal Carbonaceous Particles (SCPs), which have no natural sources, are also deposited from coal-fired power stations and are used as unambiguous markers of anthropogenic impacts on the environment (Curtis *et al*., 2009; Rose *et al*., 2020). Historical records represent direct records of combustion where SCP's and Hg for example, represent true proxies for pollution within the environmental system.

Minor contaminants may not be measurable in palaeo records using direct measures for pollution (e.g. SCPs, Hg, NO_x) as these measures only describe the situation at the time of sampling (Gökçe, 2016). Direct measures do not relay ecosystem impacts nor determine contamination over time, therefore more direct ecological indicators are needed. Bioindicator tolerance ranges and disturbance thresholds provide biologically significant pollutant values over a temporal scale (Gökçe, 2016; Tang *et al*., 2017). There is a need to reconstruct contaminant loads through time and determine the impact

on the environmental systems and identifying thresholds could provide direct evidence for the prevention of biological degradation (Tang *et al*., 2017). Diatoms for example are a type of algae that are relatively small in comparison to other aquatic bioindicators but are also sensitive to minor changes in concentrations of pollutant loads (Gökçe, 2016). Diatoms are used as a secondary proxy to the direct measures of pollutants, providing information on how pollutants may affect water bodies.

There are both natural and anthropogenic sources for atmospheric pollution, with the associated atmospheric deposition acting as the pathway for distributing the pollutants (Panichev *et al*., 2019). Natural sources of atmospheric pollution (e.g. wind-blown desert dust or wildfires) and natural atmospheric depositional fluxes are crucial contributors of important biogeochemical elements within aquatic environments (Castillo *et al.,* 2017). A large source of pollutants affecting natural systems in South Africa can be attributed to point-source atmospheric emissions from coal combustion processes (Edenebe *et al*., 2017). These activities release toxicants in large proportions and depending on the pollutant load, meteorology and transport pattern from the source, the accumulated atmospheric pollution will eventually be deposited on both land and water surfaces, leading to a potential loss in freshwater ecosystem quality within the surrounding environment (Castillo *et al*., 2017; Edenebe *et al*., 2017). The plumes of pollutants emitted into the atmosphere from these stations can reach heights of up to 300m and are transported over vast distances and areas (Langerman and Pauw, 2018). These pollutant inputs enter soils, water bodies and associated sediments and bind to both the sediment particles and the available organic material and in freshwater areas exposed to their deposition, trace metal enrichment has been observed (Dalton *et al.,* 2018). Mercury for example is a toxic substance that has a long-range transport property and is persistent within the atmosphere, and once deposited it accumulates in food chains and presents as a major environmental concern (Garnham and Langerman, 2016; Panichev *et al*., 2019).

Shallow lakes and endorheic pans have primary production as a major biotic process and are valuable sentinels of environmental change (Curtis *et al*., 2009; Das *et al*., 2015). The sediments act as naturally accumulating archives and as such, can be used to identify the fluxes, trends and impacts of pollutant inputs (Venter *et al*., 2013; Rose *et al*., 2020). Lake sediments contain sensitive indicators of atmospherically deposited pollutant inputs such as diatoms, which can provide early signals of ecosystem response to toxic contamination (Curtis *et al*., 2009; Das *et al*., 2015). There are few paleolimnological studies on South African lakes looking for ecological responses to atmospheric pollutants with a scarcity of relatively undisturbed catchments that can act as appropriate sites for atmospheric impact studies. In largely anthropogenically altered catchments (e.g. from agriculture and/or industry) other impacts may overshadow signals from atmospheric pollution deposition, whereas in undisturbed catchments, atmospheric deposition is more likely to be the only source of pollutants. However with changing climates, including the quantity and timing of rainfall and increase in temperatures (Rose *et al*., 2020) and changing air flows, this may impact pollution signals.

The focus of this study is to examine two contrasting locations at different ends of the pollution gradient. The Chrissiesmeer pans including Lake Chrissie in the Mpumalanga Province, are potentially impacted from point-source atmospheric pollution deposition given their proximity to major industrial contaminant sources. Comparatively, Lesotho has no major fossil-fuel combustion practices and very minor toxic emissions (Rose *et al*., 2020). Letšeng-la Letsie is a remote mountain lake located at high altitudes in the Maloti-Drakensburg range (Kahlolo *et al*., 2021) in Lesotho and is located at a relatively further distance from these coal-stations. This lake is a relatively pristine site providing baseline conditions; but is potentially affected by long-range pollutant transport from these distal industrial sources (Rose *et al*., 2020).

Diatoms belonging to the family Bacillariophyceae are diverse, ubiquitous, and distinct unicellular eukaryotic organisms that inhabit aquatic environments (Matlala *et al*., 2011). Diatoms are readily

preserved within lake sediments and are identified by their preserved valves, allowing these fossils to be related to contemporary autecological data (Reid *et al*., 1995). Some of these organisms tolerate a narrow range of environmental conditions, with species composition shifting according to the differences in water depth, temperature, salinity, acidity (pH) and alkalinity (Riato *et al.,* 2017). Diatoms are sensitive to changes in water quality caused by the deposition of pollutants; therefore their fossils can provide the baseline information necessary to determine both the nature and extent of pollutant loading over time (Das *et al*., 2015). Diatoms can be used to determine the ecological responses to stressors such as perturbations of acid rain, climate change and eutrophication (Kociolek, 2012). Diatoms are sensitive to ecological changes, have high dispersal and rapid growth rates and are widely used as indicators of biological integrity and physico-chemical conditions within aquatic ecosystems (e.g. Matlala *et al*., 2011).

Diatoms can be used to understand ecosystems over different spatial and temporal scales as they provide the first indication of changes within the environment (Matlala *et al*., 2011; Kociolek, 2012). Diatoms are also potentially indicative of natural characteristics including the geomorphology, geology, climate and physico-chemical conditions within the environment in which they inhabit (Alikaj *et al*., 2019). Additionally, ecosystem inferences can be made by observing diatom species changes concurrent with pollutant loading, which have shown strong correlations between changing chemical and physical parameters and diatom assemblage composition (Matlala *et al*., 2011). Globally, diatoms have been found to be one of the most effective biological indicators and the fossil assemblages found within aquatic sediments, can be used to reconstruct past lake conditions and contemporary limnological conditions (Reid *et al*., 1995). Water quality (e.g. Matlala *et al*., 2011) and paleoenvironmental (e.g. Stager *et al*., 2013; Kirsten, 2014; Fitchett *et al*., 2016a,b) research in southern Africa using diatoms has seen an increase over time, however, there remains insufficient literature available (Fitchett, 2015).

1.2. Rationale

The amount of pollution emitted from coal-fired power stations changes over time and critical ecological thresholds of the distribution and deposition of these pollutants, are arguably unknown for southern Africa. Eskom however annually emits around 1.6 million tons of SO_2, 804 000 tons of NO_x, 71 tons of PM and 206.8 million tons of CO_2 in total from all its power stations (Garland and Langerman, 2021). This project comprises a case study comparison, tracking what has occurred in terms of pollution deposition and to determine if these environmental systems are reacting. Volatile compounds including NO2 and SO2 along with PM, participate in the formation of acidic particles which eventually settle into the ground and seep into the water, leading to acidification of freshwater lakes (Lafond, 2022). However, Lake sensitivity to various pressures (e.g. acidification and eutrophication) is determined by numerous factors including their trophic status, geology, soils and vegetation (Rhodes *et al*., 2017) among other factors such as land use. The critical loads for acidification and eutrophication may occur at different levels of N and S-deposition, within the same lake or when comparing lake systems (Sheibley *et al*., 2014). For example, shallow, high-elevation oligotrophic lakes are more strongly affected by and sensitive to N and S increases (Sheibley *et al*., 2014; Rhodes *et al*., 2017). Increases in atmospheric N and S-deposition can increase the lake water concentrations of these variables, which in turn cause shifts in diatom species compositions (Rhodes *et al*., 2017). Therefore diatoms can respond to N-deposition as a nutrient or S deposition as an acidifying agent, but the lake system in which they inhabit needs to be sensitive to these pressures. It is additionally difficult to disentangle which pollutant diatoms are responding to in many instances.

The Mpumalanga pans are situated within the Mpumalanga Highveld power station belt, while Lake Letšeng-la Letsie is within a remote mountain area of Lesotho and can be considered a pristine catchment. Sediment cores were retrieved where the historical records represented the direct record of combustion and true proxies for pollution including SCPs, Hg and nitrates were investigated (Rose

et al., 2020). This study is using diatoms as a secondary proxy where they are representative of pollution and how pollutants affect water bodies, as they display sensitivities to pollutant loads. This study is seeking evidence for a diatom-based response, comparing findings for the sites. Different diatom assemblages are expected between the sites, even if unpolluted. Additionally, it is expected that a regime shift occurred from pollutant intolerant diatom species during periods of lower pollution, to more pollutant tolerant species within a more polluted environment. If a shift occurred, in the absence of other possible local drivers, the results within this study provide independent evidence for pollutant impacts. The outcome of this study is to reconstruct pollutant loading from diatoms, forming a pioneering study for both lakes where diatoms are representative of pollution within these systems..

1.3. Aims and Objectives

This project aims to find signals for historical air pollution from coal-fired power stations over the past 200 years, using diatoms as a representation of pollution in both lake systems. However, diatoms respond to many important environmental variables not associated with pollution including water depth, temperature, total phosphorous (TP), salinity and pH (Riato *et al.*, 2017; Cormier *et al*., 2020).

The objectives of the study are to:

1. Identify diatom valves to reconstruct the community assemblage for the two sites.
2. Determine trends, changepoints and their environmental significance of the diatom assemblages over time.
3. Compare the records for the sites to the observed variations in contamination between the sites, as indicated by other lake sediment proxies of fossil fuel combustion-based contamination.

1.4. Structure of the Dissertation

Following the introductory chapter, the literature review introduces anthropogenic sources for atmospheric pollution in southern Africa, with focus on coal-fired power stations in South Africa and the pollutants and particulates derived from coal and related coal-fired practices. The transport and deposition of these in both regional and distal aquatic ecosystems and the response these sentinel systems have to pollutants are investigated. Freshwater ecosystem monitoring using bioindicators is overviewed with focus on diatoms, which introduces their ecology, sensitivities to environmental variables, preservation in aquatic sediments and value as pollutant indicators. Lastly, southern African research using diatoms for water quality and paleoenvironmental research and of the diatoms of Lesotho, are explored.

The regional setting chapter introduces the general geography, geomorphology and geology, along with the hydrology and general climate for each lake system. Major environmental challenges within the region of each lake brings into focus coal-fired power stations and the threats posed to both local and distal ecosystems.

The methods chapter outlines techniques used for species counts and literature used for taxonomic identification, followed by statistical analysis that included ordination and clustering and stratigraphy which are graphically presented. The results chapter presents findings of the species identified with maximum percent occurrence within the samples within each lake system. These results are visually represented as dendrograms, bi-plots and as stratigraphic graphs.

The discussion chapter introduces the use of diatoms for environmental inferences and of species pollution tolerances in a broader context. The species found for each site, ecological characteristics and pollution tolerances are presented. Direct evidence of pollutants is investigated along with the

relationship between species habitats and water depth. The species are stratigraphically presented, grouped according to habitat and ordered according to pollution tolerance. A palaeoenvironmental reconstruction presents pollution trends, hydrological changes and potentially climatic shifts as interpreted from the diatom record. An inter-site comparison is made with focus on these three trends and is followed by comparisons made with global and southern African literature. A broader regional understanding introduces the history of pollution contamination in these systems with focus on the sources within South Africa. A look at the implications of environmental pollution on ecosystems, climate change and on human health is followed by pollution mitigation and management. The research limitations are presented, followed by the conclusions chapter, where key findings and outcomes of the aim and objectives are highlighted and with avenues for future work suggested.

CHAPTER 2: LITERATURE REVIEW

2.1. Introduction

There are few studies investigating atmospherically deposited contamination within lake sediments of remote freshwater systems throughout southern Africa (Rose *et al*., 2020). Natural standing surface waters are relatively scarce in South Africa, with permanent inland lakes rarely found and poorly described (Dunnink *et al*., 2016). The main anthropogenic sources of atmospheric pollution in South Africa arise from industrial activities, including coal combustion (Hajizadeh *et al*., 2017); where huge quantities of waste pollute the ecosystem in local and distal locations (Edenebe *et al*., 2017; Rose *et al*., 2020). In South Africa, large coal-fired power plants are mostly clustered and concentrated around the coal mines within the Highveld Region of the Mpumalanga Province (Dalton *et al*., 2018; Langerman *et al*., 2018). The deposition of atmospheric pollutants from anthropogenic combustive origins may be archived within aquatic sediments, through the potential influence on the preserved chemical constituents and micro-fossils (Adams *et al*., 2019). Biological indicators including microscopic algae (e.g. diatoms) are found within many aquatic environments (Alikaj *et al*., 2019) and when derived from both contemporary and historical samples, they are powerful indicators of environmental change within aquatic ecosystems (Harding and Taylor, 2014).

Diatoms comprise of an ecologically ubiquitous, diverse and distinctive group of microscopic single-celled (eukaryotic) algae, belonging to the phylum Bacillariophyta (Battarbee *et al*., 2001; Cameron, 2018). The most distinguishing characteristic is the presence of their siliceous cell walls (Dalu and Froneman, 2016) composed of two valves making up a frustule (Battarbee *et al*., 2001), which are unique features used for species-level identification (Pajunen *et al*., 2020). A large proportion of the estimated 10,000 species of diatoms are ecologically sensitive, owing to their rapid reproduction and short lifespan of between four to ten days, leading these assemblages to rapidly colonize new habitats

(Battarbee *et al*., 2001; Cheng *et al*., 2019). These ecologically successful organisms (Kock *et al*., 2019) are the most species-rich and widespread algal groups (Reid *et al.,* 1995) and are globally abundant, inhabiting most freshwater, brackish and marine environments (Battarbee *et al*., 2001; Matlala *et al.,* 2011). Diatoms are found in abundance within various lake habitats, including being attached to substrates (e.g. sediments, rocks or plants) or submerged within the planktonic and benthic region of the aquatic system (Battarbee *et al*., 2001). Under natural conditions their formation is related to tolerances (e.g. ecological optima) due to abiotic limiting factors and biotic interactions among species (Gökçe, 2016). Diatom cells are mostly solitary, while some connect and form chains linked by spines, resulting in some taxa forming colonies of various shapes and sizes (Battarbee *et al*., 2001). The growth of diatom species depends on the range of available habitats concurrent with the combination of chemical, physical, and biological conditions within the system (Battarbee *et al*., 2001). Deformities in diatoms may affect the valve shape due to toxic chemical contamination, preventing spine connections, potentially indicating any stress present within the system (Lavoie *et al*., 2018).

This chapter explores atmospheric pollution transport and deposition in relation to coal-fired power combustion practices. Potential environmental responses to deposited emissions are highlighted, introducing freshwater systems from a brief global view. The value of lakes as sentinel systems and as natural archives for detecting environmental change for effective freshwater ecosystem monitoring, through examining lake sediments is discussed. The ecological impacts of pollution on lake systems and of potential biological responses are highlighted, followed by a brief overview of freshwater ecosystem monitoring and the use of biomonitoring and bioindicators in pollution research. Through fossil preservation within aquatic sediments and their unique ecology and sensitivity to environmental variables, this lends to the value of diatoms as pollutant indicator species. Lastly, water quality and palaeoenvironmental research using diatoms in southern Africa including South Africa and Lesotho is investigated, drawing comparisons to existing global literature.

2.2. Atmospheric Pollution in Southern Africa

2.2.1. Natural Sources

There are both natural and anthropogenic sources for atmospheric pollution, with the associated atmospheric deposition acting as a pathway for pollutant transport and distribution (Panichev *et al*., 2019). Depending on the pollutant load, meteorology and transport pattern from the source, the accumulated atmospheric pollution eventually reaches the Earths' surface (Castillo *et al*., 2017; Adams *et al*., 2019). In Africa, the fine particles of natural contaminants or particulate matter (PM) are dominated by windblown dust from deserts (e.g. Namib and Sahara), oceans and wildfires (Hajizadeh *et al*., 2017; Marais *et al*., 2019). Natural sources of atmospheric pollution and associated depositional fluxes are crucial contributors of necessary biogeochemical elements including Nitrogen (N), Phosphorous (P) and Iron (Fe) among others, within aquatic environments (Castillo *et al*., 2017). Some heavy metals are considered vital micronutrients positively influencing the metabolic and physiological processes of biological organism's, of these however, Pb and Hg (among others) are biologically unimportant and toxic to biota within the system (Edenebe *et al*., 2017).

Geothermal activity (e.g. volcanic eruptions) release ash and metals including Hg into the atmosphere, potentially resulting in harmful deposition within the environment (Panichev *et al*., 2019). Other natural sources for atmospheric Hg include mineral geological deposits and the effect of re-emission occurring through previous atmospheric Hg deposits on the Earth's surface (Panichev *et al*., 2019). Atmospheric Hg remains a particularly persistent and highly (eco)toxic substance that once deposited, even in low concentrations (Chetty and Pillay, 2019) accumulates in food chains and presents as a major environmental concern (Garnham and Langerman, 2016). However the global high energy demands and associated combustion of fossil fuels, remain as one of the main causes for toxic atmospheric pollution and the resulting deposition of Hg and other contaminants (Hajizadeh *et al*., 2017) on both terrestrial and aquatic surfaces.

2.2.2. Anthropogenic Origins

The degradation of air quality in Africa is expected to rise with ongoing, rapid population and economic growth (Marais and Wiedinmyer, 2016). In most developing countries there is a lack of knowledge at the local level, and this is mostly attributed to data shortages along with a lack of funding for research (Selin *et al*., 2020). Consequently, there is a paucity of data on the status of toxic emissions for southern Africa (Garnham and Langerman, 2016) and inventories of pollutant emissions are potentially uncertain, underestimated and unreliable (Marais and Wiedinmyer, 2016). Southern Africa does have the means and resources to lessen the dependence on fossil fuels and rather adopt renewable energy sources, including solar and wind energy (Marais *et al*., 2019). This is crucial, as most pollution deposition occurring in South Africa and Lesotho, predominantly originates from the coal combustion sources (Marais and Wiedinmyer, 2016) situated in the Mpumalanga Province.

2.2.2.1. South Africa

A large source of pollutants affecting natural systems in South Africa can be attributed to point-source atmospheric emissions from coal combustion processes (Edenebe *et al*., 2017). South Africa's burgeoning energy sector and heavy dependence on coal makes the country the largest atmospheric polluter in Africa (Dunnink *et al.,* 2016; Dalton *et al*., 2018). The various local coal burning regions experience some of the highest levels of pollution within the country (Langerman *et al*., 2018). Nineteen official coal fields span five provinces in South Africa, where the Highveld in the Mpumalanga Province (northeast) has the highest concentration of 12 coal-fired power stations in the country, of which three are amongst the largest in the southern Hemisphere (Edenebe *et al*., 2017; Panichev *et al*., 2019; Rose *et al*., 2020). These include South Africa's state-owned energy utility Eskom's power stations namely, Arnot, Camden, Grootvlei, Komati, Kusile, Duvha, Hendrina, Kendal, Kriel, Majuba, Tutuka and Matla (Eskom, 2022c). Globally, the Mpumalanga Province is called the largest air pollution hotspot and Eskom the worst polluting power company (Garland and Langerman, 2021).

The Permian/Gondwanan coal used in South Africa are mostly bituminous, high in ash content and contain carcinogens, with the associated coal combustion activities contributing to toxic atmospheric emissions containing; SO_2, NO_x and PM, along with being sources of heavy and trace metal (e.g. Hg) deposition within the environment (Pretorius *et al*., 2015; Dalton *et al*., 2018; Langerman and Pauw, 2018). Air pollution from coal-fired power stations and are known as combustion by-products (Garland and Langerman, 2021). Eskom's thermal power plants constitute the largest contributor of toxic emissions of SO_2, NO_x and the greenhouse gas CO_2 and are the second highest contributor to PM emissions in South Africa (Pretorius *et al*., 2015; Garland and Langerman, 2021). Electricity generation plants within South Africa are uncontested as the highest contributors to Hg emissions within the environment (Garnham and Langerman, 2016) especially during the thermal treatment of coal when transformed into liquid fuels (Panichev *et al*., 2019). All of Eskom's power stations annually emit a total of around 1.6 million tons of SO_2, 804 000 tons of NO_x, 71 tons of PM and 206.8 million tons of CO_2 (Garland and Langerman, 2021).

The emitted plume of pollutants from power stations ages over time (e.g. the oxidation of SO_2 and NO_x) forming PM emissions, which overall is typically a function of the ash content from the coal burnt and the efficacy of any abatement technology (not) used (Pretorius *et al*., 2015). Between 1928 and 2021, there has been a marked annual increase in the amount of coal burnt (Mt) along with SO_2 (kt) and Hg (t) emissions in South Africa (Figure 2.1). It has been suggested that Eskom mines low-quality coal, which is also cheaper, however higher in sulphur content (Evans, 2022). Interestingly, a decrease in the amount of coal burnt between 2010 and 2013 in particular, coincides with a relative increase in SO_2 emissions (Figure 2.1). Eskom's SO_2 emissions are higher than that of the US, China and the European Union power sector Garland and Langerman, 2021). Additionally, industrial processes of fossil fuel combustion produce a particulate known as fly-ash which is released into the atmosphere (Rose, 2008; Rose *et al*., 2012). Spheroidal Carbonaceous Particles are a component of fly-ash and are solely produced from the high-temperature combustion of coal (Rose, 2008; Curtis *et al*., 2010).

.

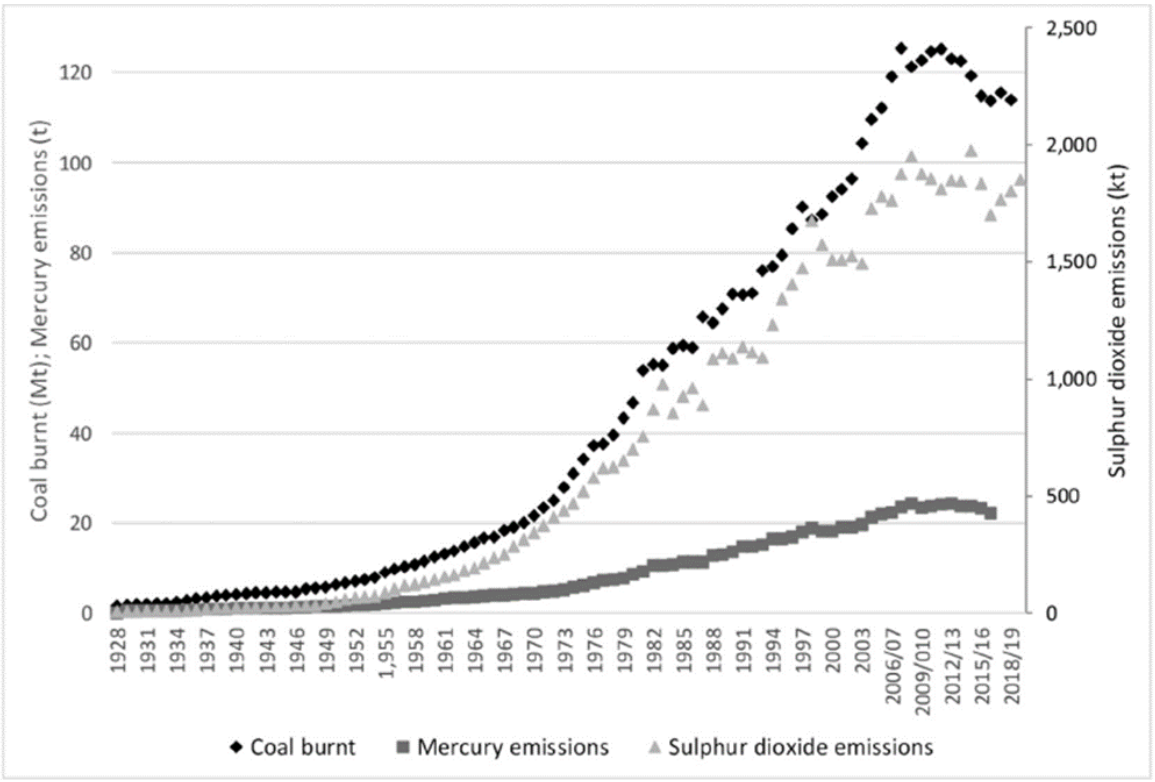

Figure 2.1. Annual coal combustion (Mt) for power generation in South Africa from 1927 to 2018/19, and annual mercury emissions (t) and sulphur dioxide emissions (kt) from coal-fired power stations for the same period (Rose *et al*., 2020).

The primary contributor to atmospheric particle pollution is through fossil fuel combustion and could be accomplished with cleaner alternatives (Camfil, 2018). South Africa (unlike other countries) substantially decreased air pollutant emissions, albeit technologies available to accomplish this (Garland and Langerman, 2021). Duvha power station was the first in the world to be retrofitted with pulse jet fabric filter plants which remove 99.9% of the fly ash (Eskom 2022c). Most of the ash generated from coal-combustion is captured and removed through filter plants (e.g. electrostatic precipitators), however criteria pollutants are still released from the power plant flue stacks (Dalton *et al*., 2018; Langerman and Pauw, 2018). Three power stations, Camden, Grootvlei and Komati were mothballed in the late 1980's and early 1990's but were returned to service in 2003 due to the sharp

increase in the demand for electricity (Eskom, 2022c). Interestingly, a sharp increase in the amount of coal burnt coinciding with increased SO_2, NO_x and CO_2 emissions are observed between 2003 and 2006, coinciding with the return of these three stations (Figure 2.2). As it currently stands, Kusile coal-fired power plant is the only facility with technology (flue gas desulphurisation) installed to reduce SO_2 emissions in South Africa (Evans, 2022).

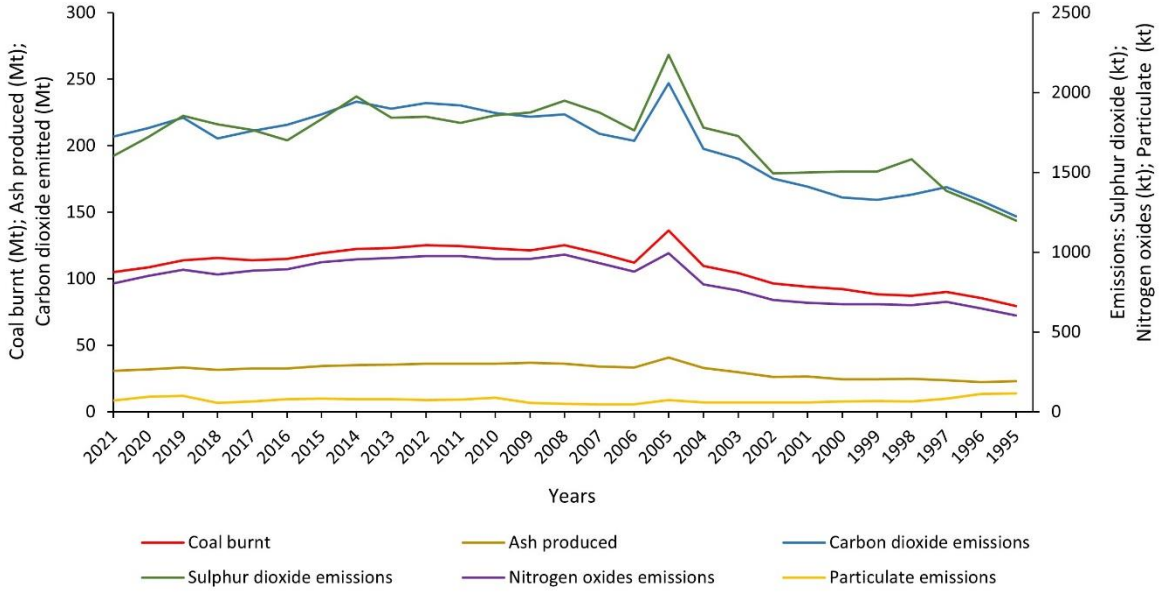

Figure 2.2. Increase in the amount of coal burnt (Mt), ash produced (Mt), CO_2 (Mt), SO_2 (kt), NO_x (kt) and particulate (kt) emissions, adapted from the Eskom annual reports 1995-2021 (Eskom, 2022a).

The apportionment of the origin of PM is challenging as the bulk of PM is formed within the atmosphere (Langerman and Pauw, 2018). Even though fossil fuel using facilities like power plants are heavy contributors to PM pollution (Camfil, 2018) it is derived from numerous combustion sources, not solely from power stations (Langerman and Pauw, 2018). Particulate matter is both naturally or anthropogenically derived from a wide variety of sources, can be in liquid or solid for and it can differ in sizes or shapes (Camfil, 2018). A large proportion of the ambient toxic PM from fossil fuel combustion found in Africa for example, is predominantly sourced from both distal (e.g. Europe) and

local locations, such as South Africa (Marais *et al*., 2019). However, minimum emission standards were introduced in South Africa in 2010 (Garland and Langerman, 2021) as Eskom's coal-fired power stations is in part responsible for the bulk of air pollution (and greenhouse gas emissions) on the entire continent (Evans, 2022). The power stations were given 10 years to comply with the limits for SO_2, NO_2 and particulates, requiring new technology (to be installed and by 2020); with currently only one coal-fired power station in full compliance (Garland and Langerman, 2021). Fossil fuel combustion is a harmful anthropogenic activity which is additionally expected to be regulated with Hg capture policies, to enforce emission reductions into the environment (Kwon *et al*., 2020).

Dalton *et al*. (2018) found that background concentrations of heavy metals in parts of South Africa are naturally high, without the additional impacts of anthropogenic inputs. However, elements such as Hg are still purposefully mined, processed and released into the environment as a by-product of coal combustion activities (Selin *et al*., 2018). Mercury is considered one of the top ten chemicals of public health concerns, as listed by the World Health Organisation (Kwon *et al*., 2020). Regulations on hazardous emissions are critically needed within South Africa (Garnham and Langerman, 2016) as data on atmospheric Hg emissions and results from analytical determinations of Hg content within coals, are controversial and not without uncertainties (Panichev *et al*., 2019). Often awareness and resource availability for effective management of the environmental impacts caused by Hg are limited and regionally isolated within developing countries (Selin *et al*., 2020).

A global treaty known as the Minamata Convention on mercury was adopted in October of 2013 for the reduction of Hg emissions and came into effect in August of 2017 (Hilson *et al*., 2018). The main objective of the convention included protecting the environment and human health from Hg through outlining the production, emissions and uses including the handling and disposal of this toxic metal (Selin *et al*., 2018). The convention highlighted the broad use Hg has in anthropogenic activities and the results of emissions that led to atmospheric, soil and water pollution (Hilson *et al*., 2018). Globally,

countries voluntarily decided to be party to the cause and once committed, the provisions would be legally binding (Selin *et al*., 2018). The convention hosted global negotiations among 140 countries, with a consensus that considered it an environmental victory for regulations around Hg emissions (Hilson *et al*., 2018). South Africa signed the Minamata Convention on mercury in 2013, but no legislation was employed with regards to emissions thereafter (Garnham and Langerman, 2016). Moreover, in 2015 and as a condition of atmospheric emission licences in South Africa, the Department of Environmental Affairs (DEA) introduced air quality offsets, but once more, no regulations governed the implementation at each power station (Langerman *et al*., 2018).

As coal continues to be the dominant source of energy in South Africa (Akinbami *et al*., 2021) there is a critical need to reduce the magnitude of these toxic atmospheric emissions (Langerman and Pauw, 2018). South Africa is considered to have advanced air quality policy and monitoring programmes, compared to many other African countries, however, enforcing compliance to the regulations, remain critically unmanaged (Marais *et al*., 2019). As debates continue over the large investments required to reduce toxic emissions, extensive areas remain impacted (Langerman and Pauw, 2018) as anything that involves combustion continues to release particles into the air (Camfil, 2018). The deposition of these atmospheric toxicants threatens aquatic ecosystems both within local and source regions such as the Mpumalanga Province, along with distal locations, including Lesotho (Mangadze *et al*., 2019).

2.3. Pollution Transport and Deposition

Coal predominantly comprises of ash, carbon, sulphur and metals and upon combustion SO_2, NO_x, PM, and trace concentrations of toxic elements (e.g. Hg) are emitted into the atmosphere (Larsen, 2000; Garnham and Langerman, 2016). Coal combustion related anthropogenic activities release large plumes that potentially reach heights of up to 300m and accumulate in the atmosphere (Pretorius *et al*., 2015; Langerman and Pauw, 2018). The released plume dilutes and undergoes chemical

transformations within the atmosphere and is transported over large distances and areas (Hajizadeh *et al*., 2017). The plume is eventually deposited within surrounding environments (Castillo *et al*., 2017) including land and water surfaces (Edenebe *et al*., 2017), potentially posing adverse ecological effects (Langerman and Pauw, 2018). Under favourable climatic conditions, trace metals and particulates can be long-range transported for thousands of kilometres, within the industrial plumes before eventually deposited (Rose *et al*., 2012). Some pollutants that are long-range transported from coal combustion sources include NO_x, trace metals, ash particles and Hg (Adams *et al*., 2019). Elemental Hg travels within the atmosphere across large distances and is deposited onto land and aquatic surfaces as a particulate-bound, oxygenated Hg species (Kwon *et al*., 2020). A methyl mercury (MeHg) species is formed within ecosystems of high biological activity, which can easily and adversely accumulate in various biological organisms (e.g. Panichev *et al*., 2019).

The air flow originating from the Mpumalanga Highveld coal-combustion regions situated within the interior of South Africa, occurs in association with continental anticyclones and with slow-moving air-masses (Rose *et al*., 2020). The atmospheric stability of this sub-tropical Highveld region is strengthened by these prevailing anti-cyclonic conditions, causing the suppression of vertical motion and resulting in subsiding air (Langerman *et al*., 2018). When wind speeds are low, emitted pollutants have been found trapped below the inversion layer within local stable atmospheres (Langerman *et al*., 2018) potentially inhibiting the long-range transportation of these contaminants. The recirculating, anticyclonic flow from the Highveld region transports these pollutants to both local and distal locations (Rose *et al*., 2020) before the emitted flue-gases and particles are removed from the atmosphere by dry and wet depositional processes (Larsen, 2000). Coal combustion PM emissions (e.g. ash) is windblown and dispersed on local land and water surfaces as dry deposition (Pretorius *et al*., 2015; Dalton *et al*., 2018). Under certain climatic conditions all locally dispersed particulates can stay in the atmosphere for days to weeks and be transported and deposited over greater distances (Larsen, 2000; Garland and Langerman, 2021).

Wet deposition transports and delivers acidic components including contaminants and gases potentially laden with pollutants such as trace and heavy metals, derived from coal combustion to the Earths' surface in the forms of acidic rain, snow, mist and dust (Castillo *et al*., 2017; Hajizadeh *et al*., 2017). As the polluted plume ages most of the SO_2 and NO_x is converted to secondary fine PM within the atmosphere, which reacts with water, oxygen and other gases to form fine droplets of sulfuric acid, ammonium nitrate and nitric acid (Hajizadeh *et al*., 2017; Langerman and Pauw, 2018). The fine acidic droplets formed in the atmosphere adhere to rain to form wet or solid acidic PM deposition (Hajizadeh *et al*., 2017). Particulate matter pollution contributes to acid rain and can change weather patterns, potentially leading to droughts (Camfil, 2018). Industrial coal combustion practices are attributed as one of the major causes of climate change and global warming (Barreira *et al*., 2017; Olufemi *et al*., 2018).

Changing climates impact the quality and quantity of water resources through conditions including flooding (Netshakhuma, 2021) and droughts (Bailey *et al*., 2021; Olaleye *et al*., 2021); where Climate change further exacerbates these drought conditions such as by further impacting increasing temperatures, high humidity and declining water levels (Mandela, 2019). The Mpumalanga Province experienced extreme drier years in 1935, 1945, 1965, 1982, 1992, 1994, 2003 and in 2015 (Netshakhuma, 2021) with an ongoing drought condition existing since 2012 (Mandela, 2019). Wetter climatic periods above average annual rainfall for the Mpumalanga Province occurred in 1939, 1955, 1996, 2000 along with in 2021; when the province experienced a wet period that caused flooding and flash flooding events (Netshakhuma, 2021). The climate in Lesotho is mainly influenced by altitude (Bailey *et al*., 2021), the El Niño Southern Oscillation (ENSO) and the effects of continentality and latitude (Noome and Fitchett, 2019; Bailey *et al*., 2021) and is vulnerable to natural hazards such as droughts and floods (Acaps, 2022). Lesotho experienced droughts in the years 1983, 1990, 2002, 2007, 2011, 2016, 2019 and 2020; further experiencing the longest drought in almost 200 years between 1991 and 1995 (CCKP, 2021). Most regions in Lesotho are affected by drought events (acaps, 2022).

Stresses such as increased contaminant loading and climate change potentially leads to the degradation of aquatic ecosystems and water quality (Rose *et al.,* 2020). Acid rain is primarily formed from fossil fuel combustion, with acidic deposition leading to increased acidic levels of surface waters and soils, causing potential changes in the biotic composition of aquatic ecosystems (Dunnink *et al*., 2016). Many aquatic species cannot tolerate increased levels of acidity from polluted rainwater (Lafond, 2022). Freshwater ecosystems form a fundamental component of biogeochemical cycles, acting as transport pathways, elemental transformations and storage sites for chemical constituents (Dalu and Froneman, 2016). They are regarded amongst the most endangered ecosystems in the world and the effects of pollution including acid rain, nutrient enrichment, along with heavy and trace metal depositions can impact lakes on a local, regional and global scale (Mangadze *et al*., 2019).

2.4. Environmental Response to Pollutants

2.4.1. Aquatic Ecosystems-A Brief Global Overview

There is many causes of aquatic ecosystem instability and include anthropogenic pollution, nutrient enrichment and climate change (Curtis *et al*., 2010). The former introduces multiple types and varied levels of pollutants into the environment (Chetty and Pillay, 2019) and is globally one of the most pervasive and widespread threats to natural aquatic ecosystems (Dunnink *et al*., 2016). Coal mining and agricultural practices increase the risk of main sources of water gaining contamination with acid mine drainage (AMD) seepage which is a serious environmental concern for the long-term sustainability of freshwater systems (Edenebe *et al*., 2017). Freshwater ecosystems are extremely sensitive to anthropogenic practices including mining, industry and agriculture (Kock *et al*., 2019) which extensively contribute to the introduction of various pollutants in into the system (Chetty and Pillay, 2019) both locally and in distal locations. Significant impacts on some remote lakes structure and functioning in Siberia (e.g. Adams *et al*., 2019) were found due to the deposition of long-range transported pollutants from distal coal-fired power stations. Nearly two decades prior in Europe,

Larsen (2000) conducted a site comparison study between two lakes in Norway to determine the impact of either point-source or long-range pollutant transport and deposition on these aquatic systems. In both cases, anthropogenic activities formed a major source of pollution for these aquatic systems; where these and other lake studies in parts of Europe (e.g. Curtis *et al*., 2009) found that these isolated aquatic ecosystems are not as pristine as their remoteness might have suggested. Globally, shallow lakes are the most abundant lentic or still water body, natural ecosystems that are often considered threatened (Riato and Leira, 2020). Southern African freshwaters are experiencing a period of unprecedented threat from the rapid increase and release of pollutants from industrial emissions (Rose *et al*., 2020); where a standard assessment for shallow lakes has yet to be determined and is crucial (Riato and Leira, 2020). There is a paucity of natural permanent standing waters such as freshwater lakes and pans throughout southern Africa (Van Deventer, 2021) with limited literature focussing on freshwater critical loads and surface water sensitivities to acidic atmospheric pollution deposition (Dunnink *et al*., 2016).

As the contamination of South African aquatic environments by pollutants remains widely acknowledged (Rose *et al*., 2020), the increasing and unabated coal mining and agricultural operations within the Mpumalanga Highveld region have contributed to substantial loss and degradation of the surrounding and distal environments (Riato *et al*., 2017). The main stressors are usually toxic heavy and/or trace metal contamination and nutrient enrichment, with direct impacts on both water and sediment quality (De Klerk *et al*., 2012). In a regionally novel study Dunnink *et al*. (2016) established the critical loads for the Maloti-Drakensberg tarns which are isolated mountain lakes and determined their sensitivity and tolerance to the acidic deposition from toxic atmospheric pollution originating in distal coal-fired power stations emissions in Mpumalanga. Depressional wetlands including endorheic pans densely occur in the Mpumalanga Highveld region of South Africa (Riato *et al*., 2017), which is known as the Mpumalanga Lake District (MLD) and consists of around 320 pans (Van Deventer, 2021). There is a paucity of information available on these pans, whilst at continued risk from the impacts of

these anthropogenic activities (De Klerk *et al*., 2012); with only a single study for this region which has determined the surface waters critical loads (e.g. Van Tienhoven *et al*., 1995). The Mpumalanga Province is considered an area to have the highest acidic deposition loads and is where most of South Africa's coal-fired power stations are situated (Dunnink *et al*., 2016). Lakes and endorheic pans are valuable sentinels and archives of environmental change (Das *et al*., 2015) and these naturally accumulating archives have globally been used to identify impacts of environmental pollutants inputs to natural ecosystems (Rose *et al*., 2020).

2.4.2. Sentinel Systems

Isolated lakes can act as valuable sentinels of environmental change (e.g. Williamson *et al*., 2008; Curtis *et al*., 2010) and can provide a system for detecting the effects of climate change (e.g. Adrian *et al*., 2009). Mountain lakes are widely recognised as sentinel ecosystems as their contaminant sources are often solely atmospherically derived and these aquatic systems may exhibit the earliest signals of ecosystem response to contaminants (Rose *et al.,* 2020). Pollutants entering freshwater systems bind to sediment particles, organic and inorganic matter and render the lake a potential long-term accumulator and archive (De Klerk *et al*., 2012; Rose *et al*., 2018). To reconstruct the history of lake sediments, dating the sedimentation record from the deepest part of a lake provides an assessment of anthropogenic change within the system (Bichet *et al*., 2014). Freshwater lakes and endorheic pans may act as natural sinks for the accumulation of sediment but are susceptible nonetheless to anthropogenic pollution (Kock *et al*., 2019). Industrial and mining operations release toxicants at increasing rates and proportions (Edenebe *et al*., 2017) and these deposited toxic heavy metals and particulates often accumulate in the sediments of aquatic ecosystems (Chetty and Pillay, 2019). There is a wide range of atmospherically deposited pollutants such as Hg and Pb and contaminants such as SCPs, that may impact the aquatic system (De Klerk *et al*., 2012; Rose *et al*., 2018).

Sediment pollutant accumulation rates vary between aquatic systems but are nonetheless affected by the atmospheric fallout of heavy metals (Larsen, 2000; Curtis *et al*., 2009). Heavy metals including Hg and Pb are some of the most common pollutant by-products from industrial processes (Chetty and Pillay, 2019) and their presence, especially when above threshold levels, leads to environmental pollution (Edenebe *et al*., 2017). Sediment analysis is an effective way to evaluate metal contamination within natural systems (Chetty and Pillay, 2019) and the analysis of Hg within lake sediments can provide evidence of possible industrial contamination (e.g. Curtis *et al*., 2010; Pelletier *et al*., 2021). As SCPs have no natural sources and are morphologically distinct, they can be used as unambiguous indicators of atmospherically deposited industrial contamination from high-temperature fossil fuel combustion activities (Rose *et al*., 2012; Adams *et al*., 2019). These particulates are used for indicating deposition arising from fossil fuel combustion as any presence of SCPs, even in low concentrations, may be considered anthropogenic contamination of the system (Curtis *et al*., 2010; Rose *et al*., 2012; 2020). An absence of SCPs within lake sediments can also indicate baseline periods of no anthropogenic impacts, as revealed within remote alpine lakes in Europe (e.g. Curtis *et al*., 2009); potentially providing beneficial insights into the natural variability and baseline conditions prior to the interactions between humans and the environment (Adams *et al*., 2019).

Therefore, sediment records help identify directions of change (e.g. improvement or deterioration) of the aquatic system along with the scale and input rates of anthropogenic contamination (Rose *et al*., 2020). However, other toxicants, including SO_2, and NO_x do not leave reliable historical records in lake sediments, as they are involved in various chemical and biological processes within the ecosystem (Larsen, 2000). However, it is important to note that there are many stressors determining the contemporary status of many freshwater systems (Rose *et al*., 2018) such as the depth of a lake which can impact water quality and in turn affect the lake ecosystem and ecology (Princeton Hydro, 2015). Sediments with high pollutant concentrations that have accumulated over time potentially threaten

the aquatic environment (De Klerk *et al*., 2012) and potentially results in acidification and/or eventual eutrophication (Hajizadeh *et al*., 2017; Rose *et al*., 2018)

2.4.3. Ecological Impacts and Biological Responses

Aquatic systems may be valuable candidates for studying the negative effects of contamination, including acidifying atmospheric pollution, sulphur and varying levels of N deposition (Curtis *et al*., 2009; Dunnink *et al*., 2016) causing common problems within aquatic ecosystems including acidification, salinization and nutrient enrichment (Reid *et al*., 1995). Coal dust and ash contain high levels of PM and trace metals and in areas exposed to their deposition, trace metal enrichment has been observed within soils (Dalton *et al*., 2018). As lakes and pans act as sinks, they are vulnerable to the effects of acidic deposition such as acid rain (Curtis *et al*., 2010; Kock *et al*., 2019). Acidic deposition is produced by sulphur and N compound emissions from fossil fuel combustion practices among other anthropogenic activities (Curtis *et al*., 2010; Kock *et al*., 2019). Increased acid rain can influence water quality variables, including dissolved oxygen and pH, which can lead to acidification of surface waters and soils (De Klerk *et al*., 2012; Hajizadeh *et al*., 2017). These deposited acidic compounds may also lead to the potential loss in freshwater ecosystem quality within surrounding environments (Castillo *et al*., 2017; Edenebe *et al*., 2017). Lake acidification in parts of Europe and North America (e.g. Curtis *et al*., 2010) was linked to changes in lake nutrient status from emitted and deposited SO_2, NO_x and N.

Possible sources for increasing nutrients are from industrial atmospheric pollution, agricultural activities and fires, or are naturally released from soils in lake catchments (Curtis *et al*., 2010; Dalu and Froneman, 2016). Nutrient concentrations are influenced by natural and anthropogenic factors; however, the latter of which activities modify physical habitats and water chemistry (Tang *et al*., 2017). Industries remain a major source of inorganic pollution and nutrient enrichment of nitrate, nitrite, and phosphate (Dalu and Froneman, 2016; Adams *et al*., 2019) with nitrates often solely derived from and

more widely associated with agricultural-based activities (Chetty and Pillay, 2019). As lakes and pans act as sinks, they are susceptible to nutrient enrichment (Curtis *et al*., 2010; Kock *et al*., 2019). Nutrients are an important driving force in aquatic ecosystems but an abundance of N and P deposited into aquatic environments (e.g. lakes) may result in eutrophication (Gökçe, 2016; Kock *et al*., 2019). Consequently, eutrophication is a process whereby an ecosystem is organically enriched through an increase of nutrients, either naturally and/or anthropogenically and results in the potential progression of aquatic ecosystem degradation (De Klerk *et al*., 2012).

High concentrations of nitrate pollutants are responsible for the low oxygen concentrations in water due to excessive algal blooms and which often leads to eutrophication of the system (Chetty and Pillay, 2019). Algal assemblages (e.g. diatoms) can reveal or indicate the effects of the degeneration of the aquatic ecosystem, derived from these pollutant inputs (Curtis *et al*., 2009; Gökçe, 2016). Biotic communities affected by anthropogenic stressors can be observed through their response patterns to the nature of the prevailing physical and chemical conditions (Mangadze *et al*., 2019); as chemical stressors can result in impaired functioning or loss of a sensitive species and change in community structure (Mangadze *et al*., 2019). Lake sediments contain these sensitive indicators of atmospherically deposited pollutant inputs such as diatoms, which provides early signals of ecosystem response to toxic contamination (Curtis *et al*., 2009; Das *et al*., 2015).

2.5. Freshwater Ecosystem Monitoring

2.5.1. A Brief Overview

Globally, freshwater lakes are under threat from interacting stressors including contamination and enrichment from anthropogenic activities (Adams *et al*., 2019). Toxic by-products from coal combustion emissions are rapidly threatening the sustainability of freshwater systems with severe impacts extending over vast areas (Langerman and Pauw, 2018; Pajunen *et al*., 2020). Characterising

the diversity, structure and function of freshwater ecosystems is becoming increasingly urgent (Mangadze *et al*., 2019). To explore aquatic ecosystem responses to catchment activities and for the effective management of freshwaters, including lakes and pans, a broader understanding the system primary production is warranted (Das *et al*., 2015). To monitor aquatic ecosystems a complete spectrum of information including the chemical, physical and biological measurements are needed (Kock *et al*., 2019). The physico-chemical variables include among others, pH, temperature, conductivity, phosphates, organic material, dissolved oxygen and CO_2, where the biological variable refers to both living and fossilized organisms found within the aquatic system (Cheng *et al*., 2019).

There are however significant shortcomings in assessing only the physico-chemical variables for water quality (Cameron, 2018) as these instantaneous measurements only depict the water conditions at the time of sampling (Dalu and Froneman, 2016) and ignore any temporal variations (Mangadze *et al*., 2019). As these physicochemical analyses only describes the transient picture of current aquatic situations and conditions, there is an increased probability of inadvertently missing pollutant fluxes, especially when they occur in lower concentrations (Gökçe, 2016). Therefore, biomonitoring is an effective technique used for aquatic ecosystem health management, through assessing aquatic organism's responses to environmental change (Cameron, 2018). Biomonitoring provides a direct measure of ecological integrity through the integration of various stressors, allowing long-term environmental effects to be detected and providing a broad measure of their collective impacts (Dalu and Froneman, 2016). This compliments the traditional physico-chemical indicators and facilitates a better assessment and management of freshwater ecosystems (Mangadze *et al*., 2019). Bioindicators are widely used in ecological assessments as they are valuable in evaluating the impact of the past, current or for predicting any future anthropogenic stresses on aquatic ecosystems (Reid *et al*., 1995; Pajunen *et al*., 2020).

2.5.2. Biomonitoring and Bioindicators

Aquatic communities integrate and reflect the effects of environmental disturbances and provide a time integrated indication of ecological conditions and a cohesive measure of health (Dalu and Froneman, 2016; Kock *et al*., 2019). The main advantage of using the biological approach is that it examines organisms whose exposure to pollutants is continuous and reflects both past and present water quality histories (Dalu and Froneman, 2016). Biological methods typically integrate responses to combinations of contaminants and other sources of environmental stressors with any potential response thus indicating the overall effects within the ecosystem (Mangadze *et al*., 2019). However, a common challenge in establishing an effective bioassessment within shallow lakes, arises in attempts to determine and separate the natural sources of variation from any anthropogenic stressors (Riato and Leira, 2020). Nevertheless, through the regular and systematic use of living organisms as indicators to evaluate changes in the environment (Mangadze *et al*., 2019) the potential presence and severity of pollutants may be indicated through the observed species diversities (Gökçe, 2016). and reflect the environmental conditions within contemporary ecosystems (Pajunen *et al*., 2020).

Biological monitoring programmes have gained popularity around the world, particularly in southern Africa, as they provide comprehensive approaches for assessing the effects of environmental stressors on aquatic ecosystems over time (Mangadze *et al*., 2019). Beyene *et al*. (2009) conducted a biomonitoring comparative study between different bioindicators including macroinvertebrates and diatoms, with aims in ascertaining which organism was best in determining water pollution in multiple rivers in Addis Ababa, Ethiopia; highlighting the various methods and use of the many potential bioindicators. In South Africa, while biological assessment techniques for river health assessments (e.g. Schoeman, 1976; Dalu *et al*., 2016) and estuarine environments (e.g. Bate and Smailes, 2008) are established; there is no definitive method for assessing the ecological condition of wetlands (Riato *et al*., 2017) including freshwater lakes and pans. As endorheic pans and shallow lakes are characterised

by variations in water depth it has often been found difficult to use invertebrates or fish as biological indicators (Kock *et al*., 2019), thus requiring a more effective and reliable indicator for these systems. Algae for example can detect environmental changes that might otherwise be overlooked when using physico-chemical assessments (Dalu and Froneman, 2016).

As bioindicators are widely used to infer the ecological status of ecosystems, it must be noted however that the robustness of this relies on the known environmental preferences of these indicator species (Pajunen *et al*., 2020). Organisms and species assemblages are intertwined with the aquatic ecosystem and environment they inhabit and untangling this integrated information, is key for using reliable indicators (Dalu and Froneman, 2016). Algae qualify as bioindicators due to their nutrient requirements, short life cycle, rapid reproduction rates and as they respond to a wide range of ecological situations, including alterations in water chemistry and increases in anthropogenic pollution (Gökçe, 2016). Within many freshwater ecosystem studies, microscopic algae, including diatoms are the most used bioindicators (Pajunen *et al*., 2020) as they provide a good understanding of the relationship between any environmental changes or physico-chemical parameters and the species community (Kock *et al*., 2019).

2.6. Diatoms as Pollutant Markers

2.6.1. Ecology

Various environmental settings and limiting resources are main drivers of diatom community composition (Reid *et al*., 1995) and within an ecological niche, the appearance of the organism is affected by (non)anthropogenic environmental factors (Gökçe, 2016). Regarding water quality parameters, many taxa have distinct ecological requirements and tolerances with communities and rapidly respond to any prevalent environmental stresses and/or changes (Battarbee *et al*., 2001; Pajunen *et al*., 2020). There are multiple (a)biotic factors influencing species assemblage structuring

and heterogeneity in freshwater lakes and pans (Riato and Leira, 2020). Diatoms depend on inorganic carbon mechanisms (e.g. uptake and enrichment) for cell productivity for their vital role as primary producers within the ecosystem (Rivera-Rondón and Catalan, 2019). They are also potentially indicative of natural characteristics including the geomorphology, geology, climate and physico-chemical conditions within the environment in which they inhabit (Alikaj *et al*., 2019).

Diatoms play a role in global nutrient, silica, and oxygen cycling (Kociolek, 2012) along with the carbon cycle (Kock *et al*., 2019). They form part of the process of both the transport and removal of metals from the environment (Matlala *et al.,* 2011) and play a pivotal role in oxygen production especially in ecosystems where sediments may lack oxygen (Kock *et al*., 2019). Diatoms are amongst the main and integral part of primary producers, forming a major biotic process in aquatic ecosystems (Dalu and Froneman, 2016; Kock *et al*., 2019). They form a dynamic position at the base of the trophic web (Dalu and Froneman, 2016) and are a crucial source of food for benthic consumers (Kock *et al*., 2019). As diatoms are abundant in aquatic environments (Reid *et al*., 1995) and are of significant ecological importance (Dalu and Froneman, 2016) they are used to understand the status, trends, and health within these ecosystems (Kociolek, 2012). The highly specific morphology of diatoms provides species-level identification and the accurate indication of an array of environmental conditions (Battarbee *et al*., 2001). Diatoms can be used to monitor both natural and anthropogenic changes within aquatic systems (Dalu and Froneman, 2016) and are successfully used as ecological indicators of freshwaters environmental situations including temperature, pH, salinity and nutrient conditions (Rivera-Rondón and Catalan, 2019) and pollution. Ionic concentration and composition are the most important factors influencing the structure of temporary wetland diatom communities due to seasonal and climate-driven changes (Riato *et al*., 2017)

2.6.2. Indicator Species

2.6.2.1. Sensitivity to Environmental Variables

Diatom communities have specific environmental requirements and rapidly respond to changes and tolerate a narrow range of environmental conditions, that ultimately affects species composition (Dalu and Froneman, 2016; Riato *et al.*, 2017). As diatoms are exposed to the aquatic environment for a prolonged period, which is their entire lifetime, they can potentially reflect the physical and chemical disturbances within the ecosystem (Kock *et al*., 2019). Each species has a defined set of thresholds and respond to many important environmental variables including water depth, temperature, total phosphorous (TP), salinity and pH (Riato *et al.*, 2017; Cormier *et al*., 2020) among other contributing factors. However, it is important to note there are multiple drivers for change within diatom community assemblages, with the degrees of changes differing regionally (Curtis *et al*., 2009). There is a strong relationship that exists with water chemistry and related parameters and the subsequent diatom community assemblages (Reid *et al.,* 1995). Species react rapidly to changes in environmental conditions including acidification, eutrophication, organic enrichment, salinization and changes in pH (Matlala *et al.,* 2011). Species composition is mainly controlled by pH (Battarbee *et al*., 2001) with water acidity often found as a main environmental factor determining the composition of assemblages in freshwater environments (Rivera-Rondón and Catalan, 2019).

There is a rapid response to stresses induced by anthropogenic activities as diatoms are sensitive to the deposition of pollutants (Das *et al*., 2015) and any subsequent changes in water chemistry (Riato *et al.*, 2017). Cosmopolitan diatom species have been found in a variety of habitats impacted by differing pollutants (e.g. Mangedze *et al*., 2014) within southern African aquatic systems (Dalu and Froneman, 2016). Similarly, species composition was found to be predominantly affected by toxic contaminant stressors from varied anthropogenic origins in a global review (e.g. Stevenson, 2014). Diatoms are sensitive to water chemistry changes with each species having its own specific water

quality requirements (Reid *et al*., 1995; Kock *et al*., 2019). Therefore, multiple environmental factors play a role in diatom community structures and produces distinct assemblages within these freshwater systems (Riato and Leira, 2020). Algae, acquire sulphur as sulphate and the availability therein affects the overall metabolism of algal cells as it is pivotal to their cell physiology (Giordano *et al*., 2008). Nitrogen plays a crucial role in aquatic ecosystems with nutrient availability playing an important role in structuring the diatom community (Gökçe, 2016).

Nutrients have significant effects on diatom species composition, as excess nutrients may lead to algal blooms when environmental conditions are favourable (Tang *et al*., 2017). The limitation of one nutrient over another can favour certain diatom species to dominate over the other, where P is the main variable responsible for driving diatom productivity and species change (Das *et al*., 2015). Thus, the N:P ratio can be used to identify which algae genera are dominant, present, or absent in nutrient impacted aquatic ecosystems (Gökçe, 2016). Interestingly, emitted solid particles (fly-ash) of the generated flue gas from coal combustion activities, have mostly no effect on diatoms and may in fact provide mineral elements used as a form of nutrition by the cells (Cheng *et al*., 2019). The strategies adopted by algal including diatom species in acquiring and assimilating sulphur in different environments can reflect fluctuations in anthropogenic sulphur emissions, as concentrations in lakes may become limiting or enriched (Giordano *et al*., 2008). In terms of diatoms and climate, in a study of the eastern Lesotho Highlands wetlands, Fitchett *et al*. (2016a,b) presented palaeoenvironmental reconstructions, with findings of changes between drier and warmer periods that were interrupted with pronounced cold events, detected from the diatom record.

2.6.2.2. Diatom-based Indices

Using diatom-based indices for biomonitoring can be an effective method and useful tool for evaluating the ecological status of aquatic systems (Alikaj *et al*., 2019), forming a significant

component of biological monitoring processes for assessing water quality (Gökçe, 2016). The development of standard assessment methodologies in lake monitoring programmes, can be somewhat attributed to numerous developed diatom-based indices (Riato and Leira, 2020) which have used different approaches in their application (Lavoie *et al*., 2018). These indices are often based on the notion that the most abundant species present, are those residing in optimal water quality conditions (Musa and Greenfield, 2018). Raju and Perumal (2015) successfully used diatom-based indices in monitoring the environmental quality of riverine ecosystems in India. Alikaj *et al*. (2019) showed a good relationship between water quality assessments and using diatom indices with physico-chemical parameters in an Albanian lake. Similarly, Tan *et al*. (2020) determined the performance of diatom indices in assessing the temporal changes in water quality in aquatic systems in China. Within South African water systems, Schoeman (1970; 1982) identified numerous diatom species and contributed to the creation of various indices (Das *et al*., 2015). These were developed and used for effective water quality management practices (e.g. Bate *et al.,* 2004) and for determining species assemblages' sensitivities to pollutants (e.g. Taylor *et al*., 2007b) within local water bodies, including impacts from external nutrients inputs (Das *et al*., 2015). In some cases, indices are not developed to assess toxic contaminants including metals directly (Lavoie *et al*., 2018).

The South African Diatom Index (SADI) was developed as a modified form of the Specific Pollution Sensitivity Index (SPI) to include endemic diatom species (Mangadze *et al*., 2019). Diatoms are not restricted by physical barriers; however, an assumption is made that certain water bodies that share water quality characteristics, would play host to comparable diatom species assemblages (Musa and Greenfield, 2018). The SADI is thought to have universal applicability across geographic areas and environments because of the cosmopolitan nature of most diatom species (Mangadze *et al*., 2019). However, the observed optima and tolerances of diatom species might vary between geographical regions, resulting in one regions' index not being applicable for another region's diatoms (Pajunen *et al*., 2020). Nevertheless, the SADI has demonstrated its utility in identifying sources of impairment and

in determining the extent of impacts within ecological systems, however input from regional studies is still required and necessary (Mangadze *et al*., 2019). The South African National Diatom Collection (SANDC) provides historical resources of baseline conditions, for most of South Africa and other southern African countries (Harding and Taylor, 2014). However, despite their widespread recognition as a valuable indicator tool in biological assessments, research on their use to assess the biological condition of pans in South Africa is limited (Riato *et al*., 2017).

2.6.2.3. Fossil Preservation in Aquatic Sediments

Diatoms can be abundantly preserved in aquatic sediments (Reid *et al*., 1995) for extended periods, even if the system dries out, due to their siliceous cell walls (Cameron, 2018); making diatoms unique from other algae (Kock *et al*., 2019). Taxonomic identification of diatom species is largely based on their preserved silica valves which are taxon-specific fossilised cells, that can be related to modern autecological data (Reid *et al*., 1995; Cameron, 2018). Identification is based on morphological characters including the shape, symmetry, raphe, stria density and any other observable ornamentation (Lavoie *et al*., 2018). Diatoms are sensitive to many environmental variables, but their highly resistant silica valve structure enclosing their cells, may be potentially well preserved within aquatic sediments under the right conditions (Reid *et al*., 1995; Cameron, 2018). This preservation process is considered best within cold lakes at higher latitudes and poorest in warm saline lakes at lower latitudes (Battarbee *et al*., 2001). Consequently, diatom assemblages are rich in high mountain lakes, of which the sediment record can provide short and long-term historical perspectives of any changes over time (Rivera-Rondón and Catalan, 2019). However, physical damage through breakage, abrasion and chemical dissolution of these siliceous remains do occur and may be found within both alkaline and/or saline waters (e.g. Reid *et al*., 1995).

As diatoms comprise the major component of the microphytobenthos (Dalu and Froneman, 2016) they collectively can be source communities for the sediment record (Battarbee *et al*., 2001). To

investigate the source of sedimentary organic matter in a shallow freshwater lake in Verlorenvlei located in South Africa, Das *et al*. (2015) used multiple biogeochemical proxies, including N concentrations. However, due to the lakes oxygenated water column and shallow sediment-water interface, organic matter rapidly degrades, which resulted in the organic geochemical record not being preserved (e.g. Das *et al*., 2015) within the lake sediments. The sedimentary records containing diatoms from aquatic systems, including lakes and pans, can provide important insights into ecosystem change in response to multiple anthropogenic stressors such as from toxic contaminants (Adams *et al*., 2019). Any fossil assemblages found within aquatic sediments can be used to reconstruct past lake conditions and contemporary limnological conditions (Reid *et al*., 1995) and used to detect lake acidification (Larsen, 2000) for example and for stratigraphic comparisons between and within sediment cores (Stager *et al*., 2013). Therefore, sediment cores offer a temporal view of these preserved microfossils and can represent potential reference conditions of baseline assemblages, prior to anthropogenic impacts (Larsen, 2000; Adams *et al*., 2019). Importantly, post cell death, the diatom frustules are preserved as sequences within the sediments (Cameron, 2018); but as previously mentioned, these organisms may experience post-depositional dissolution, which is problematic, as it possibly inhibits the accurate taxonomic identification of the indicator species of relevance (Reid *et al*., 1995). Notwithstanding, this sensitivity to variable aspects of water quality makes these organisms valuable in archaeological investigations (Cameron, 2018).

2.6.3. Value as Pollutant Indicators

Globally, algal communities are found as one of the most effective indicators (Reid *et al*., 1995) of biological integrity and physico-chemical conditions within aquatic ecosystems (Matlala *et al.,* 2011). They are used to explore and interpret many ecological and practical problems (Kociolek, 2012), to monitor past and present environmental conditions (Kock *et al*., 2019) and provide useful tools for detecting anthropogenic impacts (Gökçe, 2016). A species has a fundamental ecological niche which

is often described as an optimum and range of tolerances for environmental conditions (Pajunen *et al*., 2020) and may be classified as a good indicator if it has a strong correlation to the environmental variable of importance, a narrow tolerance, a well-defined optimum and a high abundance (Riato *et al*., 2017). Interestingly, the effect of atmospheric Hg from coal combustion emissions were determined through using lichens as a pollutant bioindicator within the Mpumalanga Province (e.g. Panichev *et al*., 2019), but it has been stated that diatoms still constitute the more reliable bioindicator (Reid *et al*., 1995; Cormier *et al*., 2020).

Diatoms are more frequently used as indicators for monitoring aquatic ecosystems as they are widely distributed, microscopic, species rich, with few habitat restrictions, react to water disturbance , rapidly respond to environmental changes and are potentially more sensitive to the impacts of pollution at lower concentrations (Gökçe, 2016; Kock *et al*., 2019). Diatom assemblages possess attributes which contribute to their suitability as biological indicators (Reid *et al*., 1995) given that they rapidly respond to environmental changes and anthropogenic activities present in most aquatic environments (Kock *et al*., 2019). Diatoms are useful as biological indicators (Kock *et al*., 2019) as they are less habitat dependant than macroinvertebrates (Reid *et al*., 1995), have high dispersal and rapid growth rates (Matlala *et al.,* 2011); with frequent changes in species composition (Gökçe, 2016), they have a cosmopolitan distribution (Reid *et al*., 1995) and are sensitive to ecological changes (Matlala *et al.,* 2011). Therefore, any observed community composition variations represent diatom species rapid responses to any changes within the environment due to specific physico-chemical factors (Reid *et al*., 1995; Dalu and Froneman, 2016).

By using autecological based analysis, one can determine past and contemporary anthropogenic impacts and the ecological responses of species to those perturbations (Kociolek, 2012). This can be achieved using standard international diatom flora texts (e.g. Lange-Bertalot, 2001) and southern African floras (e.g. Schoeman, 1982; Harding *et al*., 2005; Taylor *et al*., 2007a) and are identified to the

lowest taxonomic level possible (Riato and Leira, 2020). Information on the response of organisms to human-induced disturbances is a limited and important component of biological assessments within freshwater systems (Riato *et al*., 2017). Alikaj *et al*. (2019) researched various lakes in Albania, finding they were rich in diatom species diversity and that this tended to decrease within the more polluted systems. It can be posited that in general, a healthier ecosystem with less pollution will potentially have higher diatom species diversity, where poor diversity often indicates a more polluted ecosystem (Gökçe, 2016). Several diatoms' species are endemic and/or show regionally restricted distributions (Dalu and Froneman, 2016) and with species differences between and among regions and the potential environmental differences, this may modify species responses to environmental change (Mangadze *et al*., 2019).

Often the more tolerant taxa are more responsive than sensitive taxa along environmental and anthropogenic gradients (Tang *et al*., 2017). For instance, the relative sensitivity of diatom species to several natural variables associated with main environmental gradients were determined by Rivera-Rondón and Catalan (2019), for the Pyrenees Mountain lakes situated between France and Spain. Whereas, in a study on the Nairobi River in Kenya, Ndiritu *et al*. (2003) determined the characterization of environmental gradients, through using physico-chemical measurements and diatom densities. Comparatively, Riato *et al*. (2017) investigated the suitability of diatoms as indicators of changing environmental conditions, examining the temporal and spatial responses of diatom communities to natural environmental disturbances (Kock *et al*., 2019) within relatively undisturbed wetlands in the Mpumalanga Province. Importantly, the threshold responses of diatom assemblages to natural environmental variables should be noted, as the influence of these factors on species composition must be considered for detecting accurate thresholds of human disturbance (Tang *et al*., 2017). Globally, diatoms have been used in ecological assessments for environmental change (e.g. Hecky *et al*., 1999; Bate and Smailes, 2008) and for the effects of pollution (e.g. Della Bella and Mancini, 2009; Stevenson, 2014; Tang *et al*., 2017); as environmental preferences of many species are known, with

many species having specific tolerance ranges for pH and/or nutrient enrichment (Dalu and Froneman, 2016; Pajunen *et al*., 2020).

2.7. Southern African Research Using Diatoms

2.7.1. Water Quality

Water quality is one of the most important factors influencing an aquatic ecosystem's integrity, as the distribution of freshwater organisms is mainly controlled by these aquatic characteristics, including dissolved oxygen, acidity and nutrient content (De Klerk *et al*., 2012). Traditionally, monitoring of water quality deterioration has largely been based on physico-chemical analysis, however this approach only provides a measure of the water at the time of sampling (Mangadze *et al*., 2019) and does not explain the ecological relevance of the detected variability in the water quality (Gökçe, 2016). Cholnoky (1899-1972) posited that only performing physico-chemical analyses for water quality was insufficient but through studying the associated diatom communities, water characteristics could be more consistently determined (Dalu and Froneman, 2016). Therefore, diatoms are used as diagnostic and effective tools for water quality assessments (Mangadze *et al*., 2019) providing the biological component, alongside the physical and chemical properties of the water (Gökçe, 2016). However, it must be noted that their use as indicators is based on the concept that species distributions are ubiquitous within aquatic systems and restricted only by local environmental variables to similar degrees, across many regions (Pajunen *et al*., 2020). Most water quality analyses use diatoms as a measure of organic pollution, using varied classification systems including pollution tolerance, pH, and salinity ranges (Reid *et al*., 1995). These organisms rapidly respond to environmental change from variables including light, temperature, moisture and nutrients, leading to their general use in assessing overall water quality (Alikaj *et al*., 2019).

A large collection of international diatom related studies within the northern Hemisphere has expanded knowledge on the relationships between diatoms and multiple factors including pollution and water chemistry (Reid *et al*., 1995). For instance, Larsen (2000) calculated the heavy metal and SCP concentrations from sediment cores in two lakes in Norway and derived a pH reconstruction from the changes in the preserved diatom assemblages. A case study on a freshwater river system in Italy (e.g. Tolotti *et al.,* 2018) revealed the impact of mining and metal pollutants and the response of benthic diatom communities to the anthropogenic contamination. More recently, Pajunen *et al*. (2020) was able to infer important water chemistry including pH and P concentrations and temperature related climatic variables, from diatom assemblages in various streams in Finland and Sweden. However, diatoms are more recognized as under-utilized in water quality monitoring within the southern counterpart regions of the globe, including Australia (e.g. Reid *et al*., 1995), India (e.g. Padhi *et al.,* 2010) and Brazil (e.g. Salomoni *et al*., 2011).

More recently, for the sub-Saharan African region, Dalu and Froneman (2016) summarise the challenges and prospects for employing diatoms as a biomonitoring tool in water quality monitoring. However, some African scholars (e.g. Archibald, 1972; Schoeman, 1976,1979) used diatoms as indicators of water quality, before a defined biomonitoring method based on diatoms was being used in African waters (Dalu and Froneman, 2016). To monitor any changes within aquatic health, attempts in using diatoms as bioindicators in water quality studies in Africa have been used in Ethiopia (e.g. Beyene *et al.,* 2009); Nigeria (e.g. Gdadebo *et al.,* 2019); Malawi (e.g. Hecky *et al*., 1999); Kenya (e.g. Ndiritu *et al.,* 2003); Tanzania (e.g. Oberg *et al*., 2012) and have become more common within southern Africa (e.g. Mangadze *et al*., 2019) including Botswana (e.g. Mackay *et al*., 2012) and Zimbabwe (e.g. Bere *et al*., 2014), for the assessment of short- and long-term water quality and environmental change assessments. Water quality studies for southern Africa are critically important and can simultaneously be used with the dominant diatom species to represent the environmental conditions over time (Kock *et al*., 2019).

In South Africa, Archibald (1972) assessed the diversity of diatom associations to their relations with water quality, marking one of the earliest studies of its kind for the country; where Schoeman (1976; 1979) and Harding and Taylor (2014) have since illustrated the use of benthic diatoms to monitor biotic integrity of freshwater ecosystems in South Africa (Dalu and Froneman, 2016). Matlala *et al*. (2011) results showed a strong correlation between diatom assemblage composition and aquatic physico-chemical parameters, within various wetland ecosystems in South Africa (Kock *et al*., 2019). By assessing the relationship between diatom species occurrence and environmental water of both physical and chemical variables, Riato *et al*. (2017) discovered the important structuring effect of environmental variables, especially alkalinity and ionic composition on diatom communities (Kock *et al*., 2019) within the Mpumalanga Highveld region. To infer variability in the ratio of precipitation: evaporation, Stager *et al*. (2013) investigated the hydrological fluctuations at Lake Sibiya, the largest natural coastal freshwater lake in KwaZulu-Natal, by using high-resolution diatom records. More recently, Kock *et al*. (2019) determined the diatom community structure for Lake Sibiya and their relationship with selected water quality parameters; with findings revealing that the ecosystem and water quality was nutrient enriched and heavily impacted by pollution. Therefore, common diatom taxa correlated with water quality factors, coupled with the narrow tolerance ranges within freshwater environments, may facilitate the identification of anthropogenic impacts based on their presence/absence and/or changes in abundance (Riato *et al*., 2017). The increasing need in South Africa for conservation of aquatic resources is of critical importance due to a decline in water quality and impacts of increased anthropogenic pollution within these ecosystems (De Klerk *et al*., 2012).

Increasing research attention is being given to developing lake quality assessment tools for shallow lakes, as larger and deeper lakes have taken precedence over the last two decades (Riato and Leira, 2020). It is important to note that there are no guideline values available for the water quality variables within shallow lakes and endorheic pans in South Africa (De Klerk *et al*., 2012). It has become more common to use multivariate techniques to model modern diatom communities with contemporary

water chemistry (Cameron, 2018). These models can be applied to fossil diatom assemblages found within sediments and through using these organisms, the historical pollution impacts for water ecosystems can be evaluated (Cameron, 2018; Alikaj *et al*., 2019). Water quality conditions can be palaeolimnologically reconstructed from fossil diatom assemblages, representing periods before the onset of human impacts on aquatic ecosystems (Reid *et al*., 1995). It is crucial to understand which threats are most important for individual systems and species, albeit different threats have different sources and causes, thus, to discern when the first major impact began, a long-term perspective is warranted (Adams *et al*., 2019).

2.7.2. Palaeoenvironmental Research

Palaeolimnological analyses are critically important, they allow for ecological sensitivities, thresholds, responses and evidence for transitions in aquatic ecosystems on account of human activities, to be evaluated (Adams *et al*., 2019). Multivariate statistical techniques facilitate the reconstruction of past lake conditions and provides the accurate estimation of contemporary limnological environmental conditions (Reid *et al*., 1995). Undisturbed, temperate lakes and remote mountain lake sediments are valuable archives of environmental change and act as good reference points for comparing diatom diversity with lakes in other regions, that may have contrasting impact histories (Curtis *et al*., 2009; Adams *et al*., 2019). When exploring the effects of pollution on aquatic systems and to assess the scale of potential impact, it is beneficial to conduct a data comparison between sites (Rose, 2008). Diatom-based reconstruction archaeology is an important part of multi-proxy palaeoenvironmental studies (Cameron, 2018) as these palaeolimnological records can provide useful insights into natural variability and baseline conditions before human-environment interactions (Adams *et al*., 2019).

Palaeolimnological reconstructions often represent the only means of obtaining quantitative water quality data within aquatic ecosystems, where pre-impact chemical measurements are unavailable

(Reid *et al*., 1995). Diatoms are useful indicators of important environmental variables and are analysed from sediment cores to infer past conditions (Cormier *et al*., 2020) as their fossils can provide the baseline information necessary to determine both the nature and extent of pollutant loading over time (Das *et al*., 2015). Through the careful exploration of lake sedimentary archives, including observing chemical constituents and preserved microfossils, it is possible to reconstruct historical environmental impacts on a lake ecosystem from anthropogenic pollutants (Adams *et al*., 2019). The value of diatoms as bioindicators in contemporary and palaeolimnological studies has been well established in the northern Hemisphere (Reid *et al*., 1995) with the global ability to use diatoms to evaluate present and past conditions increasing since the turn of the century (Dalu and Froneman, 2016). Adams *et al*. (2019) reconstructed diatom assemblages from sediment cores in Lake Gusinoye located in Siberia to determine the response of primary producer communities to centuries of environmental change from multiple human-induced stressors. A decade prior, the usefulness of diatoms as a biological assessment tool was demonstrated in pans within United States of America (e.g. Della Bella and Mancini, 2009) of indicator species along a gradient of anthropogenic pressure within Mediterranean climate regions (Riato *et al*., 2017).

Through examining 12 lakes in Alberta within Canada, Curtis *et al*. (2010) found that all sediment cores showed evidence of industrial contamination based on SCPs and changes in diatom assemblages, which was found consistent with nutrient enrichment from anthropogenic N deposition. Similarly, Curtis *et al*. (2009) had previously identified within remote alpine lakes in Europe, that fossil diatom community changes were consistent with recognized environmental problems, including anthropogenic sources for N deposition and acidification. Battarbee *et al*. (2014) assessed the recovery of lakes in the United Kingdom (UK) to acidification, using palaeoecological diatom assemblage data and observed changes. Conversely, a palaeolimnological study of a lake in northern Finland, Korhola *et al*. (2002) suggested that the effects of climate change were the most likely causative mechanism of changes in diatom communities over time (Curtis *et al*., 2009). There is

demonstrated success in using diatoms as biological indicators to assess climate change within lake systems in the northern Hemisphere including North America (e.g. Sivarajah *et al*., 2018); Europe (e.g. Kuefner *et al*., 2020), Russia (e.g. Solovieva *et al*., 2008) and Asia (e.g. Bannister *et al*., 2019). It is important to note that ultimate factors including climate (e.g. Bate and Smailes, 2008) may explain more variation in diatom communities and species distributions, than local or distal pollutant factors (Pajunen *et al*., 2020).

Diatom assemblages are more frequently being used for palaeoenvironmental interpretations of freshwater systems in Africa, including in Niger (e.g. Gasse, 1987), Ethiopia (e.g. Chalie and Gasse, 2002), Cameroon (e.g. Nguetsop *et al*., 2013), Malawi (e.g. Dulanya and Trauth, 2019) and in Egypt (e.g. Hamdan *et al*., 2020); along with in East Africa (e.g. Kiage and Liu, 2006) including Kenya (e.g. Goman *et al*., 2017) and in southern Africa including Madagascar (e.g. Gasse and Van Campo, 1998) and Mozambique (e.g. Sitoe *et al*., 2017). Some palaeoenvironmental studies in southern Africa, including South Africa (e.g. Stager *et al*., 2013; Kirsten and Meadows, 2016) have used diatoms as a secondary source of evidence to support other findings, not looking at pollution within the ecological systems, nor of the potential relationship with diatoms.

More than two decades ago Garcia-Rodriguez *et al*. (2007) examined an urban lake in South Africa to determine the palaeolimnological anthropogenic impacts through observing the relationship with diatom assemblages. Recently, Musa and Greenfield (2018) determined and categorised anthropogenic impacts on South African river systems using diatoms indices. Riato *et al*. (2014) investigated the heavily impacted Mpumalanga Highveld Region freshwater pans, and the distribution and ecology of diatom assemblages were described. However, it is crucial to note that there is a general paucity of information on diatom communities and challenges remain in using these organisms as bioindicators (Mangadze *et al*., 2019). More work is still needed specifically in terms of

diatom community tolerances, ecological preferences and ecophysiology specifically within southern African freshwater systems (Dalu and Froneman, 2016; Kock *et al*., 2019).

2.7.3. Diatoms of Lesotho

Lesotho is considered one of the least developed countries throughout the world but has a rising textile industry that significantly contributes to the economy (Chatanga *et al*., 2019). The economy is largely based on agriculture and livestock, with mining and other industrial practices (Rose *et al*., 2020) simultaneously polluting numerous aquatic systems (Chatanga *et al*., 2019). Industrialised areas of the country release toxic effluents upstream, which was found to significantly affect surface water quality of local rivers (e.g. Pullanikkatil and Urama, 2011). Within the more western region of the country lies Maseru City, which is the most industrialised area in Lesotho and all associated practices threaten nearby aquatic ecosystems (e.g. Chatanga *et al*., 2019). These locally polluted waterways are often predominantly derived from anthropogenic activities including industrialisation, agriculture and urbanisation (Chatanga *et al*., 2019). Any observed anthropogenic contamination in Lesotho is potentially derived from the long-range transport from South African sources, as the country has very minor pollutant emissions and no industrial fossil-fuel combustion practices (Rose *et al*., 2020).

Remote and high-altitude lakes are attributed as sentinels of global change, mostly for research of long-distance atmospheric pollution and the effects of climate change (Rivera-Rondón and Catalan, 2019). These mountain lakes are recognised as sentinel ecosystems, despite their remoteness from sources of anthropogenic atmospheric pollutant emissions (Dunnink *et al*., 2016). Thus, naturally accumulating archives (e.g. lake sediments) potentially containing fossilized diatom species in remote areas (e.g. Letšeng-la Letsie) in Lesotho, may be used to identify the scale and rates of atmospherically deposited inputs into natural aquatic ecosystems (Rose *et al*., 2020). Lesotho has relatively under-researched regions that are of environmental significance to southern African research (Fitchett *et al*.,

2016b). **V**arious species of diatoms within parts of Lesotho and South Africa (e.g. Schoeman, 1970) were examined and formed rare taxonomic data for these environments; where Schoeman (1973) further developed a systematic and ecological study of the Lesotho diatom flora, in special reference to water quality.

Palaeoenvironmental research (e.g. Fitchett *et al*., 2016a; Norström *et al*., 2018) and palaeoclimate variability (Fitchett *et al*., 2016b) were investigated within various wetlands of the eastern Lesotho Highlands, by using a multi-proxy analysis including records of diatom assemblages. In the eastern Lesotho Highlands wetlands, Fitchett *et al*. (2016a,b) presented palaeoenvironmental reconstructions based on multiple proxies, including diatoms; with findings of drier and warmer periods, interrupted with pronounced cold events, that were detected from the diatom record (Fitchett *et al*., 2016a, b). For instance, an increase in aerophilic diatom species, including *Diploneis* and *Eunotia* taxa revealed extreme drying events within the environment, conversely the high relative abundances of *Aulacoseira ambigua* indicated wetter conditions (Fitchett *et al*., 2016a). Additionally, the concurrent relative abundance of *Fragilaria* species represented environmental change and more specifically, colder and harsher conditions over time (Fitchett *et al*., 2016a, b).

Norström *et al*. (2018) found that an absence of planktonic diatom species supported evidence for a drier environment within the Ladybird wetland in Lesotho. Thus the presence or absence of these assemblages may be indicative of fluctuations between wetter and drier climatic conditions (Fitchett *et al*., 2016b). More recently, Rose *et al*. (2020) presented the first palaeolimnological records for Lesotho of Letšeng-la Letsie and more broadly, the first high resolution multi-pollutant records for southern Africa. Determining the extent of these anthropogenic contributions is critical and may elucidate on the extent of impact from industrial emitted contaminants on the environment.

2.8. Concluding Remarks

Ongoing anthropogenic pressures highlight the importance of reliable assessments of the ecological status of southern African freshwaters (Pajunen *et al*., 2020). As with all ecological assessments, it is important to understand the spatial and temporal context of the study regions and the ecology of the indicator organisms (Cormier *et al*., 2020). Diatoms are some of the most sensitive indicators of ecological response to disturbance, that may provide the evidence for the impact from anthropogenic stressors and pollutant deposition. Further research is critical for freshwater bodies within the southern African environment, given their potential role as sentinel ecosystems, their rarity and importance as unique aquatic habitats (Dunnink *et al*., 2016). Long-term monitoring provides a source of information; however these records are often rare and unavailable for many freshwater systems in the southern Hemisphere (Adams *et al*., 2019), including for South Africa and Lesotho alike.

CHAPTER 3: REGIONAL SETTING

3.1. Introduction

The sites were determined by the larger project that this study forms part of. Lake Chrissie (Figure 3.1A) was chosen for its proximity to the coal-fired power stations in the Mpumalanga Province and Letšeng-la Letsie (Figure 3.1B) in the Quthing district of Lesotho, was chosen as it is represented as an isolated mountain lake. This chapter describes the geography and land use, geomorphology, (catchment) geology, hydrology including bathymetry and current lake water quality for these lake systems. Thereafter there is a brief consideration for the general climate, lake ecology and environmental problems experienced within both lake systems. These numerous factors contribute to the sensitivity of the lake to various pressures such as acidification and eutrophication (Rhodes *et al*., 2017). Therefore, it is important to note that there are many stressors determining the contemporary status of many freshwater systems (Rose *et al*., 2018).

Figure 3.1. A. Lake Chrissie (Photo by: Louise Pavid, 2021) and B. Letšeng-la Letsie (Rose *et al*., 2020).

Lake Chrissie is situated in relatively close proximity (~100km) to some of Eskom's coal-fired power stations located within the Mpumalanga Province (Figure 3.2). In comparison, Letšeng-la Letsie within Lesotho is situated over ~400km from these pollutant sources and found within a mountainous region of the country (Figure 3.2). These respective lakes are found at altitudes of 1676m.asl and 2402m.asl (Google Earth, 2022a,b). Thus any contamination from coal-fired power stations detected in Letšeng-la Letsie must be atmospherically derived and long range transported, as Lesotho has no coal-fired power stations (Rose *et al*. 2020).

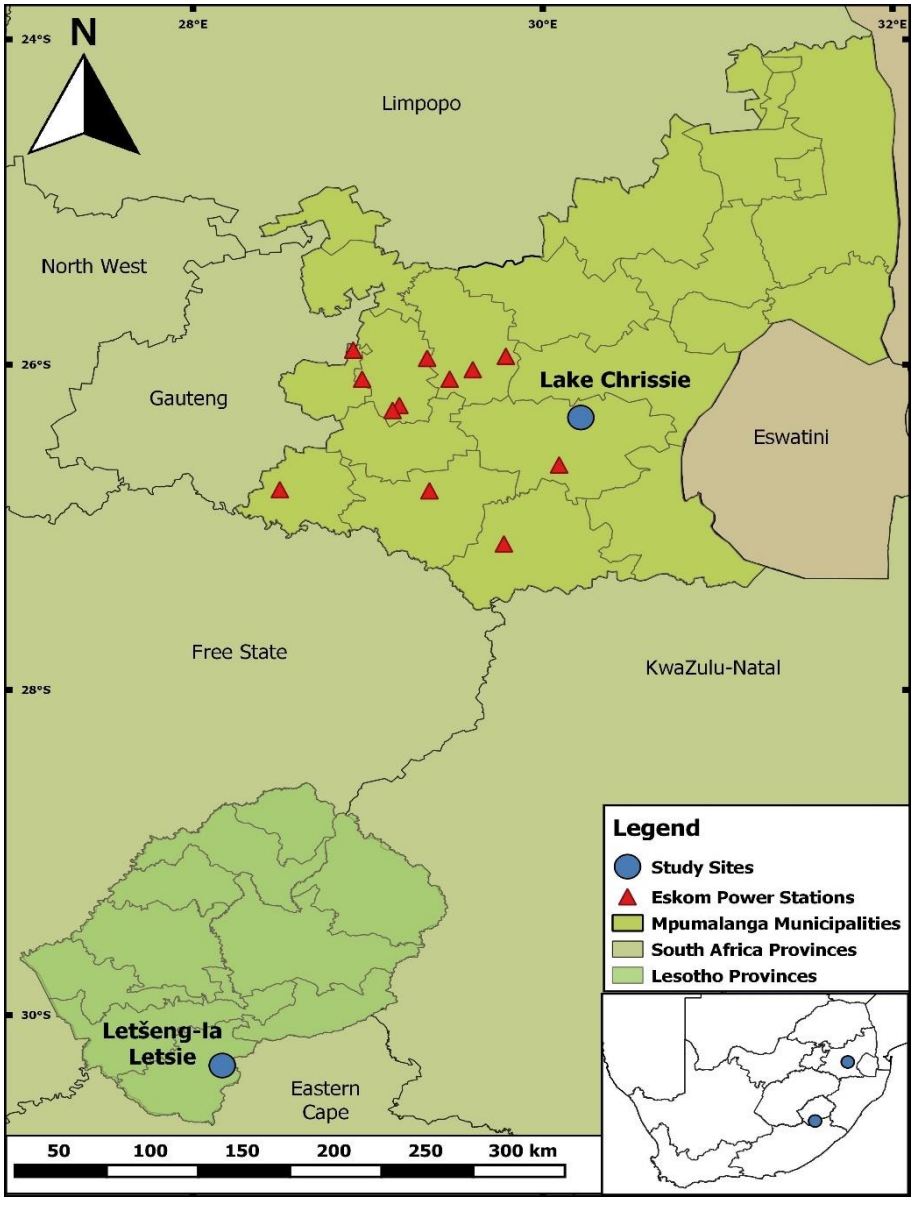

Figure 3.2. Map of the study sites and Eskom's coal-fired power stations.

3.2. South Africa (Mpumalanga Province: Lake Chrissie)

3.2.1. General Geography

Mpumalanga (Figure 3.3) is the second smallest of the nine provinces in South Africa and borders four provinces, namely the Free State, Gauteng, Limpopo and KwaZulu-Natal (Simpson *et al*., 2019; Matlakala and Von Kallon, 2021) and two countries, Mozambique and eSwatini (Matlakala and Von Kallon, 2021). Mpumalanga has 17 local municipalities separated within three districts, namely Ehlanzeni, Gert Sibande and Nkangala (Maponya *et al*., 2013; Municipalities, 2021). Eskom is South Africa's largest power entity, generating ~96% of the country's electricity (Akinbami *et al.,* 2021). Lake Chrissie (26°16'52.02"S and 30°12'38.92"E) is situated adjacent to the town of Chrissiesmeer within Msukaligwa, the largest local municipality within the Gert Sibande district (De Klerk and Wepener, 2013; Municipalities, 2021) of the Mpumalanga Province in South Africa.

Figure 3.3. Mpumalanga Province administrative map, showing Lake Chrissie and the power stations.

3.2.2. Land Use

Mpumalanga contains a large number of urban and rural areas, encompassing ~7% of South Africa's land area and more than half of the country's arable land (Simpson *et al*., 2019; Matlakala and Von Kallon, 2021). Primary land use includes agriculture, supporting ~25% of South Africa's staple food (BirdLife, 2015; Simpson *et al*., 2019) with a combination of commercial, subsistence, livestock and crop farming (Municipalities, 2021). Livestock farming is predominantly of sheep, with crops including maize, sunflowers, wheat, nuts and vegetables among others (BirdLife, 2015; Simpson *et al*., 2019; Municipalities, 2021). Agriculture along with tourism are not primary sectors but are growing within Mpumalanga (Municipalities, 2021). However, beneath Mpumalanga's arable lands are coal fields, which are subsequently surrounded by coal mines and power stations (Simpson *et al*., 2019; Matlakala and Von Kallon, 2021). Thus, major sectors in Mpumalanga include mining and manufacturing as it is rich in coal reserves and is a key resource area of South Africa's coal supply (Simpson *et al*., 2019; Municipalities, 2021). Twelve of Eskom's major coal-fired power stations are situated in the southwestern part of the Mpumalanga Province (Simpson *et al*., 2019) with some shown in Figure 3.4.

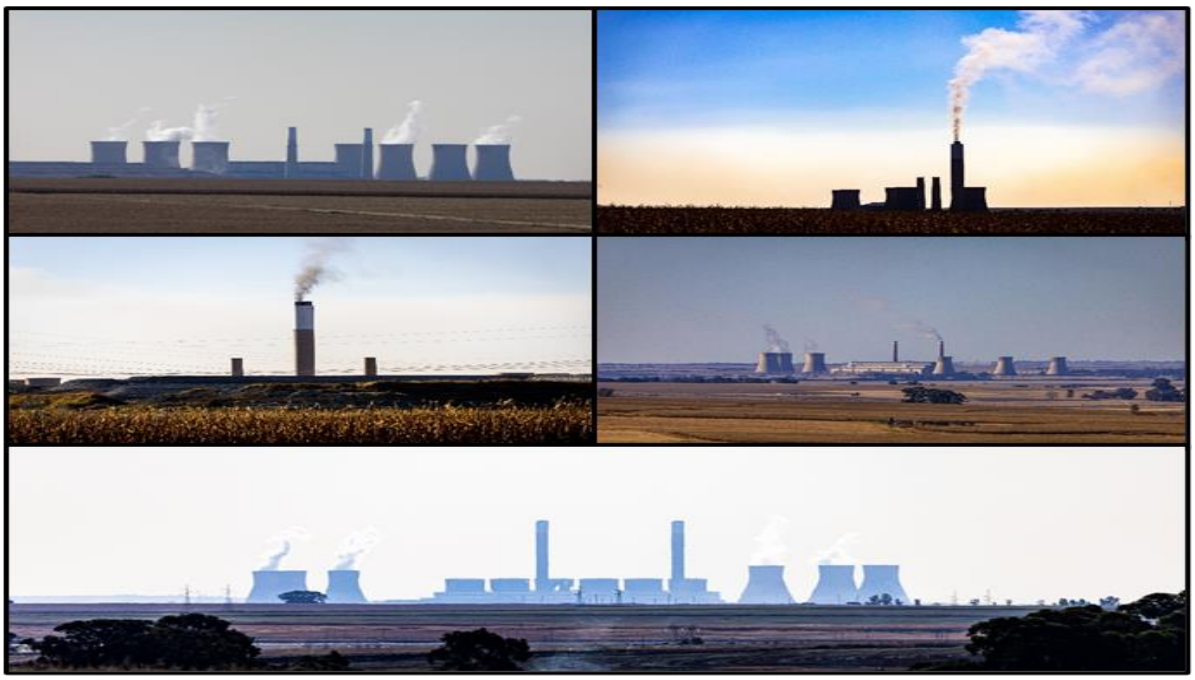

Figure 3.4. Some of Eskom's coal-fired power stations in Mpumalanga (Photo by: Louise Pavid, 2021)

3.2.3. Geomorphology and Geology

Mpumalanga is situated on the high plateau grasslands of the Middleveld and divided by an escarpment into two regions, the Highveld and the Lowveld (Figure 3.5) which extends eastwards (Foster *et al*., 2015; Municipalities, 2021). Most of eastern Highveld geology is underlain by Ecca Group rocks of the Karoo Supergroup, predominantly made up of sandstones and shales with resistant dolerite in some areas (McCarthy *et al*., 2013; Foster *et al*., 2015). The Highveld grasslands region has permanent depressional wetlands such as pans fields (Erasmus and Taylor, 2021) with immediate bedrock formed by the Vryheid Formation of the Ecca Group (McCarthy *et al*., 2013). The MLD is situated in the Highveld and is densely covered with ~320 pans (Ferreira *et al*., 2012; Hallowes and Munnik, 2016). The MLD at an altitude of ~1700m.asl, is part of one of the oldest land surfaces in southern Africa (Foster *et al*., 2015; Hallowes and Munnik, 2016); where the pans are situated on elevated ground, on one of the highest plateaus in the Highveld (McCarthy *et al*., 2013; BirdLife, 2015).

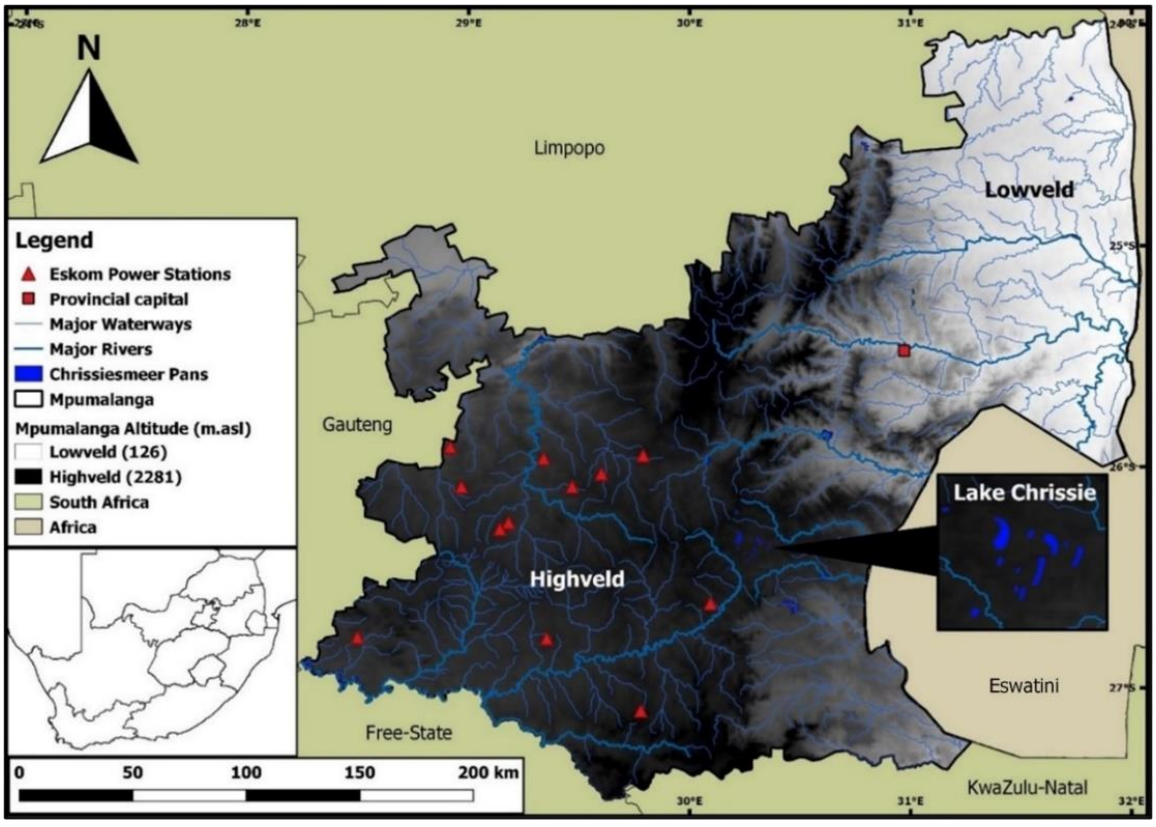

Figure 3.5. Mpumalanga Province elevation, major rivers and the coal-fired power stations.

The MLD is a unique geomorphic feature within South Africa (De Klerk *et al*., 2012; Foster *et al*., 2015), where little erosion has taken place in 65 million years (Hallowes and Munnik, 2016). The pans typically have exposed bedrock on the western margins, with the eastern margins having thick sand deposits (McCarthy *et al*., 2013). These rocks consist mainly of sandstones, with lesser siltstone and shale (Fuls, 2013). These pans have shapes and features making them unique in the country (Foster *et al*., 2015; Hallowes and Munnik, 2016) and include open-water and/or salt pans (Erasmus and Taylor, 2021).

3.2.4. Hydrology

The major rivers (Figure 3.6) that run through Mpumalanga include the Usutu, Crocodile, Sabie-Sand and Komati (Matlakala and Von Kallon, 2021). The MLD, including Lake Chrissie (Figure 3.6) is part of remnant catchments situated in the middle of an extensive drainage system between the Usutu, Vaal, Olifants, Komati and Mpuluzi river systems **(**De Klerk *et al*., 2012; Hallowes and Munnik, 2016).

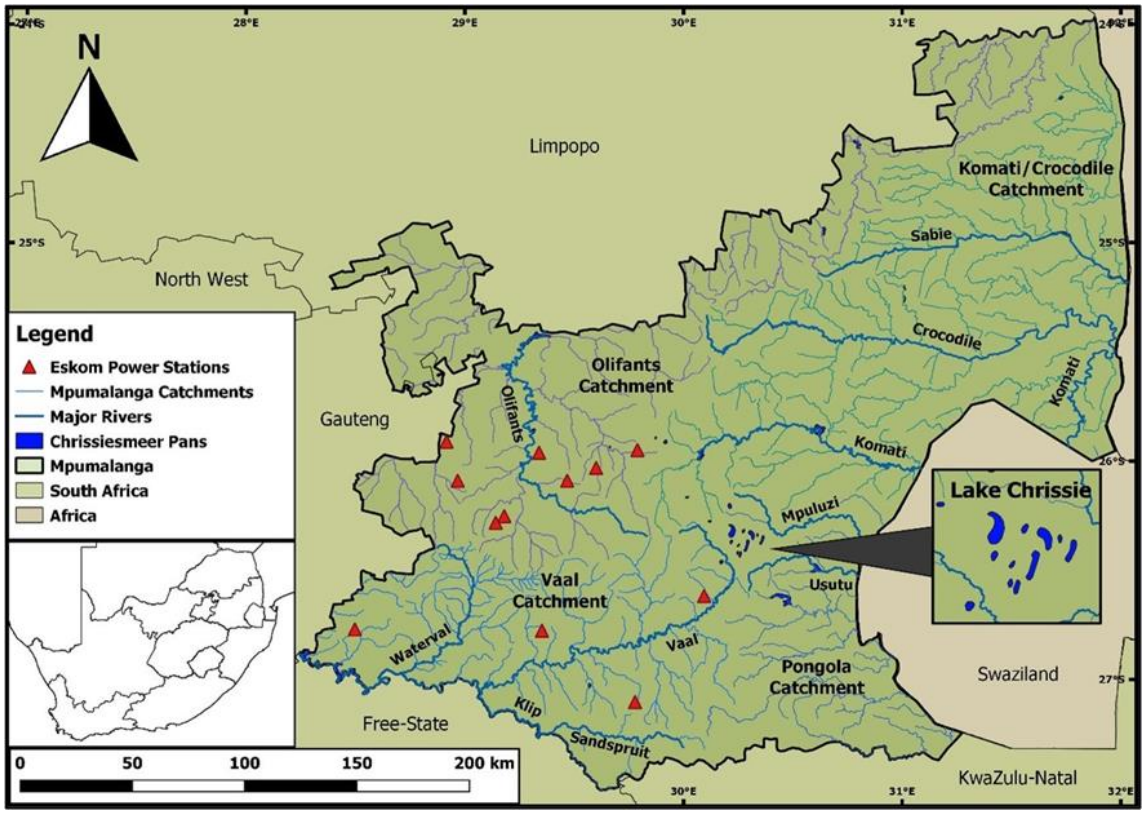

Figure 3.6. Mpumalanga major catchments and rivers, showing Lake Chrissie and power stations.

The MLD pans are situated in proximity to Chrissiesmeer and are also known as the Lake Chrissie area (Ferreira *et al*., 2012) as these pans are mostly situated on private lands and are centred on Lake Chrissie (Figure 3.6) at an altitude of more than 1670m.asl (Google Earth, 2022a; Mapcarta, 2022). Lake Chrissie is the largest natural inland lake in South Africa (McCarthy *et al*., 2013; Hallowes and Munnik, 2016) and is nine kilometres in length, three kilometres wide and has a maximum depth of six meters (Mapcarta, 2022). The pans are isolated, usually oval in shape and many are perennially flooded, making the Lake Chrissie pan fields different from other pan fields in the country (McCarthy *et al*., 2013). Drainage within the pan field is mostly closed but has several major river systems that arise around the pan field including the Usutu, Vaal, Olifants, Komati and Mpuluzi rivers (McCarthy *et al*., 2013; BirdLife, 2015). The pans in the MLD predominantly receive water from direct precipitation, surface runoff or through subsurface inflows (McCarthy *et al*., 2013; Erasmus and Taylor, 2021) with no outflow from the pans including Lake Chrissie, except during floods (Hallowes and Munnik, 2016). This ground water regime forms an important part of pan hydrology (McCarthy *et al*., 2013) where the pans are either ephemeral or perennial (Erasmus and Taylor, 2021) and where evaporation is the most important way in which water leaves (McCarthy *et al*., 2013). Salinity and water quality is seasonally variable between different pans, with salinity ranging from ~200-8000 parts per million total dissolved solids; with 1900 part per million as a maximum limit for human consumption (Fuls, 2013). However, Lake Chrissie is classified as a saline eutrophic lake and is naturally nutrient rich (Ferreira, 2021).

3.2.5. Lake Ecology

The Lake Chrissie area is important for the conservation of manty species of plants and animals, especially birds (Ferreira, 2021) and is renowned as a bird-watcher's paradise (Terblanche, 2022). The geomorphological uniqueness and variability in water access creates a rich variety of ecosystems which is associated with endemism (IMCG, 2021). There is an estimated 300 bird species and 13 frog species recorded populating the wetlands area around the lake (Ferreira, 2021; Terblanche, 2022). Species attracted to Lake Chrisie include herons, grebes, Egyptian and Spurwing Geese, Yellow-billed

Duck, Pochard, Coot, Glossy Ibis, Stilts, crakes and rails in the wetter years and in the drier years there are predominantly flamingos, Cape Teal , Avocets and migrant waders (Fuls, 2013; IMCG, 2021). When the pans are wet, there are regularly more than 20 000 birds, of which the wattled and grey crane, along with lesser flamingo are globally threatened and the greater flamingo is regionally threatened (BirdLife, 2015). The blue, grey and wattled crane are all found all year round and it is rare to find all three crane species together in one place, making Lake Chrissie unique (Terblanche, 2022).

3.2.6. Climate

The majority of South Africa is characterized by warm, wet summers and cold, dry winters (Erasmus and Taylor, 2021) and at higher altitudes, nights are colder (Olaleye *et al*., 2021). The interior regions of the country are described with a semi-arid to sub-arid climate (Noome and Fitchett, 2019) where annual rainfall declines from east to west (Roffe *et al*., 2020). The eastern region ranges from ~600-1500mm in annual rainfall whereas the western region experiences <400mm each year (Roffe *et al*., 2020). South Africa has an average annual rainfall of ~500mm and is globally classified as water stressed and the 30th driest country (Simpson *et al*., 2019; Netshakhuma, 2021). Rainfall in South Africa is produced by the surrounding oceans, both the Atlantic and Indian and the associated cold Benguela and warm Agulhas currents (Roffe *et al*., 2020). Additionally, the latitudinal position, the physical relief, seasonality and various weather systems of the country, all contribute to rainfall production (Roffe *et al*., 2020). Summer rainfall is additionally produced by thermal low-pressure systems associated with the tropical easterlies and convective cloud formation (Roffe *et al*., 2020).

Mpumalanga is in a summer rainfall region which makes up the majority of the annual rainfall (Foster *et al*., 2015; Simpson *et al*., 2019) with the climate overall characterised by minimal rainfall (Netshakhuma, 2021). This ranges from ~400-600mm annual average rainfall in the north-eastern regions, to ~600-800mm in the western and with >1000mm in the central zone; also known as the

high rainfall area (Simpson *et al*., 2019). Annual evaporation increases from the eastern region with ~1600 mm to western areas across the province to >2000mm (McCarthy *et al*., 2013; Foster *et al*., 2015). The Mpumalanga Highveld has moderate summers and cold, frosty winters while the Lowveld is characterised with a subtropical climate and mild winters (Foster *et al*., 2015). The MLD has warm and wet summers and is situated in a relatively humid area with an average annual rainfall between ~800-1000mm (De Klerk *et al*., 2012; De Klerk and Wepener, 2013) and winters are characterised as dry, with little rainfall (Foster *et al*., 2015).

3.3. Lesotho (Quthing District: Letšeng-la Letsie)

3.3.1. General Geography and Land Use

Lesotho (Figure 3.7) is a small (>30,300 km^2), independent mountain Kingdom in southern Africa and situated between the longitudes 27°E and the latitudes of 31° S (Noome and Fitchett, 2019; Grab and Nash, 2020). Completely landlocked by South Africa (Grab and Nash, 2020; Olaleye *et al*., 2021) the country has a population of >2 million people with ~27% of the population living in urban areas such as Maseru, the capital city (Chatanga *et al*., 2019; Noome and Fitchett, 2019). Letšeng-la Letsie (Figure 3.7) situated at 30°18’39.7”S and 28°09’59.3”E and an altitude of 2402m.asl (Google Earth, 2022b), is a mountain lake in the Quthing Province of Lesotho (Rose *et al*., 2020; Kahlolo *et al.*, 2021). It is located ~200km south-east of Maseru and close to the border between Lesotho and the Eastern Cape Province in South Africa (Rose *et al*., 2020; Smit and Van Rensburg, 2021). Lesotho has four agro-ecological zones including the mountains, lowlands, foothills and Senqu River Valley and respectively occupy 59%, 17%, 15%, and 9% land area in the country (Bailey *et al*., 2021; Olaleye *et al*., 2021). Lesotho is globally considered one of the least developed, low-income nations with high levels of poverty and income inequality (Chatanga *et al*., 2019; Noome and Fitchett, 2019).

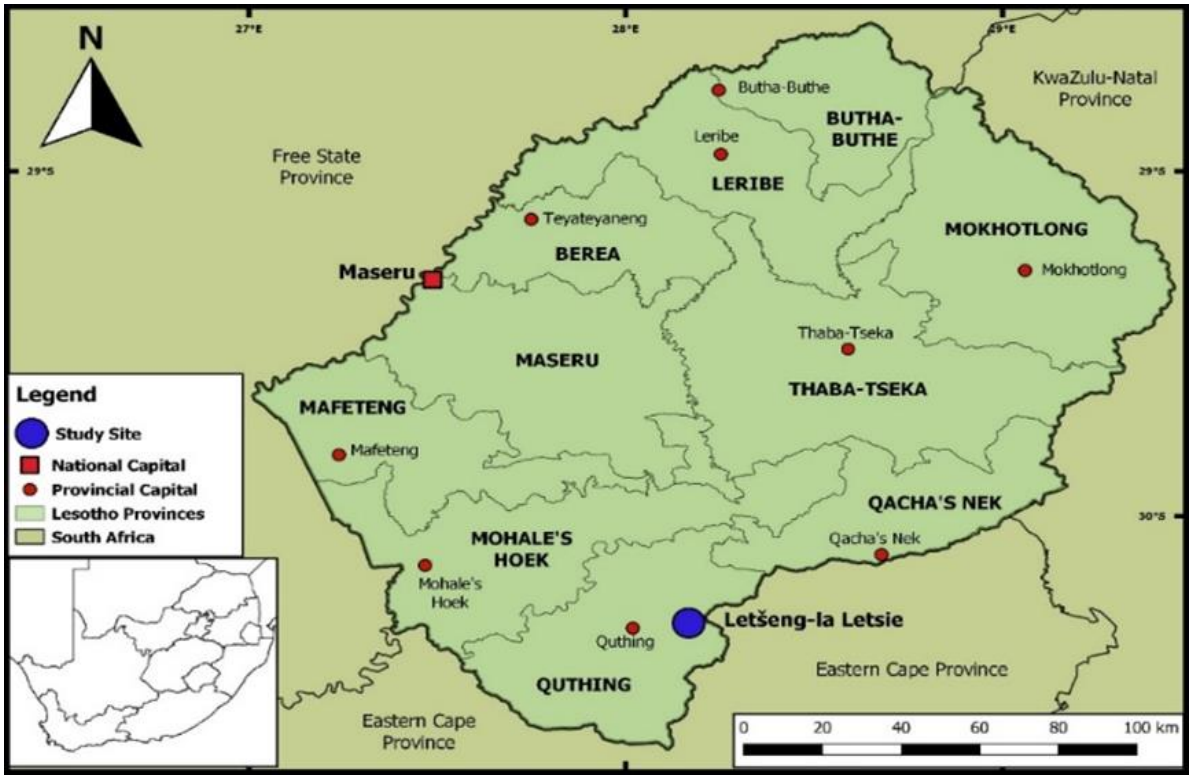

Figure 3.7. Lesotho administrative map and location of Letšeng-la Letsie.

The main economic activities such as increased development of textile industries, are predominantly located in the lowlands, foothills and along the Senqu River valley (Chatanga *et al*., 2019; Bailey *et al*., 2021). The textile factories both generate foreign currency and provide jobs (Chatanga *et al*., 2019), but water resources and nature-based tourism remain the main sources of income for the country (Hoogendoorn *et al*., 2020; Olaleye *et al*., 2021); where only 11% of the land is suitable for agriculture (Bailey *et al*., 2021). Water is a resource Lesotho has in abundance (Olaleye *et al*., 2021) with the Lesotho Highland wetlands having significant hydrological importance to southern Africa, as they store and regulate large reservoirs of water (Norström *et al*., 2018). Many households in Lesotho own grazing livestock, including cattle, sheep and goats with sheep as the most dominant (Rose *et al.,* 2020). Letšeng-la Letsie catchment area is important for provision of grass for thatching, as a source of water, medicinal plants, wood, for fishing and as grazing lands (Ramsar, 2022).

3.3.2. Geomorphology and Geology

Lesotho has diverse topography from the western lowlands to the eastern highlands (Figure 3.8) which are more mountainous with altitudes ranging from ~1400m.asl. to >3400m.asl. (Grab and Mills, 2011; Grab and Nash, 2020). The lowlands in the western section of Lesotho form a high elevation plateau (Bailey *et al*., 2021) while the eastern part has rugged topography (Noome and Fitchett, 2019) and is mountainous with rugged terrains (Olaleye *et al*., 2021). Geographically Lesotho is positioned just west of the Great African Escarpment which forms a natural eastern border of Lesotho, known as the Drakensberg (Grab and Nash, 2020).

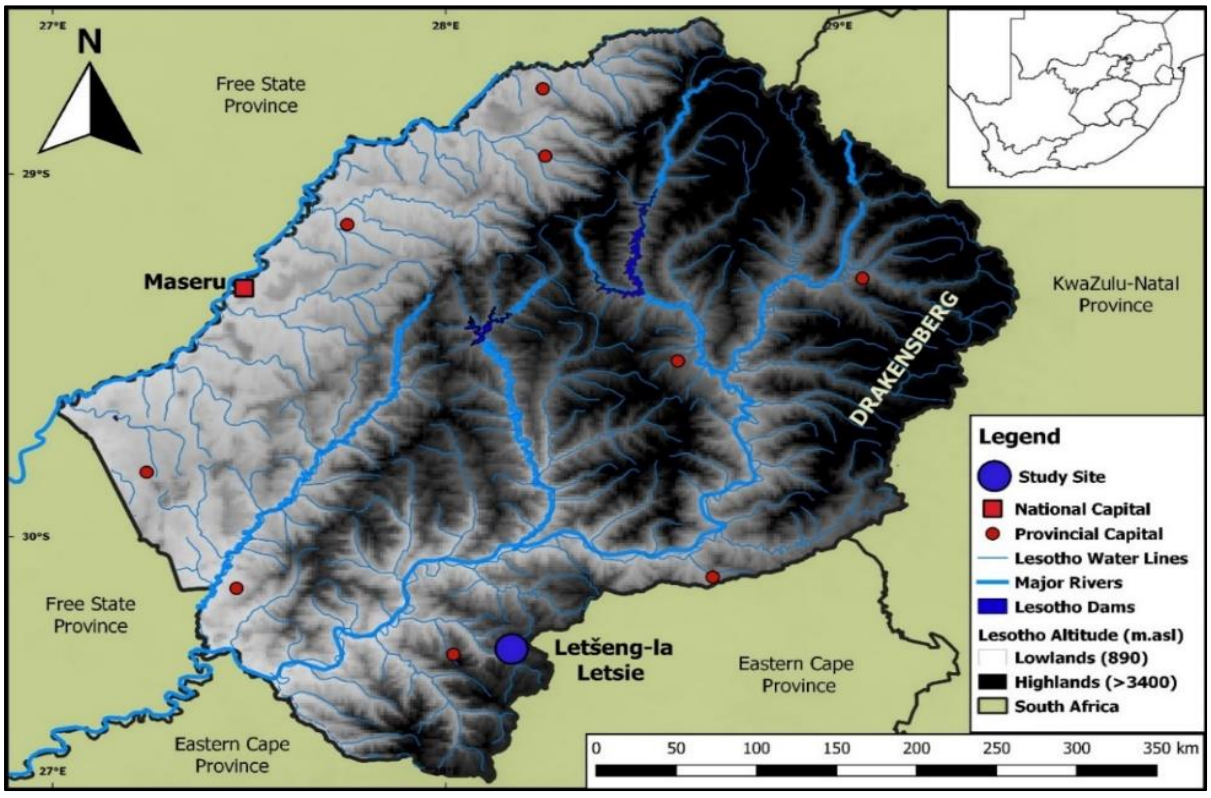

Figure 3.8. Lesotho elevation map, showing major rivers and the location of Letšeng-la Letsie.

Several high mountain ranges of >3000m.asl such as the Drakensberg in the East and the Maloti mountains in the North, along with the Thaba and Putsoa ranges contribute to the mountainous region of Lesotho, making up a third of the country's land area (Grab and Mills, 2011; Bailey *et al*., 2021).

These mountainous areas of Lesotho supply a significant portion of southern Africa's water resources (Bailey *et al*., 2021). Lesotho is generally underlain by sedimentary Karoo rocks with a dominant geology of igneous formations (Olaleye *et al*., 2021). Letšeng-la Letsie catchment area is completely bound by mountains that rise to 2820m.asl and with a dominant geology of basaltic with dolerite intrusions, with recent alluvial deposits in the valley and lake floor (Rose *et al*., 2020).

3.3.3. Hydrology and Lake Ecology

The Orange-Senqu River, known as the Orange in South Africa and the Senqu in Lesotho, flows across Lesotho before flowing westward into South Africa (Chatanga *et al*., 2019) with other major rivers including Caledon and Makhaleng (Figure 3.9). The Lesotho Highlands is dissected by major fluvial systems including the Senqu and Makhaleng, forming deep gorges (Grab and Nash, 2020).

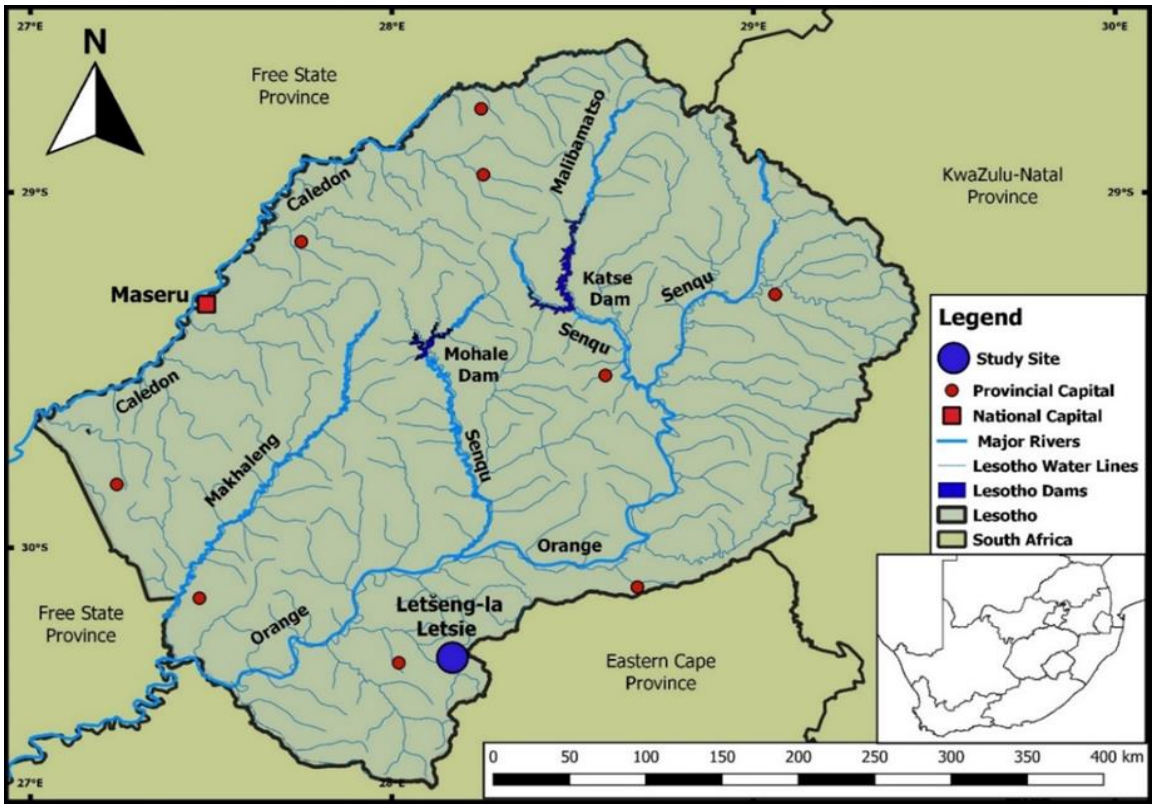

Figure 3.9. Lesotho major rivers, showing the location of Letšeng-la Letsie.

Letšeng-la Letsie, is the source of the Quthing River, one of the streams which feed into the great Senqu River (Lesotho Times, 2014). The lake has a mean depth of ~1m and maximum of 1.4m was impounded by a small dam in 1968, across the Mohlakeng River (Rose *et al*., 2020). There are signs that all is not well in the ecosystems as seen by the poor quality of the water (Lesotho Times, 2014). The Letšeng-la Letsie catchment region is dominated by grasses, sedges and woody shrubs signalling Afromontane and Afroalpine vegetation (Rose *et al*., 2020; Ramsar, 2022). Letšeng-la Letsie is part of the Ramsar protected area (Smit and Van Rensburg, 2021) part of the Maloti-Drakensburg Mountains known as a biodiversity hotspot, as it has >30% endemism of predominantly bird species (Rose *et al*., 2020). Due to its role in regulating water regimes and habitat supporting special wildlife, especially water-birds, Letšeng-la-Letsie is of global importance (Lesotho Times, 2014). A number of vulnerable species occur among the 110 bird species recorded at this site, including the Wattled and Blue Cranes, the Lesser Kestrel and the Bald Ibis Ramsar, 2022).

3.3.4. Climate

Lesotho is one of the windiest countries in Africa and experiences numerous extreme weather events including droughts and flooding (Rose *et al*., 2020; Bailey *et al*., 2021). The lowest winds are experienced in the summer months where the strongest winds in late winter are linked to the frontal systems associated with the westerlies (Rose *et al*., 2020). The climate is characterised as semi-arid to sub-humid (Noome and Fitchett, 2019; Grab and Nash, 2020) and mainly influenced by altitude (Bailey *et al*., 2021), the El Niño Southern Oscillation (ENSO) and the effects of continentality and latitude (Noome and Fitchett, 2019; Bailey *et al*., 2021). These factors contribute to the distinct seasonality in Lesotho (Grab and Nash, 2020) which is generally characterised with wetter, warmer summers and drier, cooler winters (Noome and Fitchett, 2019). These interannual variations in rainfall are significant with prolonged dry or wet periods, which are directly linked to El Niño and La Niña events, respectively (Bailey *et al*., 2021; Olaleye *et al*., 2021).

Lesotho is a summer rainfall region with an average precipitation greater than most other regions of southern Africa (Bailey *et al*., 2021; Olaleye *et al*., 2021). The rainfall season spans October through April with an average of ~800mm per year (Noome and Fitchett, 2019; Bailey *et al*., 2021). It is estimated that >80% of the annual precipitation occurs within these seven months (Bailey *et al*., 2021; Olaleye *et al*., 2021). Mean annual rainfall ranges from <600mm in the lower Senqu Valley to <740mm in the western and southwestern lowlands, to ~1000mm along the mountain ranges and to >1600mm in the north-eastern highlands (Grab and Nash, 2020; Olaleye *et al*., 2021). Most summer precipitation originates from moisture transported from the Indian Ocean and the uplift along the Great Escarpment (Norström *et al*., 2018). Depending on elevation, peak daily rainfall rates are reached either as rain or snow (Grab and Linde, 2014; Bailey *et al*., 2021). Temperatures in Lesotho are strongly influenced by high elevation gradients and are highest during the summer months between December and February; where January is described as the hottest month, reaching maximum temperatures of 26℃ (Rose *et al*., 2020; Bailey *et al*., 2021).

By April and May precipitation amounts decrease, with <10% mean annual rainfall occurring during the winter months spanning from May through August and reaching very low levels in June and July (Grab and Nash, 2020; Bailey *et al*., 2021). Snow, sleet or hail occur anytime during the year with snowfalls more common in the winter months (Grab and Linde, 2014; Grab *et al.,* 2017). Annually, snowfall predominantly occurs between March and November around eight times a year in the highlands and intermittently in the lowlands (Norström *et al*., 2018; Noome and Fitchett, 2019). Frost is widespread throughout Lesotho from May to September (Grab and Nash, 2020) but annually occurs >80 days in the lowlands and >250 days in mountainous areas with elevations of >3000m.asl. (Grab *et al.,* 2017; Olaleye *et al*., 2021). July is the coldest month experiencing snow and frost in the highest elevations (Grab and Linde, 2014; Bailey *et al*., 2021). Temperatures begin to decrease at the end of

the rainy season and range from a minimum of 1℃ to a maximum of ~17℃ in June and from a maximum of -5℃ to a minimum of -22℃ in July (Rose *et al*., 2020; Bailey *et al*., 2021) each year.

3.4. A Brief Consideration for Climate Change

Globally, the largest adverse impacts of climate change are changes in seasonality of rainfall and any reductions associated with the retreat in the Antarctic sea-ice and expansion of the Hadley cell (Roffe *et al*., 2020). Global warming is associated with subtropical cyclones ENSO and the Indian Ocean Dipole (IOD) in southern Africa (Gaughan *et al*., 2016) along with the Southern Annular Mode (SAM) and the poleward shift of easterly and westerly wave circulation systems (Sousa *et al*., 2018). There is a close link between climate systems and freshwater resources (Olaleye *et al*., 2021) with climate change raising the likelihood of both natural and anthropogenically influenced disasters (Netshakhuma, 2021). Climate change impacts the quality and quantity of water resources in southern Africa, with chronic conditions including periodic droughts (Bailey *et al*., 2021; Olaleye *et al*., 2021) and floods, which are both expected globally (Netshakhuma, 2021). Droughts in South Africa have caused reduced river flows and water levels while in extreme droughts, these sources may dry up completely, challenging water supply in many provinces (McCarthy *et al*., 2013; Matlakala and Von Kallon, 2021).

Changes in rainfall seasonality in South Africa may be detrimental to water surface supplies (Roffe *et al*., 2020) with climate change and global warming posing serious implications for future snowfall (Noome and Fitchett, 2019) both affecting Lesotho's hydrological cycle and future water availability (Olaleye *et al*., 2021). Lesotho and South Africa are in close proximity to each other, thus subject to the same meteorological conditions and possible future changes in the climate system (Gilili, 2021). Global warming increasing surface water temperatures and ongoing anthropogenic pollution have led to increased nutrient levels in lake systems and in phytoplankton growth (Olaleye *et al*., 2021).

3.5. Environmental Challenges

Primary activities in Mpumalanga and land-use practices in the MLD are diverse and of concern (De Klerk *et al*., 2012; Ferreira *et al*., 2012). The area is affected by various degrees of anthropogenic influence including coal mining, factories, agriculture and livestock practices, and sewage disposal (Ferreira *et al*., 2012; De Klerk and Wepener, 2013). Pollution in the MLD area is predominantly related to mining activities with over 60% of the province surface area subject to mining rights and agriculture (Simpson *et al*., 2019). Coal mining is a source of contaminants for these pans, both polluting the waters and disrupting the hydrology of these aquatic systems (De Klerk and Wepener, 2013; McCarthy *et al*., 2013). Old mines pollute surface and groundwater through AMD which affects nearby agricultural lands and is directly derived from coal mining activities (Erasmus and Taylor, 2021; Matlakala and Von Kallon, 2021). Coal mines and associated power stations produce acid rain which reduce the pH and affects alkaline pans, which in turn interferes with the functioning of the pans resulting in modifying the fauna and flora within these systems (BirdLife, 2015).

Agricultural practices are diverse in Mpumalanga and include livestock and the production of maize but with this diversity, results in varied environmental impacts (Ferreira, 2022). Agricultural development may cause contamination and eutrophication of pan systems due to the runoff of pesticides and fertilizers (De Klerk and Wepener, 2013; BirdLife, 2015). Other environmental impacts associated with agricultural practices include livestock waste, soil erosion and associated nutrient loss leading to the eutrophication process (Ferreira, 2022). The endorheic nature of pans exacerbates this problem and toxic substances subsequently concentrate in their basins (BirdLife, 2015). Ploughing and livestock further damage shoreline vegetation, increase wind erosion, sedimentation and change pan characteristics (BirdLife, 2015; De Klerk and Wepener, 2013). These activities present the most serious threats to wetland ecosystems such as of pan fields situated within the Mpumalanga Highveld

and threaten the health, the unique ecology and diversity within these endorheic pans (BirdLife, 2015; Erasmus and Taylor, 2021) and lakes.

Lesotho water catchments and wetland ecosystems including lakes, rivers and dams are subject to anthropogenic impacts such as industry and mining along with agricultural activities (Norström *et al*., 2018; Olaleye *et al*., 2021). Additional threats include livestock grazing and associated trampling, overgrazing, leading to overexploitation and a loss of biodiversity, and ecosystem services with soil erosion and siltation often derived from these activities (Kahlolo *et al*., 2021; Smit and Van Rensburg, 2021). It is not just grazing on Letšeng-la-Letsie which is disturbing but also other practices such as farming on the banks of the Senqu River for example (Lesotho Times, 2014). There is cause for concern over the conservation status of the Letšeng-la Letsie catchment along with socio-economic considerations, as it is a valuable grazing resource for local herdsman (Smit and Van Rensburg, 2021).

As Lesotho has no coal-fired power production, any pollution from industrial sources in the Mpumalanga Highveld needs to be long-range transported, to be deposited in Maloti mountains of southern Lesotho, such as in Letšeng-la Letsie (Rose *et al*., 2020). A back-trajectory analysis for the reconstruction of air-mass pathways found that this transport to Letšeng-la Letsie takes between two to three days (Rose *et al*., 2020). However, the Mpumalanga Highveld air flow associated with continental, recirculating anticyclones and slow-moving air-masses are infrequent, which may lead to low levels of pollution in Letšeng-la Letsie (Rose *et al*., 2020). It is projected that Letšeng-la Letsie will be less influenced by westerly flow and more by anticyclonic flow, resulting in an increase in polluted air from industrialised regions (Rose *et al*., 2020).

CHAPTER 4: METHODS

4.1. Introduction

This project involves the identification and interpretation of diatoms in sediment samples obtained from sediment cores obtained from Lake Chrissie in the Mpumalanga Province of South Africa and Letšeng-la Letsie situated in the south-eastern region of Lesotho. Sediment cores were obtained in April 2018 using a gravity corer, as part of a larger multi-proxy National Geographic funded project (Rose *et al*., 2020). While this study focusses only on diatoms, using these bioindicators of the hydrological system response to pollution deposition, the results will be compared with the SCP, Hg and other results previously obtained for the sites as part of the larger project.

4.1.1. Sediment Coring and Physico-Chemical Analysis

Using standard methods of the palaeolimnological approach, lacustrine sediment cores were collected from Lake Chrissie and from Letšeng-la Letsie (Rose *et al*., 2020) prior to the commencement of this MSc. This was achieved with a gravity corer with an 86mm diameter plastic tube that is pushed through the sediments of the deepest part of the lakes (Dulanya and Trauth, 2019; Rose *et al*., 2020). The cores are carefully extruded vertically (Dulanya and Trauth, 2019; Rose *et al*., 2020) where a threaded bar pushes increments of the sediment out from the bottom to be sliced from the top of the coring tube (Curtis *et al*., 2010; Das *et al*., 2015). The extruded sediments were sliced at 0.5cm intervals in the field, the samples separated and stored on ice at 4℃ and transported, refrigerated and kept in a dark and frozen environment thereafter of -20℃ (Dulanya and Trauth, 2019; Rose *et al*., 2020). Without age control the sediments cannot be linked to the broader context of lake history (Beck *et al*., 2019); thus, estimates of the sediment accumulation rates and age of the cores can be determined through dating techniques (Dulanya and Trauth, 2019). The ^{210}Pb chronologies were calculated for both lakes using the constant rate of ^{210}Pb supply (CSR) dating models. All dates are within the last

200-years and therefore AD is not used within the dissertation except within *Chapter 5: Results*. The Lake Chrissie ^{210}Pb core chronology can be seen in Table 4.1.

Table 4.1. ^{210}Pb chronology of core CM01 taken from Chrissiesmeer, South Africa.

Depth	Drymass	Chronology			Sedimentation Rate		
		Date	Age				
cm	g cm-2	AD	yr	±	g cm-2 yr-1	cm yr-1	± %
0	0	2017	0				
0.25	0.0113	2017	0	2	0.1233	1.978	15
2.75	0.1714	2016	1	2	0.1157	1.483	15.3
5.25	0.4014	2013	4	2	0.0766	0.754	9.5
8.25	0.7306	2009	8	2	0.0844	0.739	11.1
10.75	1.0297	2005	12	2	0.0639	0.407	6.5
13.25	1.5151	1996	21	2	0.0423	0.186	7.3
14.25	1.8252	1988	29	2	0.0376	0.099	7.6
15.25	2.2783	1978	39	2	0.0544	0.101	10.3
16.25	2.9061	1967	50	3	0.0673	0.107	16.8
17.25	3.5338	1958	59	4	0.0701	0.104	17.5
18.25	4.2554	1946	71	5	0.0525	0.073	22.3
19.25	4.982	1932	85	8	0.0503	0.068	27.7
20.25	5.7418	1916	101	12	0.0425	0.054	45.8
21.25	6.5423	1898	119	19	0.047	0.059	69.5
22.25	7.3428	1882	135	29	0.0571	0.069	109.2
23.25	8.2079	1853	164	37	0.0144	0.017	138.6

The CRS dating model places the 1963 depth between 16.25 and 17.25cm for Lake Chrissie and the sedimentation rates calculated by the ^{210}Pb data suggest that from the 1880s to the 1900s, the sedimentation process was relatively stable and followed by an increase in present day. The radiometric chronologies and sedimentation rates of the core can be seen in Table 4.1 and Figure 4.1; where the solid line shows age while the dashed line indicates sedimentation rate (Figure 4.1). An error bar stretches to 200 years ago to 1820 (Figure 4.1), where the modelled date is for 1853, which is 180 years ago. Therefore the age model was extrapolated back using an average sedimentation rate for a 240-year age model for the Lake Chrissie site

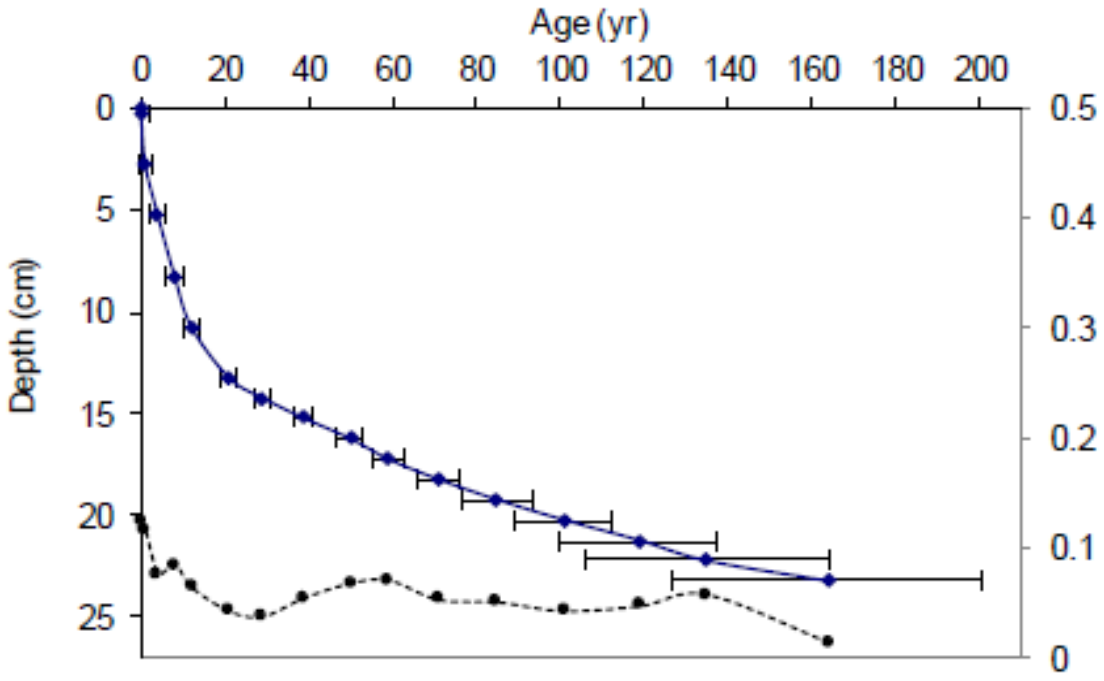

Figure 4.1. Radiometric chronology of the Lake Chrissie core, showing the CRS model, ^{210}Pb dates and sedimentation rates.

Sediment chronologies were determined for Letseng-la Letsie (Table 4.2). The ^{210}Pb records and dating confirmed a coherent stratigraphy with continuous accumulation and no problems with sample recovery in Letšeng-la Letsie (Rose *et al*., 2020).

Table 4.2. ^{210}Pb chronology of soil core LETS-P3 taken from the catchment of Lake Letsie, South Africa.

Depth	Drymass	Chronology			Accumulation Rate		
		Date	Age				
cm	g cm-2	AD	yr	±	g cm-2 yr-1	cm yr-1	± %
0	0	2018	0				
0.25	0.105	2018	0	2	0.6367	0.98	30.7
4.25	2.7625	2013	5	2	0.4587	0.563	17.7
8.25	6.6225	2005	13	2	0.4595	0.482	21.7
10.25	8.4775	2001	17	3	0.573	0.588	26.6
12.25	10.5175	1997	21	3	0.4949	0.518	39.2
14.25	12.3025	1992	26	3	0.2519	0.262	23.6
16.25	14.3625	1985	33	4	0.3112	0.295	27.7

18.25	16.5175	1977	41	5	0.2665	0.231	32
20.25	18.9825	1966	52	5	0.1924	0.157	36
22.25	21.4275	1952	66	7	0.1526	0.126	37.3
23.25	22.6175	1944	74	8	0.1399	0.118	44.4
25.25	24.9875	1920	98	15	0.0674	0.059	53.9
26.25	26.0175	1899	119	23	0.0332	0.035	57.1

The CRS dating model places the 1963 depth at around 20.5cm where the soil accumulation rates show a gradual increase from the beginning of the 1900s to the 1980s, followed by some fluctuations till present day (Figure 4.2). The radiometric chronologies and sedimentation rates of the core can be seen in Table 4.2 and Figure 4.2; where the solid line shows age while the dashed line indicates sedimentation rate.

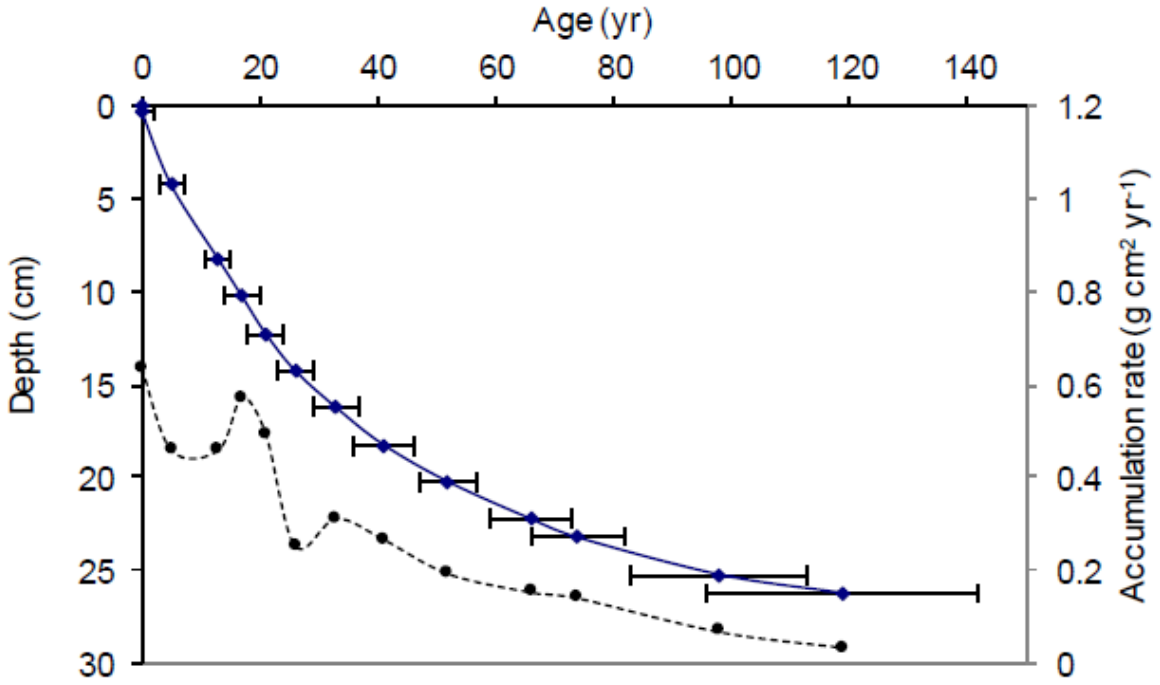

Figure 4.2. Radiometric chronology of the Letseng-la Letsie core, showing the CRS model, ^{210}Pb dates and sedimentation rates.

4.1.2. Sample Preparation

Diatom preparation was undertaken in the laboratories of the Department of Geography at the Royal Holloway University of London (RHUL), using standard techniques of Battarbee *et al*. (2001). To allow optimal comparison between proxies, and due to travel restrictions related to COVID-19, all preparation work was conducted in London. Key methods include the removal of organic material and inorganic carbonate matter from the sample slides (Dulanya and Trauth, 2019; Westover *et al*., 2019). This is achieved through cleaning the samples by using hydrogen peroxide (H_2O_2) and hydrochloric acid (HCl), respectively (Dulanya and Trauth, 2019; Zou *et al*., 2020). Samples were dried onto cover slips and prepared using Naphrax©, then mounted onto microscope slides (Beck *et al*., 2019; Westover *et al*., 2019; Zou *et al*., 2020). Modern ecological changes can also be investigated from these accumulated sediment samples (Dulanya and Trauth, 2019) and these samples can additionally be used for diatom diversity analysis (Zou *et al*., 2020). The prepared and mounted slides allow for microscopy to determine the diatom counts and to identify the diatom assemblages to the highest taxonomic level possible (Beck *et al*., 2019). This has been summarised as a flow chart seen in Appendix A as Figure A.1 and Figure A.2.

4.2. Laboratory Work: Microscopy

4.2.1. Species Counts and Taxonomic Identification

All diatom microscopy (Figure 4.3) was undertaken in the laboratory of the School of Geography, Archaeology and Environmental Studies (GAES) at the University of the Witwatersrand (Wits) using a Zeiss Primorstar Light Microscope (LM). The slides were analysed at 1000x magnification under oil immersion and 300 diatom valves were counted per sample (Adams *et al*., 2019; Kock *et al*., 2019; Westover *et al*., 2019), where possible. Poorly preserved frustules or valve fragments were not counted and excluded from the sample (Westover *et al*., 2019).

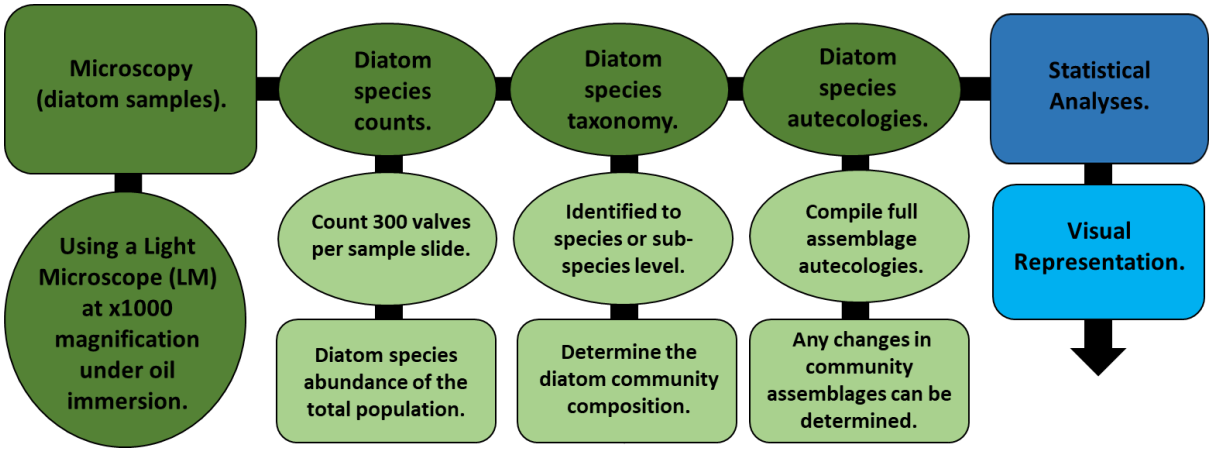

Figure 4.3. Workflow diagram of diatom microscopy (Adapted from Fitchett, 2015).

Diatom taxonomic identifications were mainly based on local and international literature (Sitoe *et al*., 2017; Zou *et al*., 2020). Consulted literature from Africa ranges from countries in the North such as Egypt (e.g. Zaky *et al*., 2020), and in the West with Benin (e.g. Olodo *et al*., 2013) to eastern Africa (e.g. Stager and Johnson, 2000) including Zambia (e.g. Taylor and Cocquyt, 2016), Kenya (e.g. Beck *et al.,* 2019; Westover *et al.*, 2019) and Malawi (e.g. Dulanya *et al*., 2019; Dulanya and Trauth, 2019). Southern African reference material includes Mozambique (e.g. Sitoe *et al*., 2017), Lesotho (e.g. Fitchett *et al.,* 2016a,b) and South Africa (e.g. Taylor *et al*., 2007a; Venter *et al*., 2013; Dalu *et al*., 2016). Other consulted international literature includes a range from Siberia (e.g. Adams *et al.*, 2019) to Australia (e.g. Beck *et al*., 2020), in North America (e.g. Sivarajah *et al.,* 2018), Europe (e.g. Buczkó *et al.,* 2019; Cohu *et al*., 2020), the middle east (e.g. Oğuz *et al*., 2020), Asia (e.g. Bannister *et al*., 2019; Yang *et al*., 2020) including studies in China (e.g. Zou *et al*., 2020) and India (e.g. Humane *et al*., 2020).

Diatoms have a highly specific morphology and where possible, the frustules can aid identification to species level (Battarbee *et al*., 2001; Fitchett *et al*., 2016b). Broadly, diatoms frustules are classified as either pennate or centric and form as indicator groups of diatoms and are associated with oligotrophic and eutrophic waters, respectively (Battarbee *et al*., 2001). For species-level identification considerations are made for the size, shapes, patterning and frequency of the striae and presence of

a raphe (Battarbee *et al*., 2001) along with the valve outline, apex shape and difference in the raphe (Taylor *et al*., 2007a). Diatom assemblage autecologies are then compiled for further analyses. Diatom species have specific optima and tolerances for environmental conditions and are used to determine the nature and extent of pollutant loading over time (Curtis *et al.,* 2010*;* Riato *et al.,* 2017). Once identified to species level, such as the differences between *Aulacoseira sp.* (Figure 4.4) the habitats and autecologies are tabulated and the species pollution tolerances determined. This involves making a distinction between species intolerant of polluted conditions and those not affected; if no distinction can be made, the species is labelled as unknown with regards to pollution tolerances. Thereafter, through statistical analysis, changes from sensitive communities to pollutant tolerant species can then be determined for both the study sites.

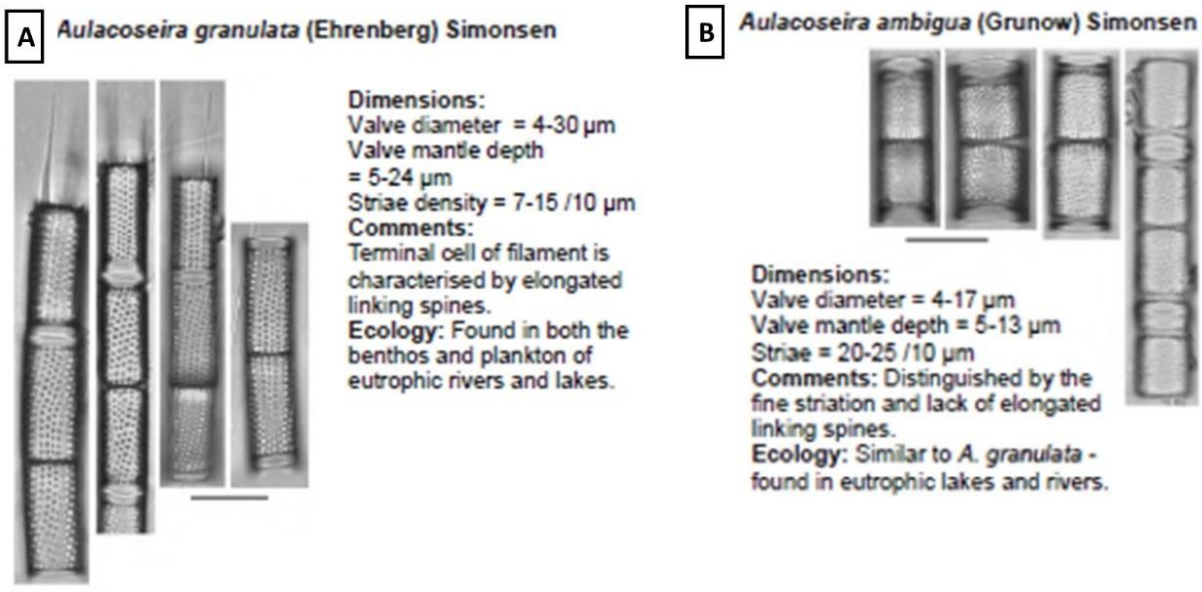

Figure 4.4. Differences between species such as *Aulacoseira granulata* and *Aulacoseira ambigua.*

4.3. Statistical Analysis

4.3.1. Ordination and Clustering

Determining periods in which notable diatom species assemblage changes might have occurred was the main aim for statistical analysis in this study (Fitchett, 2015). The workflow of all analyses and visual representation are seen in Figure 4.5. All statistical analysis was undertaken using the code-based statistical platform R except for the stratigraphic plots which were produced using C2 software (Fitchett *et al*., 2016a,b). The raw counts are expressed as percent relative abundance of the total number of valves counted per sample slide for the sites (Pajunen *et al*., 2020; Zou *et al*., 2020). Species occurring with <2% frequency throughout the cores are removed (Dong *et al*., 2008; Tang *et al*., 2017), allowing major trends to be examined (Adams *et al*., 2019). Species percent occurrence and maximum individual percent occurrence are tabulated along with the depths of the core profile in which they occur. Through the different relative abundances of the identified species, the diatom diversity can be examined and analysed (Olodo *et al*., 2020). Clustering and ordination techniques (Figure 4.5) detect major patterns of variations within the diatom assemblage zones and provide tools for assessing the degree of changes (Adams *et al*., 2019).

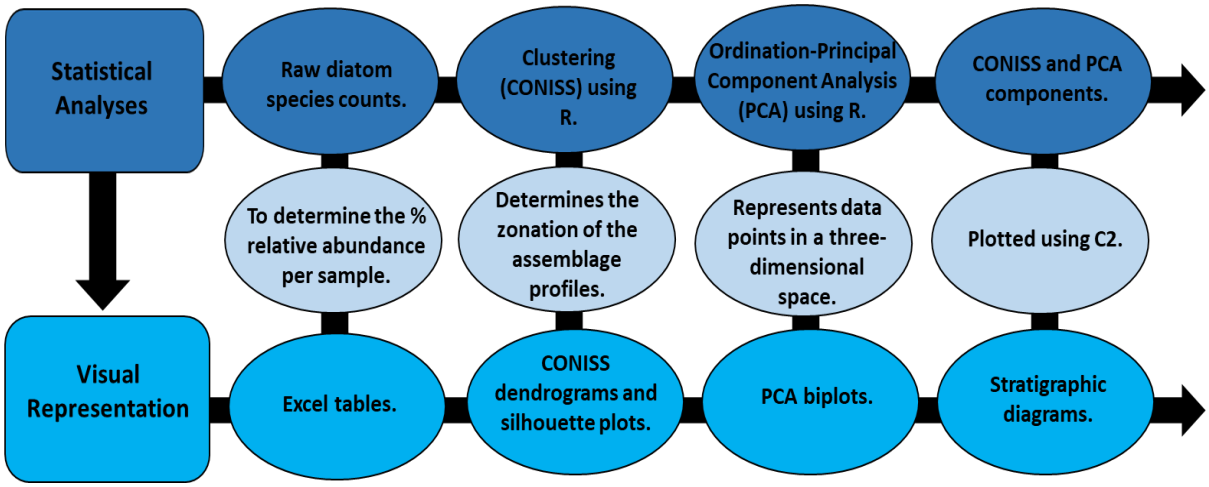

Figure 4.5. Workflow diagram of diatom statistical analyses (Adapted from Fitchett, 2015).

Constrained Incremental Sum of Squares (CONISS) and Principal Component Analysis (PCA) are clustering, and ordination techniques used to determine various groups of diatom assemblages and any gradients of change (Fitchett *et al*., 2016a; Zou *et al*., 2020). Stratigraphic zonation or Diatom Assembly Zones (DAZ) are defined using CONISS calculations (Sitoe *et al*., 2017; Buczko *et al*., 2019) Thus, major patterns of variation in the data are investigated using the indirect ordination technique (PCA) on the percent composition of diatoms (Fitchett *et al*., 2016a; Adams *et al*., 2019). The derived CONISS clusters are used to classify samples using PCA scaling and ordination scores (Mackay *et al*., 2012). Clustering is used to classify the samples and determine dominant diatom species within these major groups and throughout the core profile (Yang *et al*., 2020). By plotting the relative abundance of diatom species in each sample, periods of change and clusters can be visually explored (Figure 4.4).

4.3.2. Visual Representations

Through zonation performed in CONISS, the groups are visually displayed as a dendrogram that are colour coded to separate the clusters (Fitchett, 2015). A silhouette plot shows the optimal number of groups that can be determined; with optimal number of clusters having values closest to one while negative values suggest incorrect sample groupings (Fitchett, 2015). A PCA is conducted to identify the major variables that may be influencing the diatom assemblages (Yang *et al*., 2020). The sample scores from the PCA are plotted within a two-dimensional space, with scaling ordination scores relative to the first and second principal components (Conradie *et al*., 2016; Fitchett *et al*., 2016b). These produced biplots and constrained data points indicate diatom species composition changes over time (Conradie *et al*., 2016). This multi-dimensional space containing the produced set of axes allows data variability to be explored within one dimension (Ferreira *et al*., 2012; Fitchett *et al*., 2016b). The (dis)similarities between the samples, inter-specific relationship within communities, relationship with the sites and any contaminants can be explored (Ferreira *et al*., 2012; Fitchett *et al*., 2016b) allowing shifts in pollution (in)tolerant assemblages to be determined (Fitchett, 2015).

Stratigraphic zone boundaries were defined by using CONISS software in R (Dulanya and Trauth, 2019) where the stratigraphic diagrams were drawn using C2 software (Zou *et al*., 2020). This plots the counts of each species of diatom against depth throughout the core (Fitchett, 2015) and is achieved through the creation of a .csv file of the tabulated data, derived from Excel software which includes the PCA scores. The sample scores from the first and second principal components from the PCA are plotted to indicate periods of change in species composition (Fitchett, 2015). The species are arranged according to their species PC1 scores in order to demonstrate a clear gradient of change (Fitchett, 2015). The stratigraphic diagrams in the *Discussion* section (Chapter 6) are plotted against age and grouped according to habitats that are colour-coded to aid in similarities between species. The habitats, with a visual representation as silhouette plots of total abundances is presented, along with the corresponding PC1 and PC2 curves; with species grouped to their ecological traits and ordered from most to least pollution tolerant within these habitats. This facilitates comparisons with existing published palaeoenvironmental reconstructions for these regions, further enhancing environmental inferences (Fitchett, 2015).

4.4. Conclusion

Using standard methods in laboratory preparations and taxonomic identification of the diatom samples and analysis facilitates the reproducibility of results and improves comparisons between sites (Fitchett, 2015). Difficulties faced throughout the methodological processes are of value to future studies in South Africa and Lesotho. Loss-on-ignition (LOI) sediment analysis was not carried out and as such the percent organic and carbonate content in the samples could not be determined (Fitchett *et al*., 2016a; Dulanya and Trauth, 2019). Additionally, the microsphere method was not accomplished, including the addition of a known quantity of the microspheres to the samples prior to slide mounting (Westover *et al*., 2019). Identified microsphere quantities allow an estimation of diatom valve concentrations (Adams *et al*., 2019; Beck *et al*., 2019).

CHAPTER 5: RESULTS

5.1. Lake Chrissie (CM1)

5.1.1. Microscopy

The Lake Chrissie core profile consists of 52 depth samples spanning the depth of 25.75cm (~1780s AD) to 0.25cm in 2017 AD, from which a total of 56 diatom species were identified (Table 5.1). The Simpson's index of diversity (D) for Lake Chrissie is 0.5. There were 36 species identified with a maximum occurrence of >2% at some point throughout the core samples; of these *Navicula trivialis* with a 0.2% total occurrence is the least abundant species, with a 2.8% maximum occurrence at the depth of 13.25cm during the mid ~1990s AD (Table 5.1). *Eupodiscus radiatus* (65.4%) was the most dominant species with the highest maximum occurrence of 100% at the depths of 25.75cm (~1780s AD), 25.25cm (~1790s AD) and 22.25cm (~1880s AD), respectively (Table 5.1). *Aulacoseira sp*. was the second dominant species (15.4%) and the second highest maximum occurrence (64.7%) at the depth of 6.25cm in the early ~2010s AD (Table 5.1). *Cyclotella meneghiniana* (4.3%) is the third most dominant species, with the fourth highest maximum occurrence (50%) at the depth of 24.75cm (~1800s AD); where *Fragilaria famelica* with a 2.3% total abundance has the third highest maximum occurrence (60%) at the depth of 16.75cm during the early ~1960s AD (Table 5.1).

Table 5.1. The 56 identified diatoms in Lake Chrissie ordered by maximum percent occurrence within a sample.

Diatom species	Total individual % occurrence	Maximum individual % occurrence	Sample depth (cm) of the maximum individual % occurrence
Eupodiscus radiatus Bailey	65.4	100	22.25, 25.25, 25.75
Aulacoseira sp.	15.4	64.7	6.25
Fragilaria famelica Kützing	2.3	60	16.75
Cyclotella meneghiniana Kützing	4.3	50	24.75
Navicula goeppertiana Bleish	0.1	50	23.75

Nitzschia sp.	1.4	50	24.75
Amphora ovalis Kützing	1.7	28.6	16.25
Surirella ovalis Brébisson	0.5	25	18.75
Hantzschia amphioxys Ehrenberg	0.5	25	18.25
Eunotia eruca Ehrenberg	<0.1	18.2	24.25
Rhopalodia gibba Ehrenberg	0.1	15.0	15.75
Nitzschia amphibia Grunow	0.9	13.5	14.25
Fragilaria construens Ehrenberg	0.9	12.9	13.75
Pinnularia borealis Ehrenberg	0.4	12.5	15.25, 19.25
Cymbella cistula Ehrenberg	0.1	11.1	17.75
Eunotia bilunaris Ehrenberg	<0.1	11.1	22.75
Stauroneis phoenicentron Ehrenberg	0.2	10.4	14.75
Fragilaria fasciculata Lange-Bertalot	1.3	10	21.25
Navicula antonii Lange-Bertalot	0.1	9.4	15.25
Achnanthes exigua Grunow	<0.1	9.1	24.25
Aulacoseira granulata Ehrenberg	<0.1	9.1	24.25
Gomphonema minutum Agardh	0.1	7.1	21.75
Pinnularia divergens Smith	0.5	7.1	21.75
Fragilaria ulna Lange-Bertalot	0.3	6.4	13.75
Diploneis sp.	0.1	6.3	15.25
Fragilaria pinnata Ehrenberg	1.4	5.8	14.25
Gomphonema parvulum Kützing	0.1	5.6	17.25
Achnanthes minutissima Kützing	0.1	5.0	15.75
Eunotia minor Kützing	0.2	5.0	15.75
Pinnularia viridis Ehrenberg	<0.1	4.8	16.25
Anomoeneis sphaerophora Ehrenberg	0.2	4.7	15.25
Nitzschia acidoclinata Lange-Bertalot	0.4	4.4	13.25
Gomphonema sp.	<0.1	4.2	19.25
Navicula sp.	<0.1	3.1	15.25
Navicula veneta Kützing	0.1	3.1	15.25
Navicula trivialis Lange-Bertalot	0.2	2.8	13.25
Fragilaria capucina Lange-Bertalot	0.1	1.7	14.75
Stauroneis anceps Ehrenberg	0.1	1.7	14.75
Cyclostephanos dubius Fricke	0.1	1.6	2.75
Stauroneis sp.	0.1	1.6	14.25
Stephanodiscus agassizensis Håkansson & Kling	<0.1	1.3	3.75
Cyclotella psuedostelligera Hustedt	<0.1	1.2	0.25
Fragilaria sp.	<0.1	1.0	8.75
Gomphonema clavatum Ehrenberg	0.1	1.0	14.25
Navicula erifuga Müller	0.1	1.0	9.25
Cymbella silesiacum Bleisch	<0.1	0.9	14.75
Gomphonema truncatum Ehrenberg	<0.1	0.7	3.25

Caloneis sp.	<0.1	0.3	12.25
Cymbella aspera Ehrenberg	<0.1	0.3	1.25
Cymbella minuta Hilse	<0.1	0.3	13.25
Diatoma vulgaris Bory	<0.1	0.3	13.25
Frustulia vulgaris Thwaites	<0.1	0.3	13.25
Nitzschia frustulum Kützing	<0.1	0.3	6.25, 7.25
Nitzschia palea Kützing	<0.1	0.3	5.75
Rhopalodia operculate Agardh	<0.1	0.3	11.75

A total of 300 valves were only counted for 28 of the 52 depth samples, as 24 of these samples had low diatom abundances and counting a total of 300 valves was not possible. For three of these 24 samples, at the depths of 25.75cm (~1780s AD), at 25.25cm (~1790s AD) and at 22.25cm (~1880s AD), the counted valves were 100% identified as *Eupodiscus radiatus* (Table 5.1). This species was found in fragments and thus there may have been other species present that were perhaps not well preserved. The remaining 21 samples and associated counted valves coincided with 36 identified species that had a maximum occurrence of >2% at some point throughout the core samples.

Species with high maximum percent occurrences but with relatively low total abundances includes both *Nitzschia sp.* and *Navicula goeppertiana* with 50% at the respective depths of 24.75cm (~1800s AD) and 23.75cm (~1830s AD) and with 1.4% and 0.1%, respectively (Table 5.1). Additionally, *Amphora ovalis* has a maximum occurrence of 28.6% at the depth of 16.25cm (late ~1960s AD) and a 1.7% total abundance (Table 5.1). Both *Surirella ovalis* and *Hantzschia amphioxys* have a maximum occurrence of 25% at the respective depths of 18.75cm (late ~1930s AD) and 18.25cm (~1940s AD) and with a 0.5% total abundance, respectively (Table 5.1). Four species with a relatively low total abundances of <0.1% but with high maximum occurrences include *Eunotia bilunaris* with 11.1% at the depth of 22.75cm (~1860s AD), along with *Eunotia eruca* with 18.2% and both *Achnanthese exigua* and *Aulacoseira granulata* with 9.1% and all coinciding at the depth of 24.25cm (~1820s AD), respectively (Table 5.1). The 20 species with <2% maximum individual percent frequencies from *Fragilaria capucina* through to *Rhapolodia operculate* (Table 5.1) are removed for all subsequent statistical analyses.

5.1.2. Statistical Analyses

Two statistically significant clusters are identified for the Lake Chrissie core profile using CONISS, each coincidentally containing 26 of the 52 depth samples (Figure 5.1). Group 2 (zone CM1Z2) of 26 samples displayed in red, extends from the bottom of the core profile at the depth of 25.75cm during the ~1820s AD, to 13.25cm during the mid ~1990s AD and represents ~210-years (Figure 5.1). Group 1 (zone CM1Z1) samples presented in black, span the depths from 12.75cm during the late ~1990s AD to the core surface depth of 0.25cm which coincides with 2017 AD and represents the comparatively shorter period of ~20-years (Figure 5.1).

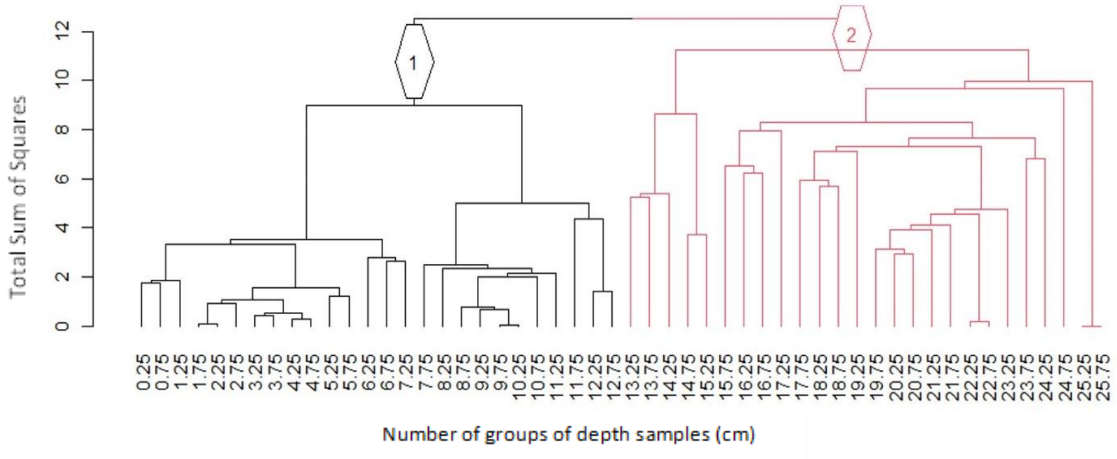

Figure 5.1. CONISS analysis separating the Lake Chrissie core profile into two clusters.

The PCA biplot results reveal two clusters, which align with the CONISS dendrogram (Figure 5.1; 5.2). Both zone CM1Z2 samples in red and zone CM1Z1 samples in black are distributed across all quadrants (Figure 5.2). The majority of zone CM1Z2 samples are in the first quadrant and share a strong affinity with *Eupodiscus radiatus* the main driver species; where the majority of zone CM1Z1 samples are found in the second quadrant and share an affinity with *Aulacoseira sp.,* the main driver and only species within this quadrant (Figure 5.2). Zone CM1Z2 samples in the third quadrant strongly associate with *Nitzschia sp., Cyclotella meneghiana* and *Fragilaria famelica* in the fourth quadrant; zone CM1Z1 samples do not seem to correspond with any species vector in these quadrants (Figure 5.2).

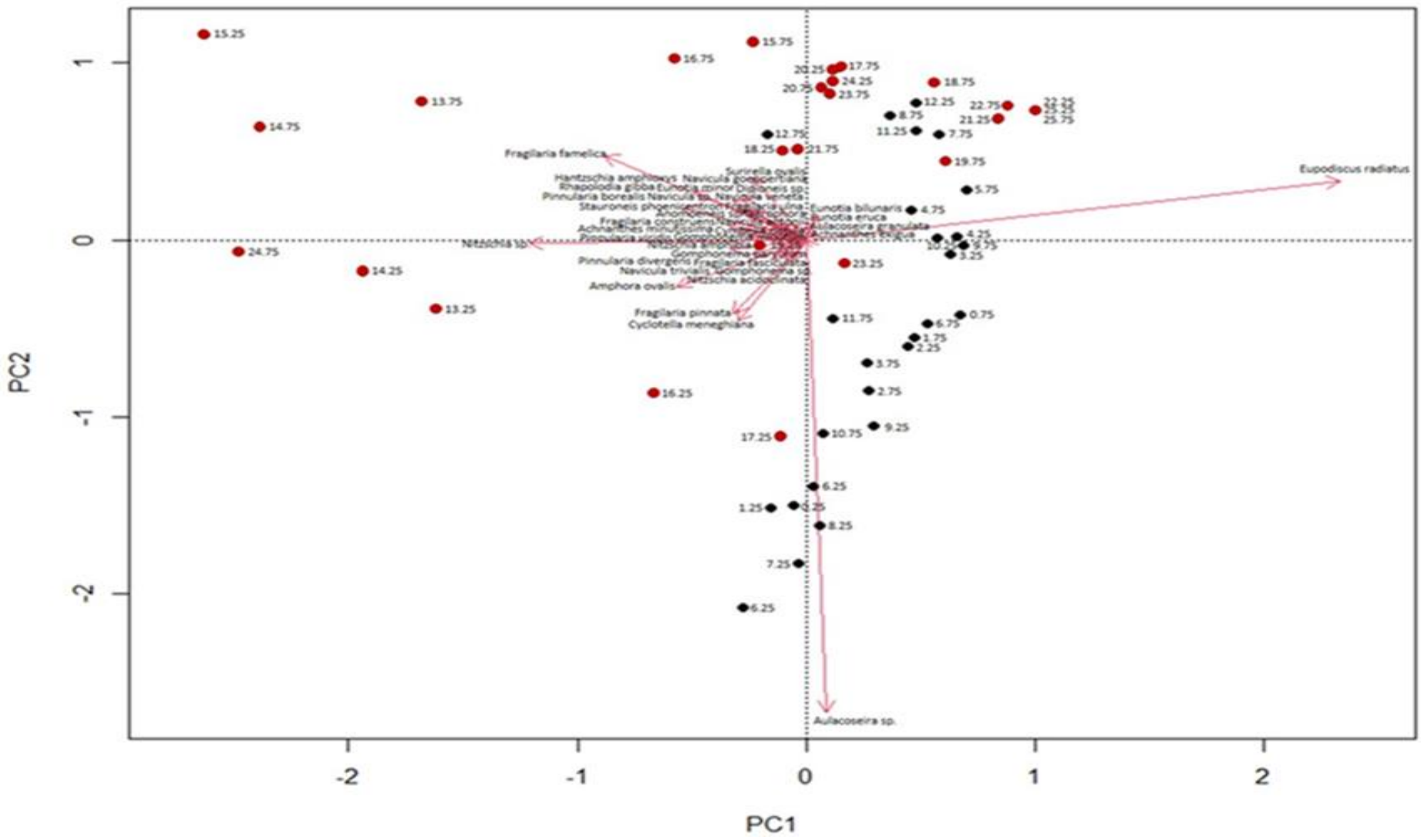

Figure 5.2. PCA biplot for the 52 depth samples separated into group 1 (black) and group 2 (red), along with the identified diatom species for Lake Chrissie.

PC1 accounts for 25.2% of the variance in identified diatom species compositions across the 52 samples from the Lake Chrissie core (Appendix A1.1). Species with the highest PC1 scores include *Eupodiscus radiatus* with a calculated score of 2.33, *Aulacoseira sp.* with 0.09, *Eunotia bilunaris* with 0.05, *Eunotia eruca* with 0.01 and *Aulacoseira granulata* 0.01 (Appendix A1.2). Species with the lowest PC1 scores included *Nitzschia sp*. with -1.21, *Fragilaria famelica* with -0.88, *Amphora ovalis* with -0.57, *Pinnularia borealis* with -0.54 and *Hantzschia amphioxys* with a score of -0.49 (Appendix A1.2).

PC2 accounts for 22% of the variance in identified diatom species compositions across the 52 samples for the Lake Chrissie core (Appendix A1.1). Species with the highest PC2 scores include *Fragilaria famelica* with 0.48*, Surirella ovalis* with 0.35*, Eupodiscus radiatus* with 0.33*, Hantzschia amphioxys* with 0.28 and *Navicula goeppertiana* with 0.26 (Appendix A1.2). Species with the lowest PC2 scores include *Aulacoseira sp.* with -2.67, C*yclotella meneghiania* with -0.46, *Fragilaria pinnata* with -0.41, *Amphora ovalis* with -0.26 and *Gomphonema parvulum* with -0.11 (Appendix A1.2). PC1 and PC2 explain a cumulative total of 47% of the variance in the Lake Chrissie core profile (Appendix A1.1).

The samples, species and PC scores are stratigraphically presented (Figure 5.3). The Lake Chrissie core sample depths are presented on the y-axis, beginning with the first sample depth of 25.75cm during the ~1780s AD through to the core surface depth of 0.25cm in 2017 AD (Figure 5.3). This is divided into two zones, with zone CM1Z2 spanning the depth of 25.75cm during the ~1780s AD to the depth of 13.25 AD during the mid ~1990s AD and zone CM1Z1 spanning thereafter the depths from 12.75cm during the late ~1990s AD, to the core surface in 2017 at the depth of 0.25cm (Figure 5.3). The species total abundances per sample depth are presented as a percentage on the x-axis as bar graphs and the identified diatom species are additionally arranged in descending species PC1 scores, which range from *Eupodiscus radiatus* with the highest PC1 score of 2.33, to *Nitzschia sp.* with the lowest PC1 score of -1.21 (Figure 5.3). Lastly, the PC1 and PC2 depth scores are presented as line graphs (Figure 5.3).

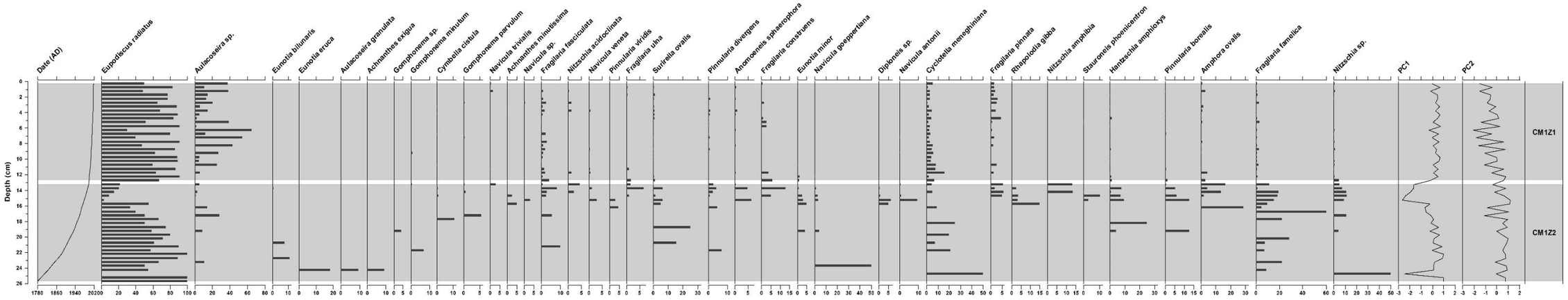

Figure 5.3. Stratigraphic diagram of the diatom record for the Lake Chrissie profile, including core depth (cm) and date (AD), with species ordered from highest to lowest PC1 scores.

Zone CM1Z2, 25.75cm (~1780s AD) to 13.25cm (mid *~1990s AD)*

Eupodiscus radiatus is the most dominant species within this zone, with an individual occurrence ranging from 0% at the depth of 24.75cm (~1800s AD), to 100% at the depths of 25.75cm (~1780s AD), 25.25cm (~1790s AD) and 22.25cm (~1880s AD), respectively (Figure 5.3). All 36 identified diatom species are recorded within this zone with nine species exclusively found and include: *Eunotia bilunaris* with 11.1%, 7.7% and 0.6% found at the respective depths of 22.75cm (~1860s AD), 20.75cm (~1900s AD) and at 13.75cm (early ~1990s AD); *Pinnularia viridis* with 4.8% at the depth of 16.25cm (late ~1960s AD) and with 3.1% at the depth of 15.25cm (~1970s AD); *Diploneis sp.* with 5%, 6.3%, 0.9% and 0.6% total abundances and *Rhapolodia gibba* with 15%, 3.1%, 3.5% and 2.3%, that respectively coincide at four depths including 15.75cm (early ~1970s AD), 15.25cm (late ~1970s AD), 14.75cm (early ~1980s AD) and at 13.75cm (early ~1990s AD); along with *Nitzschia amphibia* with 13.5% and 13.1% at the depth of 14.25cm (late ~1980s AD) and at 13.25cm (mid ~1990s AD), respectively (Figure 5.3). There were four species identified in only a single sample within the core, three of these species coincide at the depth of 24.25cm (~1820s AD) and include *Eunotia eruca* with 18.2%*,* both *Aulacoseira granulata* and *Achnanthes exigua* with 9.1% where *Gomphonem*a *sp.* was found with 4.2% at the depth of 19.25cm (~1930s AD), respectively (Figure 5.3).

PC1 scores within this zone range from -3 to +1 and overall decrease from 1.00 to -1.62 from the depths of 25.75cm (~1780s AD) to 13.25cm (mid ~1990s AD), respectively (Figure 5.3). This PC1 curve strongly coincides with the relative abundance of *Eupodiscus radiatus* which decreases from 100% to 21.6%, between these respective depths (Figure 5.3). The PC1 curve in this zone is characterised by two major troughs extending to a calculated score of -3 and include minimum scores of -2.48 and -2.63 located at the depths of 24.75cm (~1800s AD) and at 15.25.cm (late ~1970s AD), respectively (Figure 5.3). The first of these minimum PC1 scores coincides with an abrupt absence of *Eupodiscus radiatus*, from a 100% occurrence in the preceding sample (Figure 5.3). This decrease at the depth of 24.75cm (~1800s AD) additionally coincides with a 50% maximum occurrence of both *Nitzschia sp.* and

Cyclotella meneghiana (Table 5.1; Figure 5.3). Thereafter, an increase in PC1 scores to 0.11 at the depth 24.25cm (~1820s AD) demarcates the beginning of the relatively constant, but fluctuating central area, that extends to the depth of 15.75cm (early ~1970s AD) and is situated between these two major troughs (Figure 5.3). An increasing trend in PC1 scores from 0.11 to 1.00 between the depths of 24.25-22.25cm (~1820-1880s AD) coincides with an increase in *Eupodiscus radiatus* abundances from 54.5% to 100%, respectively (Figure 5.3). During this period there is also the first identification in the record of *Eunotia eruca* with 18.2%, along with *Aulacoseira granulata* and *Achnanthes exigua* with 9.1%, all coinciding at the depth of 24.25cm (~1820s AD); *Navicula goeppertiana* to 50% at the depth of 23.75cm (~1830s AD); *Fragilaria famelica* with 22.2% and *Aulacoseira sp.* with 11.1% at the depth of 23.25cm (~1850s AD), respectively; and *Eunotia bilunaris* with 11.1% found at the depth of 22.75cm and corresponding to during the ~1860s AD (Figure 5.3).

The PC1 curve thereafter decreases from -0.04 at the depth of 21.75cm (early ~1890s AD) to -0.67 at the depth of 16.25cm (late ~1960s AD) and coincides with an overall decrease in *Eupodiscus radiatus* abundances from 57.1% to 33.3%, respectively (Figure 5.3). This period is interrupted with four major peaks in PC1 scores: to 0.84 from -0.04; to 0.61 from 0.15; to 0.56 from -0.21 and to 0.12 from -0.10 (Figure 5.3). The four major PC1 peaks in scores are found at the depths of: 21.25cm (late ~1890s AD) from 21.75cm (early ~1890s AD); of 19.75cm (~1920s AD) from 20.25cm (~1910s AD); of 18.75cm (late ~1930s AD) from 19.25cm (early ~1930s AD and of 17.75cm (early ~1950s AD) from 18.25cm (~1940s AD), respectively (Figure 5.3). These observed peaks in PC1 scores and associated sample depths, additionally coincide with increased *Eupodiscus radiatus* abundances: to 90% from 57.1%; to 80% from 71.4%; to 75% from 58.3% and to 66.7% from 50%, respectively (Figure 5.3). The increased PC1 score of 0.84 at the depth of 21.25cm (late ~1890s AD) coincides with the first identification of the species *Fragilaria fasciculata* within the Lake Chrissie core with a 10% abundance (Figure 5.3). The increased PC1 scores of 0.61 at the depth of 19.75cm (~1920s AD) coincides with increased *Cyclotella meneghiana* abundances to 20% from a short-lived absence at the depth of 20.25cm coinciding with

the ~1920s AD (Figure 5.3). The increased PC1 score of 0.56 at the depth of 18.75cm (~1930s AD) coincides with increased *Surirella ovalis* abundances to 25% from a relatively sustained absence, since an abundance of 15.4% at the depth of 20.75cm during the ~1900s AD (Figure 5.3). Other species that increase in abundance between the depths of 21.75-15.75cm (early ~1890-1970s AD) includes *Fragilaria famelica* which increases to: 28.6% at the depth of 20.25cm (~1910s AD) from 7.7% at the depth of 20.75cm (~1900s AD); to 22.2% at the depth of 17.75cm (early ~1950s AD) from a relatively prolonged absence since the abundance of 28.6% at depth of 20.25cm (~1910s AD) and to 10% at the depth of 15.75cm (early ~1970s AD) from 4.8% at the depth of 16.25cm (late ~1960s AD), respectively (Figure 5.3). Species first identified in this zone between the depths 21.75-15.75cm (early ~1890-1970s AD) include: *Cymbella cistula* with a 11.1% abundance at the depth of 17.75cm (early ~1950s AD); both *Achnanthes minutissima* and *Diploneis sp*. with 5% and *Rhapolodia gibba* with 15%, all found at the depth of 15.75cm (early ~1970s AD), respectively (Figure 5.3).

There are five major decreases in PC1 scores between the depths 21.75-15.75cm (early ~1890-1970s AD) and include reduced scores to: -0.04 from 1.00; to 0.07 from 0.84; to -0.21 from 0.61; to -0.10 from 0.56 and to -0.67 from -0.58 (Figure 5.3). These reduced PC1 scores are found at the depths: 21.75cm (early ~1890s AD) from the depth of 22.25cm (~1880s AD); 20.75cm (~1900s AD) from 21.25cm (late ~1890s AD); 19.25cm (early ~1930s AD) from 19.75cm (~1920s AD); 18.25cm (~1940s AD) from 18.75cm (late ~1930s AD) and the depth of 16.25cm (late ~1960s AD) from 16.27cm (early ~1960s AD), respectively (Figure 5.3). These scores and associated depths additionally coincide with a decrease in *Eupodiscus radiatus* abundances to 57.1% from 100%; to 61.5% from 90%; to 58.3% from 80%; to 50% from 75% and to 33.3% from 40%, respectively (Figure 5.3). The lowest PC1 score calculated as -2.63 at the depth of 15.25cm (late ~1970s AD) and coincides with the lowest abundance of *Eupodiscus radiatus* with 3.1% since a brief absence at the depth of 24.75cm during the ~1800s AD (Figure 5.3). The top portion of this zone between the depths of 14.75cm (early ~1980s AD) and 13.25cm (mid ~1990s AD) is characterised by an overall increase in PC1 scores from -2.39 to -1.62,

respectively (Figure 5.3). This increasing trend coincides with an overall respective increase in six species abundances and include: *Eupodiscus radiatus* to 21.6% from 8.7%; *Amphora ovalis* to 16.3% from 1.7%; *Fragilaria pinnata* to 5.6% from 5.2%; along with *Aulacoseira sp.* to 5.3%, *Pinnularia divergens* to 2.5% and *Fragilaria ulna* to 1.6%, all from 0.9%, respectively (Figure 5.3). *Fragilaria construens* is first identified in the core profile with a 5.2% abundance at the depth of 14.75cm (early ~1980s AD); where there is also an increase in *Achnanthese minutissima* to 2.6% at this depth, from the depth of 15.25cm (late ~1970s AD) with a short-lived absence (Figure 5.3). Both *Nitzschia amphibia* and *Nitzschia acidoclinata* are first identified in the core profile with 13.5% and 2.3% abundances at the coinciding depth of 14.25cm (late ~1980s AD), respectively (Figure 5.3). Additionally at this depth, there is an increase in *Cyclotella meneghiana* to 5.1%, after a prolonged absence since an abundance at the depth of 16.25cm (late ~1960s AD) with 9.5% (Figure 5.3).

There is an increase in *Fragilaria fasciculata* abundances to: 2.6% at the depth of 14.75cm (early ~1980s AD) from a relatively prolonged absence since an abundance of 5.6% at the depth of 17.25cm (late ~1950s AD) and thereafter to 2.9% and to 8.2%, at the consecutive depth samples of 14.25cm (late ~1980s AD) and 13.75cm (early ~1990s AD), respectively (Figure 5.3). At the depth of 13.75cm (early ~1990s AD) *Fragilaria construens* abundances increase to 12.9% and both *Fragilaria ulna* and *Surirella ovalis* increase to 6.4%, all from short-lived absences at the depth of 14.25cm during the late ~1980s AD (Figure 5.3). Additionally there is both an increase in in *Anomoeneis sphaerophora* to 4.7% and *Navicula veneta* to 1.2% at the depth of 13.75cm (early ~1990s AD) and both from a relatively prolonged absences since the depth of 15.25cm (late ~1970s AD), with an abundance of 6.3% and 3.1%, respectively (Figure 5.3). *Cyclotella meneghiana* increases to 4.7% at the depth of 13.25cm (mid ~1990s AD) from the depth of 13.75cm (early ~1990s AD) with 0.6% (Figure 5.3). Additionally, *Nitzschia amphibia, Nitzschia acidoclinata* and *Navicula trivialis* respectively increase to 13.1%, 4.4% and 2.8% at the depth of 13.25cm (mid ~1990s AD) and all from a short-lived absence at the depth of 13.75cm during the early ~1990s AD (Figure 5.3). Species that decrease in abundance between the respective

depths of 14.75cm (early ~1980s AD) and 13.25cm (mid ~1990s AD) include: *Fragilaria famelica* from 18.3% to 1.6%; *Nitzschia sp*. from 11.3% to 5.3%; *Pinnularia borealis* from 6.1% to 0.6%; along with *Hantzschia amphioxys* from 7% and *Navicula goeppertiana* from 2.6% and both to 0.3%, respectively (Figure 5.3).

PC2 scores within this zone spanning the depths of 25.75cm (~1780s AD) to 13.25cm (mid ~1990s AD) and range in scores from -2 to +2 but overall decrease from 0.73 to -0.39, respectively (Figure 5.3). Extending from the bottom of the core at the depth of 25.75cm (~1780s AD) to slightly past midway at the depth of 17.75cm (early ~1950s AD) there is a relatively regular fluctuation in PC2 scores between -1 and +1; with scores ranging from a minimum of -0.13 at the depth of 23.25cm (~1850s AD) to a maximum at the depth of 20.25cm (~1910s AD) with 0.97 (Figure 5.3). PC2 scores between the depth of 25.75cm (~1780s AD) and 17.75cm (early ~1950s AD) overall increase from 0.73 to 0.96, respectively (Figure 5.3). This positive trend however coincides with an overall decrease in *Eupodiscus radiatus* abundances from 100% to 66.7%, respectively (Figure 5.3). There are five major peaks in PC2 scores during this period and include: an increase to 0.90 from -0.06; to 0.76 from -0.13; to 0.97 from 0.86; to 0.89 from -0.03 and to 0.96 from 0.50 (Figure 5.3). These five peaks in PC2 scores were calculated for the depths: of 24.25cm (~1820s AD) from 24.75cm (~1800s AD); of 22.75cm (~1860s AD) from 23.25cm (~1850s AD); of 20.25cm (~1910s AD) from 20.75cm (~1900s AD); of 18.75cm (late ~1930s AD) from 19.25cm (early ~1930s AD) and the depth of 17.75cm (early ~1950s AD) from 18.25cm (~1940s AD), respectively (Figure 5.3). *Eupodiscus radiatus* was found to coincide with these PC2 peaks in scores and respectively increased to 54.5% from a short-lived absence; to 88.9% from 66.7%; to 71.4% from 61.5%; to 75% from 58.3% and to 66.7% from 50% (Figure 5.3). There is additionally an increase in seven other species at these peaks in PC2 scores and include: the first identification of *Eunotia eruca* with 18.2% along with *Fragilaria famelica, Aulacoseira granulata* and *Achnanthese exigua* all with a 9.1% abundance and all respectively found at the depth of 24.25cm (~1820s AD); along with the first occurrence of *Eunotia bilunaris* with 11.1% found at the depth of

22.75cm (~1860s AD); there is an increase in *Fragilaria famelica* to 28.6% at the depth of 20.25cm (~1910s AD) from 7.7% at the depth of 20.75cm (~1900s AD); of *Surirella ovalis to* 25% at the depth of 18.75cm (late ~1930s AD) from an absence since an abundance of 15.4% at the depth of 20.75cm (~1900s AD); followed by the first identification of *Cymbella cistula* with 11.1% at the depth of 17.75cm (early ~1950s AD) along with an increase in *Fragilaria famelica* to 22.2% at this depth from an absence in the core since the depth of 20.25cm (~1910s AD) with an abundance of 28.6% (Figure 5.3).

Between the depths of 17.25cm (late ~1950s AD) and 13.25cm (mid ~1990s AD) there are abrupt fluctuations between PC2 scores of between +2 and -2 over this period and overall increase in scores from -1.11 to -0.39, respectively (Figure 5.3). The PC2 curve in this zone is characterised by three maximum scores of: 1.02 at the depth of 16.75cm (early ~1960s AD) from -1.11 at the depth of 17.25cm (late ~1950s AD); 1.12 at the depth of 15.75cm (early ~1970s AD) from -0.86 at the depth of 16.25cm (late ~1960s AD) and 1.16 located at the depth of 15.25cm during the late ~1970s AD (Figure 5.3). These peaks in PC2 scores coincide with a respective increase in *Fragilaria famelica* to 60% from a short-lived absence; to 10% from 4.8% and consecutively thereafter to 15.6% (Figure 5.3). Additional species that increase at these peaks include: *Eupodiscus radiatus* to 55% at the depth of 15.75cm (early ~1970s AD) from 33.3% at the depth of 16.25cm (late ~1960s AD); *Surirella ovalis* to 5% at the depth of 15.75cm (early ~1970s AD) from an absence since an abundance of 25% at the depth of 18.75cm (late ~1930s AD); *Pinnularia viridis* to 3.1% at the depth of 15.25cm (late ~1970s AD) after a short-lived absence at the depth of 15.75cm (early ~1970s AD); *Navicula goeppertiana* to 3.1% at the depth of 15.25cm (late ~1970s AD) from an absence in the core since an abundance of 4.2% at the depth of 19.25cm (early ~1930s AD); *Diploneis sp.* to 6.3% at the depth of 15.25cm (late ~1970s AD) from 5.5% at the depth of 15.75cm (early ~1970s AD); *Pinnularia borealis* to 12.5% at the depth of 15.25cm (late ~1970s AD) from an absence in the core since an abundance of 12.5% at the depth of 19.25cm (early ~1930s AD); *Hantzschia amphioxys* to 9.4% at the depth of 15.25cm (late ~1970s AD) from an absence in the core since an abundance of 25% at the depth of 18.25cm (~1940s AD); along

with *Nitzschia sp*. to 9.4% at the depth of 15.25cm (late ~1970s AD) from an absence in the core since the depth of 17.25cm (late ~1950s AD) with an abundance of 11.1% (Figure 5.3). The first identification in the Lake Chrissie core of five species was found to coincide at these peaks in PC2 scores and include: *Rhapolodia gibba* with 15%, along with both *Achnanthese minutissima* and *Diploneis sp.* with 5% abundances all located at the depth of 15.75cm (early ~1970s AD); along with *Navicula antonii* with 9.4%, *Anomoeneis sphaerophora* with 6.3% and *Navicula veneta* with 3.1% all located at the depth of 15.25cm (late ~1970s AD), respectively (Figure 5.3). There is an additional peak in PC2 scores calculated as 0.78 at the depth of 13.75cm from a score of -0.18 at the depth of 14.25cm and both coinciding with the early ~1990s AD (Figure 5.3). This peak was found to coincide with the respective increase in: *Eupodiscus radiatus* to 20.5% from 14.8%; *Fragilaria fasciculata* to 8.2% from 2.9%; *Hantzschia amphioxys* to 7.6% from 0.6%; *Pinnularia divergens* to 4.1% from 2.3%; *Pinnularia borealis* to 5.3% from 0.3*%; Fragilaria construens* to 12.9%, along with *Fragilaria ulna* and *Surirella ovalis* to 6.4% and *Navicula goeppertiana* to 1.2% all from a short-lived absences, respectively; along with *Anomoeneis sphaerophora* to 4.7% from an absence since the depth of 15.25cm (late ~1970s AD) with abundance of 6.3% (Figure 5.3).

Zone CM1Z1, 12.75cm (late ~1990s AD) to 0.25cm (2017)

Compared to zone CM1Z2 there is reduced species diversity within zone CM1Z1, where only 27 identified diatom species are recorded (Figure 5.3). *Eupodiscus radiatus* is the most dominant species with an individual occurrence within this zone ranging from a maximum of 91.4% at the depth of 7.75cm (late ~2000s AD) to a minimum at the depth of 6.25cm (early ~2010s AD) with 30% (Figure 5.3). The second most dominant species is *Aulacoseira sp.* ranging from short lived absences in five samples at the depths of 12.75cm (late ~1990s AD), 12.25cm (late ~1990s AD), 11.25cm (early ~2000s AD), 8.75cm (late ~2000s AD) and at 7.75cm (late ~2000s AD), to a maximum occurrence at the depth of 6.25cm (early ~2010s AD) with 64.7% (Figure 5.3). *Eupodiscus radiatus* and *Aulacoseira sp.* were found to have fluctuating abundances, except when both species simultaneously increase at three

depth samples and include 9.75cm (mid ~2000s AD), 4.25cm (early ~2010s AD) and 1.75cm coinciding with the mid ~2010s AD (Figure 5.3). PC1 and PC2 curve trends were found to predominantly coincide, except where PC1 scores increase to 0.68, at the depth of 9.75cm (mid ~2000s AD) from 0.57 at the depth of 10.25cm (mid ~2000s AD) and to 0.66 at the depth of 4.25cm (early ~2010s AD) from 0.46 at the depth of 4.75cm (mid ~2010s AD); where PC2 scores were found to respectively decrease to -0.03 from 0.01 and to 0.02 from 0.17 (Figure 5.3).

PC1 scores range between -1 and +1 and overall increase from -0.17 at the depth of 12.75cm (mid ~1990s AD) to -0.05 at the depth of 0.25cm (2017 AD) at the core surface (Figure 5.3). This trend overall coincides with *Aulacoseira sp.* increasing from a short-lived absence to 37.7%, respectively (Figure 5.3). The maximum PC1 score within this zone CM1Z1 of 0.70 is located at the depth of 5.75cm (early ~2010s AD) and is an increase from the minimum PC1 score at the depth of 6.25cm (early ~2010s AD) with -0.28 (Figure 5.3). This peak in PC1 score predominantly coincides with an abrupt increase in *Eupodiscus radiatus* abundances to 91.2% from 30%, respectively, which is the lowest recorded abundances of this species within this zone of the core (Figure 5.3). PC2 scores in zone CM1Z1 range between -3 and +1 and overall decrease from 0.59 at the depth of 12.75cm (mid ~1990s AD) to -1.50 at the core surface (Figure 5.3). This negative trend predominantly coincides with the overall decrease in *Eupodiscus radiatus* abundances from 67% to 49.8%, respectively (Figure 5.3). There are two maximum PC2 scores calculated as 0.77 at the depth of 12.25cm (late ~1990s AD) and at the depth of 8.75cm (late ~2000s AD) with 0.71 (Figure 5.3). These peaks in PC2 scores predominantly coincide with the respective increase in *Eupodiscus radiatus* abundances to 91.1% from 67% and to 86% from 62.7% (Figure 6.3). There is also an abrupt increase in *Fragilaria fasciculata* to 2% at the depth of 8.75cm (late ~2000s AD) from the depth of 9.25cm (mid ~2000s AD) with 1% (Figure 5.3). Both minimum PC1 and PC2 scores of -0.28 and -2.07, coincide at the depth of 6.25cm (early ~2010s AD) which additionally coincides with the lowest occurrence of *Eupodiscus radiatus* in zone CM1Z1 with 30% (Figure 5.3).

5.2. Letšeng-la Letsie (Lets2)

5.2.1. Microscopy

The Letšeng-la Letsie core profile consists of 57 samples spanning from the depth of 28.25cm (~1850s AD) to 0.25cm (2018 AD) from which a total of 75 diatom species were identified (Table 5.2). Simpson's index of diversity (D) is 0.7. There were 39 species identified with a maximum individual occurrence of >2% at some point throughout the core samples; of these *Pinnularia borealis* with a 0.3% total occurrence is the least abundant species, with a maximum occurrence at the depth of 21.25cm (late ~1950s AD) of 2% (Table 5.2). *Aulacoseira granulata* (53.1%) was the most dominant species with a maximum occurrence of 92.2% at the depth of 18.75cm (early ~1970s AD) and was found across all samples (Table 5.2). *Cymbella cistula* with a sum of 4% is the second most dominant species with the second highest maximum occurrence of 26.1% at the depth of 21.25cm (late ~1950s AD); where *Nitzschia sp.* with a sum of 5.8% is the third most dominant taxa with the third highest maximum occurrence of 21.1% at the depth of 13.25cm in the mid ~1990s AD (Table 5.2).

Table 5.2. The 75 Identified diatoms in Letšeng-la Letsie ordered by maximum percent occurrence within a sample.

Diatom species	Total individual % occurrence	Maximum individual % occurrence	Sample depth (cm) of the maximum individual % occurrence
Aulacoseira granulata Ehrenberg	53.1	92.2	18.75
Cymbella cistula Ehrenberg	7.4	26.1	21.25
Nitzschia sp.	5.8	21.1	13.25
Navicula veneta Kützing	1.2	13.7	22.25
Gyrosigma acuminatum Kützing	1.9	12.8	15.75
Fragilaria famelica Kützing	3.8	12.7	27.25
Cymatopleura solea Brébisson	2.4	11.5	1.75
Navicula trivialis Lange-Bertalot	1.4	8.8	15.25
Fragilaria construens Ehrenberg	2.2	7.3	20.75
Fragilaria capucina Lange-Bertalot	3.5	6.9	3.25
Fragilaria ulna Lange-Bertalot	1.2	6.9	1.75
Cymbella tumida Brébisson	1.4	6.1	1.25

Cyclotella meneghiniana Kützing	0.2	5.2	28.25
Caloneis schumanniana Grunow	1.4	5.1	15.75
Nitzschia palea Kützing	0.5	5.1	22.25
Diploneis subovalis Cleve	1.4	4.9	14.75
Navicula erifuga Müller	0.7	4.9	28.25
Cyclotella sp.	0.3	4.6	26.25
Gomphonema minutum Agardh	1.0	4.6	23.25
Aulacoseira ambigua Grunow	0.4	4.3	3.25
Fragilaria pinnata Ehrenberg	0.9	3.9	21.75
Gyrosigma sp.	0.1	3.9	10.25
Navicula antonii Lange-Bertalot	0.4	3.9	21.75
Gomphonema parvulum Kützing	0.8	3.8	15.25
Fragilaria biceps Kützing	0.1	3.6	6.75
Eunotia minor Kützing	0.2	3.5	27.75
Fragilaria fasciculata Lange-Bertalot	0.3	3.4	22.75
Cyclotella pseudostelligera Hustedt	0.3	3.3	28.25
Cocconeis placentula Ehrenberg	0.6	2.9	13.25
Hantzschia amphioxys Ehrenberg	0.5	2.8	2.75
Achnanthes minutissima Kützing	0.3	2.6	28.25
Melosira varians Agardh	0.3	2.6	21.75
Pinnularia viridis Ehrenberg	0.4	2.6	21.25
Gomphonema clavatum Ehrenberg	0.3	2.3	12.75
Pinnularia divergens Smith	0.5	2.3	11.75
Rhopalodia gibba Ehrenberg	0.2	2.3	11.25
Fragilaria sp.	0.1	2.2	22.25
Cyclostephanos dubius Fricke	0.1	2.1	26.25
Pinnularia borealis Ehrenberg	0.3	2.0	21.25
Amphora ovalis Kützing	0.3	1.9	5.25
Surirella angusta Kützing	0.1	1.9	22.75
Gomphonema truncatum Ehrenberg	0.3	1.7	11.75
Nitzschia frustulum Kützing	0.1	1.7	23.25
Frustulia vulgaris Thwaites	0.2	1.3	14.75
Navicula cryptotonella Lange-Bertalot	<0.1	1.3	0.25
Nitzschia filiformis Smith	0.1	1.3	22.25
Cymbella silesiaca	<0.1	1.2	13.25
Navicula capitatoradiata Germain	<0.1	1.2	0.75
Navicula pupula Kützing	0.1	1.2	13.25
Stauroneis anceps Ehrenberg	0.1	1.2	26.25
Craticula cuspidata Kützing	0.1	1.0	5.25
Diploneis elliptica Kützing	0.1	0.9	13.25
Gomphonema gracile	<0.1	0.9	0.25

Navicula sp.	<0.1	0.7	20.25
Nitzschia acidoclinata Lange-Bertalot	<0.1	0.7	20.25
Achnanthes linearis Lange-Bertalot	<0.1	0.6	13.25
Cocconeis engelbrechtii Cholnoky	<0.1	0.6	0.25
Cymbella minuta Hilse	<0.1	0.6	2.25
Diploneis oblongella Naegeli	<0.1	0.6	0.25, 2.25
Gomphonema bohemicum Reichelt & Fricke	<0.1	0.6	0.75
Gomphonema venusta Passy	<0.1	0.6	15.25
Hantzschia distinctepunctata Hustedt	<0.1	0.6	4.25
Muelleria sp.	<0.1	0.6	19.75
Navicula capitata Ehrenberg	<0.1	0.6	0.25, 0.75, 6.25, 12.25
Nitzschia sinuate Grunow	<0.1	0.6	22.25
Stauroneis kriegeri Patrick	<0.1	0.6	26.25
Craticula ambigua Ehrenberg	<0.1	0.3	13.25
Denticula kuetzingii Grunow	<0.1	0.3	2.25
Diploneis smithii Brébisson	<0.1	0.3	0.25, 4.25, 12.25
Diatoma vulgaris Bory	<0.1	0.3	16.25, 22.25
Eunotia bilunaris Ehrenberg	<0.1	0.3	1.75, 12.25
Pinnularia gentillis Cleve	<0.1	0.3	2.25
Stauroneis gracilior Reichart	<0.1	0.3	4.25
Stauroneis phoenicentron Nitzsch	<0.1	0.3	7.25
Stauroneis sp.	<0.1	0.3	5.25

A total of 300 valves were counted for the 57 Letšeng-la Letsie depth samples. *Aulacoseira granulata* were predominantly found in girdle with an observed elongated spine which allowed for species level identification and distinction from *Aulacoseira ambigua,* with no connecting spines (Taylor *et al*., 2007a). Species with high maximum percent occurrences with relatively low total abundances respectively includes: *Navicula veneta* with 13.7% at the depth of 28.25cm (~1850s AD) and with 1.2%; *Nitzschia palea* with 5.1% at the depth of 22.25cm (early ~1950s AD) and with 0.5%; *Navicula erifuga* with 4.9% at the depth of 22.25cm (early ~1950s AD) and with 0.7%; *Gyrosigma acuminatum* with 12.8% at the depth of 15.75cm (mid ~1980s AD) and with 1.9%; *Navicula trivialis* with 8.8% at the depth of 15.25cm (late ~1980s AD) and with 1.4% (Table 5.2). For all statistical analyses, the 36 species with <2% maximum frequencies from *Stauroneis sp.* to *Amphora ovalis* are removed (Table 5.2).

5.2.2. Statistical Analyses

Two statistically significant clusters are identified for the Lets2 profile using CONISS (Figure 5.4). Group 2 (zone Lets2Z2) of 35 samples displayed in red, extends from the depth of 28.25cm (~1850s AD) to 11.25cm (late ~1990s AD) and spans ~140-years (Figure 5.4). Group 1 (zone Lets2Z1) with 22 samples displayed in black, span the depths from 10.75cm (~2000s AD) to the core surface depth of 0.25cm (2018 AD) which represents the comparatively shorter period of ~20-years (Figure 5.4).

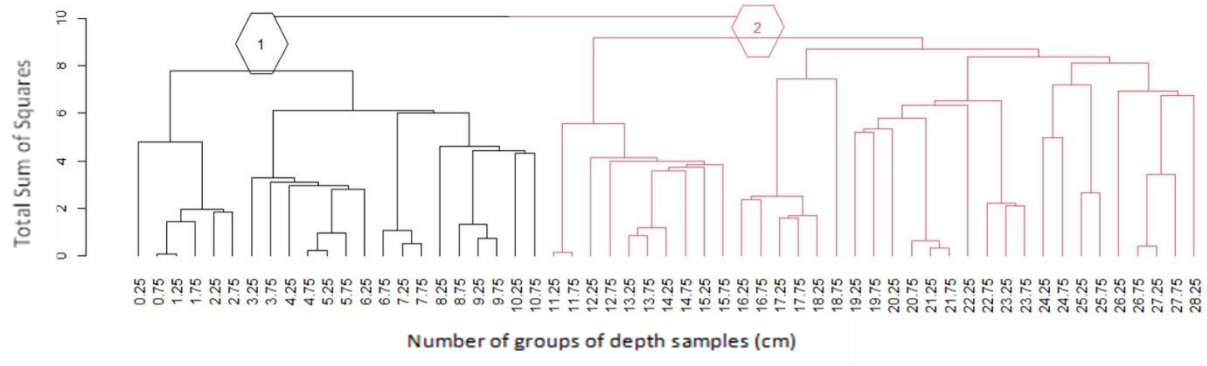

Figure 5.4. CONISS analysis separating the Letšeng-la Letsie core profile into two clusters.

The PCA biplot results demonstrate two clusters, which align with the CONISS dendrogram (Figure 5.4; 5.5). Zone Lets2Z2 samples displayed in red are found across all quadrants; where the remaining 22 samples in zone Lets2Z1 presented in black, are only found in the first and second quadrants (Figure 5.5). The majority of zone Lets2Z2 samples are found in the third quadrant and share an affinity with *Cymbella cistula*, *Fragilaria famelica* and *Cymatopleura solea* (Figure 5.5). A further 12 zone Lets2Z2 samples are found in the fourth quadrant and share an affinity with *Nitzschia sp., Navicula veneta, Navicula trivialis* and *Nitzschia palea* (Figure 5.5). The majority of zone Lets2Z1 samples are found in the second quadrant and share an affinity with *Cymbella tumida* and *Rhapolodia gibba,* the only species present within this quadrant (Figure 5.5). The remaining eight zone Lets2Z1 samples are located in the first quadrant and are strongly driven by *Aulacoseira granulata*, but also share an affinity with *Fragilaria pinnata, Gyrosigma sp.* and *Aulacoseira ambigua* (Figure 5.5).

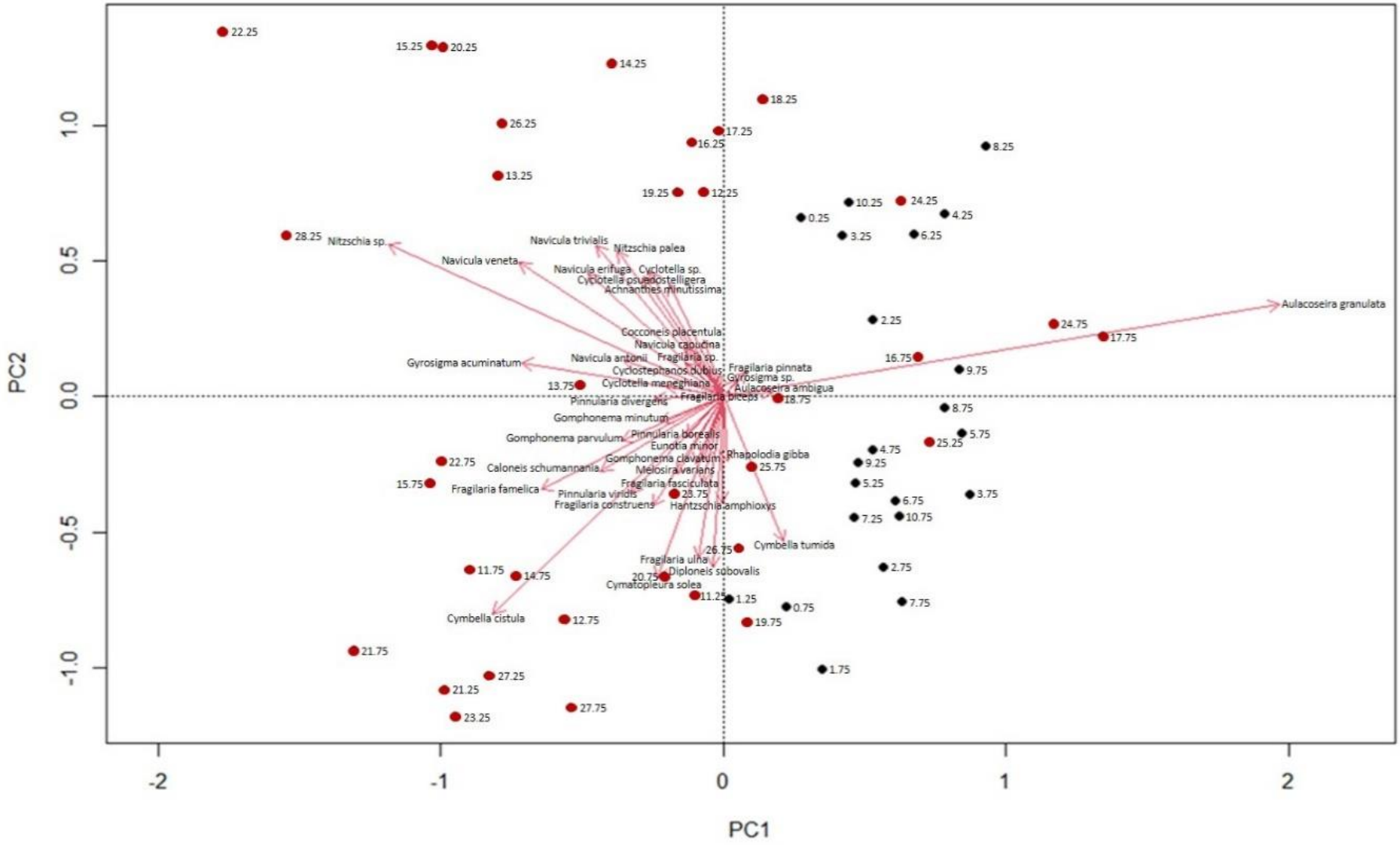

Figure 5.5. PCA biplot for the 57 depth samples separated into group 1 (black) and group 2 (red), along with the identified diatom species for Letšeng-la Letsie.

PC1 accounts for 30.2% of the variance in identified diatom species compositions across the 57 samples from the Letšeng-la Letsie core (Appendix A2.1). Species with the highest PC1 scores include *Aulacoseira granulata* with 1.97, *Cymbella tumida* with 0.21, *Aulacoseira ambigua* with 0.18, *Fragilaria pinnata* with 0.08 and *Gyrosigma sp.* with a score of 0.05 (Appendix A2.2). Species with the lowest PC1 scores include *Nitzschia sp.* with -1.19, *Cymbella cistula* with -0.81, *Navicula veneta* with -0.72, *Gyrosigma acuminatum* with -0.71 and *Fragilaria famelica* with a score of -0.64 (Appendix A2.2).

PC2 accounts for 17.8% of the variation in the identified diatom species composition across the 57 samples for the Letšeng-la Letsie core (Appendix A2.1). Species with the highest PC2 scores include *Nitzschia sp.* and *Navicula trivialis* with 0.56, *Nitzschia palea* with 0.54*, Navicula veneta* with 0.50 and *Cyclotella sp.* with 0.46 (Appendix A2.2). Species with the lowest PC2 scores include *Cymbella cistula* with -0.80, *Diploneis subovalis* with -0.63, *Cymbella tumida* with -0.53 along with *Fragilaria construens* and *Hantzschia amphioxys* both with a PC2 score of -0.40 (Appendix A2.2). PC1 and PC2 scores explain a cumulative total of 48% of the variance in the Letšeng-la Letsie core profile (Appendix A2.1).

The sample depths, species and both PC scores are stratigraphically presented (Figure 5.6). The Letšeng-la Letsie core sample depths are presented on the y-axis, beginning with the first sample depth of 28.25cm during the ~1850s AD through to the core surface depth of 0.25cm in 2018 (Figure 5.6). The core profile is divided into two zones, with zone Lets2Z2 spanning the depth of 28.25cm during the ~1850s AD to the depth of 11.25 AD during the late ~1990s AD and zone Lets2Z1 spanning thereafter the depths from 10.75cm during the early ~2000s AD, to the core surface in 2018 at the depth of 0.25cm (Figure 5.6). The species total abundances per sample depth are presented as a percentage on the x-axis and as observed as bar graphs; where the identified diatom species are additionally arranged in descending species PC1 scores, which range from *Aulacoseira granulata* with the highest PC1 score of 1.97, to *Nitzschia sp.* with -1.19.and lowest PC1 species score (Figure 5.6). Lastly, the PC1 and PC2 sample depth scores are presented as line graphs (Figure 5.6).

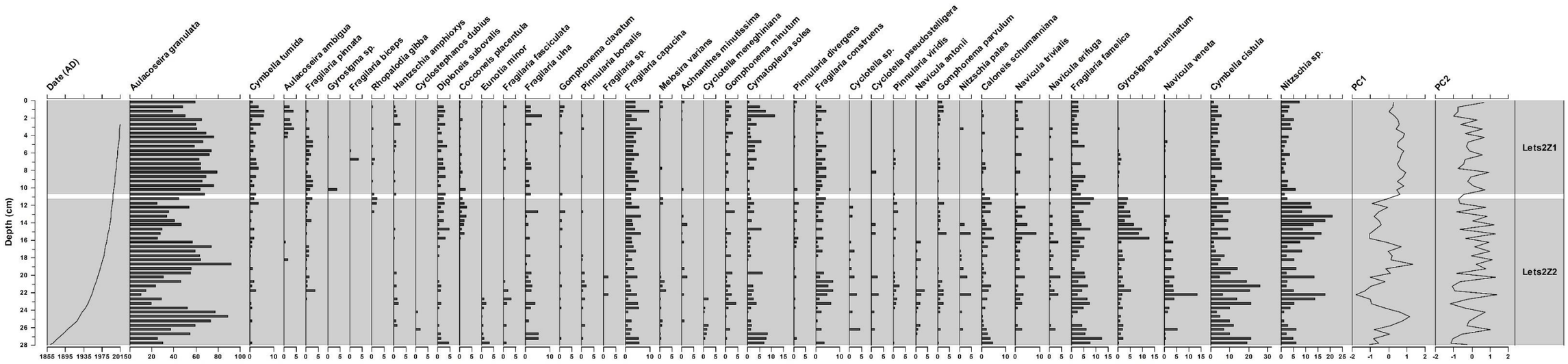

Figure 5.6. Stratigraphic diagram of the diatom record for the Letšeng-la Letsie profile, including core depth (cm) and date (AD), with species ordered from highest to lowest PC1 scores.

Zone Lets2Z2, 28.25cm (~1850s AD) to 11.25cm (~1990s AD)

The most dominant species within zone Lets2Z2 is *Aulacoseira granulata*, with an individual occurrence ranging from 10.5% at the depth of 22.25cm (early ~1950s AD) to a maximum at the depth of 18.75cm (early ~1970s AD) with 92.2% (Figure 5.6). *Cyclotella meneghiana* and *Fragilaria sp.* are exclusively found in this zone with respective maximum occurrences of 5.2% at the depth of 28.25cm (~1850s AD) and at the depth of 22.25cm (early ~1950s AD) with 2.2% (Table 5.2; Figure 5.6). *Gyrosigma sp.* is the only identified diatom species not recorded within this zone (Figure 5.6). PC1 scores within this zone range from -2 to +2, with an overall increase from -1.55 at the depth of 28.25cm (~1850s AD), to -0.10 at the depth of 11.25cm (late ~1990s AD) coinciding with an increase in *Aulacoseira granulata* relative abundances from 16.1% to 45.3%, respectively (Figure 5.6). It was found that PC1 scores in this zone predominantly follow the trends in *Aulacoseira granulata* relative abundances; except at the depths of 28.25cm (~1850s AD), at 22.75cm (late ~1940s AD), at 19.25cm (early ~1970s AD), along with at 17.75cm (late ~1970s AD); PC1 scores decrease at the first three of these depths and increases at the lattermost depth, where the opposite observed in *Aulacoseira granulata* abundances (Figure 5.6).

The PC1 curve in this zone is characterised with three minimum scores extending to -2 and three maximum scores reaching +2 (Figure 5.6). The minimum PC1 scores were found to predominantly coincide with decreased *Aulacoseira granulata, Fragilaria famelica, Cymbella cistula, Cymatopluera solea* and *Caloneis schumanniana* abundances; with maximum scores strongly coinciding with increased *Aulacoseira granulata* abundances (Figure 5.6). The first minimum PC1 score of -1.55 at the depth of 28.25cm (~1850s AD) coincides with a period of a relatively low *Aulacoseira granulata* abundance of 16.1%, which is the third lowest occurrence of this species in this zone (Figure 5.6). A maximum PC1 score of 1.17 at the depth of 24.75cm (late ~1920s AD) coincides with an increase in *Aulacoseira granulata* abundances to 89.6%, from 73.8% at the depth of 25.25cm (early~1920s AD)

which marks the second maximum occurrence of this species throughout the core profile (Figure 5.6). There is also an increase in *Fragilaria famelica* to 0.9% and *Gyrosigma acuminatum* to 1.3% at this depth of 24.75cm (late ~1920s AD) and from a respective short-lived absence and from 1% at the depth of 25.25cm (early ~1920s AD), respectively (Figure 5.6).

After the maximum PC1 score of 1.17 at the depth of 24.75cm (late ~1920s AD) there is a steep decrease in PC1 scores at the depth of 22.25cm (early ~1950s AD) to a minimum score of -1.77 (Figure 5.6). This coincides with a decrease in *Aulacoseira granulata* abundances from 89.6% to 10.5%, respectively (Figure 5.6). At this minimum PC1 score at the depth of 22.25cm (early ~1950s AD) there is additionally a decrease in species including *Fragilaria famelica* to 2.5%, *Cymbella cistula* to 6.3% and *Pinnularia viridis* to 0.6%; from 6.5%, 13.9% and 1.5% at the depth of 22.75cm (late ~1940s AD), respectively (Figure 5.6). Species that increase however between the depth of 24.75cm (late ~1920s AD) and the depth of 22.25cm (early ~1950s AD) include: *Nitzschia sp.* to 18.1%, *Navicula veneta* to 13.7%, *Nitzschia palea* to 5.1%, *Navicula erifuga* to 3.8%, *Navicula antonii* to 2.5% and *Gomphonema parvulum* to 2.5% all from relatively short-lived absences, respectively; along with *Fragilaria capucina* from 0.3% to 4.8%, *Navicula trivialis* from 0.3% to 3.5% and *Gomphonema minutum* from 0.6% to 2.5%, respectively (Figure 5.6). The highest maximum occurrence of both *Nitzschia palea* and *Navicula veneta* across the core profile additionally coincide at the depth of 22.25cm coinciding with the early ~1950s AD (Table 5.2; Figure 5.6).

PC1 scores thereafter increase from the minimum PC1 score at the depth of 22.25cm (early ~1950s AD) to the maximum PC1 score zone Lets2Z2 at the depth of 18.75cm (early ~1970s AD) with 1.34 (Figure 5.6). This overall increase in PC1 scores coincides with an increase in *Aulacoseira granulata* abundances from 10.5% to 92.2%, respectively (Figure 5.6). Conversely, *Nitzschia sp.* were found to decrease between these depths from 18.1% to 0%, respectively (Figure 5.6). The overall increase in

PC1 scores between these depths is interrupted with two minimum PC1 scores of -0.99 at the depth of 20.25cm (mid ~1960s AD) and at the depth of 19.25cm (early ~1970s AD) with a score of -0.16 (Figure 5.6). These minimum PC1 scores coincide with the respective decrease in species including: *Fragilaria construens* to 2%, from 7.3% at the depth of 20.75cm ()early ~1960s AD) and to 0.3%, from 3.5% at the depth of 19.75cm (late ~1960s AD); *Aulacoseira granulata* and *Cymbella cistula* decrease to 31.1% and 4.9% the depth of 20.25cm (mid ~1960s AD), respectively and from 46.8% and 18.9%, respectively at the depth of 20.75cm (early ~1960s AD); along with *Fragilaria famelica* decreasing to 1.5% at the depth of 19.25cm (early ~1970s AD) from the depth of 19.75cm (late ~1960s AD) with 5.5% (Figure 5.6).

Species that increase at these two troughs in PC1 scores at the depths of 20.25cm (mid ~1960s AD) from the depth of 20.75cm (early ~1960s AD) and at the depth of 19.25cm (early ~1970s AD) from the depth of 19.75cm (late ~1960s AD), respectively include: *Nitzschia sp.* to 13.8% from 2.7% and to 6.3% from 2.3%; *Fragilaria capucina* to 4.9% from 1.3% and to 3.8% from 0.9%; *Navicula erifuga* to 4.6% from 0.7% and to 1.5% from 0.3%; *Navicula veneta* to 4.3% from 2% and to 3% from a short-lived absence; *Navicula trivialis* to 3.9% from 0.3% and to 1.8% from a short-lived absence; along with *Nitzschia palea* to 3.3% and to 1.8% from short-lived absences, respectively (Figure 5.6). Additionally, there is an increase in *Fragilaria famelica* to 5.9% at the first aforementioned PC1 trough at the depth of 20.25cm (mid ~1960s AD) from 3% the depth of 20.75cm (early ~1960s AD); along with an increase at the second trough at the depths of 19.25cm (early ~1970s AD) from the depth of 19.75cm (late ~1960s AD) in *Aulacoseira granulata* abundances to 55.9% from 55.3% and *Cymbella cistula* to 14.2% from 10.4%, respectively (Figure 5.6). From the maximum PC1 score of 1.34 at the depth of 18.75cm (early ~1970s AD), PC1 scores overall decrease at the depth of 15.75cm (mid ~1980s AD), to the third lowest minimum score of -1.04 in zone Lets2Z2 (Figure 5.6). This negative trend coincides with an overall decrease in *Aulacoseira granulata* abundances from 92.2% to 26%, respectively (Figure 5.6).

Species that overall increase during this period however include: *Nitzschia sp.* to 18.8%, *Fragilaria famelica* to 5.4%, *Navicula trivialis* to 2.9% and *Pinnularia divergens* to 1.9% all from short-lived absences, respectively (Figure 5.6). There is additionally an increase in *Gyrosigma acuminatum* from 0.7% to 12.8%, *Cymbella cistula* from 4.2% to 10.6%, *Caloneis schumannania* from 0.7% to 5.1% and *Diploneis subovalis* from 0.3% to 3.5% between these depths, respectively (Figure 5.6). This overall decrease is interrupted with the third highest maximum PC1 score calculated as 0.69 in this zone, at the depth of 16.75cm (early ~1980s AD) which coincides with an increase in *Aulacoseira granulata* to 74% and *Fragilaria famelica* to 5.3%, from 59.6% and 3.1% from the depth of 17.25cm (early ~1980s AD), respectively (Figure 5.6). From the minimum PC1 score of -1.04 at the depth of 15.75cm (mid ~1980s AD) there is an overall increase in PC1 scores at the depth of 11.25cm (late ~1990s AD) to -0.10 (Figure 5.6). This coincides with an overall increase in *Aulacoseira granulata* relative abundances from 26% to 45.3%, respectively (Figure 5.6). Other species that overall increase in abundance between these depths include *Fragilaria construens* from 3.2% to 4.2% along with *Fragilaria famelica* from 5.4% to 9.1%, respectively (Figure 5.6). Species that decrease during this period include *Nitzschia sp.* from 13.8 % to 2.6%, *Cymbella cistula* from 10.6% to 9.4% and *Gyrosigma acuminatum* from 12.8% to 4.2%, respectively (Figure 5.6). These increasing PC1 scores are interrupted with two minimum PC1 scores calculated as -0.80 at the depth of 13.25cm (early ~1990s AD) and at the depth of 11.75cm (late ~1990s AD) with -0.90 (Figure 5.6). This coincides with a decrease in *Aulacoseira granulata* abundances to 33.8% from 40.7% at the depth of 13.75cm (early ~1990s AD) and to 24.9% from the depth of 12.25cm (mid ~1990s AD) with 54.4% (Figure 5.6).

PC2 scores within this zone range from -2 to +2 and overall decrease from the score of 0.59 at the depth of 28.25cm (~1870s AD) to the depth of 11.25cm (late ~1990s AD) with -0.73 (Figure 5.6). This overall decreasing trend predominantly coincides with an overall respective decrease in *Nitzschia sp.* from 13.8% to 2.6%, *Cymbella cistula* from 10.5% to 9.4%, *Fragilaria capucina* from 5.6% to 2.3%,

Cymatopluera solea from 3.9% to 1.6%, along with *Navicula erifuga* from 4.9% and *Navicula trivialis* from 3% to short-lived absences, respectively (Figure 5.6). The PC2 curve in this zone is characterized by six maximum scores calculated as 1.01, 1.35, 1.29, 1.10, 1.29 and 1.23; located at the depths of 26.25cm (~1890s AD), 22.25cm (early ~1950s AD), at 20.25cm (mid ~1960s AD), 18.25cm during the late ~1970s AD, at 15.25cm (late ~1980s AD) and at 14.25cm (early ~1990s AD), respectively (Figure 5.6). These scores respectively increased from -0.56, -0.24, -0.66, 0.22, -0.32 and -0.66, and from the depths of 26.75cm (~1880s AD), 22.75cm (~1940s AD), 20.75cm (early ~1960s AD), 18.75cm (early ~1970s AD), 15.75cm (mid ~1980s AD) and at the depth of 14.75cm (early ~1990s AD), respectively (Figure 5.6). These maximum PC2 scores and related depths predominantly coincides with increases in four species including: *Nitzschia sp.* to 6.4% from 2.3%, to 18.1% from 13.9%, to 13.8% from 2.7%, to 5.6% from a brief absence, to 16.5% from 13.8% and to 13.5% from 8.9%; of *Navicula trivialis* to 3% from 0.3%, to 3.5% from 2.2%, to 3.9% from 0.3%, to 1.9% from a brief absence, to 8.8% from 2.9% and to 5% from 0.7%; of *Navicula veneta* to 5.5% from 0.6%, to 13.7% from 4.3%, to 4.3% from 2%, to 3.7% from a brief absence, to 1.8% from 1.3% and to 0.9% from a brief absence; along with *Fragilaria capucina* to 2.7% from 2%, to 4.8% from 1.2%, to 4.9% from 1.3%, to 2.8% from 0.7%, to 6.2% from 2.6%, but is conversely found to decrease slightly at the last depth to 3.2% from 3.9% (Figure 5.6).

Between the bottom of the core at 28.25cm (~1850s AD) to around the middle of this zone at the depth of 19.75cm (late ~1960s AD), there are five maximum PC2 scores calculated as 0.59, -1.03, -0.24, 1.35 and -066 (Figure 5.6). These coincide with the depths of 28.25cm (~1850s AD), 27.25cm (~1870s AD), 22.75cm (~1940s AD), 22.25cm (~1950s AD) and at 20.75cm (early ~1960s AD), respectively (Figure 5.6). These maximum PC2 scores coincide with the maximum occurrence of eight species at different depths within the core and include: both *Navicula erifuga* with 5.2% and *Cyclotella meneghiana* with 4.9% at the depth of 28.25cm (~1850s AD); *Fragilaria famelica* with 12.7% at the depth of 27.25cm (~1870s AD); *Fragilaria fasciculata* with 3.4% at the depth of 22.75cm (late ~1940s

AD); along with *Navicula veneta* with 13.7%, *Nitzschia palea* with 5.1% and *Cyclotella pseudostelligera* with 3.2% at the depth of 22.25cm (early ~1950s AD), respectively; along with *Fragilaria construens* with 7.3% at the depth of 20.25cm during the mid ~1960s AD (Table 5.2; Figure 5.6).

The PC2 curve is characterized by three minimum scores between the depth of 28.25cm (~1850s AD) and 19.75cm (late ~1960s AD); these include a score of -1.14, -1.18 and -1.08 at the respective depths of 27.75cm (~1860s AD), 23.25cm (early ~1940s AD) and at 21.25cm during the late ~1950s AD (Figure 5.6). There is a coinciding decrease in *Nitzschia sp*. to 6.4% at the depth 27.75cm (~1860s AD), from 13.8% at the depth of 28.25cm (~1850s AD) and to 2.3% at the depth of 21.25cm (late ~1950s AD), from 5.2% at the depth of 21.75cm (mid ~1950s AD); along with a decrease in *Aulacoseira granulata* to 19.8% at the depth 23.25cm (early ~1940s AD) from the depth of 23.75cm (late ~1930s AD) with 52.4% (Figure 5.6). Between the depth of 19.25cm (early ~1970s AD) and 11.25cm (late ~1990s AD), the PC2 curve is characterized by numerous, relatively stable but alternating peaks and troughs extending from the scores of +2 to -1 (Figure 5.6). The two maximum PC2 scores of 1.29 at the depth of 15.25cm (late ~1980s AD) and of 0.82 at the depth of 13.25cm (early ~1990s AD), coincide with the maximum occurrence of three species including: *Navicula trivialis* with 8.8% and *Gomphonema parvulum* 3.8% at the depth of 15.25cm (late ~1980s AD); along with *Nitzschia sp*. at the depth of 13.25cm (early ~1990s AD) with 21.1% (Table 5.2; Figure 5.6).

Zone Lets2Z1, 10.75cm (~2000s AD) to 0.25cm (~2010s AD)

The most dominant species in this zone is *Aulacoseira granulata*, with an individual occurrence ranging from a maximum of 79.5% at the depth of 8.25cm (mid ~2000s AD) to a minimum of 39.2% at the depth of 1.25cm (mid ~2010s AD) for zone Lets2Z1 (Figure 5.6). There were 37 identified diatom species recorded in this zone, excluding the two species C*yclotella meneghiana* and *Fragilaria sp.* (Figure 5.6). The second most dominant species is *Fragilaria capucina* ranging from a minimum of 1.2%

at the depth of 9.75cm (early ~2000s AD) to a maximum occurrence throughout the core at the depth of 1.25cm (mid ~2010s AD) with of 9.7% (Figure 5.6). PC1 scores within this zone range from zero to +1 and overall decrease from 0.62 at the depth of 10.75cm (early ~2000s AD) to 0.28 at the core surface depth of 0.25cm (2018 AD), respectively (Figure 5.6). This negative curve coincides with a decrease in *Aulacoseira granulata* from 68.7% to 59.4%, respectively (Figure 5.6). Overall, PC1 scores in this zone and *Aulacoseira granulata* relative abundances follow the same fluctuating trajectories, except at the depths of 7.25cm (mid ~2000s AD) and at 2.25cm (mid ~2010s AD); where PC1 scores decrease to 0.46 and 0.53 and *Aulacoseira granulata* abundances increase to 65.2% and 65.4%, respectively (Figure 5.6). The reverse is also observed in this trend at the depths of 6.75cm (late ~2000s AD) and both depths of 3.75cm and 2.75cm (early ~2010s AD) where PC1 scores increase to 0.61, 0.87 and 0.57 and where *Aulacoseira granulata* abundances decrease to 63%, 69.5% and 60.4%, respectively (Figure 5.6)

The PC1 curve in this zone is characterised with three maximum scores of 0.93, 0.84 and 0.87 located at the depths of 8.25cm (mid ~2000s AD), 5.75cm and 3.75cm (early ~2010s AD), respectively; along with three minimum PC1 scores of 0.02, 0.22 and 0.28 which were found at the depths of 1.25cm and 0.75cm (mid ~2010s AD) and at 0.25cm (2018 AD), respectively (Figure 5.6). The maximum PC1 scores at the depths of 8.25cm (mid ~2000s AD) and at 5.75cm (early ~2010s AD) coincide with a respective increase in *Aulacoseira granulata* abundances to 79.5% and to 74.5%, from 69.3% at the depth of 8.75cm (mid ~2000s AD) and from the depth of 6.25cm (late ~2000s AD) with 72.8% (Figure 5.6). The second highest maximum PC1 score in this zone of 0.87 at the depth of 3.75cm (early ~2010s AD), coincides with an increase in five species abundances from a lesser percentage at the depth of 4.25cm (early ~2010s AD) and include respectively: *Fragilaria capucina* to 4.5% from 3.5%, *Cymbella cistula* to 3.6% from 1.5%, *Fragilaria construens* to 3.2% from 0.9%, along with both *Cyclotella tumida* and *Fragilaria famelica* to 2.6% from 0.3%, respectively (Figure 5.6). The three lowest minimum PC1 scores

in this zone are calculated as initially a decrease to 0.02 and increases thereafter to 0.22 and to 0.28, at the respective depths of 1.25cm and 0.75cm (mid ~2010s AD), along with at 0.25cm at the core surface (Figure 5.6). The first of these minimum PC1 scores coincides with a decrease in *Aulacoseira granulata* abundances to 39.2% and the increases thereafter to 48.7% and to 59.4%, respectively (Figure 5.6).

PC2 scores range from -1 to +1 and overall increase from -0.44 at the depth of 10.75cm (early ~2000s AD) to a score of 0.66 at the depth of 0.25cm (2018 AD) at the core surface (Figure 5.6). This positive trend coincides with an overall increase in *Nitzschia sp.* relative abundances from 1.6% to 7.5%, respectively (Figure 5.6). The lowest PC2 score of -1.00 at the depth of 1.75cm (mid ~2010s AD) coincides with a decrease in *Aulacoseira granulata* abundances to 51.1% from 65.4% along with *Nitzschia sp*. to 1.3% from 5.2%, from the depth of 2.25cm (mid ~2010s AD), respectively (Figure 5.6). This minimum PC2 score however, additionally coincides with an abrupt increase and maximum occurrence of *Cymatopluera solea* to 11.5% from 1.7%, along with *Fragilaria ulna* to 6.9% and *Hantzschia amphioxy*s to 1.6% from short-lived absences, respectively (Table 5.2; Figure 5.6). The PC2 curve in this zone is characterised by two maximum PC2 scores of 0.72 from -0.44 and of 0.93 from -0.04 at the depths of 10.25cm (early ~2000s AD) from the depth of 10.75cm (early ~2000s AD) and at 8.25cm (mid ~2000s AD) from 8.75cm (early ~2000s AD), respectively (Figure 5.6). These peaks in PC2 scores coincide with an increase in *Nitzschia sp.* to 6% from 1.6% and to 1.6% from a short-lived absence; along with *Fragilaria capucina* to 4.5% from 2.3% and to 4.9% from 3.9%, respectively (Figure 5.6). Thereafter, PC2 scores increase to 0.60 at the depth of 3.25cm (early ~2010s AD) from a score of -0.38 at the depth of 3.75cm (early ~2010s AD); to -0.74 at the depth of 1.25cm (mid ~2010s AD) from a score of -1.00 at the depth of 1.75cm (mid ~2010s AD); and at the core surface depth to 0.66 from the depth of 0.75cm (late ~2010s AD) with -0.78 (Figure 5.6). These peaks in PC2 scores coincide with the maximum occurrence of three species in this zone and include: *Aulacoseira ambigua* with 4.3% at

the depth of 3.25cm (mid ~2010s AD), both *Fragilaria capucina* with 9.7% and *Cymbella tumida* with 6.1% at the depth of 1.25cm (mid ~2010s AD); along with *Nitzschia sp*. with 7.5% at the core surface (Table 5.2; Figure 5.6).

5.3. Inter-site Comparison

Lake Chrissie is situated in the highveld plateau of the Mpumalanga Province in South Africa within the MLD (Ferreira *et al*., 2012; Hallowes and Munnik, 2016); while Letšeng-la Letsie is located below the Maloti Mountains (Kahlolo *et al*., 2021; Smit and Van Rensberg, 2021). These lake systems are geographically located in different regions at altitudes of 1676m.asl and 2402m.asl, respectively, with a difference in elevations of 726m.asl and distance of 734Km (Google Earth, 2022a,b). The highest concentration of 12 of Eskom's coal-fired power stations are located within the Mpumalanga Province (Panichev *et al*., 2019; Rose *et al*., 2020). Lake Chrissie is situated in relatively close proximity to these stations (Figure 3.2). Comparatively, Letšeng-la Letsie is located at over ~400km from these pollutant sources and found within mountainous regions of Lesotho, at higher altitudes (Figure 3.2). Thus, any contamination from coal-fired power stations in Letšeng-la Letsie must be atmospherically derived and long range transported, as Lesotho has no coal-fired power stations (Rose *et al*., 2020).

There are 24 identified diatom species common to both lake systems and three dominant species in Lake Chrissie with the highest maximum occurrence includes: *Fragilaria famelica* with 60% in the early ~1960s AD; both *Nitzschia sp.* and *Cyclotella meneghiana* with 50% during the ~1780s AD (Table 5.1,5.2; Figure 5.3,5.6). In Letšeng-la Letsie, the three most dominant species and maximum abundances include: *Aulacoseira granulata* with 92.2% in the early ~1970s AD; *Cymbella cistula* with 26.1% in the late ~1950s AD and *Nitzschia sp.* with 21.1% in the early ~1990s AD (Table 5.1,5.2; Figure 5.3,5.6). *Nitzschia sp.* was found to be dominant in both lake systems, in comparison however, *Fragilaria famelica* was found with 12.7% in the ~1870s AD and *Cyclotella meneghiana* with a

maximum of 5.2% during the ~1850s AD in Letšeng-la Letsie; where *Aulacoseira granulata* had a maximum abundance of 9.1% during the ~1880s AD and *Cymbella cistula* with 11.1% in the early ~1950s AD, in Lake Chrissie (Table 5.1,5.2; Figure 5.3,5.6). The fourth most dominant species in Lake Chrissie was identified as *Hantzschia amphioxys* with 25% during the ~1940s AD; where this species was found with a maximum occurrence of 2.8% in the early ~2010s AD in Letšeng-la Letsie (Table 5.1,5.2; Figure 5.3,5.6). The fourth most dominant species in Letšeng-la Letsie was identified as *Navicula veneta with* 13.7% during the early ~1950s AD; where this species was found with a maximum occurrence of 3.1% during the late ~1970s AD in Lake Chrissie (Table 5.1,5.2; Figure 5.3,5.6).

The remaining 17 species found in both Lake Chrissie and Letšeng-la Letsie, respectively, are presented with their maximum occurrences in descending Lake Chrissie order and include: *Rhapolodia gibba* with 15% in the early ~1970s AD and with 2.3% in the late ~1990s AD; *Fragilaria construens* with 12.9% in the early ~1990s AD and with 7.3% in the early ~1960s AD; *Pinnularia borealis* with 12.5% during the late ~1970s AD and with 2% in the late ~1950s AD; *Fragilaria fasciculata with* 10% in the late ~1890s AD and with 3.4% during the late ~1940s AD; *Navicula antonii* with 9.4% in the late ~1970s AD and with 3.9% in the mid ~1950s AD; *Achnanthes minutissima* with 9.1% during the ~1820s AD and with 2.6% during the ~1850s AD; *Gomphonema minutum* with 7.1% in the early ~1890s AD and with 4.6% in the early ~1940s AD; *Pinnularia divergens* with 7.1% in the early ~1890s AD and with 5% during the mid ~1980s AD; *Fragilaria ulna* with 6.4% in the early ~1990s AD and with 6.9% in the mid ~2010s AD; *Fragilaria pinnata* with 5.8% in the late ~1980s AD and with 3.9% during the mid ~1950s AD*; Gomphonema parvulum* with 5.6% in the late ~1950s AD and with 3.8% in the late ~1980s AD; *Eunotia minor* with 5% in the early ~1970s AD and with 3.5% during the ~1860s AD; *Pinnularia viridis* with 4.8% in the late ~1960s AD and with 2.6% in the late ~1950s AD; *Navicula trivialis* with 2.8% during the mid ~1990s AD and in the late ~1980s AD with 8.8% (Table 5.1,5.2; Figure 5.3,5.6). The remaining three species *Navicula erifuga, Fragilaria capucina* and *Gomphonema clavatum* were found in Letšeng-la

Letsie however with maximum abundances of 4.9% during the ~1850s AD, with 6.9% in the early ~2010s AD and with 2.3% during the mid ~1990s AD, respectively; while these species were found with <2% maximum occurrences in Lake Chrissie (Table 5.1,5.2; Figure 5.3,5.6).

The maximum abundance of five species unique to Lake Chrissie include: *Eupodiscus radiatus* with 100% during the ~1780s AD, ~1790s AD and ~1880s AD; *Aulacoseira sp*. with 64.7% in the early ~2010s AD; *Amphora ovalis with* 28.6% during the late ~1960s AD; *Surirella ovalis* with 25% in the late ~1930s AD; along with *Anomoeneis sphaerophora* during the late ~1970s AD with 4.7% (Table 5.1; Figure 5.3). The maximum abundance of eight species unique to Letšeng-la Letsie include: *Gyrosigma acuminatum* with 12.8% in the mid ~1980s AD; *Cymatopluera solea* with 11.5% in the mid ~2010s AD; *Cymbella tumida* with 6.1% in the mid ~2010s AD; *Caloneis schumannania* with 5.1% in the mid ~1980s AD; *Diploneis subovalis* with 4.9% in the early ~1990s AD; *Aulacoseira ambigua* with 4.3% in the early ~2010s AD; *Cocconeis placentula* with 2.9% in the early ~1990s AD; along with *Melosira varians* in the ~1950s AD with 2.6% (Table 5.2; Figure 5.6).

Seven planktonic and facultative planktonic species were identified in the Lake Chrissie core, with 81% total abundances (Figure 5.7). *Aulacoseira granulata* (0.2%) was found with the lowest average frequency within this habitat; where *Eupodiscus radiatus* with 63% was the most dominant species, followed by *Aulacoseira sp.* with 9.9% (Figures 5.7). Fifteen benthic species were identified and represent a total abundance of 10% with *Gomphonema sp*. reflecting the lowest average abundance of 0.1% and *Fragilaria famelica* the most dominant benthic species with 5% (Figure 5.7). Ten epiphytic, epilithic and epipelic species were identified with a total abundance of 5% (Figure 5.7). *Gomphonema parvulum* had the lowest average of 0.1% where *Nitzschia sp*. with 2.4% is the most dominant species within this group (Figure 5.7). Four aerophilic species were identified with a total abundance of 4% with *Hantzschia amphioxys* the most dominant species in this habitat with 1.2% (Figure 5.7).

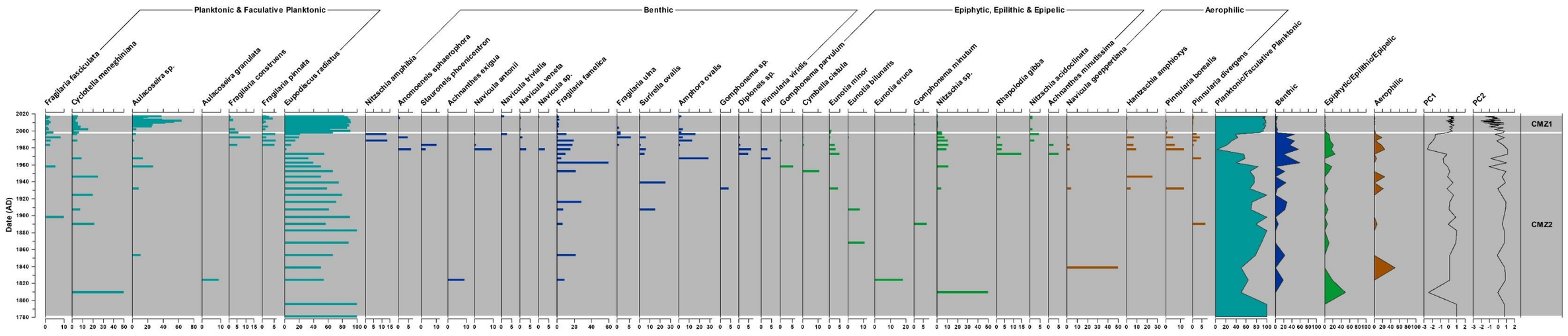

Figure 5.7. Stratigraphic diagram of the 36 identified diatom species throughout the Lake Chrissie core profile, grouped according to habitats and ordered from highest (left) to lowest (right) pollution tolerance within each group.

Twelve planktonic and facultative planktonic species were identified in the Letšeng-la Letsie core with a 59% total abundance (Figures 5.8). Three species including *Cyclostephanos dubius, Fragilaria biceps* and *Fragilaria sp*. had the lowest average frequency within this habitat with 0.1% where *Aulacoserira granulata* with 53% was dominant (Figures 5.8). Eleven benthic species were identified with a total abundance of 16%, where *Gomphonema sp*. was found with the lowest average abundance of 0.1% and *Fragilaria famelica* as the most dominant species within this habitat with 3.8% (Figure 5.8). Thirteen epiphytic, epilithic and epipelic species were identified with a total abundance of 24% and the lowest average frequency of 0.2% was found for *Eunotia minor* and *Rhapolodia gibba*, respectively *Cymbella cistula* with 7.5% is the most dominant species in this group (Figure 5.8). Three aerophilic species were identified with a total abundance 1%, with *Hantzschia amphioxys* found as the most dominant species in this habitat with 0.5% (Figure 5.8).

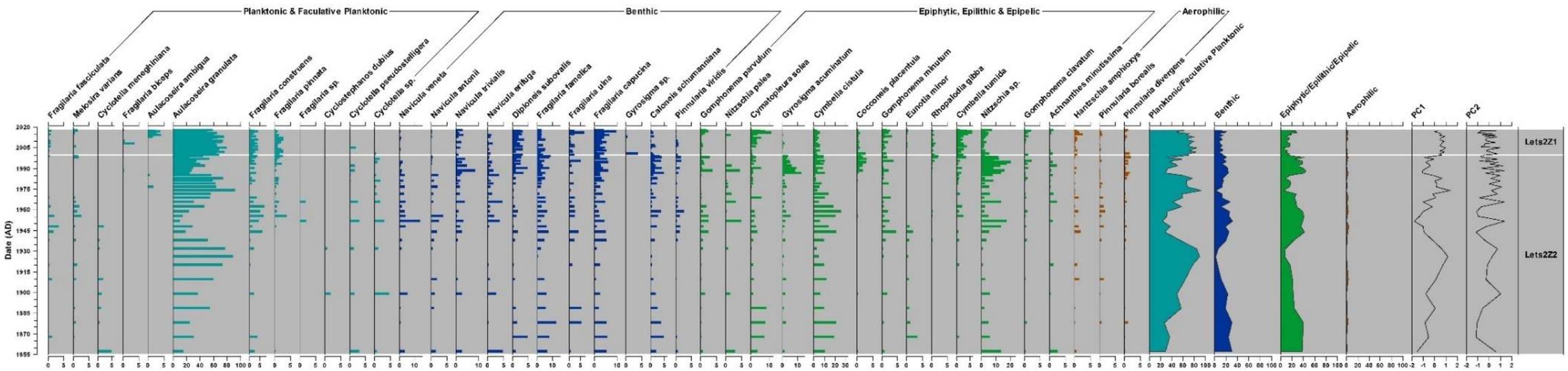

Figure 5.8. Stratigraphic diagram of the 39 identified diatom species throughout the Letšeng-la Letsie core profile, grouped according to habitats and ordered from highest (left) to lowest (right) pollution tolerance within each group.

5.4. Conclusion

There are 24 identified diatom species common to both lake systems, with five species unique to Lake Chrissie and eight species unique to Letšeng-la Letsie (Figure 5.3,5.6). The epiphytic, epipelic and epilithic species *Nitzschia sp.* was found in both systems as part of the top three most dominant species; while the benthic species *Fragilaria famelica* was also found in relatively high abundances in both lake cores (Table 5.1,5.2; Figure 5.3,5.6).). *Eupodiscus radiatus* is the most dominant species throughout the Lake Chrissie core with an average abundance of 54.5% in zone CM1Z2 and with 71.4% in zone CM1Z1 (Figure 5.3). *Aulacoseira granulata* is the most dominant species throughout the Letšeng-la Letsie core profile with an average abundance of 45.3% in zone Lets2Z2 and with 64.6% in zone Lets2Z1 (Figure 5.6).

The Lake Chrissie core spans ~240-years from the ~1780-2017 AD and extends from the depths of 25.75cm to the core surface of 0.25cm, respectively (Figure 5.3). The core is divided into two zones, zone CM1Z2 extends from the bottom of the core profile from ~1780s AD to the mid ~1990s AD, spanning ~220-years from the depth of 25.75cm to 13.25cm, respectively (Figure 5.3). Zone CM1Z1 extends for ~20-years from the mid ~1990s AD to the core surface in 2017 AD and spanning the depths of 12.75cm to 0.25cm (Figure 5.3). The Letšeng-la Letsie core spans the comparatively shorter period of ~170-years and extends from the ~1850s AD to the core surface in 2018 AD, spanning the depths of 28.25cm to 0.25cm, respectively (Figure 5.6). The core is divided into two zones, zone Lets2Z2 extends from the bottom of the core profile in the ~1850s AD to the late ~1990s AD and spans ~150-years from the depths of 28.25cm to 11.25cm, respectively (Figure 5.6). Zone Lets2Z1 extends for the comparatively shorter period of ~20-years from the early ~2000s AD to the core surface in 2018 AD, spanning the depths of 10.75cm to 0.25cm, respectively (Figure 5.6).

CHAPTER 6: DISCUSSION

6.1. Introduction

The aim of this research is to use diatoms as a representation of historical air pollution from coal-fired power stations and other pollutants deposited in water bodies in South Africa and Lesotho over the past ~200 years. The results of the diatom analyses from the Lake Chrissie and Letšeng-la Letsie core profiles are presented in the *Results (Chapter 5).* This chapter begins with investigating environmental inferences and introduces the identified diatom species recorded for both sites. Comparisons relating to water depth and pollution are made between the sites and with global literature, followed by a southern African perspective. A broader regional understanding of pollution history in terms of contexts around lakes and environmental pollution in South Africa and Lesotho, is discussed. This brings into focus the history of coal-fired power stations within the Mpumalanga Province of South Africa. The implications of this research are outlined, broadly discussing lakes and environmental pollution, with a brief consideration for the climate and the effects of pollution on human health and well-being. Potential mitigation action is discussed in the context of pollution emitted from coal-fired power stations in South Africa. Lastly the limitations of this research are outlined.

6.2. Environmental Inferences

6.2.1. Diatoms and Pollution Tolerances

Diatoms are globally used as ecological indicators to determine contemporary and past environmental conditions of freshwater systems, such as lakes (Rivera-Rondon and Catalan, 2019; Humane *et al*., 2020). Species are sensitive to physical parameters including light conditions, convective mixing and the effects of various climatic conditions (Venter *et al.,* 2013; Westover *et al.*, 2019); where fluctuations in pH, conductivity/salinity, nutrient concentrations and pollution, are some factors

influencing diatom species composition (Humane *et al*., 2020; Zou *et al*., 2020). Diatoms have been proven to be useful water quality indicators, to monitor changes in the physical and chemical properties of the aquatic system including fluctuating lakes levels (e.g. Bannister *et al*., 2019) and salinisation (e.g. Sitoe *et al.,* 2015*;* Zaky *et al*., 2020) among others (Buczkó *et al*., 2019; Humane *et al*., 2020). They have globally been used as indicators of contamination such as industrial pollution (e.g. Adams *et al*., 2019) including sewage effluents (e.g. Bere *et al*., 2014) and eutrophication (e.g. Bannister *et al*., 2019; Yand *et al*., 2020) of many aquatic systems (Buczkó *et al*., 2019; Rivera-Rondon and Catalan, 2019).

The 53 diatoms identified from sediment profiles at Lake Chrissie and Letšeng-la Letsie represent a range of environmental attributes and habitats, with 20 species overlaps between the sites, 15 species unique to Lake Chrissie and 18 unique to Letšeng-la Letsie (Table 6.1). The benthic species *Fragilaria famelica* was found in relatively high abundance in both sites, throughout the cores; with the planktonic *Eupodiscus radiatus* as the most dominant species in Lake Chrissie and the planktonic *Aulacoseira granulata* as the most dominant species found in Letšeng-la Letsie. The most pollution tolerant species found in both lake systems includes *Fragilaria fasciculata, Gomphonema parvulum, Navicula trivialis, Navicula antonii, Navicula veneta, Cyclotella meneghiniana, Hantzschia amphioxys;* along with *Achnanthes exigua, Anomoeneis sphaerophora, Navicula goeppertiana* and *Nitzschia amphibia* in Lake Chrissie; with *Cymatopleura solea, Gyrosigma acuminatum, Melosira varians, Navicula erifuga, Diploneis subovalis* and *Nitzschia palea* found in Letšeng-la Letsie (Table 6.1). Species with moderate to high pollution tolerances that are identified in the cores for both sites include *Fragilaria famelica, Cymbella cistula* and *Fragilaria ulna;* along with *Aulacoseira sp.* and *Stauroneis phoenicentron* in Lake Chrissie and with *Aulacoseira ambigua* and *Fragilaria biceps* found in Letšeng-la Letsie (Table 6.1). Species with moderate pollution tolerances found at both sites includes *Aulacoseira granulata, Fragilaria construens, Fragilaria pinnata, Eunotia minor, Gomphonema*

minutum, Pinnularia borealis, Pinnularia divergens; along with *Amphora ovalis, Surirella ovalis, Eunotia eruca, Eunotia bilunaris* in Lake Chrissie and *Fragilaria capucina* found in Letšeng-la Letsie (Table 6.1). Species that indicate a diverse range in pollution tolerances found in both sites includes *Nitzschia sp*., with *Diploneis sp, Gomphonema sp.* and *Navicula sp.,* found in Lake Chrissie along with *Fragilaria sp.* and *Gyrosigma sp.,* within Letšeng-la Letsie (Table 6.1). Moderate-high pollution sensitive species found in both lake systems includes *Pinnularia* viridis and Rhopalodia *gibba*; with *Nitzschia acidoclinata* found in Lake Chrissie and *Caloneis schumanniana, Cymbella tumida, Cyclostephanos dubius* found in Letšeng-la Letsie (Table 6.1). Lastly, species with low pollution tolerances include *Achnanthes minutissima* found in both sites along with *Eupodiscus radiatus* in Lake Chrissie and *Gomphonema clavatum, Cocconeis placentula, Cyclotella pseudostelligera* and *Cyclotella sp.* in Letšeng-la Letsie (Table 6.1).

Table 6.1: The habitat and autecologies of the 53 diatom species identified in both the Lake Chrissie and Letšeng-la Letsie sediment cores.

Diatom Species	Site	Habitat	Ecological Characteristics	Pollution Tolerance
Achnanthes exigua Grunow	CM1	Benthic (Niyatbekov and Barinova, 2018).	Brackish, alkaline waters with moderate to high electrolyte content, increased salinity, high temperatures and low light condition, found in industrial wastewaters (Taylor *et al*., 2007a; Zaky *et al*., 2020).	High.
Achnanthes minutissima Kützing	CM1 LETS2	Epiphytic (Zou *et al*., 2020).	Well oxygenated, clean, fresh and brackish waters with increased salinity (Taylor *et al*., 2007a; Zaky *et al*., 2020).Pollution sensitive species (Benhassane *et al*., 2020).	Low.
Amphora ovalis Kützing	CM1	Benthic (Humane *et al*., 2020).	Alkaline, brackish and mesotrophic waters with moderate electrolyte content; may reflect lake shallowing, low flooding and hyper-arid conditions (Taylor *et al*., 2007a; Humane *et al*., 2020; Zaky *et al*., 2020).	Moderate.
Anomoeneis sphaerophora Ehrenberg	CM1	Benthic (Niyatbekov and Barinova, 2018).	Brackish and mesotrophic waters, with moderate-high electrolyte content and found in waters with critical levels of pollution (Taylor *et al*., 2007a; Niyatbekov and Barinova, 2018; Dulanya *et al*., 2019).	High.
Aulacoseira ambigua (Grunow) Simonsen	LETS2	Planktonic (Fitchett *et al*, 2016b).	Alkaline, meso-eutrophic waters with strongly mixed water columns, with associated high wind speeds and wetter climate conditions (Fitchett *et al.,* 2016b; Sivarajah *et al.,* 2018).	Moderate-High.
Aulacoseira granulata Ehrenberg	CM1 LETS2	Planktonic (Taylor *et al*., 2007a; Westover *et al.*, 2019).	High water levels, wetter conditions, well mixed water columns, high wind speeds, mesotrophic waters (Sitoe *et al*., 2017; Buczkó *et al.,* 2019) with slightly elevated-abundance	Moderate.

			of P and silica (Si) levels (Beck *et al.,* 2019; Westover *et al.*, 2019). Sinks out of photic zone when water column mixing decrease and lake stratifies (Adams *et al.*, 2019).	
Aulacoseira sp.	CM1	Planktonic (Taylor *et al*., 2007a; Westover *et al.*, 2019).	Alkaline, well-mixed lake, high productivity, windy conditions (Stager and Johnson, 2000; Beck *et al*., 2019). Abundance supports wet climatic conditions (Zaky *et al*., 2020). Favoured under a high Si:P ratio and good light competitors, surviving with limiting light; replaced by *Nitzschia sp*., when convective mixing less is intense (Burge *et al*., 2017; Westover *et al*., 2019). Found in meso-eutrophic waters (Stager and Johnson, 2000; Beck *et al*., 2019) and are highly adaptable to environmental change (Burge *et al*., 2017; Westover *et al*., 2019).	Moderate-High.
Caloneis schumanniana (Grunow) Cleve	LETS2	Benthic (Nevrova and Petrov, 2019).	Cosmopolitan species, oligotrophic waters with moderate electrolyte content and may indicate an unstable and changing environment (Taylor *et al*., 2007a; Buczkó *et al*., 2019).	Low-Moderate.
Cocconeis placentula Ehrenberg	LETS2	Epiphytic (Taylor *et al*., 2007a).	Found on plants and is indifferent to salinity (Taylor *et al*., 2007a; Sitoe *et al*., 2017). Pollution sensitive taxa (Benhassane *et al*., 2020).	Low.
Cyclostephanos dubius (Fricke) Round	LETS2	Planktonic (Taylor *et al*., 2007a).	Inland waters with elevated chloride concentration as well as calcareous, alkaline waters (Taylor *et al*., 2007a). Low-moderate pollution tolerance (Mangadze *et al*., 2017).	Low-Moderate.
Cyclotella meneghiniana Kützing	CM1 LETS2	Planktonic (Westover *et al*., 2019).	Electrolyte rich, shallow waters, medium-high conductivity (Taylor and Cocquyt, 2016; Dulanya and Trauth, 2019). Can live in freshwater lakes during highly evaporative conditions (Sitoe *et al*., 2017). Found in organically polluted and eutrophic waters and associated with organic waste and brackish waters, where their presence may indicate polluted waters that are silted up (Bannister *et al*., 2019; Dulanya *et al*., 2019).	High.
Cyclotella pseudostelligera Hustedt	LETS2	Planktonic (Taylor *et al*., 2007a).	Found in plankton of fresh inland lakes and are sensitive to metal contamination (Taylor *et al*., 2007a; Hansika and Yatigammana, 2019).	Low.
Cyclotella sp.	LETS2	Planktonic (Sivarajah *et al*., 2018).	Low wind conditions and can signify responses to climate warming, found in low nutrient conditions (Sivarajah *et al*., 2018; Westover *et al*., 2019). Sensitive to metal contamination (Hansika and Yatigammana, 2019).	Low.
Cymatopleura solea (Brébisson) W Smith	LETS2	Epiphytic, (Taylor and Cocquyt, 2016).	Moderate-high electrolyte content to brackish but favours alkaline waters and found in eutrophic conditions (Taylor *et al.,* 2007a).	High.
Cymbella cistula Ehrenberg	CM1 LETS2	Epiphytic and epilithic (Taylor *et al*., 2007a).	Circumneutral to slightly alkaline waters with moderate-high electrolyte content with meso-eutrophic waters (Taylor *et al.,* 2007a).	Moderate-High.
Cymbella tumida (Brébisson) Van Heurck	LETS2	Epilithic (Cohu *et al*., 2020).	Alkaline waters with moderate electrolyte content and found in oligo-mesotrophic waters (Taylor *et al*., 2007a; Cohu *et al*., 2020).	Low-Moderate.
Diploneis sp.	CM1	Benthic (Taylor and Cocquyt, 2016).	Found in acidic or alkaline, oligotrophic waters with high conductivity (Taylor and Cocquyt, 2016). Good competitor for nutrient rich environment (Dalu *et al*., 2014).	Diverse.
Diploneis subovalis Cleve	LETS2	Benthic (Dalu *et al*., 2014).	Found in fresh to brackish waters, with moderate to high electrolyte content (Taylor *et al*., 2007a) and also associated with eutrophic conditions (Tuturí *et al*., 2021).	High.
Eunotia bilunaris Ehrenberg	CM1	Epiphytic (Fitchett *et al*., 2016a).	Prefer acidic waters with low electrolyte content (Taylor *et al*., 2007a; Taylor and Cocquyt, 2016).	Moderate.

Eunotia eruca Ehrenberg	CM1	Epiphytic (Kociolek and Spaulding, 2003).	Prefers acidic waters (Kociolek and Spaulding, 2003; Taylor and Cocquyt, 2016).	Moderate.
Eunotia minor Kützing	CM1 LETS2	Epilithic (Kim and Lee, 2017).	Found in circumneutral waters but prefers acidic environments (Taylor *et al*., 2007a; Taylor and Cocquyt, 2016).	Moderate.
Eupodiscus radiatus Bailey	CM1	Planktonic (Perez *et al.,* 2017; Onyema, 2018).	Found in marine-brackish habitats (Onyema, 2018) and in drier climatic conditions (Varona-Cordero *et al*., 2010). Indicative of high salinity and low trophic conditions or organic matter (Perez *et al*., 2017) in the system.	Low.
Fragilaria biceps Kützing	LETS2	Planktonic (Wu *et al*., 2010).	Found in mesotrophic to eutrophic waters (Taylor *et al*., 2007a).	Moderate-High.
Fragilaria capucina Lange-Bertalot	LETS2	Benthic (Niyatbekov and Barinova, 2018).	Found in mesotrophic, circumneutral waters with moderate electrolyte content (Taylor *et al*., 2007a; Niyatbekov and Barinova, 2018).	Moderate.
Fragilaria construens Ehrenberg	CM1 LETS2	Planktonic and facultative planktonic (Fitchett *et al*., 2016a,b).	Clean, shallow waters, indifferent to salinity and tolerates ice, cold water, colder climatic conditions; where decreased abundances suggest warming and reflect an unstable and changing environment (Fitchett *et al.,* 2016a,b; Sitoe *et al*., 2017).	Moderate.
Fragilaria famelica Kützing	CM1 LETS2	Benthic (Fitchett *et al*., 2016a).	Snow tolerant, found in sodium-sulphate deeper standing, mesotrophic waters levels with elevated conductivity but prefers nutrient rich waters (Fitchett *et al*., 2016a; Niyatbekov and Barinova, 2018). Alkalophilic, fresh-brackish with elevated mineral content (Antón-Garrido *et al*., 2013; Aude *et al*., 2020) metals and nutrients (Belando *et al.,* 2017).	Moderate-High.
Fragilaria fasciculata Lange-Bertalot	CM1 LETS2	Planktonic (Niyatbekov and Barinova, 2018).	Favours moderate to high electrolyte concentrations and found in critically polluted industrial wastewater (Taylor *et al*., 2007a).	High.
Fragilaria pinnata Ehrenberg	CM1 LETS2	Planktonic and facultative planktonic (Fitchett *et al.,* 2016a, b).	Clean, shallow waters, with moderate-high electrolyte content, reflects colder climatic conditions and an unstable and changing environment (Taylor *et al*., 2007a; Fitchett *et al.,* 2016a,b).	Moderate.
Fragilaria sp.	LETS2	Planktonic (Venter *et al*., 2013).	Oligo-mesotrophic conditions, r-strategists and tolerate harsh, unstable and changing environments (Fitchett *et al*., 2016a,b; Bartozek *et al.,* 2018).	Diverse.
Fragilaria ulna Lange-Bertalot	CM1 LETS2	Benthic (Taylor and Cocquyt, 2016).	Alkaline meso-eutrophic lakes with low-moderate conductivity (Taylor *et al*., 2007a; Taylor and Cocquyt, 2016).	Moderate-High.
Gomphonema clavatum Ehrenberg	LETS2	Epilithic (Taylor *et al*, 2007a).	Found in oligotrophic waters with high electrolyte content (Taylor *et al*, 2007a).	Low.
Gomphonema minutum Agardh	CM1 LETS2	Epiphytic and epipelic (Wojtal, 2003).	Eutrophic waters but not tolerant of more than moderate levels of pollution (Taylor *et al*., 2007a).	Moderate.
Gomphonema parvulum Kützing	CM1 LETS2	Epiphytic, epipelic, epilithic (Wojtal, 2003).	Found in high mineralization levels of water (Aude *et al*., 2020). Tolerant of extremely polluted conditions and indicates anthropogenic impact (Schneck *et al*., 2007; Çelekli *et al*., 2018).	High.
Gomphonema sp.	CM1	Benthic (Taylor and Cocquyt, 2016).	Range of waters with low-moderate conductivity (Taylor and Cocquyt, 2016; Sitoe *et al*., 2017). Oligo-eutrophic waters and indicates eutrophication and pollution (Taylor and Cocquyt, 2016; Sitoe *et al*., 2017).	Diverse
Gyrosigma acuminatum (Kützing) Rabenhorst	LETS2	Epipelic, epilithic (Taylor *et al*., 2007a).	Electrolyte rich to brackish, mesotrophic waters and tolerates critical levels of organic pollution (Taylor *et al*., 2007a; Niyatbekov and Barinova, 2018).	High.
Gyrosigma sp.	LETS2	Benthic (Taylor and Cocquyt, 2016).	Range of oligo-eutrophic waters with low-moderate conductivities (Taylor and Cocquyt, 2016).	Diverse.

Hantzschia amphioxys (Ehrenberg) Grunow	CM1 LETS2	Aerophilic (Jahn *et al*., 2014).	Periodically dry habitats, washed in with soils (Taylor *et al*., 2007a; Fitchett *et al*., 2016b). High tolerance for disturbance (Antonelli *et al*., 2017) found in soil polluted by mining waste (Minaoui *et al*., 2021).	High
Melosira varians Agardh	LETS2	Planktonic (Taylor *et al*., 2007a).	Slightly brackish but eutrophic waters and is tolerant of organic pollution (Schneck *et al*., 2007; Taylor *et al*., 2007a; Yang *et al*., 2020).	High.
Navicula antonii Lange-Bertalot	CM1 LETS2	Benthic (Oğuz *et al*., 2020).	Waters with moderate-high electrolyte content, (hyper)eutrophic, tolerant of strongly polluted conditions, good indicator for anthropogenic impacts (Taylor *et al.,* 2007a).	High.
Navicula erifuga Müller	LETS2	Benthic (Oğuz *et al*., 2020).	Brackish waters with a high electrolyte content, eutrophic waters and tolerates critical pollution levels (Taylor *et al*., 2007a).	High.
Navicula goeppertiana Bleish	CM1	Aerophilic (Sitoe *et al*., 2015).	Sub-aerial and electrolyte rich environments, found in eutrophic waters and tolerant of heavily polluted conditions (Schneck *et al*., 2007; Taylor *et al*., 2007a).	High.
Navicula sp.	CM1	Non-planktonic taxa (Zaky et al., 2020).	Increase in abundance may reflect lake shallowing, low flooding and arid/hyper arid conditions (Zaky et al., 2020). Abundant in areas with moderate disturbance (Antonelli *et al*., 2017) but found in treated wastewaters with increased organic matter (Minaoui *et al*., 2021).	Diverse.
Navicula trivialis Lange-Bertalot	CM1 LETS2	Benthic (Oğuz *et al*., 2020).	Moderate electrolyte content, eutrophic waters and is tolerant of desiccation and strongly polluted conditions (Taylor *et al*., 2007a; Çelekli *et al*., 2018).	High.
Navicula veneta Kützing	CM1 LETS2	Benthic (Taylor *et al*., 2007a; Niyatbekov and Barinova, 2018).	Alkaline, electrolyte rich-brackish waters and indicates organic pollution, eutrophicated waters; species is very pollution tolerant and dominant in industrially impacted waters (Taylor *et al*., 2007a; Yang *et al*., 2020).	High.
Nitzschia acidoclinata Lange-Bertalot	CM1	Epiphytic (Földi *et al*., 2018).	Found in oligotrophic, electrolyte-poor and slightly acidic waters (Taylor *et al*., 2007a).	Low-Moderate.
Nitzschia amphibia Grunow	CM1	Benthic (Sitoe *et al*., 2017).	Found in electrolyte poor-rich waters and indicates eutrophication and pollution (Taylor *et al*., 2007a; Sitoe *et al*., 2017).	High.
Nitzschia palea Kützing	LETS2	Epilithic, (Taylor *et al*., 2007).	Waters with moderate-high electrolyte content, tolerant of hypereutrophic conditions and organic pollution (Taylor *et al*., 2007a; Bannister *et al*., 2019).	High.
Nitzschia sp.	CM1 LETS2	Epiphytic, epilithic, epipelic (Lowe, 2003).	Lower salinity, weaker winds, reduced mixing and stronger stabilization of the water column, reflects warmer conditions and decrease in *Aulacoseira sp.* (Sivarajah *et al*., 2018; Zaky *et al*., 2020). Abundant in areas with moderate disturbance (Antonelli *et al*., 2017) but found in treated wastewaters with increased organic matter (Minaoui *et al*., 2021).	Diverse-High
Pinnularia borealis Ehrenberg	CM1 LETS2	Aerophilic (Sitoe *et al*., 2015).	Aerial habitats, slightly alkaline environments and indicates increased organic matter (Taylor *et al*., 2007a; Humane *et al*., 2020).	Moderate.
Pinnularia divergens Smith	CM1 LETS2	Aerophilic (Beck *et al*., 2020).	Found in electrolyte-poor waters with oligotrophic conditions but reflects acidic waters (Taylor *et al*., 2007a).	Moderate
Pinnularia viridis Ehrenberg	CM1 LETS2	Benthic (Cohn, 2001).	Indicating circumneutral waters with low-moderate electrolyte content and indicating oligo-mesotrophic waters with low-moderate organic pollution (Taylor *et al.,* 2007a; Yang *et al*., 2020).	Low-Moderate.
Rhopalodia gibba Ehrenberg	CM1 LETS2	Epiphytic, epilithic, epipelic (Lowe, 2003).	Oligo-mesotrophic waters with moderate-high electrolyte content (Taylor *et al*., 2007a; Niyatbekov and Barinova, 2018).	Low-Moderate.

Stauroneis phoenicentron Ehrenberg	CM1	Benthic (Niyatbekov and Barinova, 2018).	Meso-eutrophic waters, sometimes polluted lakes (Taylor *et al*., 2007a; Niyatbekov and Barinova, 2018).	Moderate-high.
Surirella ovalis Brébisson	CM1	Benthic (Niyatbekov and Barinova, 2018).	Found in mesotrophic waters with high electrolyte content (Taylor *et al*., 2007a; Niyatbekov and Barinova, 2018).	Moderate.

6.2.2. Evidence of Pollutants.

Lakes may contain high pollution levels, which are related to the surrounding environment and can reduce overall water quality; with the level of impact dependent on properties such as the level of toxicity and the lifetime of the particular pollutant (Hicks, 2020). Direct indicators of industrial contamination in lake systems includes anthropogenic N deposition and Hg, which can provide evidence of possible industrial contamination (Curtis *et al*., 2010). Agricultural practices release fertilizers which enter lakes and cause elevated levels of N and P, often leading to eutrophication of the system (Hicks, 2020); where pesticides including polychlorinated biphenyl (PCBs) may be found in sediments such as at Letšeng-la Letsie (Rose *et al*., 2020). Nutrient loading from agricultural practices can accelerate carbon fixation by algae (Vander Zanden and Vadeboncoeur, 2020) and in turn the nutrient signals in diatom assemblages can be used to indicate anthropogenic impacts within a lake system (Wolin and Stone, 2010). However, it is difficult to disentangle which pollutant diatoms are responding to in many instances.

Diatoms can be used for biomonitoring of organic pollutants and heavy metals in aquatic systems (Datta *et al*., 2019) providing information about changing pollutant loading through shifts between oligotrophic and eutrophication tolerant taxa and more generally, between pollutant tolerant and intolerant species including of heavy metals such as Hg. Limiting and non-limiting resources favour certain species that are superior competitors at particular resource ratios, and once the resource ratios are changed, these species may suffer from a loss of competitiveness and will probably be replaced by other species (Lei *et al*., 2021). Some diatom species are very tolerant to a wide-range of

ecological variance, where other species have tolerance levels that are distinct and narrow optima for many environmental variables (Datta *et al*., 2019).

Individual diatom species have specific nutrient requirements over a broad spectrum of lake trophic status, making them indicators of nutrient concentration (Lei *et al*., 2021). Diatoms may respond to nutrient flux by changing their community structure as a species response where certain species dominate nutrient-rich waters and others prefer nutrient-depleted conditions (Datta *et al*., 2019). Diatom communities mainly dominated with oligotrophic species are potentially indicative of weak anthropogenic impacts (Wu *et al*., 2022). Oligotrophic species include for example *Gomphonema clavatum, Caloneis schumanniana* and both *Fragilaria pinnata and Fragilaria construens* (Fitchett *et al*., 2016a,b; Buczkó *et al*., 2019). *Achnanthes minutissima* is both a species associated with oligotrophic conditions and is considered a pollution sensitive species (Benhassane *et al*., 2020). Other pollution sensitive species include *Cocconeis placentula* and *Gomphonema minutum* (Datta *et al*., 2019; Benhassane *et al*., 2020). The planktonic species *Cyclotella pseudostelligera* for example is sensitive to metals (Hansika and Yatigammana, 2019). A shift from species indicative of oligotrophic lake conditions to those indicative of eutrophication within the system is suggestive of increased pollution within the aquatic system (Fontana *et al*., 2014).

Shifts from oligotrophic diatom species such as *Eunotia sp.* to eutrophic species such as *Aulacoseira granulata*, *Aulacoseira ambigua, Cyclotella meneghiana* and *Nitzschia sp.* is indicative of higher nutrient concentrations in lakes (e.g. Fontana *et al*., 2014; Wu *et al*., 2022). Centric diatoms tend to be favoured in nitrogen-enriched environments, such as the planktonic species *Aulacoseira granulata* which are known for their high N requirements and have been defined as a typical indicator of eutrophic waters (Lei *et al*., 2021). Other species indicative of eutrophic lake conditions includes *Diploneis subovalis* (Tuturí *et al*., 2021) and of organic pollution within the system such as *Nitzschia*

sp. (Minaoui *et al*., 2021) including *Nitzschia palea* (Datta *et al*., 2019) and the aerophilic *Pinnularia borealis* (Humane *et al*., 2020). Diatoms exist in almost all aquatic environments and are found in industrial wastewaters, due to their ability to bind heavy metals and assimilate N and P (Chonova *et al*., 2019). Species such as the planktonic *Cyclotella meneghiniana* is indictive of (hyper)eutrophic conditions and is a species tolerant of wastewater and industrial pollution (Fontana *et al*., 2014). Benthic species including *Fragilaria famelica* and *Fragilaria capucina* are indicative of organic pollution and of heavy metals within the system (Belando *et al*., 2017; Datta *et al*., 2019). The effects of heavy metals on diatom assemblages are observed in the absence of the most sensitive taxa and increase in relative abundance of the most tolerant taxa (e.g. Fontana *et al*., 2014). Other species considered extremely pollution tolerant includes *Nitzschia palea* and *Gomphonema parvulum* (Datta *et al*., 2019).

The results from this study indicate that there has been nutrient enrichment in Lake Chrissie from the early ~1930s to the early ~2000s and thereafter between the mid ~2010s and during 2017 at the core surface. Periods of greatest evidence of industrial related pollution in Lake Chrissie is between the late ~1950s to the to the mid ~2010s. The Letšeng-la Letsie results indicate that there has been increased nutrient enrichment with the greatest evidence of hypereutrophic and industrially polluted conditions between the ~1960-1980s and from the ~2010s to the core surface. Periods of least evidence of pollution in Lake Chrissie and Letšeng-la Letsie occurs prior to the ~1930s. Ther are however multiple stressors aside from eutrophication and heavy metal contamination that influence diatom communities and include hydrological changes within the system (Fontana *et al*., 2014).

6.2.3. Habitats and Water Depth

Diatom assemblage compositions change across a water depth gradient within a lake (Buczkó *et al*., 2019; Zou *et al*., 2020) and water depth changes in freshwater systems are often recorded from increases in planktonic diatoms (Wolin and Stone, 2010). Planktonic diatoms, however, may not be

sensitive indicators of water depth by themselves, but are when observing the ratio of planktonic to benthic diatom species (Westover *et al*., 2019; Zou *et al*., 2020). Benthic species such as *Fragilaria famelica* for example are indicative of deeper standing waters when in abundance (Niyatbekov and Barinova, 2018). The planktonic species *Aulacoseira granulata* is indicative of increased water levels (Buczkó *et al.,* 2019) where the planktonic species *Cyclotella meneghiniana* and benthic *Amphora ovalis* are indicative of lake shallowing (Dulanya and Trauth, 2019; Zaky *et al*., 2020). *Nitzschia sp*. indicates increased stratification of the water column (Zaky *et al*., 2020).

The Lake Chrissie diatom record results indicate deeper waters in the ~1950s to the early ~1960s and from the ~1970s to the mid ~1990s, predominantly indicated by the increased abundance of *Fragilaria famelica,* which was the most dominant benthic species in the Lake Chrissie core. These periods are interrupted with periods of shallow waters during the ~1940s, in the late ~1960s, the late ~1990s to the early ~2000s and from the early ~2010s to 2017 at the core surface. Increased lake levels are found between the mid ~2000s and the early ~2010s within the Lake Chrissie profile. Letšeng-la Letsie profile is characterised with more fluctuations in lake levels, with deeper waters found between the early ~1930s and mid ~1960s along with during the ~1990s, which is interrupted with fluctuating but increased lake levels between the late ~1960-1980s and from the early ~2000s to 2018 at the core surface. *Aulacoserira granulata* is the most abundant planktonic species in the Letšeng-la Letsie core and predominantly indicates water depth changes (Buczkó *et al.,* 2019). The benthic to planktonic ratio is therefore associated with fluctuations in water levels (Fontana *et al*., 2014) but periods dominated with aerophilic species, relative to those dominated by benthic and planktonic species, can be interpreted as representing drier climatic conditions (Fitchett *et al*., 2016a). The aerophilic species *Hantzschia amphioxys* in abundance is indicative of drier climatic conditions (Fitchett *et al*., 2016b). Climate changes, as shifts between wetter and drier periods are usually inferred indirectly in palaeolimnological studies from evidence for water-level changes (Wolin and Stone, 2010).

6.3. Paleoenvironmental Reconstruction

Biotic proxies such as preserved diatoms are often used to reconstruct environmental impacts and ecosystem changes on lake ecosystems (Burge *et al*., 2017; Adams *et al*., 2019). These organisms are used in palaeoenvironmental reconstructions as they preserve well in sediments, their autecologies are well known and they rapidly respond to environmental change (Dulanya *et al*., 2019). The analyses of a single proxy can provide specific stressor identification, such as the historical deposition of metal waste in lakes, from industrial and mining activities (Burge *et al*., 2017; Dulanya *et al*., 2019). Paleoenvironmental reconstructions for Lake Chrissie and Letšeng-la Letsie are made based on inferences of the identified diatom species and their autecologies (Table 6.1) and the stratigraphic diagrams observed as Figure 5.7 and Figure 5.8.

6.3.1. Lake Chrissie

6.3.1.1. Zone CM1Z2, from ~1780s to the mid ~1990s (25.75-13.25cm)

Zone CM1Z2 represents the oldest section of the core profile spanning ~220-years (Figure 5.7). All 36 identified diatom species were found within this zone with varying abundances (Figure 5.7). The planktonic and facultative planktonic species *Eupodiscus radiatus* is the most dominant species in this zone with an average abundance of 54.5% (Table 6.1). *Eupodiscus radiatus* abundances range from 0% in the ~1800s to a maximum occurrence during the ~1780-1790s and the ~1880s of 100%, respectively (Figure 5.7). When in abundance *Eupodiscus radiatus* may be indicative of lower lake trophic conditions and drier climates, with increased salinity (Varona-Cordero *et al*., 2010; Perez *et al.,* 2017). An overall decrease in this species abundance allows one to suggest increasing lake trophic conditions and decreasing salinity (Table 6.1). The benthic species *Fragilaria famelica* has an average occurrence of 9.1% and is the second most dominant species in zone CM1Z2 (Table 6.1). *Fragilaria* famelica abundances range from 0% in 12 depth samples, to a maximum in the early ~1960s with 60% (Figure 5.7). An increase in *Fragilaria famelica* may indicate nutrient enriched, deeper waters with

colder climates (Fitchett *et al*., 2016a; Belando *et al.,* 2017). The planktonic species *Cyclotella meneghiana* is the third most dominant species in zone CM1Z2 with an average appearance of 5.5% (Table 6.1). *Cyclotella meneghiana* abundances range from 0% in 17 of the 26 depth samples, to a maximum of 50% within the ~1800s (Figure 5.7). An increase in *Cyclotella meneghiana* indicates eutrophic waters with organic enrichment, lake shallowing and highly evaporative climatic conditions (Sitoe *et al*., 2017; Dulanya *et al*., 2019).

6.3.1.1.1. Pollution Trends

Spanning ~110-years between the start of the core from the ~1780-1880s there is little indication of pollution trends; however the 100% abundance of *Eupodiscus radiatus* during the ~1780s and the ~1880s may be indicative of periods with lower trophic conditions (Varona-Cordero *et al*., 2010; Perez *et al.,* 2017). During the ~1820s and the ~1850s there is an abrupt increase in *Fragilaria famelica* abundances to 9.1% and to 22.2% from short-lived absences, respectively (Figure 5.7). An increase in *Fragilaria famelica* may indicate periods of nutrient enrichment (Fitchett *et al*., 2016a; Belando *et al.,* 2017). The results show that overall during these ~110-years there are lower trophic conditions potentially interrupted with periods of nutrient enrichment during the ~1820s and the ~1850s.

Over the next four decades from the early ~1890-1920s, there is an overall increase in *Eupodiscus radiatus* abundances from 57.1% to 80%, respectively (Figure 5.7). *Eupodiscus radiatus* may overall indicate lower trophic conditions during these decades (Varona-Cordero *et al*., 2010; Perez *et al.,* 2017). From a 100% abundance in the ~1880s, *Eupodiscus radiatus* decreases to 57.1% in the early ~1890s, then abruptly increases to 90% in the late ~1890s , followed by a decrease during the ~1900s to 61.5% (Figure 5.7). The decrease in *Eupodiscus radiatus* to 57.1% in the early ~1890s coincides with an abrupt increase in the benthic species *Fragilaria famelica* to 7.1% along with the epiphytic, epilithic and epipelic species *Gomphonema minutum,* respectively (Figure 5.7). This decrease in *Eupodiscus*

radiatus is indicative of increasing trophic conditions where the coinciding increase in *Fragilaria famelica* and *Gomphonema minutum* may support this as they are both indicative of increasing nutrient enrichment within the system (Varona-Cordero *et al*., 2010; Perez *et al.,* 2017). The decrease in *Eupodiscus radiatus* abundances to 61.5% during the ~1900s coincides with an increase in the benthic species *Surirella ovalis* to 15.4% and *Fragilaria famelica* to 7.7% from short-lived absences in the late ~1890s, respectively (Figure 5.7). *Surirella ovalis* and *Fragilaria famelica* are both indicative of mesotrophic waters (Belando *et al.,* 2017; Niyatbekov and Barinova, 2018). Overall, the results show that this ~40-year period may indicate fluctuating lake trophic conditions, but with overall lower trophic conditions suggested. However, this is interrupted with periods of increased nutrient enrichment in the early ~1890s and the ~1900s, respectively.

Over the next five decades from the ~1930-1970s there is an overall decrease in the planktonic sum from 66.6% to 3.1%, respectively (Figure 5.7). A decrease in the planktonic sum coincides with the overall decrease in *Eupodiscus radiatus* abundances from 58.3% to 3.1%, respectively (Figure 5.7). The results show that this overall decrease indicates a period of increasing lake trophic conditions (Varona-Cordero *et al*., 2010; Perez *et al*., 2017). This is supported by the overall increase in the benthic sum from 4.2% to 56.3% and in the epiphytic, epilithic and epipelic species sum from 8.4% to 15.6% during this ~50-year period (Figure 5.7). There is additionally an increase in benthic species such as *Surirella ovalis* to 25% in the late ~1930s from an absence since the ~1990s with 15.4% (Figure 5.7). This species is predominantly indicative of mesotrophic waters (Niyatbekov and Barinova, 2018). From an absence in the core since the early ~1930s there is an increase during the ~1940s in the planktonic species *Cyclotella meneghiana* to 25% (Figure 5.7). *Cyclotella meneghiana* is indicative of eutrophic waters and is often associated with organic pollution (Sitoe *et al*., 2017; Dulanya *et al*., 2019).

Other benthic species that increase between the ~1930-1970s includes *Fragilaria famelica* to 22.2% in the early ~1950s, following a sustained absence since the ~1910s with a 28.6% abundance (Figure 5.7). *Fragilaria famelica* is indicative of mesotrophic waters but is a species that prefers a more nutrient-rich environment (Fitchett *et al*., 2016a). The epiphytic, epilithic and epipelic species *Cymbella cistula* made its first appearance in the core profile with 11.1% in the early ~1950s and is indicative of mesotrophic lake conditions (Taylor *et al.,* 2007a; Fitchett *et al*., 2016a). In the late ~1950s there is an abrupt increase to 5.6% in both the planktonic species *Fragilaria fasciculata* from an absence since the late ~1890s and the first identification in the core of the epiphytic, epipelic and epilithic species *Gomphonema parvulum* (Figure 5.7). *Fragilaria fasciculata and Gomphonema parvulum* are both species indicative of polluted conditions such as of industrially derived wastewaters (Taylor *et al*., 2007a; Çelekli *et al*., 2018).

The benthic species *Fragilaria famelica* increases to 60% in the early ~1960s from a short-lived absence during the ~1950s followed by an abrupt decrease in the late ~1960s to 4.8 % (Figure 5.7). *Fragilaria famelica* when in abundance is indicative of mesotrophic lake conditions that are potentially more nutrient enriched (Fitchett *et al*., 2016a; Belando *et al.,* 2017). The increases of *Fragilaria famelica* abundances in the early ~1960s coincides with an increase in *Aulacoseira sp*. to 14.3% from a short-lived absence in the early ~1960s and of *Cyclotella meneghiana to* 9.5% from an absence since ~1940s with 25% (Figure 5.7). Both *Aulacoseira sp*. and *Cyclotella meneghiana* are indicative of meso-eutrophic lake waters (Stager and Johnson, 2000; Beck *et al*., 2019) with the potential of organic enrichment (Sitoe *et al*., 2017; Dulanya *et al*., 2019). *Fragilaria famelica* increases to 15.6% in the late ~1970s from 10% in the early ~1970s and indicates a mesotrophic to nutrient-rich environment (Fitchett *et al*., 2016a). Other notable benthic species that increase in the late ~1970s include: the first identification of *Navicula antonii* with 9.4%, *Anomoeneis sphaerophora* with 6.3% and *Navicula veneta* with 3.1%, in the core (Figure 5.7). Collectively *Navicula antonii*, *Anomoeneis sphaerophora* and

Navicula veneta are indicative of eu-hypereutrophic waters with critical levels of (organic)pollution and are good indicators of industrially impacted waters (Taylor *et al.,* 2007a; Yang *et al*., 2020). Overall, the results show that this ~50-year period spanning the ~1930s-1970s has periods of increasing nutrient enrichment with a shift from mesotrophic to more eutrophic lake conditions. Additionally, the results show that there is evidence from the diatom record of industrially derived pollution specifically within the late ~1950s and the late ~1970s.

Over the next ~20-years from the early ~1980s to the mid ~1990s, the planktonic species *Fragilaria pinnata* and *Fragilaria construens* both increase from 5.2% to 5.6% and to 12.9%, respectively (Figure 5.7). *Fragilaria pinnata* and *Fragilaria construens* are both indicative of an unstable and changing environment (Fitchett *et al.,* 2016a,b). There is an increase from 2.6% in the early ~1980s to 8.2% in the early ~1990s in *Fragilaria fasciculata* abundances (Figure 5.7) and it is a species that indicates critically polluted industrial wastewaters (Taylor *et al*., 2007a). Benthic species such as *Surirella ovalis* increase from 0.9% in the late ~1980s to 6.4% in the in the early ~1990s and indicate meso-eutrophic waters (Niyatbekov and Barinova, 2018). There is an increase in *Anomoeneis sphaerophora* abundances to 4.7% in the early ~1990s from an absence since the late ~1970s with 6.3% (Figure 5.7). *Anomoeneis sphaerophora* is indicative of waters with critical levels of pollution (Taylor *et al*., 2007a; Dulanya *et al*., 2019).

Nitzschia amphibia first appears in the core with 13.5% in the late ~1980s, followed by a short-lived absence in the early ~1990s and an abrupt increase in the mid ~1990s to 13.1% (Figure 5.7). *Nitzschia amphibia* is indicative of eutrophication and pollution within the system (Taylor *et al*., 2007a; Sitoe *et al*., 2017). There is also an increase in *Navicula trivialis* abundances to 2.8% in the mid ~1990s from the early ~1990s with a short-lived absence (Figure 5.7). *Navicula trivialis* is tolerant of desiccation and strongly polluted conditions (Taylor *et al*., 2007a; Çelekli *et al*., 2018). Additionally there is an overall

increase in *Cyclotella meneghiana* in the mid ~1990s to 5.6% from 1.8% in the early ~1990s, indicating eutrophication and organic enrichment within the system (Sitoe *et al*., 2017; Dulanya *et al*., 2019). Overall, the results show that over a ~20-year period from the early ~1980s to the mid-1990s, Lake Chrissie had industrially derived pollution specifically in the early ~1980s with eutrophication, increased organic enrichment and pollution suggested.

6.3.1.1.2. Water Depth Changes

Spanning ~80-years between the start of the core from ~1780-1850s the planktonic assemblages' total sum overall decreases from a peak of 100% to 77.8%, respectively (Figure 5.7). There is an abrupt appearance in the planktonic and facultative planktonic species *Cyclotella meneghiana* with a 50% abundance during the ~1800s and this may indicate a period of shallow waters (Dulanya and Trauth, 2019; Dulanya *et al*., 2019). During the ~1820s the benthic sum is introduced with 18.2% which is followed by a short-lived absence during the ~1830s and abrupt reappearance thereafter during the ~1850s to 22.2% (Figure 5.7). This coincides with an introduction of *Fragilaria famelica* with 9.1% during the ~1820s and increase thereafter to 22.2% in the ~1850s from the ~1830s with a short-lived absence (Figure 5.7). *Fragilaria famelica* is indicative of deeper waters when in abundance (Fitchett *et al*., 2016a; Belando *et al.,* 2017).

Over the next seven decades from ~1860-1920s there is an overall increase in the planktonic and facultative planktonic sum from 88.9% to 100%, respectively (Figure 5.7). This coincides with the abrupt increase in *Cyclotella meneghiana* to 21.4% during the early ~1890s following an absence in the core since 50% in the ~1800s (Figure 5.7). *Cyclotella meneghiana* is indicative of periods of shallow waters (Dulanya and Trauth, 2019; Dulanya *et al*., 2019). There is an increase in the benthic sum to 23.1% in the ~1900s from a short-lived absence in the late ~1890s followed by an increase during the ~1910s to 28.6% (Figure 5.7). This positive trend coincides with an increase in the benthic species

Fragilaria famelica to 7.7% in the ~1900s and a direct increase thereafter during the ~1910s to 28.6% (Figure 5.7). *Fragilaria famelica* is indicative of deeper waters when in abundance (Fitchett *et al*., 2016a; Belando *et al.,* 2017). Additionally during the ~1900s, there is also an increase in the planktonic species *Cyclotella meneghiana* to 7.7% from a short-lived absence in the late ~1890s and is indicative of periods of shallow waters (Dulanya and Trauth, 2019; Dulanya *et al*., 2019). Thereafter, *Cyclotella meneghiana* increases to 20% during the ~1920s from the ~1910s with a short-lived absence (Figure 5.7). Overall, the results show that this ~150-year period from ~1780-1920s may reflect shifts between planktonic and benthic species indicative of fluctuating lake levels. Shallow waters are suggested from the results during the ~1800s, the late ~1890s and the ~1920s and interrupted with deeper waters during the ~1820s, the ~1850s, the ~1900s and during the ~1910s. Interestingly, Wellington (1943) states that local farmers recorded Lake Chrissie to have dried out in the years 1901-03.

Over the next four decades from the ~1930-1960s the planktonic assemblages' total sum overall decreases from 66.6% to 57.1% and the benthic sum increases from 4.2% to 38.2%, respectively (Figure 5.7). There is an abrupt increase in the planktonic species *Cyclotella meneghiana* abundances to 25% during the ~1940s and to 9.5% in the late ~1960s, from brief absences in the late ~1930s and the early ~1960s, respectively (Figure 5.7). *Cyclotella meneghiana* indicates periods of shallow waters when in abundance (Dulanya and Trauth, 2019; Dulanya *et al*., 2019). This is interrupted with abrupt increases in the benthic species *Fragilaria famelica* to 22.2% in the early ~1950s from an absence since the ~1910s with a sum of 28.6% (Figure 5.7). Thereafter there is an increase in *Fragilaria famelica* abundances to a peak of 60% in the early ~1960s from the late ~1950s with a short-lived absence (Figure 5.7). *Fragilaria famelica* indicates periods of deeper waters when in abundance (Fitchett *et al*., 2016a; Belando *et al.,* 2017). Thereafter, between the early ~1970s to the mid ~1990s the planktonic assemblages' total sum overall decreases from 55% to 38.1% and the benthic sum increases from 20% to 46.6%, respectively (Figure 5.7). This positive trend coincides with an overall increase in the benthic

species *Fragilaria famelica* abundances from 10% to 11.6%, respectively with a peak of 19.3% in the late ~1980s from the early ~1980s with 18.3% (Figure 5.7). *Fragilaria famelica* is indicative of deeper lake waters during these decadal periods (Fitchett *et al*., 2016a; Belando *et al.,* 2017). Overall, the results show that this ~40-year period may be indicative of fluctuations in water depth from shallow waters during the ~1940s shifting to deeper waters in the early ~1950s to the early ~1960s; followed by shallow waters in the late ~1960s and deeper waters from the ~1970s to the mid ~1990s.

6.3.1.1.3. Climate Trends

From the start of the core from ~1780-1920s spans ~150-years. During the ~1800s the planktonic and facultative planktonic species *Cyclotella meneghiana* and the epiphytic, epipelic and epilithic species *Nitzschia sp.,* are first identified in the core with 50% abundance, respectively (Figure 5.7 *Cyclotella meneghiana* is indicative of high evaporation and drier climatic conditions (Sitoe *et al*., 2017; Dulanya *et al*., 2019) and *Nitzschia sp.* indicates warmer climatic conditions (Sivarajah *et al*., 2018; Zaky *et al*., 2020). Following short lived absences in the ~1800s there is an increase in the benthic sum to 18.2% during the ~1820s which coincides with an increase in *Fragilaria famelica* abundances to 9.1% (Figure 5.7). The increase in *Fragilaria famelica* could be indicative of a shift to colder climatic conditions (Fitchett *et al*., 2016a; Belando *et al.,* 2017). During the ~1830s the aerophilic sum and the species *Navicula goeppertiana* are introduced into the system with a respective 50% abundance (Figure 5.7) and indicates drier climatic conditions (Taylor *et al*., 2007a). There is an increase in the benthic sum to 22.2% in the ~1850s and coincides with the abrupt increase in *Fragilaria famelica* abundances to 22.2%, from the ~1830s with a short-lived absence (Figure 5.7) and is indicative of a shift to colder climatic conditions (Fitchett *et al*., 2016a; Belando *et al.,* 2017). There is an overall increase in the planktonic species *Eupodiscus radiatus* from 54.5% in the ~1820s to 80% in the ~1920s and is indicative of drier environmental conditions, over this ~110-year period (Varona-Cordero *et al*., 2010; Perez *et al.,* 2017).

There is an increase in the planktonic and facultative planktonic species *Cyclotella meneghiana* to 21.4% in the early ~1890s from a relatively prolonged absence since the ~1800s with an abundance of 50% (Figure 5.7). Thereafter this species increases to 7.7% in the ~1900s after a brief absence in the late ~1890s (Figure 5.7). This is followed by a by a brief absence once more in *Cyclotella meneghiana* abundances in the ~1910s and increase thereafter in the ~1920s to 20% (Figure 5.7). *Cyclotella meneghiana* indicates high evaporation and drier climatic conditions (Sitoe *et al*., 2017; Dulanya *et al*., 2019). An abrupt increase in *Fragilaria famelica* to 7.1% in the early ~1890s and to 7.7% in the ~1900s is followed by an increase to 28.6% in the ~1910s (Figure 5.7) and is indicative of increasing colder climatic conditions (Fitchett *et al*., 2016a; Belando *et al.,* 2017). Overall, the results show that this ~150-year period may indicate drier environmental conditions, with specific increases identified during the ~1800s, the ~1830s, the early ~1890s, the ~1900s and during the ~1920s, respectively (Figure 5.7). It is additionally suggested that there is an overall increase in salinity between the ~100-year period between ~1820-1920s. Warming climatic conditions are suggested for the ~1800s with colder climates thereafter during the ~1820s and ~1850s and between the ~1890-1910s.

Over the next four decades from the ~1930-1960s there is an overall decrease in the planktonic sum from 66.6% to 57.1%, respectively (Figure 5.7). This negative trend is interrupted with an abrupt increase in the aerophilic sum to 20.9% in the early ~1930s from an absence since ~1890s with an abundance of 7.1% (Figure 5.7). Wellington (1943) states that local farmers recorded Lake Chrissie to have dried out again in 1933. Thereafter, the aerophilic sum increases to 25% in the ~1940s from the late ~1930s with a short-lived absence (Figure 5.7). Increased aerophilic species during the early ~1930s include the introduction of *Pinnularia borealis* with 12.5% and *Hantzschia amphioxys* with 4.2% (Figure 5.7). There is additionally an increase in *Navicula goeppertiana* to 4.2% from a relatively prolonged absence since the ~1830s with 50% (Figure 5.7). *Pinnularia borealis, Hantzschia amphioxys* and *Navicula goeppertiana* collectively indicate drier environmental conditions (Fitchett *et al*., 2016b;

Humane *et al*., 2020). There is an abrupt increase in *Hantzschia amphioxys* to 25% during the ~1940s from a short-lived absence in the late ~1930s with 4.2% (Figure 5.7). *Hantzschia amphioxys* predominantly indicates a periodically drier environment (Fitchett *et al*., 2016b). There is also an increase in species such *Cyclotella meneghiana* to 25% during the ~1940s from an absence since the ~1920s with 20% (Figure 5.7) and is a species that can tolerate highly evaporative conditions (Sitoe *et al*., 2017; Dulanya *et al*., 2019). There is an increase in the late ~1960s in *Cyclotella meneghiana* abundances to 9.5%, from an absence the late ~1930s with 25% (Figure 5.7). *Cyclotella meneghiana* can tolerate highly evaporative conditions (Sitoe *et al*., 2017; Dulanya *et al*., 2019). *Amphora ovalis* is first identified within the system in the late ~1960s with 28.6% (Figure 5.7) and is indicative of hyper-arid conditions (Humane *et al*., 2020; Zaky *et al*., 2020).

This drier cycle is interrupted with wetter climatic conditions in the late ~1950s as suggested from the increase in *Aulacoseira sp*. to 27.8% (Figure 5.7). Colder climatic conditions are suggested in the early ~1950s and the early ~1960s as suggested from the abrupt increase in *Fragilaria famelica* to 22% from an absence since the ~1910s with 28.6%; along with the peak to 60% after a brief absence in the ~1950s, respectively (Figure 5.7). These colder periods are interrupted with warmer climates suggested in the late ~1950s with the abrupt increase in *Nitzschia sp.* abundances to 11.1% from an absence in the core since the early ~1930s with 4.2% (Figure 5.7). Overall, the results show that this ~40-year period may predominantly indicate drier climatic conditions with high evaporation within the in the early ~1930s, in the ~1940s and in the late ~1960s. This drier cycle is interrupted with wetter conditions in the late ~1950s. Colder climates are suggested for the early ~1950s and the early ~1960s, which are interrupted with warmer climates in the late ~1950s.

Over the next three decades spanning the early ~1970s, to the mid ~1990s the aerophilic sum overall increases from a short-lived absence to 3.7%, respectively (Figure 5.7). There is a peak in the aerophilic sum to 25% in the late ~1970s from the early ~1970s with a brief absence (Figure 5.7). This peak coincides with an abrupt increase in *Hantzschia amphioxys* to 9.4% from an absence since a 25% abundance in the ~1940s, of *Pinnularia borealis* to 12.5% and *Navicula goeppertiana* to 3.1% from 12.5% and 4.2% during the early ~1930s, respectively (Figure 5.7). These species collectively indicate periodically drier habitats (Taylor *et al*., 2007a; Humane *et al*., 2020). This peak in the late ~1970s additionally coincides with an increase in the epipelic species *Nitzschia sp.* to 9.4%; after a relatively prolonged absence since 11.1% in the late ~1950s and is indicative of warming environmental conditions (Zaky *et al*., 2020). Thereafter *Nitzschia sp*., increases to a peak of 11.3% in the early ~1980s. There is an abrupt increase of the benthic species *Amphora ovalis* from a 1.7% in the early ~1980s and in the late ~1980s to 13.2% (Figure 5.7) and is a species that indicates hyper-arid conditions (Humane *et al*., 2020; Zaky *et al*., 2020).

In the late ~1980s there is an additional increase in *Cyclotella meneghiana* to 5.1% from an absence in the core since the late ~1960s with an abundance of 9.5% (Figure 5.7). This species can tolerate highly evaporative conditions (Sitoe *et al*., 2017; Dulanya *et al*., 2019). There is an increase in *Hantzschia amphioxys* to 7.6% and *Pinnularia borealis* to 5.3% in the early ~1990s from 0.6% and 0.3% abundance in the late ~1980s and collectively indicate drier climatic conditions (Taylor *et al*., 2007a; Fitchett *et al*., 2016b). There is an increase in *Amphora ovalis* to 16.3% in the mid ~1990s from 4.1% in the early ~1990s and is indicative of hyper-arid conditions (Humane *et al*., 2020; Zaky *et al*., 2020). This additionally coincides with the respective increase in *Cyclotella meneghiana* to 4.7% from 0.6% and further indicates highly evaporative conditions (Sitoe *et al*., 2017; Dulanya *et al*., 2019). Overall, the results show that this ~30-year period may predominantly indicate drier environmental

conditions, with increased aridity and evaporative conditions specifically from the late ~1970s. Warmer climates are suggested in the late ~1970s and in the early ~1980s.

6.3.1.2. Zone CM1Z1 late ~1990s to 2017 (12.75- 0.25cm)

This zone represents the youngest section of the core profile spanning ~20-years (Figure 5.7). There were 27 of the 36 identified diatom species found within this zone with varying abundances; with 24 of these species found in relatively low abundances of <5% throughout this zone (Figure 5.7). *Eupodiscus radiatus* is the most dominant species in this zone and found in relatively high abundance in each sample, ranging from the highest maximum individual occurrence of 91.4% in the late ~2000s to the lowest in the early ~2010s of 30% (Figure 5.7). An increase in *Eupodiscus radiatus* is indicative of low trophic conditions or organic matter in the system, of drier environmental conditions and increased salinity (Varona-Cordero *et al*., 2010; Perez *et al*., 2017). This is followed by *Aulacoseira sp.* with a maximum individual occurrence of 64.7% in the early ~2010s and predominantly indicates meso-eutrophic waters, increased lake levels and wetter climatic conditions (Beck *et al*., 2019; Zaky *et al*., 2020). *Cyclotella meneghiana* is the third most abundant species within this zone, with 16% in the early ~2000s and is indicative of organically polluted and eutrophic, shallow waters since it is a species that can tolerate highly evaporative conditions (Sitoe *et al*., 2017; Dulanya *et al*., 2019).

6.3.1.2.1. Pollution Trends

In terms of pollution trends, there is an overall decrease in *Eupodiscus radiatus* abundances from 67% in the late ~1990s to 49.8% at the core surface (Figure 5.7). Th results show that this may indicate a period of increasing trophic conditions and organic matter within the system (Varona-Cordero *et al*., 2010; Perez *et al.,* 2017). This is supported by the increase in *Aulacoseira sp.* from a short-lived absence in the late ~1990s to 37.7% in 2017 and is indicative of meso-eutrophic lake conditions (Beck *et al*., 2019; Zaky *et al*., 2020). *Cyclotella meneghiana* increases from 7% the late ~1990s to 16% in the

early ~2000s to 8.6% in the mid ~2000s, from the early ~2000s with 7.8% (Figure 5.7). Thereafter there is a brief decrease in this species to 2% in the early ~2010s followed by an increase to 4.8% in the mid ~2010s and thereafter to a peak of 5.6% in 2017 (Figure 5.7). This species indicates eutrophication and organic enrichment within the system (Sitoe *et al*., 2017; Dulanya *et al*., 2019). There is an increase in the abundance of *Fragilaria fasciculata* during these three decal periods, albeit in relatively low concentrations (Figure 5.7) and it is a species that can be found in critically polluted industrial wastewater (Taylor *et al*., 2007a). This occurs in the late ~1990s, with an increase to 4.3% abundance from 0.9% in the mid ~1990s and an increase to 3% in the early ~2010s from 1% in the late ~2000s; along with an increase to 2.6% in the mid ~2010s from the mid ~2010s with 0.7% (Figure 5.7). Overall, the results show that this ~30-year period may predominantly indicate increasing organic and nutrient enrichment specifically within the early ~2000s and from the mid ~2010s to the core surface in 2017. Additionally, the results show that there is indication of industrially derived pollution in the late ~1990s, early ~2010s and in the mid ~2010s.

6.3.1.2.2. Hydro-climatology

Between the late ~1990s to the early ~2000s, there is an increase in *Cyclotella meneghiana* from 7% to 16%, respectively (Figure 5.7) and is indicative of shallower waters and increased evaporation (Sitoe *et al*., 2017; Dulanya *et al*., 2019). Additionally, there is an abrupt increase in *Amphora* ovalis in the early ~2000s to 4.2% from the late ~1990s with 0.3% (Figure 5.7) and is a species that indicates hyper-arid conditions (Humane *et al*., 2020; Zaky *et al*., 2020). There is an overall increase in the planktonic and facultative planktonic *Aulacoseira sp.* from 25.4% in the mid ~2000s to a peak of 64.7% in the early ~2010 and indicates increased lake levels and turbid lake waters along with wetter climatic conditions during this period (Beck *et al*., 2019; Zaky *et al*., 2020). However thereafter, this taxon shows a negative trajectory and decreases in abundance overall to 37.7% at the core surface during 2017 (Figure 5.7). This negative trend coincides with an overall increase in *Cyclotella meneghiana*

abundances from 2.9% in the early ~2010s to 5.6% in 2017 (Figure 5.7). This species indicates shallower waters and increased evaporation (Sitoe *et al*., 2017; Dulanya *et al*., 2019). Overall, the results show that this ~30-year period may be indicative of shallow waters and drier environmental conditions between the late ~1990s to the early ~2000s and during the early ~2010s to 2017. These periods of lower lake levels and drier environmental conditions are interrupted with increased lake levels and wetter climates between the mid ~2000s to the early ~2010s.

6.3.1.3. A Brief Summary

This lake system is characterised as nutrient enriched for ~80-90 years between the early ~1930s to the early ~2000s and between the mid ~2010s and during 2017, at the core surface. There is also indication that Lake Chrissie has had industrial related pollution fluctuations for ~50-years, suggested for the late ~1950s, the late ~1970s, the early ~1980s along with between the late ~1990s to the mid ~2010s. Fluctuating water levels are suggested throughout the core profile with peak periods of shallower waters for ~70-80 years, during the ~1800s, early ~1890s, the ~1920s, during the ~1940s, in the late ~1960s, the late ~1990s to the early ~2000s and from the early ~2010s to 2017. Increased lake levels and turbidity is suggested for between the mid ~2000s and the early ~2010s which is interrupted with deeper waters for ~70-years; during the ~1820s, the ~1850s, the ~1900s, the ~1910s, the ~1950s to the early ~1960s and from the ~1970s to the mid ~1990s. Warmer climatic conditions are suggested for ~40-years during the ~1800s, the late ~1950s and between the late ~1970s to the early ~1980s. Warmer conditions are interrupted with colder climates during the ~1820s, the ~1850s, between the ~1890-1910s, the ~1950s and in the early ~1960s. Drier environmental conditions are suggested for the ~1800s, the ~1830s, the early ~1890s, the ~1900s, the ~1920s, the early ~1930s, the ~1940s, the late ~1960s, late ~1970s and between the late ~1990s to the early ~2000s and from the early ~2010s to 2017 at the core surface. Wetter climatic conditions are suggested for the late ~1950s and between the mid ~2000s to the early ~2010s.

6.3.2. Letšeng-la-Letsie

6.3.2.1. Zone Lets2Z2 ~1850s to the ~1990s (28.25-11.25cm)

Zone Lets2Z2 represents the oldest section of the core profile spanning ~150-years (Figure 5.8). Of the 39 identified diatom species, 38 were found within this zone with varying abundances (Figure 5.8). The planktonic and facultative planktonic species *Aulacoseira granulata* is the most dominant species in this zone with an average abundance of 45.3% and with an occurrence ranging from a minimum of 10.5% in the early ~1950s to a maximum in the early ~1970s of 92.2% (Figure 5.8). There is a coinciding overall increase in the planktonic and facultative planktonic species sum from 28.5% to 54.3%, respectively and with an increase in *Aulacoseira granulata* abundances from 16.1% to 45.3%, respectively (Figure 5.8). When in abundance *Aulacoseira granulata* indicates mesotrophic waters, high lake levels and wetter climatic conditions (Buczkó *et al.,* 2019). The epiphytic and epilithic species *Cymbella cistula* is the second most dominant species in this zone, with an average occurrence of 9.9% and a range in abundances from a maximum of 26.1% in the late ~1950s to a minimum in the mid ~1980s of 1.7% (Figure 5.8). When in abundance *Cymbella cistula* is predominantly indicative of meso-eutrophic waters (Taylor *et al.,* 2007a). The epiphytic, epilithic, epipelic *Nitzschia sp.* was identified as the third most dominant species in this zone, with an average appearance of 7.7% and range in abundance from an absence in the late ~1920s and the in the early ~1970s, respectively, to a maximum in the early ~1990s of 21.1% (Figure 5.8). An increase in *Nitzschia sp*. is indicative of warmer environmental conditions (Zaky *et al*., 2020).

6.3.2.1.1. Pollution Trends

Spanning ~80-years between the start of the core during the ~1850s to the late ~1920s there is little indication of a pollution trend. However an overall increase in *Aulacoseira granulata* abundances from 16.1% to 89.6%, respectively may be indicative of mesotrophic waters (Buczkó *et al.,* 2019). Rather,

the results show that the diatom record during these decadal periods indicates hydro-climatological trends. However, over the next ~40-years from the early ~1930s to the mid ~1960s there is indication of increasing polluted conditions within Letšeng-la Letsie. There is an overall coinciding increase in the mid ~1960s in benthic species such as *Fragilaria famelica* to 5.9%, *Fragilaria capucina* to 4.9% along with *Navicula veneta* to 4.3% from 2.5%, 1.3% and 1.6% in the early ~1930s, respectively (Figure 5.8). Both *Fragilaria* species are indicative of mesotrophic and potentially more nutrient rich waters (Taylor *et al*., 2007a; Fitchett *et al*., 2016a). The presence of the pollution tolerant species *Navicula veneta* is indicative of organically polluted and eutrophicated waters that may be industrially impacted (Taylor *et al*., 2007a; Yang *et al*., 2020). There is an overall increase the epiphytic, epilithic and epipelic species *Nitzschia palea* from 1% in the early ~1930s and in the mid ~1960s to 3.3% (Figure 5.8). *Nitzschia palea* is tolerant of hypereutrophic and organically polluted waters (Taylor *et al*., 2007a; Bannister *et al*., 2019). This period is interrupted with an abrupt increase in the planktonic species *Fragilaria fasciculata* to 3.4% in the late ~1940s from the early ~1940s with 1.7% (Figure 5.8). *Fragilaria fasciculata* is found in critically polluted industrial wastewaters (Taylor *et al*., 2007a).

During the early ~1950s from the late ~1940s there is a coinciding abrupt increase in species including *Navicula veneta* to 13.7% from 4.3%; *Nitzschia palea* to 5.1% after a relatively sustained absence since 1% in the early ~1930s; *Navicula erifuga* to 3.8% from 0.6%; *Navicula trivialis* to 3.5% from 2.2%; *Gomphonema parvulum* to 2.5% from 1.2% and *Navicula antonii* to 2.5% from a short-lived absence, respectively (Figure 5.8). Collectively, the results show that these aforementioned six species indicate (hyper)eutrophic, organically enriched waters and strongly polluted conditions in industrially impacted waters (Taylor *et al*., 2007a; Çelekli *et al*., 2018; Bannister *et al*., 2019; Yang *et al*., 2020). During the mid ~1950s from the early ~1950s there is a coinciding increase in species including: *Gyrosigma acuminatum* to 5.6% from 1.9%; *Navicula antonii* to 3.9% from 2.5%; *Melosira varians* to 2.6% from a short-lived absence; *Gomphonema parvulum* to 2.6% from 2.5% and *Fragilaria fasciculata*

to 2% from a short-live absence, respectively (Figure 5.8). These five species collectively indicate anthropogenically impacted meso-eutrophic waters with critical levels of organic pollution (Taylor *et al*., 2007a; Çelekli *et al*., 2018; Niyatbekov and Barinova, 2018; Yang *et al*., 2020). During the mid ~1960s there is an abrupt increase in *Navicula erifuga* to 4.6% and *Navicula trivialis* to 3.9%, from the early ~1960s with 0.7% and 0.3%, respectively (Figure 5.8). Both of these *Navicula sp*. are indicative of eu-hypereutrophic waters with critical organic pollution levels (Taylor *et al*., 2007a; Çelekli *et al*., 2018). Overall, the results show that this ~40-year period is characterised by meso-eutrophic waters with indication of being industrially polluted in the late ~1940s, during the early and mid ~1950s.

Over the next two decades from the late ~1960-1980s there is an increase in species such as *Aulacoseira granulata* to 92.2% in the mid ~1970s from the early ~1970s with 57.7% (Figure 5.8). An increase in this species is indicative of mesotrophic waters (Buczkó *et al.,* 2019). From the mid ~1970s to the late ~1970s, both benthic species *Navicula veneta* and *Navicula antonii* increase from short-lived absences to 3.7% and to 2.2%, respectively (Figure 5.8). *Navicula veneta* and *Navicula antonii* further increase in the in the mid ~1980s to 3.7% and to 2.3%, respectively and from short-lived absences in the early ~1980s along with the benthic species *Navicula erifuga* to 3.7% from 0.3%, respectively (Figure 5.8). The three aforementioned *Navicula* taxa collectively indicate (hyper)eutrophic, strongly polluted conditions and industrially impacted waters, with *Navicula veneta* and *Navicula antonii* described as very pollution tolerant species (Taylor *et al*., 2007a; Yang *et al*., 2020). The epiphytic, epilithic and epipelic species *Gyrosigma acuminatum* abruptly increases in the mid ~1980s to 1.7% and thereafter to 12.8% from the early ~1980s with a brief absence in the core (Figure 5.8). *Gyrosigma acuminatum* tolerates critical levels of organic pollution (Taylor *et al*., 2007a; Niyatbekov and Barinova, 2018). Species that increase in abundance in the late ~1980s from the mid ~1980s include the benthic species *Navicula trivialis* to 8.8% from 2.9% along with the epiphytic, epilithic and epipelic species *Nitzschia palea* to 4.7% and *Gomphonema parvulum* to 3.8% (Figure 5.8).

Navicula trivialis, *Nitzschia palea* and *Gomphonema parvulum* are indicative of anthropogenic impact such as of eutrophic waters and organically polluted conditions (Taylor *et al*., 2007a; Çelekli *et al*., 2018; Bannister *et al*., 2019). Overall, the diatom results show that this ~20-year period is characterised by (hyper)eutrophic, strongly polluted conditions with industrially impacted waters, specifically from the mid ~1970-1980s. However, although the diatom record may suggest these conditions, the extremely remote and untouched nature of Letseng-la Letsie lends one to believe that this is rather unlikely and may instead be due to stronger hydrological and/or climatic signals.

During the ~1990s there is an overall increase in *Aulacoseira granulata* abundances from 29.9% to 45.3%, respectively (Figure 5.8) and indicates mesotrophic waters (Buczkó *et al.,* 2019). However, the increase in the benthic species *Fragilaria famelica* from 7.2% to 9.1% during this period potentially indicates a more nutrient rich environment (Taylor *et al*., 2007a; Fitchett *et al*., 2016a). Other benthic species that increase include *Caloneis schumannania* to 4.3% in the early ~1990s from 1.5% in the late ~1980s and in *Cymatopluera solea* to 5.9% from 1.2%, respectively (Figure 5.8). *Caloneis schumannania* is indicative of an unstable and changing environment and *Cymatopluera solea* is indicative of eutrophic waters (Taylor *et al*., 2007a). During the early ~1990s, *Navicula trivialis* abruptly increases to 5% from 0.7%, respectively (Figure 5.8). *Navicula trivialis* is indicative of eutrophic waters and strongly polluted conditions (Taylor *et al*., 2007a; Çelekli *et al*., 2018). In the mid ~1990s there is an increase in *Fragilaria ulna* to 5.2% from 0.9%, respectively (Figure 5.8) and is indicative of meso-eutrophic waters (Taylor *et al*., 2007a). Overall, the results show that this ~10-year period is characterised by meso-eutrophic waters and strongly polluted conditions.

6.3.2.1.2. Water Depth Changes

Spanning ~80-years during the ~1850s to the mid ~1920s, there is an overall increase in the planktonic sum from 28.5% to 89.6%, respectively (Figure 5.8). This coincides with an overall respective increase

in species abundances such as *Aulacoseira granulata* from 16.1% to 73.8% (Figure 5.8). *Aulacoseira granulata* is indicative of increasing lake levels when in abundance (Buczkó *et al.,* 2019). This is interrupted however in the ~1870s with an abrupt increase in *Fragilaria famelica* to 12.7% from 8% during the ~1860s that coincides with a decrease in *Aulacoseira granulata* abundances to 25.7% from 30.7%, respectively (Figure 5.8). The increase in the benthic *Fragilaria famelica* and coinciding decrease in the planktonic *Aulacoseira granulata* indicates a period of deeper waters (Taylor *et al*., 2007a). Overall, the results show that this ~80-year period is characterised by increasing lake levels interrupted with deeper waters in the ~1870s.

Over the next ~40-years from the ~1930s to the mid ~1960s, there is an overall decrease in the planktonic sum from 84.5% to 42%, respectively and coincides with the decrease in *Aulacoseira granulata* abundances from a peak of 77.8% to 31.1%, respectively (Figure 5.8). Overall, the results show that this ~40-year period is characterised by decrease in lake levels. Between the late ~1960-1980s there is an abrupt increase in *Aulacoseira granulata* to 92.2% in the mid ~1970s from 55.9% in the early ~1970s, followed by an increase to 74% in the early ~1980s from 59.6% (Figure 5.8). *Aulacoseira granulata* is indicative of higher lake levels (Buczkó *et al.,* 2019) and the increase in this species coincides with the construction of the dam at Letšeng-la Letsie in 1968 (Rose *et* al., 2020). During the ~1990s there is an overall increase in the planktonic sum from 32.5% to 54.3%, respectively (Figure 5.8). This positive trend coincides with an overall increase in *Aulacoseira granulata* abundances from 29.9% to 45.3%, respectively (Figure 5.8) which indicates increasing lake levels (Buczkó *et al.,* 2019). Overall, between the late ~1960s and during the ~1990s the Letšeng-la Letsie diatom record over this ~30-year period is characterised by an increase in lake levels.

6.3.2.1.3. Climate Trends

Spanning ~80-years between the ~1850-1920s there is an overall increase in *Aulacoseira granulata* from 16.1% to 89.6%, respectively (Figure 5.8) and is indictive of wetter climatic conditions (Buczkó *et al.,* 2019). Over the next ~40-years from the ~1930s to the mid ~1960s there is an overall decrease in the planktonic sum from 84.5% to 42%, respectively (Figure 5.8). This negative trend coincides with the decrease in *Aulacoseira granulata* abundances from a peak of 77.8% to 31.1%, respectively (Figure 5.8) and is indicative of a decrease in wetter climatic conditions (Buczkó *et al.,* 2019). Between the ~1930s and the mid ~1960s there is an indication of drier environmental conditions, suggested by the appearance of aerophilic species such as *Hantzschia amphioxys*, *Pinnularia borealis* and *Pinnularia divergens* (Taylor *et al*., 2007a; Fitchett *et al*., 2016b; Humane *et al*., 2020); but with <5% total abundances during this period (Figure 5.8). The results show that there is a slight decrease in wetter climatic conditions during this period and potentially shifted to a drier environment. There is also an increase in epiphytic, epilithic and epipelic species such as *Nitzschia sp.* from 1.3% to 13.8%, respectively (Figure 5.8) and is indicative of warmer environmental conditions (Zaky *et al*., 2020).

Overall, during the early ~1950s there is a decrease in the planktonic sum to 23.9% from 37.7% in the late ~1940s and coincides with a decrease in *Aulacoseira granulata* abundances to 10.5% from 29.4%, respectively (Figure 5.8). The maximum occurrence of the epiphytic, epipelic and epilithic species sum of 39.3% is found during the mid ~1960s from 36.3% the early ~1960s and coincides with an increase in *Nitzschia sp.* to 18.1% from 13.9%, respectively (Figure 5.8) and is indicative of warming environmental conditions (Zaky *et al*., 2020). Overall, these ~40-years from ~1930s to the mid ~1960s is characterised by a shift from wetter to drier climates and of increasing warming conditions.

Between the late ~1960-1980s there is an overall increase in the epiphytic, epilithic and epipelic sum from 23.7% to 43.9%, respectively (Figure 5.8). This positive trend coincides with an increase in

Nitzschia sp. from 2.3% to 16.5%, respectively (Figure 5.8) and is indicative of warming environmental conditions (Zaky *et al*., 2020). Between the early ~1970s and mid ~1970s there is an increase in the planktonic sum from 57.7% to 92.2%, respectively (Figure 5.8). This positive trend coincides with a respective increase in *Aulacoseira granulata* abundances from 55.9% to 92.2% (Figure 5.8) and is indicative of wetter climatic conditions (Buczkó *et al.,* 2019). During the early ~1980s there is an increase in the planktonic sum from 66.3% to 76.6% (Figure 5.8). This increase coincides with an increase in *Aulacoseira granulata* abundances from 59.6% to 74%, respectively (Figure 5.8) and indicates wetter climatic conditions (Buczkó *et al.,* 2019). The mid ~1980s is characterised by an increase and maximum occurrence of the epiphytic, epipelic and epilithic species sum from 15.45% to 42.2%, respectively (Figure 5.8). This trend coincides with an increase in *Nitzschia sp.* from 8% to 13.8%, respectively (Figure 5.8) and indicates warmer environmental conditions (Zaky *et al*., 2020). Overall between the late ~1960-1980s is characterised by wetter and warmer climatic conditions.

During the ~1990s there is an overall increase in the planktonic sum from 32.5% to 54.3%, respectively (Figure 5.8). This increase coincides with an increase in *Aulacoseira granulata* abundances from 29.9% to 45.3%, respectively (Figure 5.8) and indicates wetter climatic conditions (Buczkó *et al.,* 2019). This is interrupted however by an increase in the late ~1990s in the aerophilic species *Pinnularia divergens* to 2.3% from the late ~1990s with 0.3% (Figure 5.8) and is indicative drier environmental conditions (Taylor *et al*., 2007a) albeit in relatively low abundances of <5% in this period (Figure 5.8). *Nitzschia sp.* abundances in the early ~1990s increase to 21.1% from 18.2%, respectively (Figure 5.8) and indicates warmer environmental conditions (Zaky *et al*., 2020). Overall during the ~1990s, the results show that predominantly wetter climatic conditions were interrupted with drier climates in the late ~1990s with warmer conditions suggested for the early ~1990s.

6.3.2.2. Zone Lets2Z1 ~2000s to 2018 (10.75-0.25cm)

Zone Lets2Z1 represents the youngest section of the core profile spanning ~20-years and of the 39 identified diatom species, 37 were found within this zone with varying abundances (Figure 5.8). The planktonic and facultative planktonic species *Aulacoseira granulata* is the most dominant in this zone with an average abundance of 64.6% and with an abundance ranging from a maximum of 79.5% % in the mid ~2000s to a minimum in the mid ~2010s of 39.2% (Figure 5.8). *Aulacoseira granulata* is indicative of increasing lake levels, wetter conditions and mesotrophic waters (Buczkó *et al.,* 2019). The benthic species *Fragilaria capucina* with an average occurrence 4.1% is the second most dominant species in zone Lets2Z1, with a range in occurrence from a minimum of 1.2% in the early ~2000s to a maximum in the mid ~2010s of 9.7% (Figure 5.8). The epiphytic, epilithic, epipelic species *Cymbella cistula* was identified as the third most dominant species in zone Lets2Z1, with an average appearance of 3.6% and range in occurrence from a minimum of 0.2% in the mid ~2000s to a maximum in the early ~2000s of 6% (Figure 5.8). *Fragilaria capucina* and *Cymbella cistula* are indicative of periods of meso-eutrophic waters (Taylor *et al.,* 2007a).

6.3.2.2.1. Pollution Trends

Spanning ~10-years during the ~2000s there is an overall increase in the planktonic species *Aulacoseira granulata* from 68.7% to 72.8%, respectively (Figure 5.8). There is also an increase during this decadal period in the benthic species *Fragilaria capucina* from 2.3% to 5.4% and *Navicula trivialis* from 1.3% to 2.6%, respectively (Figure 5.8). These three aforementioned species are all indicative of mesotrophic waters (Taylor *et al*., 2007a; Buczkó *et al.,* 2019). Spanning just under ~10-years , during the ~2010-2018 and at the core surface there is a decrease in *Aulacoseira granulata* from 74.5% to 59.4%, respectively (Figure 5.8) and is potentially indicative of increasing lake trophic conditions (Buczkó *et al.,* 2019). This is supported by the coinciding overall increase in the benthic species including: *Fragilaria capucina* from 3.1% to 4.1%; *Navicula trivialis* from 0.3% to 3.1%; and *Fragilaria*

famelica from 0% to 2.8%, respectively (Figure 5.8) and are all indicative of meso-eutrophic lake waters (Taylor *et al*., 2007a; Çelekli *et al*., 2018). There is a peak in *Cymatopluera solea* abundances during the mid ~2010s from 1.7% to 11.5%, respectively (Figure 5.8) and is a species is that is predominantly found in found in eutrophic waters (Taylor *et al.,* 2007a).

The mid ~2010s coincides with the lowest planktonic sum of 48.6% in zone Lets2Z1 and lowest relative abundance's of *Aulacoseira granulata* from 51.1% to 39.2%, respectively (Figure 5.8). A decrease in *Aulacoseira granulata* is potentially indicative of increasing lake trophic conditions (Buczkó *et al.,* 2019). There is additionally an increase in *Gomphonema parvulum* from 0.7% to a peak of 2.6%, respectively (Figure 5.8) and is a species tolerant of extremely polluted conditions and indicates anthropogenic impact (Schneck *et al*., 2007; Çelekli *et al*., 2018). In the late ~2010s there is an increase in *Fragilaria fasciculata* from an absence since an abundance of 0.9% during the early ~2010s to a peak of 1.2% (Figure 5.8) and is a species found in critically polluted industrial wastewater (Taylor *et al*., 2007a). There is an increase in the planktonic species *Melosira varians* in the late ~2010s to a peak of 1.5% from a short-lived absence since the mid ~2010s with an abundance of 0.6% in (Figure 5.8). *Melosira varians* is indicative of eutrophic waters and is tolerant of organic pollution (Taylor *et al*., 2007a; Yang *et al*., 2020). Overall, the ~20-year period can be characterised by increasing lake trophic conditions and pollution. Mesotrophic conditions are suggested for the ~2000s which shifts to eutrophic, organically enriched waters with indication of industrially polluted conditions in the ~2010s to 2018 at the core surface.

6.3.2.2.2. Hydro-climate

During the ~2000s there is an overall increase in the planktonic species *Aulacoseira granulata* from 68.7% to 72.8%, respectively (Figure 5.8) and is a species indicative of increased lake levels and wetter climatic conditions (Buczkó *et al.,* 2019). The maximum planktonic sum of 83.9% in the early ~2000s

coincides with the maximum abundance of *Aulacoseira granulata* with 79.5% in Lets2Z1 (Figure 5.8). During the early ~2010s-2018 there is an overall decrease in the planktonic sum from 80% to 62.2%, respectively and coincides with an overall decrease in *Aulacoseira granulata* from 74.5% to 59.4%, respectively (Figure 5.8). The mid ~2010s coincides with the lowest planktonic sum of 48.6% in Lets2Z1 and the lowest relative abundance of *Aulacoseira granulata* with 39.2% from 51.8% and 51.1%, respectively during the mid ~2010s (Figure 5.8). The decrease in *Aulacoseira granulata* is potentially indicative of a decadal period of decreasing lake levels and wetter climatic conditions (Buczkó *et al.,* 2019). This is supported by the increase in the aerophilic sum from 0.5% to 1.6%, respectively, albeit relatively very low (Figure 5.8).

There is an abrupt increase in the aerophilic species *Hantzschia amphioxys* in the early ~2010s from 0.3% to a peak of 2.8% in Lets2Z1 (Figure 5.8). An increase in *Hantzschia amphioxys* is indicative of a periodically drier environment (Taylor *et al*., 2007a; Fitchett *et al*., 2016b). There is an overall increase in the epiphytic, epilithic and epipelic sum between the early ~2010s-2018 from 10.4% to 17.6%, respectively (Figure 5.8). This positive trend coincides with an overall increase in the epiphytic, epilithic and epipelic species *Nitzschia sp*. from 1% to 7.5%, respectively (Figure 5.8) and indicates warming climatic conditions (Sivarajah *et al*., 2018; Zaky *et al*., 2020). Overall this ~20-year period is characterised by increased levels and wetter climatic conditions spanning the ~2000s with warmer and drier environmental conditions characterizing the early ~2010s-2018.

6.3.2.3. A Brief Summary

Letšeng-la Letsie is characterised by nutrient enrichment for ~90 consecutive years between the early ~1930s to 2018 at the core surface (Table 6.1; Figure 5.7). Between the ~1930-1960s and during the ~1990s, Letšeng-la Letsie is characterised by meso-eutrophic waters. The more meso-eutrophic conditions are however interrupted with hyper-eutrophic and strongly polluted conditions during the

late ~1960-1980s. The majority of the ~2000s is characterised by mesotrophic lake conditions that shift in the ~2010s-2018 to eutrophic and more organically enriched waters. There is also an indication that Letšeng-la Letsie has had industrial related pollution fluctuations across five decadal periods, however in relatively low concentrations and includes the late ~1940s, during the early-mid ~1950s, during the mid-late ~1970s, during the mid ~1980s and throughout the ~2010s to the core surface.

Letšeng-la Letsie is characterised by fluctuating lake levels throughout the profile. Higher lake levels are suggested for ~120-years: between the ~1850-1920s; between the late ~1960-1980s and from the early ~2000s-2018, at the core surface. Specifically, deeper waters are suggested for ~60-years: during the ~1870s, between the early-mid ~1930-1960s and during the ~1990s. Letšeng-la Letsie is predominantly characterised with wetter climatic conditions, suggested for ~130-years: between the ~1850-1920s; between the late ~1960-1980s and between the ~1990-2000s. Wetter climatic conditions are interrupted with ~40-years of drier environmental conditions suggested for: the late ~1940s; mid ~1950s; the late ~1990s and during the ~2010s-2018, at the core surface. Letšeng-la Letsie can be characterised by warmer climatic conditions for ~80-years: from the early ~1930-1990s and during the early ~2010s-2018, at the core surface (Table 6.1; Figure 5.8).

6.4. Comparisons Between Sites

Lake Chrissie is situated in the highveld plateau of the Mpumalanga Province in South Africa within the MLD (Ferreira *et al*., 2012; Hallowes and Munnik, 2016); while Letšeng-la Letsie is located within the lower part of the Maloti Mountains (Kahlolo *et al*., 2021; Smit and Van Rensberg, 2021). These lake systems are geographically located in different regions at altitudes of 1676m.asl and 2402m.asl, respectively, with a difference in elevations of 726m.asl and distance of 734Km between them (Google Earth, 2022a,b). Diatoms common to both systems that are indicative of nutrient enrichment and/or

industrially derived pollution include the planktonic and facultative planktonic species *Fragilaria fasciculata, Cyclotella meneghiana*, *Aulacoseira granulata* and *Fragilaria ulna*; benthic species such as *Navicula antonii*, *Navicula trivialis, Navicula veneta* and *Fragilaria famelica;* epiphytic, epilithic and epipelic species such as *Gomphonema parvulum*, *Nitzschia sp.*, *Gomphonema minutum*, *Cymbella cistula and Eunotia minor*; and aerophilic species including *Hantzschia amphioxys, Pinnularia divergens* and *Pinnularia borealis.*

The Lake Chrissie diatom record shows an increase in industrial related pollution fluctuations during the ~1950s, during the ~1970s and in the early ~1980s and an increase in these conditions from the late ~1990s to the mid ~2010s (Figure 6.1). The species displayed in light red are particularly indicative of industrial based pollution such as from coal-fired power stations, where those in dark red are indicative of generalised extremely polluted conditions. The species in dark green are more indicative of organic pollution and eutrophic lake conditions, where the species in turquoise are indicative of more mesotrophic-eutrophic conditions. The species in light green are indicative of moderate pollution and mesotrophic conditions, where the species in dark blue are indicative increased acidity.

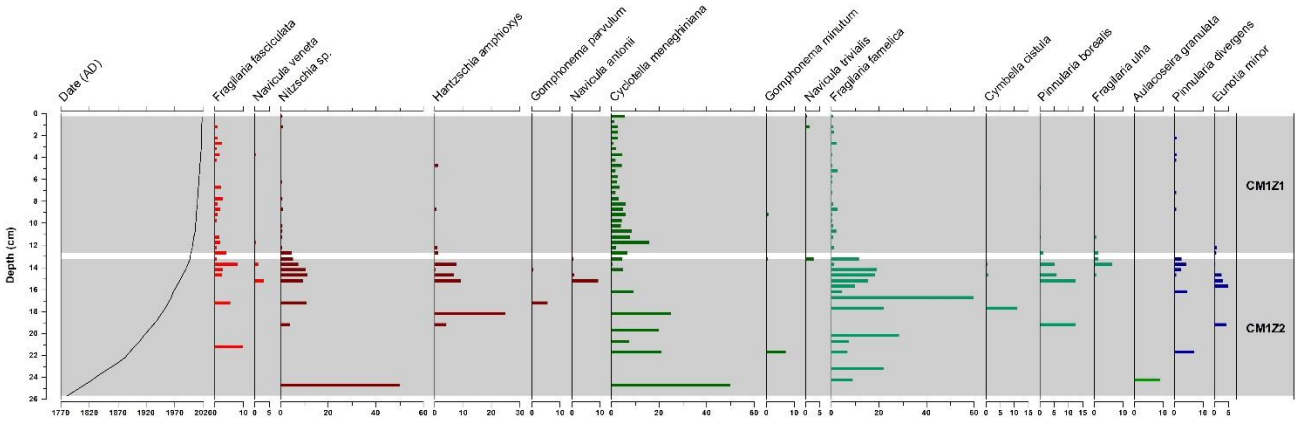

Figure 6.1. Age plot and % abundance of pollution tolerant species in Lake Chrissie.

There is indication that both Lake Chrissie and Letšeng-la Letsie have had industrial related pollution fluctuations coinciding during the ~1950s and during the ~1970s (Figure 6.1; 6.2). Thereafter, there is a delay observed in Letšeng-la Letsie with an increase again in the mid ~1980s, followed by a brief hiatus in these conditions until indication once more of an increase during the ~2010s to 2018 (Figure 6.2). The results show that Letšeng-la Letsie had a delay in industrial based contamination post ~1980s and is indicative of low concentrations throughout the Letšeng-la Letsie profile, as indicated by the diatom profile. The air originating over the industrialized Highveld is advected over Letšeng-la-Letsie, however infrequently, which may explain the low level of contamination seen at the site (Rose *et al.,* 2020). The species in Figure 6.2 are colour-coded to those found in Lake Chrissie in Figure 6.1. There is a greater abundance in pollution tolerant species in Letšeng-la Letsie than in Lake Chrissie.

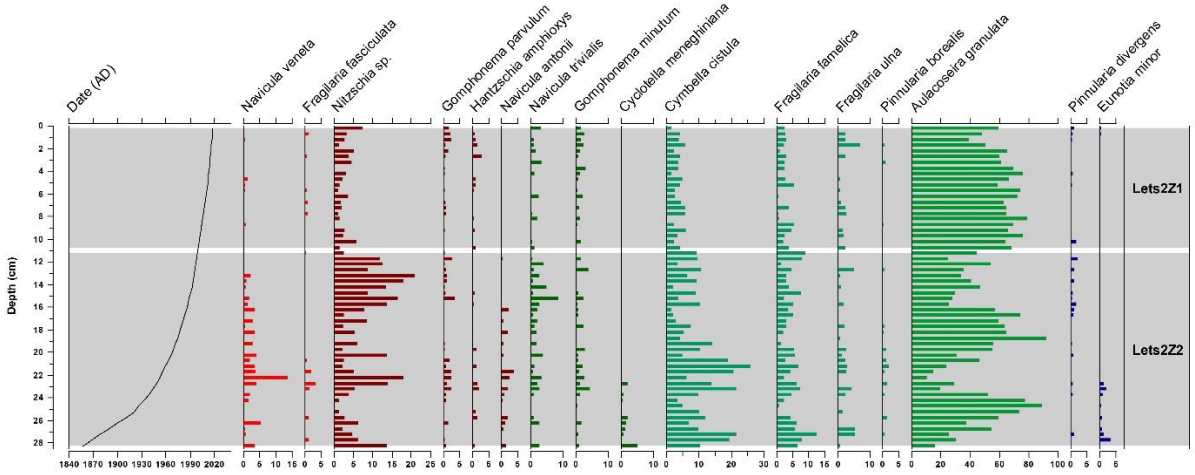

Figure 6.2. Age plot and % abundance of pollution tolerant species in Letseng-la Letsie.

Diatoms common to both systems that are indicative of hydro-climatic conditions include the planktonic and facultative planktonic species *Aulacoseira granulata, Cyclotella meneghiana, Fragilaria construens* and *Fragilaria pinnata*; benthic species such as *Fragilaria famelica*; epiphytic, epilithic and epipelic species such as *Nitzschia sp.;* along with aerophilic species including *Pinnularia borealis* and *Hantzschia amphioxys.* Hydrologically, both sites' records indicate deeper waters during the ~1950s,

~1960s and ~1990s, however unlike Lake Chrissie, Letšeng-la Letsie was dammed in 1968 and in turn, this affected the lake levels. Both sites additionally coincide with increased lake levels between the ~2000-2010s. From a climatic perspective, both sites' records indicate wetter periods during the ~2000-2010s; drier periods during the ~1940s, the late ~1990s and during the ~2010s; along with indication of warmer periods during the late ~1950s and between the late ~1970s and early ~1980s.

The Lake Chrissie diatom record (Figure 6.3) shows an abundance of aerophilic species over planktonic and facultative planktonic species. The species displayed in orange are indicative of drier environmental conditions, where the species in light blue are indicative of wetter climatic conditions. The species in red are indicative of warmer climates, where the species in dark blue are indicative of colder climatic conditions. The record shows that from the 1990s, Lake Chrissie predominantly exhibits drier environmental conditions (Figure 6.3).

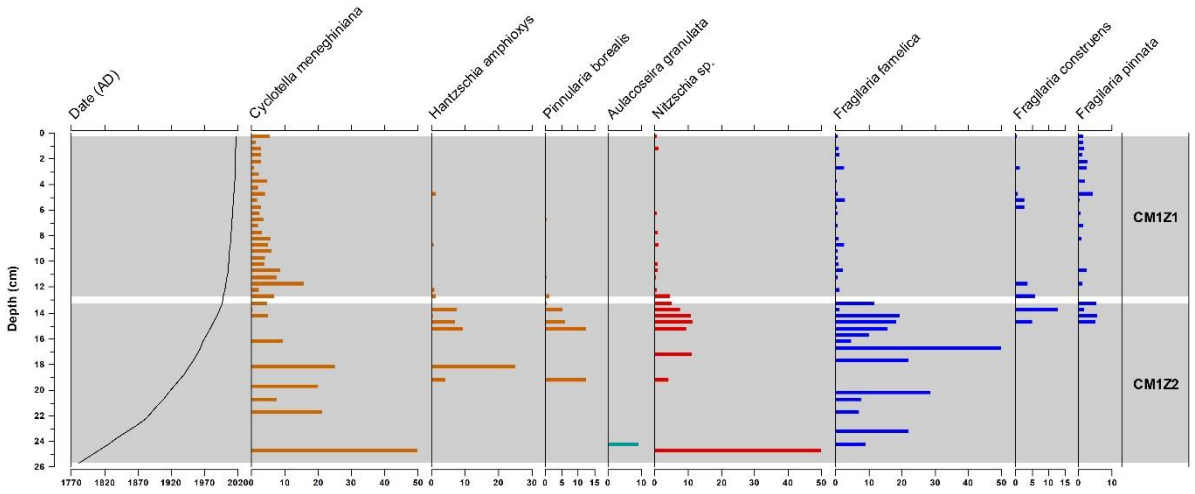

Figure 6.3. Age plot and % abundance of species indicative of hydro-climatic conditions in Lake Chrissie.

Conversely to the Lake Chrissie diatom record, the Letšeng-la Letsie diatom record (Figure 6.4) shows an abundance of planktonic and facultative planktonic species over aerophilic species. The species in Figure 6.4 are colour-coded to those found in Lake Chrissie in Figure 6.3. The record shows that throughout the diatom record, Letšeng-la Letsie exhibits predominantly wetter climatic conditions.

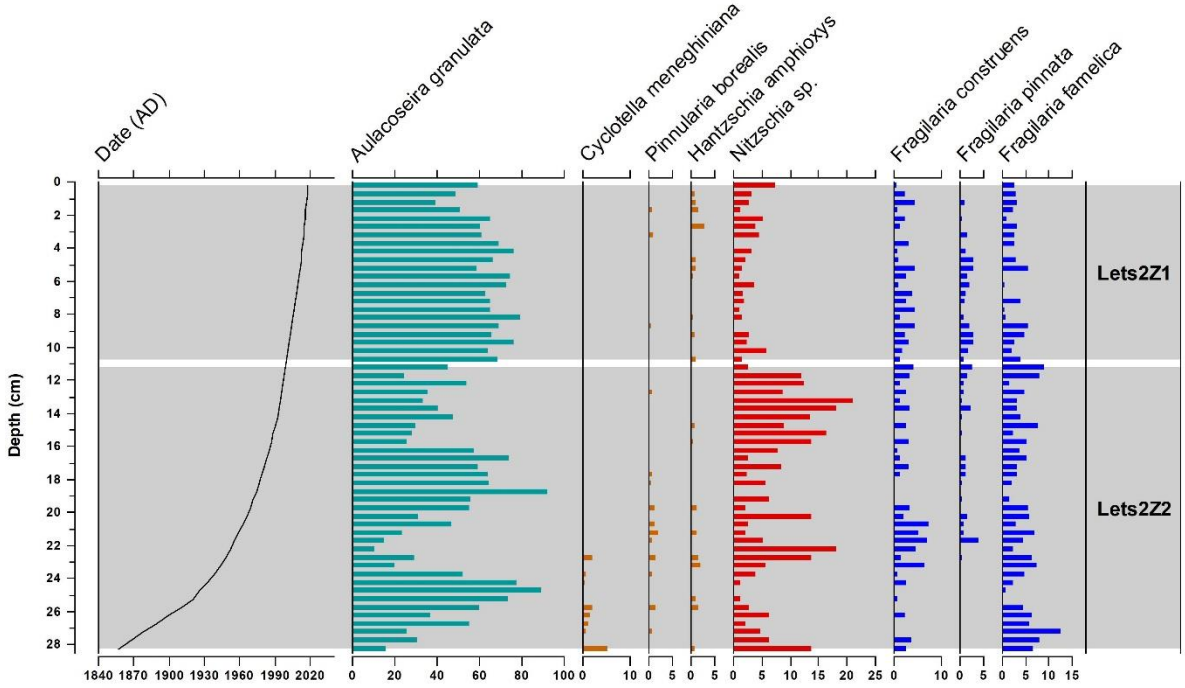

Figure 6.4. Age plot and % abundance of species indicative of hydro-climatic conditions in Letseng-la Letsie.

6.5. Global Comparisons

6.5.1. Lake Trophic Status

Globally, diatoms have been used to reconstruct changes in lake levels and in pollutant history. Lakes are abundant in the northern Hemisphere and numerous studies have therefore been conducted determining various conditions such as the tolerances of individual systems to pollutants (Dunnink *et al.*, 2016). Key indicator species found in various global research based on indications of

eutrophication, nutrient enrichment and increased organic material include: *Aulacoseira sp*., including *Aulacoseira granulata, Cyclotella meneghiana*, *Gomphonema parvulum, Fragilaria ulna, Achnanthes minutissima, Eunotia sp* and *Nitzschia spp.,* including *Nitzschia palea* and *Nitzschia amphibia*. These species are all considered pollution tolerant species (Table 6.1). *Eupodiscus radiatus* however, is intolerant to pollution and is indicative of lower trophic conditions (Table 6.1). All these species were found within this study, across both the Lake Chrissie and Letšeng-la Letsie core profiles in various abundances and at various periods.

In a study on a number of lakes in Alberta, Canada, Curtis *et al*. (2010) found that the diatom core stratigraphy showed large increases in planktonic diatom species, which was particularly indicative of strong nutrient enrichment of the lake. The finding in this study found that planktonic and facultative planktonic species dominated both the Lake Chrissie and Letšeng-la Letsie core profiles. Similarly, in various freshwater lakes in tropical east Asia, Bannister *et al*. (2019) found these systems to be characterised by eutrophication, along with nutrient fluctuations; as indicated from the increase in particular of species including *Aulacoseira granulata, Nitzschia palea*, *Cyclotella meneghiana* and *Gomphonema parvulum*. In Lake Poyang in China, Yang *et al*. (2020) found the lake to have increased N availability, organic and eutrophic levels along with increased wastewater inputs; as inferred from the presence and increased abundance of species including *Cyclotella meneghiana, Fragilaria capucina* and *Nitzschia spp*., along with the pollution tolerant species *Nitzschia palea.* Similarly, in Lake Qilu, in China Klamt *et al*., (2021) found that the diatom composition changed during the ~1990s and was mainly driven by eutrophication, nutrient enrichment and increased organic material within the system. The findings of this study on both the Lake Chrissie and Letšeng-la Letsie cores were found to align with the findings of Klamt *et al*. (2021), whereby both systems indicated nutrient enrichment during this decadal period. Wu *et al*. (2022) in a study on Lake Chenghai found that shifting trophic

levels were the main driver of diatom assemblages' changes over the ~80-year record between 1920-2010 with oligotrophic conditions before 1998 and with eutrophic conditions post-1998.

In the southern Hemisphere, Bartozek *et al*. (2018) found that species including *Cyclotella meneghiana, Nitzschia palea* and *Nitzschia amphibia* were dominant in eutrophic conditions within various reservoirs in Brazil. The findings for this study showed an increase in these species' abundances during periods of eutrophication, as suggested for both cores. Comparatively, Perez *et al*. (2017) found in an estuary in Uruguay, that an increase in *Aulacoseira sp*. was indicative of low salinity levels and higher trophic conditions, while an increase in *Eupodiscus radiatus* was indicative of higher salinity levels and lower trophic conditions. These findings directly align with the results found for the Lake Chrissie core, where there is evidence of fluctuations in abundances between *Aulacoseira sp.* and *Eupodiscus radiatus,* indicating periods of lower and higher trophic conditions, respectively. It is expected however, that lower water levels would coincide with higher salinity in Lake Chrissie, due to greater relative importance of evaporation and reduced dilution

6.5.2. Pollution from Coal-fired Power Stations

In a study on Lake Gusinoye in Siberia, Adams *et al*. (2019) found that post ~1970s diatom assemblages changed due to multiple anthropogenic stressors, including nutrient fluxes, eutrophication and pollution specifically from power plants. Through examining 12 lakes in Alberta within Canada, Curtis *et al*. (2010) found that all sediment cores showed evidence of industrial contamination, based on SCPs and changes in diatom assemblages, which was found consistent with nutrient enrichment from anthropogenic N deposition. These studies align with the results found in the Letšeng-la Letsie core, where Rose *et al*. (2020) found an increasing trend of SCPs contamination from ~1970s and the diatoms record shows an increase in pollution tolerant species during this period. Curtis *et al*. (2009) had previously identified within remote alpine lakes in Europe that fossil diatom community changes

were consistent with recognized environmental problems, including anthropogenic sources for N deposition and acidification. The results of the Lake Chrissie and Letšeng-la Letsie diatom record similarly reveals a relationship between diatoms community changes and pollution sources, where pollution tolerant species increased with periods identified with increased emissions from in coal-fired power stations. Larsen (2000) calculated heavy metal and SCP concentrations from sediment cores, where the changes in the preserved diatom assemblages were used to derive a pH reconstruction of the two lakes in Norway. A study on a freshwater river system in Italy (e.g. Tolotti *et al.,* 2018) revealed the impact of mining and metal pollutants and the response of benthic diatom communities to the anthropogenic contamination.

Adams *et al*. (2019) also revealed that the long-range atmospheric transport of pollutants from industrial activities from major cities in Russia, were found as a major source of contamination for Lake Baikal. Similarly, findings of Liu *et al*. (2019) on Lake Lugu in China suggest that long distance transport and deposition is the main source of Pb with the system; with a rapid increase in trace elements between the 2001-2010 period, deteriorating water quality. The findings in this research on Letšeng-la Letsie of pollution tolerant species that are particularly indicative of industrial based pollution support the suggestion that pollutants in this lake system are long-range atmospherically transported and deposited. Anthropogenic input of trace metals in Lake Lugu in China showed low levels but with an increasing trend over the past decade (Liu *et al*., 2019). The diatoms record in Letšeng-la Letsie similarly indicates low concentrations of pollution in the system but with increases in recent decades (e.g. Hg) and of contaminants such as SCPs (Rose *et al*., 2020). Alikaj *et al*. (2019) researched various lakes in Albania, finding they were rich in diatom species diversity and that this tended to decrease within the more polluted systems. The Lake Chrissie core profile had significantly less diatom diversity than that of the Letšeng-la Letsie core. Therefore, it can be posited that in

general, a healthier ecosystem with less pollution will potentially have higher diatom species diversity, where poor diversity often indicates a more polluted ecosystem (Gökçe, 2016).

6.5.3. Hydro-climatic Comparisons

In many global studies, planktonic species such as *Aulacoserira granulata* have been used to determine fluctuations in water depth, as they are predominantly indicative of increased lake levels and are also found associated with wetter climatic conditions; where comparatively, *Fragilaria famelica* has been used to identify periods of deeper lake waters and may indicate periods of colder climates (Table 6.1). *Fragilaria* taxa are replaced by planktonic species such as *Aulacoseira sp.* when increased water column mixing occurs (Zou *et al*., 2020). Both these species were found in the Letšeng-la Letsie core profile and were found to fluctuate in abundances and indicated changes in lake levels (Table 6.1). However, numerous lake studies have identified that diatom assemblages across the world have changed substantially, but this is mostly attributed as a response to climate change (Zou *et al*., 2020). In a study on Lake Huron in Canada, Sivarajah *et al*. (2018) found that diatom assemblage composition remained relatively stable until ~1970s AD, when a major shift occurred in these assemblages in the ~200-year record. This included an abrupt decrease in *Aulacoseira* taxa, attributed to climate-associated changes in the water column properties (Sivarajah *et al*., 2018).

In the shallow Lake Balaton in Hungary, Buczkó *et al*. (2019) found that higher ratios of planktonic species such as *Aulacoserira granulata* were indicative of high-water levels and increased depth fluctuations. The increased ratio of planktonic to benthic forms implied higher lake levels and that the shallow lake was wind-stressed and likely affected by climate conditions (Buczkó *et al*., 2019). The findings in both the Lake Chrissie and Letšeng-la Letsie cores were found to align with the findings of Buczkó *et al*. (2019). In various freshwater lakes in tropical east Asia, Bannister *et al*. (2019) along with

Klamt *et al*. (2021) on a study of Lake Qilu in China, found that diatom composition changed during the ~2000s with increases in *Aulacoseira granulata* and indicated periods of high-water turbulence. These findings were found to align with the findings in this research project, whereby increased periods of lake levels were identified for the ~2000s and within the ~2010s for the Letšeng-la Letsie core profile.

6.6. Southern African Comparisons

6.6.1. Lake Trophic Status and Coal-fired Power Stations

Southern Africa provides a valuable geographic setting for palaeoenvironmental research (Fitchett *et al*., 2016b). However, very few data exist on the scale and rate of change in contaminant inputs to freshwater systems in this region (Rose *et al*., 2020). The effects of global change can be assessed through using isolated mountain lakes with little direct human influence and often in remote areas (Rivera-Rondon and Catalan, 2019). However, there is a rarity of permanent and natural standing waters throughout southern Africa and in South Africa particularly, these inland lakes are rarely found and poorly described (Dunnink *et al*., 2016; Rose *et al*., 2021). Sitoe *et al*. (2015) in a study on Lake Lungué in Mozambique found that there was a high abundance of freshwater planktonic species such as *Aulacoseira granulata*, which indicated high nutrient concentrations. Similarly in a study on various dams in South Africa, Venter *et al*. (2013) found that an abundance of *Aulacoseira granulata* and *Cyclotella meneghiana* were typical of eutrophic impoundments and suggested that the increase in species such as *Fragilaria ulna* was indicative of decreased water quality. *Aulacoseira granulata* was found in high abundances throughout the Letšeng-la Letsie core where *Cyclotella meneghiana* was found in relatively high abundances within the Lake Chrissie core.

Letšeng-la Letsie showed low but increasing levels of contamination since ~1970s as a likely result of long-range transport from coal combustion and other industrial sources in the Highveld region of South Africa (Rose *et al.,* 2020). The diatoms found at Letšeng-la Letsie in this research study supports this finding, with an observed but low increase in pollutant tolerant species since ~1970s AD (Figure 6.5). The Letšeng-la Letsie core showed continuous sedimentation over ~85-years (Rose *et al.,* 2020) and coincides with a period where overall emissions increased through the 20th century, but climatic variability may have affected the year-to-year delivery of any pollutants into this lake. The pollutants found include Hg, SCPs and nutrient enrichment within Letšeng-la Letsie and is lake that was found in range for transport from coal combustion sources in the Mpumalanga Highveld (Rose *et al*., 2020).

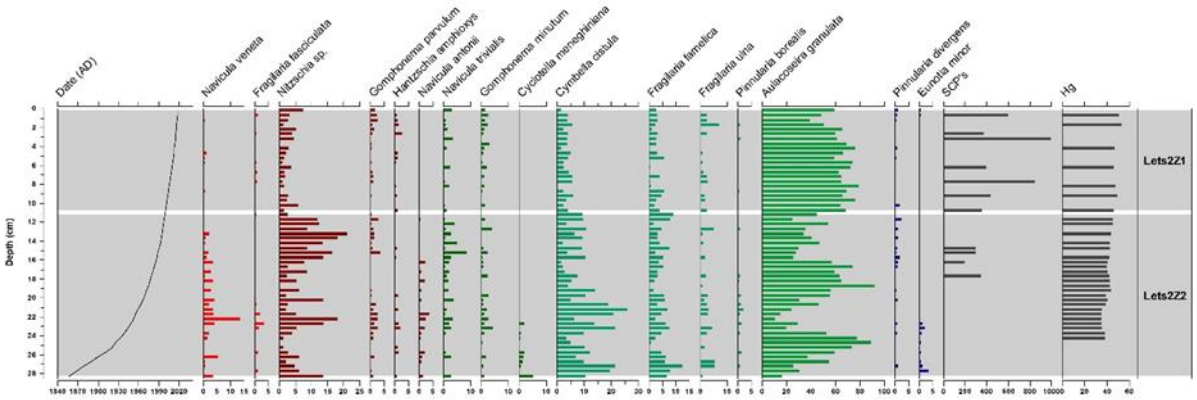

Figure 6.5. Age plot and % abundance of pollution tolerant species in Letseng-la Letsie along with the Hg and SCPs found in Rose *et al*., (2020).

6.6.2. Hydro-climatic Comparisons

In various southern Africa literature, it is found that species such as *Aulacoseira granulata* and *Aulacoseira ambigua* are indicative of increased water levels, a well-mixed lake and are associated with wetter climatic conditions. Conversely, species such as *Hantzschia amphioxys*, *Navicula*

goeppertiana, *Pinnularia borealis*, *Cyclotella meneghiania* are associated with drier climatic conditions and increased evaporative concentrations. These species were all identified in various abundances in both the Lake Chrissie and Letšeng-la Letsie core profiles. Westover *et al.* (2019) investigated various paleolakes in Kenya and found a dominance of *Aulacoseira* taxa indicating a well-mixed lake with higher water levels and were associated with increased wind speeds. Similarly, in a study on Lake Lungué in Mozambique, Sitoe *et al*. (2015) found that there was a high abundance of freshwater planktonic species such *Aulacoseira granulata*, which indicated overall higher lake levels and wetter climatic conditions. Sitoe *et al*. (2015) additionally found that the interrupted presence of aerophilous taxa, such as *Hantzschia amphioxys*, *Navicula goeppertiana* and *Pinnularia borealis* in the lake, indicated periods of relatively drier climatic conditions (Sitoe *et al*., 2015).

Fitchett *et al*. (2016b) found that alternating abundances of *Aulacoseira ambigua* and *Hantzschia amphioxys* were indicative of periods of fluctuating wetter and drier climatic conditions in a wetland in Lesotho. Fitchett *et al*. (2016b) presented a multi-proxy palaeoenvironmental reconstruction for the highest wetland known as Mafadi in southern Africa, which is based in Lesotho and found that the most dominant species included *Fragilaria* taxa; where large abundances of *Aulacoseira ambigua* suggested a shallow lake persisted in the wetland. Increased freshwater, planktonic species such as *Aulacoserira sp* which indicate lake level variability may however be primarily driven by prevailing climate conditions and flooding events (Sitoe *et al*., 2017). There is a fluctuation between species such as *Aulacoseira sp.,* including *Aulacoseira granulata* and of *Hantzschia amphioxys*, *Navicula goeppertiana* and *Pinnularia borealis* in both the Lake Chrissie and Letšeng-la Letsie core profiles, which is interpreted as potentially indicating fluctuations between wetter and drier environmental conditions.

In a recent study on Letšeng-la Letsie in Lesotho, Rose *et al.* (2020) concluded that a shallow lake has likely been present in Letšeng-la Letsie over at least the last ~85-years, as there has been uncertainty regarding the presence of a permanent waterbody at Letšeng-la Letsie, prior to the 1968 impoundment. This diatom record from this research project supports this through identified diatom autecologies, such as with the persistent and high presence of *Aulacoseira granulata* throughout the core profile and before 1968, which is interpreted as indicative of increased lake levels, prior to the dam's construction. Prior to the impoundment there was a small wetland lake with variable waters levels and the diatom record shows continued variability in water levels post-1968, as seen with continued fluctuations in *Aulacoseira granulata* abundances; until ~2000-2010s where there is a relatively stable and higher abundance of *Aulacoseira granulata* species in Letšeng-la Letsie and indicates increased lake levels. Zou *et al*. (2020) in a study in China, found that after the dam was constructed, lake water levels gradually increased as well as a continuous accumulation of lake sediments. Rose *et al.* (2020) found that Letšeng-la Letsie in Lesotho displayed no hiatus in accumulation before or after the dam construction in 1968 but found that the sediment accumulation rates before 1968 were more variable and they suggest that a more stable accumulating environment occurred after the impoundment.

6.7. Broader Regional Understanding

6.7.1. History of Pollution Contamination

South Africa is the most industrialised country in Africa and one of the largest coal-producing countries in the world (Garnham and Langerman, 2016). The country has 19 official coal fields and coal mines spread across five provinces; the Free State, Eastern Cape, KwaZulu-Natal, Limpopo and in Mpumalanga (Ebenebe *et al*., 2017). The state-owned utility Eskom uses coal combustion and provides ~95% of South Africa's electricity and generates ~45% of the total energy in Africa (Pretorius *et al*.,

2015; Williams, 2020). Eskom is one of the largest energy utilities in the world and has 14 coal-fired power stations located across South Africa (Pretorius *et al*., 2015; Garnham and Langerman, 2016). The Mpumalanga Highveld hosts 12 of these coal-fired power plants along with petroleum facilities and other industrial complexes (Williams, 2020). There are three non-Eskom owned smaller coal-fired power stations in South Africa, located in the Gauteng Province (Garnham and Langerman, 2016).

Industrial activities, including coal-combustion from power stations release pollutants that accumulate in the atmosphere and are locally dispersed or long-range transported and deposited (Barreira *et al*., 2017; Rivera-Rondon and Catalan, 2019). South Africa's reliance on coal for energy generation, has made the country the largest air polluter in Africa (Marais *et al*., 2019). The energy sector is the largest contributor to SO_2 and NO_x emissions and second highest contributor to PM emissions in the country (Pretorius *et al*., 2015). Spheroidal Carbonaceous Particles are exclusively produced by anthropogenic burning and are relatively widely dispersed in the atmosphere (Adams *et al*., 2019; Bannister *et al*., 2019). As SCPs have no natural sources, they are used as unambiguous markers of anthropogenic pollution; where any presence can be considered enrichment (Adams *et al*., 2019; Rose *et al.,* 2020). South African coal impurities are variable between regions, but nonetheless have relatively high ash content and carbon, with small amounts of sulphur and depending on the Hg content of the coal, trace amounts are released upon combustion (Pretorius *et al*., 2015; Garnham and Langerman, 2016).

Between the ~1900-1950s power generation through Eskom in South Africa accounted for ~75% of the coal used in the country (Rose *et al*., 2020). Between the ~1940-1990s the South African government built more coal-fired power stations, of which the bulk of these stations were owned by Eskom by the end of the ~1950s (Rose *et al*., 2020; Williams, 2020). Specifically during the ~1970s, South Africa saw a marked increase in electricity generation due to the numerous new, larger coal-

fired power stations developed in the Highveld (Rose *et al.,*2020). Additionally, Sasol created a refinery in the Mpumalanga Highveld during this time to produce liquid petroleum from coal (Williams, 2020). The amount of coal burnt between ~1970-1990s in this region of the Mpumalanga Province more than doubled (Rose *et al.,* 2020). Findings in both lake systems in this study show increased contamination from industrially derived pollution coinciding during the ~1950s, during the ~1970s and the early ~1980s; with a delay observed in Letšeng-la Letsie until an increased suggested for the mid ~1980s. As the majority of coal extraction and burning occurs in the Mpumalanga Highveld this region has the highest acidic deposition loads which have increased since ~1980s (Pretorius *et al*., 2015; Dunnink *et al*., 2016; Williams, 2020). South Africa faced an energy crisis between 2004-2013 and due to this, older power stations from the ~1980s and ~1990s were returned to service (Pretorius *et al*., 2015). This was to alleviate pressures on existing stations; while two newer stations came online in 2015 and in 2017 within the Mpumalanga Province (Pretorius *et al*., 2015; Garnham and Langerman, 2016). However, it was found that PM emissions between 2007-2010 doubled, amidst the energy crisis (Pretorius *et al*., 2015; Dunnink *et al*., 2016; Williams, 2020). Lake Chrissie continues to show an increase in industrially derived polluted conditions from the late ~1990s to the mid ~2010s; while Letšeng-la Letsie however, shows a brief hiatus in these conditions until indication once more of an increase during the ~2010s.

South African freshwater systems are being threatened by unsustainable anthropogenic activities including, mining and coal combustion (De Klerk *et al*., 2012). Mining activities in South Africa release large quantities of toxic heavy metals into the environment, where coal combustion is a major source for industrial Hg (Ebenebe *et al*., 2017; Rose *et al.,*2020). Mercury is a persistent and toxic substance that accumulates in food chains and has adverse ecological effects (Garnham and Langerman, 2016; Rose *et al.,* 2020). Mining and coal industry related activities have escalated in the second half of the 20th century, while global atmospheric Hg at the start of the 21st century dramatically increased since

pre-industrial times (Ebenebe *et al*., 2017; Rose *et al*., 2020). These activities generate huge quantities of wastes with harmful and hazardous heavy metals including Hg, which is released into the environment and pollutes the ecosystem (Ebenebe *et al*., 2017). This could lead to ecological regime shifts characterised by abrupt changes affecting ecosystem structure and functioning (Bannister *et al*., 2019). In South Africa however, there is limited literature on surface water sensitivities to acidic atmospheric pollution and on the levels of Hg emissions and deposition (Dunnink *et al*., 2016; Ebenebe *et al*., 2017).

Lesotho, compared to South Africa has only minor emissions and no large-scale fossil-fuel combustion (Rose *et al.,* 2020). Therefore, long-range transport is required for the deposition of industrial contaminants in most of Lesotho and is suspected to originate from sources in the Mpumalanga Highveld of South Africa (Rose *et al.,* 2020). However, Rose *et al*. (2020) found that gaseous Hg from industrial sources may have an atmospheric lifetime of around one year and so the Hg deposited in Letšeng-la Letsie is potentially from anywhere in the world. Dunnink *et al*. (2016) in a study on the Lesotho tarns, found that levels of acidifying pollution in these systems, were found to be in similar range to deposition levels across Europe and North America. Pullanikkatil and Urama (2011) found that industrialised areas of Lesotho surface water quality have been significantly affected by industrial effluents being released into them. Textile factories in Lesotho ineffectually dispose of industrial wastewater which causes local water pollution and forms part of the problem of industrial wastewater management in Lesotho (Pullanikkatil and Urama, 2011). Rose *et al.* (2020) data represent the first palaeolimnological records and the first trace contaminant data for Lesotho and found an increase in Hg concentrations over the Letšeng-la Letsie core profile.

Water quality is an important factor influencing aquatic ecosystem integrity, as the distribution of aquatic freshwater organisms is controlled mainly by water quality characteristics (De Klerk *et al*.,

2012). Water quality is largely determined by both natural and anthropogenic inputs to the systems; where lake sediments are used to identify the impacts of pollutant inputs, as they act as naturally accumulating archives (Venter *et al*., 2013; Rose *et al*., 2020). Nutrients including N and P largely control the lake trophic status and could lead to the process of eutrophication (De Klerk *et al*., 2012). Eutrophication can be defined as the degradation of an aquatic ecosystem from organic enrichment due to an increase in nutrients; where P is considered the most important (De Klerk *et al*., 2012; Venter *et al*., 2013). Agricultural practices are one of the main sources for pollutants such as P due to increased nutrients from fertilizers (De Klerk *et al*., 2012). The MLD is predominantly impacted by nearby industrial activities but is additionally affected by agriculture and livestock practices (De Klerk *et al*., 2012). Lesotho additionally has local sources of pollutants such as agricultural pesticides, burning of biomass, over-grazing and catchment soil erosion among others (Rose *et al.,* 2020). Along with toxic heavy and/or trace metal contamination, nutrient enrichment has a direct impact on aquatic environments such as lakes (De Klerk *et al*., 2012). Both the Lake Chrissie and Letšeng-la Letsie diatom records revealed nutrient enrichment throughout the core profiles, which may be attributed to local pollutant sources within the site regions along with potentially from changing hydro-climatic conditions.

6.8. Research Implications

6.8.1. Environmental Pollution

6.8.1.1. Lakes and Ecosystem Health

Anthropogenic pollution is one of the most widespread and pervasive threats to natural ecosystems, especially for aquatic systems such as lakes (Dunnink *et al*., 2016). Lakes are a dominant feature across the Earth's surface, covering ~37% total land area and hold major portions of global freshwaters (Burge *et al*., 2017; Humane *et al*., 2020). They are precious natural resources and complex ecosystems

that play a crucial role in regulating the global hydrological and biogeochemical cycles and act as important parts of the global biosphere (Buczkó *et al*., 2019; Humane *et al*., 2020). To efficiently manage freshwater ecosystems, it is crucial to identify which threats are most important for individual lakes, as different threats have different causes (Adams *et al*., 2019). A range of anthropogenic pressures adversely affect freshwater lake systems such as agricultural activities, acid mine drainage, industry, mining and the combustion of fossil fuels, such as coal among others (Rose *et al*., 2020). A long-term perspective is needed to find when the various threats first impacted the aquatic system, as sediments act as a sink for a wide range of contaminants threatening these environments (De Klerk *et al*., 2012; Adams *et al*., 2019). Metals such as Hg and Pb are usually toxic and biologically unimportant to living organisms and cannot degrade (Ebenebe *et al*., 2017). Long-term inputs of metals into the sediment bind to sediment particles and organic matter and then persist in these localities (De Klerk *et al*., 2012; Ebenebe *et al*., 2017). These harmful metals are usually transferred from water bodies to the food chain via assimilation and bioaccumulation (Ebenebe *et al*., 2017). Lake sediments usually contain pollutant concentrations far higher than that of the lake waters and form a reliable long-term indicator of these inputs (De Klerk *et al*., 2012).

The Mpumalanga Province is a region in South Africa with the highest concentration of coal fields in juxtaposition to being a source for some of South Africa's major rivers (Olufemi *et al*., 2018). Coal-burning practices in the Mpumalanga Highveld have adverse effects on the environment causing water acidification from deposition of sulfuric acids, nitric acids and ammonium (Barreira *et al*., 2017; Olufemi *et al*., 2018). These acid rains are primarily caused by the release of oxidised sulphur and N compounds from these polluting combustion activities (Dunnink *et al*., 2016). The Mpumalanga Province is additionally the largest producer and supplier of food in South Africa, but soil degeneration with high concentrations of heavy metals has occurred, due to the activities of the coal mining industry (Olufemi *et al*., 2018). In sensitive systems these polluting compounds can acidify soils and affect

nutrient cycles (Barreira *et al*., 2017). The process of eutrophication can also occur which impacts water quality and ecosystem health, resulting in oxygen depletion within the lake system and development of harmful cyanobacterial blooms (De Klerk *et al*., 2012). As primary producers however, changes in diatom assemblages can directly affect lake productivity and influence ecosystem stability (Zou *et al*., 2020). As diatoms occupy the base of the food chain, any changes in species compositions may affect the food web and ecosystem functioning (Zou *et al*., 2020). If allowed to deteriorate, the quality of water can adversely affect not only the aquatic ecosystem of the specific water resource, but groundwater quality too (De Klerk *et al*., 2012). Diatoms however may be used to indicate changes in nutrient inputs lower than those required to cause harmful algal blooms, through subtle changes in assemblages. The findings from this study reveals major periods of shifting diatom communities in both the Lake Chrissie and Letšeng-la Letsie core and these changes in species compositions may in turn affect ecosystem functioning.

Industrialization in Lesotho has had negative environmental effects, as the country has many textile companies and these industrial effluents pollute the already scarce waterways (Pullanikkatil and Urama, 2011). The water from Lesotho provides ~35% of water for the Vaal Water Supply Systems, which supplies Gauteng and the mines, industries and most coal-fired power stations in the Mpumalanga Province (Rose *et al*., 2020). Ebenebe *et al*. (2017) summarise literature on South African mines, of metals leached into the environment and their potential impact on biota in surrounding areas; but due to the long-range transport of pollutants, even remote lakes in Lesotho are no longer considered to be pristine (Adams *et al*., 2019) and untouched by these industrial pollutant sources. Southern African freshwater systems are facing unprecedented threats and there is a critical need for conservation of these resources, as increased pollution impacts water quality in regions often considered climatically vulnerable (De Klerk *et al*., 2012; Rose *et al*., 2020).

6.8.1.2. A Brief Consideration of Climate Change

Anthropogenic activities including industrial coal combustion practices are attributed as one of the major causes of climate change and global warming (Barreira *et al*., 2017; Olufemi *et al*., 2018). Climate is considered important in regulating ecosystem structure and combined with nutrients, drives changes in lake ecosystems (Bannister *et al*., 2019). Increased contaminant loading along with climate related stress potentially leads to the degradation of aquatic ecosystems and water quality (Rose *et al.,* 2020). Climate warming is both a gradual driver of ecological change and cause for abrupt shocks to ecosystems such as with changes in precipitation which influences nutrient inputs (Bannister *et al*., 2019). Both lake systems showed evidence of shifts in diatom assemblages from planktonic and benthic taxa to aerophilic which are indicative of fluctuations in regional moisture gradients. There is a need to keep the rise in global average temperatures below 2℃ in accordance with the Paris agreement as the strength and persistence of stratification in lake systems and extent of hypoxia can also be impacted by warming (Barreira *et al*., 2017; Bannister *et al*., 2019).

Rose *et al*. (2020) findings show a unidirectional trend in increasing depositions, however the diatom results of this study shows that diatom responses to increasing deposition do not follow the same unidirectional trend. Instead, records show that they are rather impacted by climatic variations, which may have a greater impact on diatom assemblages than the pollution load. Therefore with changing climates and associated recirculation patterns, this could result in changes in the amount of pollution deposited in regions. With climate change, it is expected that Letšeng-la Letsie may experience the marginal increase in the deposition of the transport of polluted air from the Mpumalanga industrial regions in the North (Rose *et al*., 2020). It has become crucial to phase out the use of coal in energy generation to both reduce environmental pollution and mitigate climate change and determining the scale of contamination at source areas is crucial for the environment and human health (Barreira *et al*., 2017; Rose *et al.,* 2020).

6.8.2. Human Health and Well-being

A challenge facing southern Africa in the 21st century is the management of clean air and accessibility to clean and safe waters, especially for rural populations (Rose *et al.,* 2020). Electricity production based on fossil fuels, coal and natural gases is one of the main sources of pollutants such as of PM, SCPs, SO_2 and NO_x among others (Barreira *et al*., 2017). These contaminants when inhaled, have been linked to a variety of ailments and a range of harmful effects on human health (Barreira *et al*., 2017; Langerman and Pauw, 2018). Inhaled fine PM enters and suppress the lungs development and function, at which point the pollutant infiltrates the bloodstream and can cause cancers (Langerman and Pauw, 2018; Williams, 2020). Development of respiratory (e.g. asthma and chronic bronchitis), cardiovascular and cardiopulmonary diseases from these pollutants have also been linked to cases of premature deaths (Barreira *et al*., 2017; Langerman and Pauw, 2018). In the Mpumalanga Highveld in South Africa, a 2019 report ranked the region one of the highest global emitters of SO_2 and NO_2 and due to heightened air pollution levels, it is also associated with hundreds of early deaths each year (Williams, 2020). Many comprehensive assessments on the impact of South African coal-fired power station emissions on human health are summarised in Langerman and Pauw (2018).

There is a need to reduce priority pollutants emitted in high quantities such as Hg and which may be deposited on southern African freshwaters (Garnham and Langerman, 2016; Rose *et al.,* 2020). Increasing levels of contamination leading to further deterioration of water quality impacts the access, especially for rural communities, to clean natural waters (Rose *et al.,* 2020). In places such as Lesotho, industrial wastewater discharges are being released into the environment at an unsustainable rate, causing water pollution (Pullanikkatil and Urama, 2011). The extent and impacts of industrial water pollution in Lesotho for example, and the associated effects on human livelihoods in the region are investigated by Pullanikkatil and Urama (2011). Research is crucial in sensitive aquatic systems such as in Lesotho, as it is an important water resource area for South Africa, that import their water from

the Lesotho Highlands Water Project (LHWP) programme (Rose *et al*., 2020). As a prerequisite for sustainable use of water resources, the health of aquatic ecosystems is essential (Rose *et al.,*2020).

6.8.3. Mitigation and Management

This study demonstrates the need for better management and mitigation of atmospheric pollution. Air pollution and subsequent deposition pose adverse effects on both the environment and on human health which is an issue faced globally (Barreira *et al*., 2017). In South Africa, there is a general lack of air quality monitoring with many monitoring stations across the country proving non-functional (Williams, 2020). Additionally, as different pollutant mitigation strategies are independent of one another and require among other factors differing technologies and infrastructure, this may limit efforts (Pretorius *et al*., 2015). Controlling and limiting polluting emissions and deposition from the coal industry is crucial; where phasing coal out provides the opportunity to reduce emissions entirely (Garnham and Langerman, 2016; Barreira *et al*., 2017). Eskom's coal-fired power stations situated in the Mpumalanga Highveld burn bituminous coal and air pollution in this region exceeds South Africa's national air quality standards (Garnham and Langerman, 2016; Williams, 2020).

Although >90% of the ash during the coal combustion processes is supposed to be removed, impurities and pollutants such as SO_2, NO_x and Hg are still released into the atmosphere (Langerman and Pauw, 2018). In South Africa, not many power stations use SO_2 and NO_x abatement technologies, where this could better address the deposition of these pollutants (Pretorius *et al*., 2015). Abatement technologies include Low NO_x Burners (LNB) and Flue Gas Desulfurization Plants (FGD) for reducing NO_x and SO_2 emissions, respectively (Pretorius *et al*., 2015). The bio-accumulation of Hg in ecosystems and food chains is a global concern and the main driver for regulations around this pollutant in South Africa (Garnham and Langerman, 2016). Through abatement technologies such as Electrostatic

Precipitators (ESPs) and Fabric Filter Plants (FFPs) of which the latter is more efficient, a reduction in the emission and deposition of PM and particulate-bound Hg can occur (Pretorius *et al*., 2015).

To reduce emissions by 2020 and comply with national standards, a management plan was published in 2012 by the South African government (Williams, 2020). Eskom however, as one of the major role players in coal combustion in South Africa, submitted in 2013 applications to postpone compliance with 11 of its coal-fired power stations (Pretorius *et al*., 2015; Williams, 2020). Eskom further filed postponement and exemption from the Minimum Emission Standards that were also set (Pretorius *et al*., 2015). There are plans however for South Africa to reduce emissions between 2025-2030 and decommission most of Eskom's coal-fired power stations by 2040 (Williams, 2020; Phillips, 2021). Additionally, to reach a net zero economy by 2050, the Low Emission Development Strategy (LEDS) was developed by the South African government (Lo, 2020). However, without emission abatement technologies or upgrades, it is unclear whether pollutant emissions and subsequent deposition from Eskom's power stations will improve or increase in severity over the next decades (Garnham and Langerman, 2016).

The Mpumalanga Highveld in South Africa was already considered a high priority air pollution hotspot back in 2007 (Williams, 2020). Pollution trends from the Lake Chrissie core indicate increased abundances of pollution tolerant species, suggesting potentially increased pollution within the system. Areas surrounding these power stations are suggested to experience increased pollution deposition from these coal burning practices, along with from other sources. Notwithstanding, energy models based on burning fossil fuels such as coal are not respectful to the environment and cannot be the basis of economic development (Barreira *et al*., 2017).

6.9. Research Limitations

There is a lack of information on the rate and extent of pollution deposition in Lake Chrissie from coal-fired power stations and of diatom related information pertaining to species identified in both lake systems. During diatom preparation, some diatom valves may have been destroyed and as such this may have impacted the total diatom counts. Limitations arose with species identification, such as *Nitzschia sp*., as these species are difficult to separate due to taxonomic similarities (Sitoe *et al*., 2017; Westover *et al.*, 2019). Challenges with interpretations include the diatom record indicating heavily industrially contaminated water at the remote Letšeng-la Letsie, where changes in diatom assemblages are potentially caused by another driver such as climate trends. As some species may respond to multiple different drivers, it is often difficult to interpret what is causing a change. Lastly, whether the results from a single sediment core are representative of the diatom diversity of an entire lake at a specific time interval, is a still posited as a fundamental question (Zou *et al*., 2020).

CHAPTER 7: CONCLUSION

7.1. Introduction

Ongoing anthropogenic pressures heighten the importance of reliable assessments of the ecological status of southern African freshwaters (Pajunen *et al*., 2020). As with all ecological assessments, it is important to understand the spatial and temporal context of the study regions and the ecology of the indicator organisms (Cormier *et al*., 2020). Diatoms are one of the most sensitive indicators of ecological response to disturbance, that may provide the evidence for the impact from anthropogenic stressors and pollutant deposition. Further research is critical for freshwater bodies within the southern African environment, given their potential role as sentinel ecosystems, their rarity and importance as unique aquatic habitats (Dunnink *et al*., 2016). Long-term monitoring provides a source of information; however these records are often rare and unavailable for many freshwater systems in the southern Hemisphere (Adams *et al*., 2019), including South Africa and Lesotho alike. However, this is important as southern African ecosystems are at threat from widespread pollution.

Mpumalanga Province is rich in both coal deposits and wildlife-based tourism; Lake Chrissie and the greater MLD are in close proximity to coal-fired operations. Letšeng-la Letsie Wetland is designated as a Ramsar protected site (Kahlolo *et al*., 2021). The Letšeng-la Letsie catchment is protected and located within a biodiversity hotspot of the Maloti-Drakensburg Mountain area in southern Lesotho (Rose *et al*., 2020). The only World Heritage Site in Lesotho is the Maloti-Drakensberg Park which borders eastern Lesotho and South Africa (Noome and Fitchett, 2019). The lake within this greater catchment area forms part of the Conserving Mountain Biodiversity initiative (Rose *et al*., 2020) and is situated within the Maloti Mountains at an altitude of 2400m.asl (Kahlolo *et al*., 2021; Smit and Van Rensberg, 2021). This project aim was to find signals for historical air pollution from coal-fired power stations over the past 200-years, in these two lakes, using changes in diatom assemblages.

7.2. Synthesis of Results

The site, years of pollution, hydrology and climate along with the indicator diatom species are summarised in Table 7.1. Both Lake Chrissie and Letšeng-la Letsie have had industrial related pollution fluctuations coinciding during the ~1950s and the ~1970s. Thereafter, there is indication of an increase in industrial-related pollution in the early ~1980s in Lake Chrissie, with a delay observed with an increase in Letšeng-la Letsie in the mid ~1980s. Lake Chrissie continues to show an increase in these conditions from the late ~1990s to the mid ~2010s; where Letšeng-la Letsie however, shows a brief hiatus in these conditions until indication once more of an increase during the ~2010s to 2018. The Letšeng-la Letsie results show a delay in industrial based contamination post ~1980s with low concentrations throughout the Letšeng-la Letsie profile. Both sites' records indicate deeper waters during the ~1950s, ~1960s and ~1990s with increased lake levels from the ~2000-2010s (Table 7.1). Both sites' records indicate wetter periods during the ~2000-2010s and drier periods during the ~1940s, the late ~1990s and during the ~2010s to the core surface (Table 7.1). Both sites indicate warmer periods during the late ~1950s and between the late ~1970s and early ~1980s (Table 7.1).

Table 7.1. Summary of the pollution and hydro-climatic conditions in both lake systems and the indicator species.

Site	Pollution	Indicator species
Lake Chrissie and Letšeng-la-Letsie	During the ~1950s, ~1970s, ~1980s, late ~1990s and ~2010s.	*Fragilaria fasciculata* *Navicula veneta* *Nitzschia sp.* *Hantzschia amphioxys* *Gomphonema parvulum* *Navicula antonii* *Cyclotella meneghiana* *Gomphonema minutum* *Navicula trivialis* *Fragilaria famelica*

Site	Hydrology	Indicator species
Lake Chrissie and Letšeng-la-Letsie	Deeper waters : During the ~1950s, ~1960s and ~1990s Increased lake levels: During the ~2000-2010s.	The benthic species *Fragilaria famelica* The planktonic and facultative planktonic species *Aulacoseira sp.* including *Aulacoseira granulata*
Site	Climate	Indicator species
Lake Chrissie and Letšeng-la-Letsie	Wetter conditions: During the ~2000-2010s Drier conditions: During the ~1940s, late ~1990s and ~2010s. Warmer climates: During the late ~1950s and between the late ~1970s and early ~1980s.	The planktonic and facultative planktonic species *Aulacoseira sp.* including *Aulacoseira granulata* The aerophilic species *Hantzschia amphioxys, Pinnularia borealis* and *Pinnularia divergens.* The epiphytic, epipelic and epilithic species *Nitzschia sp.*

The results from this study revealed that the climate signal inferred from the diatom records are clearer than that of the pollution signal. The results indicate that the pollution signal at Letšeng-la Letsie is likely more affected by air mass pathways and in some periods, pollution may not have reached the lake. Additionally, the remoteness and low pollution levels makes it difficult to identify the pollution signal in Letšeng-la Letsie, which is likely weaker and interrupted. Additionally, it cannot be argued definitively that the pollutants are from coal-fired power stations, especially given that Rose *et al*. (2020) report om the presence of PCBs and PAHs. However, in comparing the MLD and Letsie there is a site proximate and a site distal to these stations, and so the variation in pollutant loading can be hypothesised to reflect this. Related to this, the impact of other forms of pollution cannot be excluded. The majority of the pollutant signal, particularly in the MLD, likely relates to coal fired power stations, but there is a range of other pollutants.

7.3. Achievement of Study Objectives

1. Identify diatom valves to reconstruct the community assemblage for the two sites.

The results of the Lake Chrissie and Letšeng-la Letsie diatom analyses are presented in *Chapter 5*. The results of the community assemblages for Lake Chrissie can be found in *Section 5.1* including microscopy found in *Section 5.1.1,* with statistical analysis in Section *5.1.2.* The results of the community assemblages for Letšeng-la Letsie can be found in *Section 5.2,* including microscopy in *Section 5.2.1* and of statistical analysis in *Section 5.2.2.*, respectively.

2. Determine trends, changepoints and their environmental significance of the diatom assemblages over time.

The collated identified diatom species in each site are found in Chapter 6, in *Section 6.*2 and in the Table *6.*1, which lists their ecological characteristics and tolerances to pollutants. Environmental inferences of change in diatom communities, species composition and diversity within the two sites, are found in *Chapter 6.3* which includes the paleoenvironmental reconstruction for the two sites, found in *Section 6.3.1* for Lake Chrissie and in *Section 6.3.2* for Letšeng-la Letsie. There were 20 species overlaps between sites, with 15 species found unique to Lake Chrissie and 18 species unique to Letšeng-la Letsie. Pollution tolerant species were found in both sites, but in low concentrations and included *Fragilaria fasciculata, Gomphonema parvulum, Navicula trivialis, Navicula antonii, Navicula veneta, Cyclotella meneghiniana*. There was predominant indication of cycles of various lake levels, as indicated from shifts between planktonic and benthic taxa and aerophilic species, signalling hydrological fluctuations which were found stronger than signals linked to pollution.

3. Compare the records for the sites to the observed variations in contamination between the sites, as indicated by other lake sediment proxies of fossil fuel combustion-based contamination.

The inter-site comparison between species is found in *Chapter* 5, in Section *5.3.* Lake Chrissie was chosen due to its proximity to the Mpumalanga Province coal-fired power stations, while Letšeng-la Letsie may act as a relatively pristine site given its distal location from these power stations. There is a comparison between the Lake Chrissie and Letšeng-la Letsie. diatom records in *Chapter* 6, specifically found in *Section 6.4.* The results for both sites are compared with global literature in *Section 6.5*, taking into consideration lake trophic status in *Section 6.5.1*, of pollution from coal-fired power stations in *Section 6.3.2* and of the hydro-climatic differences in *Section 6.5.3.* Thereafter a comparison is made with southern African literature in Section 6.6, concerning lake trophic status and of pollution derived from coal-fired power stations, found in *Section 6.6.1*, along with the hydro-climatic conditions in *Section 6.6.2.*

7.4. Avenues for Future Work

The results from this study revealed that the climate signal inferred from the diatom records within both sediment core profiles is clearer than that of the pollution signal. The results from Rose *et al.* (2020) show low traces of pollution and contamination in Letšeng-la Letsie, that has increased since ~1970s. However this was unexpected given that South Africa exceeds international pollution levels and standards (Rose *et al*., 2021). Therefore, where this pollution is being transported and deposited is of interest, if it is not landing with higher concentrations in Lesotho and why there is not a stronger pollution signal in Lake Chrissie. However, regarding prevailing wind direction: “Most pans in the MLD are oriented in a north-south direction, perpendicular to the prevailing winds which are easterly

during summer and westerly or northerly in winter (Russell, 2008)".Potential future work can bridge this gap in knowledge with key areas of research involving performing the same physical and chemical analyses on more sites in the MLD, including on Lake Chrissie, along with the broader southern African regions. Comparing findings from this study and with other southern African aquatic systems would allow for broader comparisons to be made, to see if there are any synchronicities and/or dissimilarities in the diatom records and pollution trends.

REFERENCES

Acaps. (2022). Country: Lesotho. Available from https://www.acaps.org/country/lesotho/crisis/drought?acaps_mode=slow&show_mode=1, accessed 18 June 2022.

Adams, J.K., Peng, Y., Rose, N.L., Shchetnikov, A.A. and Mackay, A.W. (2019). Diatom community responses to long-term multiple stressors at Lake Gusinoye, Siberia. *Geography and Environment*, 6 (1): 1-19, DOI: 10.1002/geo2.72.

Adrian, R., O'Reilly, C.M., Zagarese, H., Baines, S.B., Hessen, D.O., Keller, W., Livingstone, D.M., Sommaruga, R., Straile, D., Van Donk, E., Weyhenmeyer, G.A. and Winder, M. (2009). Lakes as sentinels of climate change. *Limnology and Oceanography*, 54(6): 2283-2297.

Akinbami, O.M., Oke, S.R. and Bodunrin, M.O. (2021). The state of renewable energy development in South Africa: An overview. *Alexandria Engineering Journal,* 60: 5077-5093.

Alikaj, M., Brahushi, F. and Kupe, L. (2019). Ecological status assessment using diatom indices of water ecosystems in Gjirokastra district, Albania. *Fresenius Environmental Bulletin,* 28(2): 857-862.

Antonelli, M., Wetzel, C.E., Ector, L., Teuling, A. and Pfister, L. (2017). On the potential for terrestrial diatom communities and diatom indices to identify anthropic disturbance in soils. *Ecological Indicators,* 7(5): 73-81.

Archibald, R.E.M. (1972). Diversity in some South African diatom associations and its relation to water quality. *Water Research,* 6: 1229-1238.

Bailey, M., Heinrich, D. and Kruczkiewicz, A. (2021). Climate profiles of countries in southern Africa: Lesotho. *Climate Centre*, 1-4.

Bannister, W., McGowan, S., Santos-Borja, A.C., Quak, J., Fong, L.S., Mendoza, M., Papa, R.D.S. and Taylor, D. (2019). Potential anthropogenic regime shifts in three freshwater lakes in tropical East Asia. *Freshwater Biology*, 64(4): 708-722.

Barreira, A., Patierno, M. and Ruiz-Bautista, C. (2017). Impacts of pollution on our health and the planet: The case of coal power plants. *UN Environment Perspectives*, 28: 1-10.

Bate, G. and Smailes, P. (2008). The response of the diatom flora of St Lucia Lake and estuary, South Africa, to severe drought. *African Journal of Aquatic Science*, 33: 1-15, DOI: 10.2989/AJAS.2007.33.1.1.385.

Bate, G., Smailes, P. and Adams, J. (2004). A water quality index for use with diatoms in the assessment of rivers. *Water South Africa*, 30: 493-449.

Battarbee, R.W., Jones, V.J., Flower, R.J., Cameron, N.G. and Bennion, H. (2001). Chapter 8: Diatoms. In Smol, J.P., Birks, H.J.B. and Last, W.M. (Eds.) *Tracking Environmental Change Using Lake Sediments, Volume 3: Terrestrial, Algal, and Siliceous Indicators*, Kluwer: Dordrecht, 155-202.

Battarbee, R.W., Simpson, G.L., Shilland, E.M., Flower, R.J., Kreiser, A., Yang, H. and Clarke, G. (2014). Recovery of UK lakes from acidification: An assessment using combined palaeoecological and contemporary diatom assemblage data. *Ecological Indicators,* 37:365-380.

Beck, C.C., Allen, M.M., Feibel, C.S., Beverly, E.J., Stone, J.R., Wegter, B. and Wilson IV, C.I. (2019). Living in a swampy paradise: Palaeoenvironmental reconstruction of an African humid period lacustrine margin, West Turkana, Kenya. *Journal of African Earth Sciences*, 154: 20-34.

Benhassane, L., Oubraim, S., Mounjid, J., Fadlaoui, S. and Loudiki, M. (2020). Monitoring impacts of human activities on Bouskoura stream (Periurban of Casablanca, Morocco): 3. Bio-Ecology of epilithic distoms. *Nature, Environment and Pollution Technology,* 19(5): 1913-1930.

Bere, T., Mangadze, T. and Mwedzi, T. (2014). The application and testing of diatom-based indices of stream water quality in Chinhoyi Town, Zimbabwe. *Water South Africa.* 40: 530–512.

Beyene, A., Addis, T., Kifle, D., Legesse, W., Kloos, H. and Triest, L. (2009). Comparative study of diatoms and microinvertebrates as indicators of severe water pollution: Case study of the Kebena and Akaki Rivers in Addis Ababa, Ethiopia, *Ecological Indicators*, 9: 381-392.

Bichet, V., Gauthier, E., Massa, C. and Perren, B.B. (2014). Lake sediments as an archive of land use and environmental change in the eastern settlement, southwestern Greenland. *Journal of North Atlantic*, 6: 47-63.

BirdLife. (2015). Chrissie Pans. Available from https://www.birdlife.org.za/iba-directory/chrissie-pans/, accessed on 4 November 2021.

Buczkó, K., Ács, É., Báldi, K., Pozderka, V., Braun, M., Tihamér, K. and Korponai, J. (2019). The first high resolution diatom record from Lake Balaton, Hungary in Central Europe. *Limnetica*, 38(1): 417-430.

Cameron, N. (2018). Diatoms. In Sandra, L. and Varela, L. (Eds). *The Encyclopaedia of Archaeological Sciences*, John Wiley & Sons Inc. 1-2.

Camfil. (2018). Avoiding the Harmful Impacts of Particulate Matter Pollution. Available from https://cleanair.camfil.us/2018/01/22/avoiding-the-harmful-impacts-of-particulate-matter-pollution/, accessed 18 May 2022.

Castillo, S., Alastuey, A., Cuevas, E., Querd, X. and Avila, A. (2017). Quantifying dry and wet deposition fluxes in two regions of contrasting African influence: The North-Eastern Iberian Peninsula and the Canary Islands. *Atmosphere*, 8(5): 86-103.

Çelekli, A., Toudjani, A.A., Lekesiz, H.O. and Cetin, T. (2018). Ecological quality assessment of running waters in the North Aegean catchment with diatom metrics and multivariate approach. *Limnologica,* 73: 20-27.

Chalie, F. and Gasse, F. (2002). Late glacial-Holocene diatom record of water chemistry and lake level change from the tropical East African Rift Lake Abiyata (Ethiopia). *Palaeogeography, Palaeoclimatology, Palaeoecology,* 187: 259-283.

Chatanga, P., Ntuli, V., Mugomeri, E., Keketsi, T. and Chikowore, N.V.T. (2019). Situational analysis of physico-chemical, biochemical and microbiological quality of water along Mohokare River, Lesotho. *Egyptian Journal of Aquatic Research*, 25: 45-51.

Cheng, J., Zhu, Y., Zhang, Z. and Yang, W. (2019). Modification and improvement of microalgae strains for strengthening CO2 fixation from coal-fired flue gas in power plants. *Bioresources Technology*, 291(1): 1-12, DOI: 10.1016/j.biortech.2019.121850.

Chetty, S. and Pillay, L. (2019). Assessing the influence of human activities on river health: A case for two South African rivers with differing pollutant sources. *Environmental Monitoring Assessment*, 191(3): 168-179.

Chonova, T., Kurmayer, R., Rimet, F., Labanowski, J.M., Vasselon, V., Keck, F., Illmer, P. and Bouchez, A. (2019). Benthic diatoms communities in an alpine river impacted by waste treatment effluents as revealevd using DNA metabarcoding. *Frontiers in Microbiology*, 10(653): 1-17, DOI: 10.3389/fmicb.2019.00653.

Climate Change Knowledge Portal, CCKP. (2021). Country: Lesotho. Available from https://climateknowledgeportal.worldbank.org/country/lesotho/vulnerability#:~:text=Between%20April%201991%20and%20October,environment%2C%20economy%2C%20and%20society, accessed 8 June 2022.

Cohu, R.L., Lange-Bertalot, H., van de Vyver, B. and Tudesque, L. (2020). Analysis and critical evaluation of structural features in four *Cymbellaceae* taxa from New Caledonia*,* 20(1): 75-85.

Conradie, E.H., van Zyl, P.G., Pienaar, J.J., Beukes, J.P., Galy-Lacaux, C., Venter, A.D. and Mkhatshwa, G.V. (2016). The chemical composition and fluxes of atmospheric wet deposition at four sites in South Africa. *Atmospheric Environment*, 146: 113-131.

Cormier, E.C., Sisson, D.R., Ruhland, K.M., Smol, J.P. and Bennet, J.R. (2020). A morphological trait-based approach to environmental assessment models using diatoms. *Canadian Journal of Fisheries and Aquatic Sciences*, 77(1): 108-112.

Curtis, C.J., Flower, R. Rose, N., Shilland, J., Simpson, G.L., Turner, S., Yang, H. and Pla, S. (2010). Palaeolimnological assessments of lake acidification and environmental change in the Athabasca Oil Sands Region, Alberta. *Journal of Palaeolimnology*, 69(1): 92-104.

Curtis, C.J., Juggins, S., Clarke, G., Battarbee, R.W., Kernan, M., Catalan, J., Thompson, R. and Posch, M. (2009). Regional influence of acid deposition and climate change in European mountain lakes assessed using diatom transfer functions. *Freshwater Biology*, 54: 2555-2572.

Dalton, A., Feig, G.T. and Barber, K. (2018). Trace metal enrichment observed in soils around a coal-fired power plant in South Africa. *Clean Air Journal*, 28(2): 32-40.

Dalu, T. and Froneman, P.W. (2016). Diatom-based water quality monitoring in southern Africa: Challenges and future prospects. *Water South Africa*, 42(4): 551-559.

Dalu, T., Bere, T. and Froneman, P.W. (2016). Assessment of water quality based on diatom indices in a small temperate river system: a case of the Kowie River, South Africa. *Water South Africa*, 42: 183-193.

Dalu, T., Bere, Froneman, P.W., Chari, L. and Richoux, N.B. (2014). Colonisation and community structure of benthic diatoms on artificial substrates following a major flood event: A case of the Kowie River (Eastern Cape, South Africa). *Water SA,* 40(3): 471-480.

Das, S.K., Routh, J. and Roychoudhury, A.N. (2015). Biogeochemistry of shallow lake sediments: A case study from Verlorenvlei, South Africa. *Current Science*, 109(8): 1486-1491.

Datta, A., Marella, T.K., Tiwari, A. and Wani, S.P. (2019). The diatoms: From eutrophic indicators to mitigators. In Gupta, S.K. and Bux, F. (eds). *Applications of Microalgae in Wastewater Treatment*. Springer India, Noida: 19-40.

De Klerk, A.R., De Klerk., L.P., Chamier, J. and Wepener, V. (2012). Seasonal variations of water and sediment quality parameters in endorheic reed pans on the Mpumalanga Highveld. *Water South Africa,* 38(5): 663-672.

De Klerk, A.R. and Wepener, V. (2013). Macroinvertebrate assemblage changes as an indicator of water quality of perennial endorheic reed pans on the Mpumalanga Highveld, South Africa. *Journal of Environmental Protection,* 4: 10-21.

Della Bella, V. and Mancini, L. (2009). Freshwater diatom and macroinvertebrate diversity of coastal permanent ponds along a gradient of human impact in a Mediterranean ecoregion. In Oertli, B., Ce´re´ghino, R., Biggs, J., Declerck, S., Hull, A. and Miracle, M.R. (eds). *Pond Conservation in Europe*. Springer Netherlands, Dordrecht: 181-197.

Dong, X., Bennion, H., Battarbee, R., Yang, X., Yang, H. and Liu, E. (2008). Tracking eutrophication in Taihu Lake using the diatom record: Potential and problems. *Journal of Palaeolimnology*, 40: 413-429.

Dulanya, Z. and Trauth, M.H. (2019). Palaeoenvironmental reconstruction of the recent history of Lake Chiuta Wetland, South Malawi. *Malawi Journal of Science and Technology,* 11(1): 1-26.

Dunnink, J.A., Curtis, C.J., Beukes, J.P., van Zyl, P.G. and Swartz, J. (2016). The sensitivity of Afromontane tarns in the maloti-Drakensberg region of South Africa and Lesotho to acid deposition. *African Journal of Aquatic Sciences*, 41(4): 413-426.

Ebenebe, P.C., Shale, K., Sedibe, M., Tikilili, P. and Achilonu, M.C. (2017). South African mine effluents: Heavy metal pollution and impact on the ecosystem. *International Journal of Chemical Sciences*, 15(4): 198-209.

Environmental Protection agency, EPA. (2021). Available from https://www.epa.gov/pm-pollution/health-and-environmental-effects-particulate-matter-pm#:~:text=Particles%20can%20be%20carried%20over,waters%20and%20large%20river%20basins, accessed 22 May 2022.

Erasmus, M. and Taylor, J. (2021). A diatom-based index for acid mine drainage impacted permanent pans in the Mpumalanga Highveld region. *Coaltech Research Association*, 1-63.

Eskom. (2022a). Annual and statistical reports. Available from https://www.eskom.co.za/heritage/annual-and-statistical-reports/, accessed on 12 April 2022.

Eskom. (2022b). Arnot Power Station. Available from https://www.eskom.co.za/heritage/history-in-decades/escom-1963-1972/arnot-power-station/, accessed 10 June 2022.

Eskom. (2022c). Coal fired power stations. Available from https://www.eskom.co.za/eskom-divisions/gx/coal-fired-power-stations/, accessed 10 June 2022.

Evans, J. (2022). Eskom greenwash on coal-fired Kusile a smokescreen for terrifying overall emissions. Available from https://www.dailymaverick.co.za/article/2022-06-10-eskom-greenwash-on-coal-fired-kusile-a-smokescreen-for-terrifying-overall-emissions/, accessed 10 June 2022.

Ferreira, M. (2021). The development of methods to assess the ecological integrity of perennial pans. Submitted for the requirements of a philosophiae Doctor, University of Johannesburg.

Ferreira, M., Wepener, V. and van Vuren, J.H.J. (2012). Aquatic invertebrate communities of perennial pans in Mpumalanga, South Africa: A diversity and functional approach. *Invertebrates,* 53(2): 751-768.

Fitchett, J.M. (2015). Towards a multi-proxy Holocene palaeoenvironmental and palaeoclimatic reconstruction for Eastern Lesotho. *Degree Philosophioe Doctor Dissertation submitted to the, University of the Witwatersrand: Johannesburg.*

Fitchett, J.M., Grab, S.W., Bamford, M.K. and Mackay, A.W. (2016a). A multi-disciplinary review of late quaternary palaeoclimates and environments for Lesotho. *South African Journal of Science*, 112(7/8): 788-798.

Fitchett, J.M., Grab, S.W., Bamford, M.K. and Mackay, A.W. (2016b). A multi-proxy analysis of late Quaternary palaeoenvironments, Sekhokong Range, eastern Lesotho. *Journal of Quaternary Science*, 31(7): 788-798.

Fontana, L., Albuquerque, A.L.S., Brenner, M., Bonotto, D.M., Sabaris, T.P.P., Pires, M.A.F., Cotrim, M.E.B. and Bicudo, D.C. (2014). The eutrophication history of a tropical water supply reservoir in Brazil. *Journal of Paleolimnology*, 51: 29-43.

Foster, L., Malherbe, W., Ferreira, M. and van Vuren, J.H.J. (2015). Macroinvertebrate variation in endorheic depression wetlands in North West and Mpumalanga Provinces, South Africa. *African Journal of Aquatic Science*, 40(3): 287-297.

Fuls, F. (2013). Choosing between coal or wetlands in Chrissiesmeer. Available from http://www.chrissiesmeer.co.za/cp/19247/mining, accessed on 09 June 2022.

Garcia-Rodriguez, F., Anderson, C.R. and Adams, J.B. (2007).Paleolimnological assessment of human impacts on an urban South African lake. *Journal of Palaeolimnology,* 38: 297-308.

Garland, R. and Langerman, K. (2021). South Africa's power utility Eskom: how does it stack up in the pollution stakes? Available from https://theconversation.com/south-africas-power-utility-eskom-how-does-it-stack-up-in-the-pollution-stakes-170808, accessed on 12 June 2022.

Garnham, B.L. and Langerman, K.E. (2016). Mercury emissions from South Africa's coal-fired power stations. *Clean Air Journal*, 26(2): 14-20.

Gasse, F. (1987). Diatoms for reconstructing palaeoenvironments and paleohydrology in tropical semi-arid zones. *Hydrobiologia,* 154: 127-163.

Gasse, F. and Van Campo, E. (1998). A 40,000-yr pollen and diatom record from Lake Tritrivakely, Madagascar, in the southern tropics. *Quaternary Research,* 49: 299-311.

Gaughan, A.E., Staub. C.G., Hoell, A., Weaver, A. and Waylen, P.R. (2016). Inter- and intra-annual precipitation variability and associated relationships to ENSO and the IOD in southern Africa. *International Journal of Climatology*, 36: 1643-1656.

Gbadebo, A.M., Dimowo, B.O., Taiwo, A.M. and Omoniyi, I.T. (2019). Application of diatom-based indices in river quality assessment: A case study of lower Ogun River (Abeokuta, southwestern Nigeria) using epilithic diatoms. *In Limnology-Some New Aspects of Inland Water Ecology*, 3: 40-62.

Gilili, C. (2021). Climate crisis threatens future maize production in SA and Lesotho. Available from https://mg.co.za/environment/2021-03-26-climate-crisis-threatens-future-maize-production-in-sa-and-lesotho/?amp, accessed 29 May 2022.

Giordano, M., Norici, A. and Ratti, S. (2008). Role of sulfur for algae: Acquisition, metabolism, ecology and evolution. *Sulfur Metabolism in Phototrophic Organisms*, 2: 397-415.

Gökçe, D. (2016). Algae as an indicator of water quality. *In Algae-Organisms for Imminent Biotechnology. InTech*, 81-101.

Goman, M., Ashley, G.M., Owen, R.B., Hover, V.C. and Maharjan, D.K. (2017). Late Holocene environmental reconstructions from Lake Solai, Kenya. *The Professional Geographer*, 69(3): 438-454.

Google Earth. (2022a). Lake Chrissie, Chrissiesmeer, elevation of 1676m.asl. Available from https://earth.google.com/web/search/lake+Chrissie/@-26.32093985,30.21436235,1675.87355232a,10418.43320118d,35y,0h,0t,0r/data=CigiJgokCRmJJi9yuzRAEReJJi9yuzTAGVxPDwWyn0lAIVtPDwWyn0nA, accessed 9 November 2021.

Google Earth. (2022b). Lake Letsie, Lesotho, elevation of 2402m.asl. Available from https://earth.google.com/web/search/lake+letsie/@-0.309798,28.165087,2399.02410501a,897.17576015d,35y,30.66633958h,45t,0r/data=CigiJgokCUM9HxlfSTrAEXvqXk3wWjrAGcAfGLkSSz5AIQhdzS2uIj5A, accessed 9 November 2021.

Grab, S.W. and Linde, J.H. (2014). Mapping exposure to snow in a developing African context: Implications for human and livestock vulnerability in Lesotho. *Natural Hazards,* 71: 1537-1560.

Grab, S.W., Linde, J.H. and De Lemos, H. (2017). Some attributes of snow occurrence and snowmelt/sublimation rates in the Lesotho Highlands: Environmental implications. *Water South Africa*, 43(2): 333-342.

Grab, S.W. and Mills, S.C. (2011). Quaternary slope processes and morphologies in the upper Sehonghong Valley, eastern Lesotho. *Proceedings of the Geologists' Association,* 122: 179-186.

Grab, S.W. and Nash, D.J. (2020). "But what silence! No more gazelles…": Occurrence and extinction of fauna in Lesotho, southern Africa, since the late Pleistocene. *Quaternary International*, DOI: 10.1016/j.quaint.2020.04.030.

Hajizadeh, Y., Nemati, S., Aghapour, A.A., Abdolahnejad, A., Mohammadi, A., Panatri, H., Maghanjooghi, S.M. and Nikoonahad, A. (2017). Influence of air pollution on chemical quality of wet atmospheric deposition: A case study in Urmia, Iran. *Iranian Journal of Health, Safety and Environment*, 5(1): 904-910.

Hallowes, D. and Munnik, V. (2016). The destruction of the Highveld. *Groundwork Report,* 1: 1-211.

Hamdan, M.A., Flower, R.J., Hassan, F.A. and Hassan, S.M. (2020). The Holocene history of the Faiyum lake (Egypt) based on sediment characteristics, diatoms and ostracods contents. *Journal of Great Lakes Research,* 46: 456-475.

Hansika, R.V.H. and Yatigammana, S.K. (2019). Distribution of diatom assemblages in the surface sediments in Sri Lankan reservoirs located in the main climatic regions and potential of using them as environmental predictors. *Tropical Ecology*, 60: 415-425.

Harding, W.R., Archibald, C.G.M. and Taylor, J. (2005). Diatomology in South African biomonitoring: The South African diatom collection. *African Journal of Aquatic Science,* 30(2):221, DOI: 10.2989/16085910509503865.

Harding, W.R. and Taylor, J.C. (2014). Diatoms as indicators of historical water quality: A comparison of samples taken in the Wemmershoek catchment (Western Cape Province, South Africa) in 1960 and 2008. *Water South Africa,* 40: 601–606.

Hecky, R.E., Kling, H.J., Johnson, T.C., Bootsma, H.A. and Wilkinson, P. (1999). Algal and sedimentary evidence for recent changes in the water quality and limnology of Lake Malawi/Nyasa. *Victoria*, 1: 192-214.

Hicks, S. (2020). *Pollution*. Available from https://www.lakescientist.com/pollution/, accessed on 25 November 2021.

Hilson, G., Zolnikov, T.R., Ortiz, D.R. and Kumah, C. (2018). Formalizing artisanal gold mining under the Minamata convention: Previewing the challenge in Sub-Saharan Africa. *Environmental Science and Policy*, 85: 123-131.

Hoogendoorn, G., Stockigt, L., Saarinen, J. and Fitchett, J.M. (2020). Adapting to climate change: the case of snow-based tourism in Afriski, Lesotho. *African Geographic Review*, 40(1): 92-104.

Humane, S.S., Humane, S.K. and Borkar, N. (2020). Diatoms and phytoliths records from sediment core of Tarna-Satighat Lake, Centra India: Implications as indicators of changing wet/dry climatic phases and trophic status. *Earth Science India,* 13(2): 39-50.

Kahlolo, N., Mapeshoane, B.E., Chatanga, P., Seleteng-Kose, L. and Marake, M. (2021). Vegetation and associated environmental conditions of the high-altitude Letšeng-le Letsie palustrine wetland, a Ramsar site in Lesotho. *Wetlands*, 41(79): 2411-2502.

Kiage, L.M. and Liu, K.B. (2006). Late quaternary palaeoenvironmental changes in East Africa: A review of multiproxy evidence from palynology, lake sediments, and associated records. *Progress in Physical Geography,* 30(5): 633-658.

Kirsten, K.L. and Meadows, M.E. (2016). Late-Holocene palaeolimnological and climate dynamics at Princessvlei, South Africa: Evidence from diatoms. *The Holocene,* 26(9): 1371-1381.

Klamt, A.M., Qian, F., Hu, K., Wang, J., Huang, L., Li, R. and Chen, G. (2021). The rise and fall of primary producers and consumers in multiply-stressed shallow lake (Lake Qilu, China) over the last 200 years. *Ecological indicators*, 129: 1-14, DOI: 10.1016/j.ecolind.2021.107891.

Kociolek, P. (2012). The diatoms: Applications for environmental and earth sciences. In Smol, J.P. and Stoemer, E.F. (eds.) *Palaeontologica Electronica*, 15(1): 2-3.

Kock, A., Taylor, J.C. and Malherbe, W. (2019). Diatom community structure and relationship with water quality in Lake Sibiya, KwaZulu-Natal, South Africa. *South African Journal of Botany*, 123: 161-169.

Korhola, A., Sorvari, S., Rautio, M., Appleby, P.G., Dearing, J.A., Hu, Y., Rose, N., Lami, A. and Cameron, N.G. (2002). A multi-proxy analysis of climate impacts on the recent development of subarctic Lake Saanaja¨rvi in Finnish Lapland. *Journal of Paleolimnology*, 28: 59-77.

Kuefner, W., Ossyssek, S., Geist, J. and Raeder, U. (2020). The silicification value: A novel diatom-based indicator to assess climate change in freshwater habitats. *Diatom Research*, 35(1): 1-16, DOI: 10.1080/0269249X.2020.1722246.

Kwon, S.Y., Blum, J.D., Yin, R., Tsui, M.T., Yang, Y.H. and Choi, J.W. (2020). Mercury stable isotopes for monitoring the effectiveness of the Minamata Convention on mercury. *Earth-Science Reviews*, 203: 103-111.

Lafond, A. (2022). Available from https://foobot.io/guides/environmental-impact-of-particle-pollution.php, accessed on 25 May 2022.

Lange-Bertalot, H. (2001). *Navicula* sensu stricto, 10 genera separated from *Navicula* sensu lato, *Frustulia*. *Diatoms of Europe*, Gantner, Ruggell/Liechtenstein, pp: 526.

Langerman, K.E. and Pauw, C.S. (2018). A critical review of health risk assessments of exposure to emission from coal-fired power stations in South Africa. *Clean Air Journal*, 28(2): 68-79.

Langerman, K.E., Pauw, C.S., Smith, H. and Piketh, S. (2018). Moving households to cleaner energy through air quality offsets. *2018 International Conference on the Domestic Use of Energy*, 1-8, DOI: 10.23919/DUE.2018.8384405.

Larsen, J. (2000). Recent changes in diatom-inferred pH, heavy metals, and spheroidal carbonaceous particles in lake sediments near an oil refinery at Mongstad, western Norway. *Journal of Palaeolimnology*, 23: 343-363.

Lavoie, I., Hamilton, P.B., Morin, S., Tiam, S.K., Kahlert, M., Goncalves, S., Falasco, E., Fortin, C., Gontero, B., Heudre, D., Kojadinovic-Sirinelli, M., Manoylov, K., Pandey, L.K. and Taylor, J.C. (2018). Diatom teratologies as biomarkers of contamination: Are all deformities ecologically meaningful? *Elsevier*, 82: 539-550.

Lehana, H. and Whittle, M. (2021). Dear Green Place COP26**:** Floods, drought and typhoid: The reality of the climate crisis in Lesotho. Available from https://www.heraldscotland.com/news/homenews/19692108.cop26-floods-drought-typhoid-reality-climate-crisis-lesotho/, accessed 29 June 2022.

Lei, Y., Wang, Y., Qin, F., Liu, J., Feng, P., Luo, L., Jordan, R.W. and Jiang, S. (2021). Diatom assemblage shift driven by nutrient dynamics in a large, subtropical reservoir in southern China. *Journal of Cleaner Production*, 317: 1-13, DOI: 10.1016/j.jclepro.2021.128435.

Lesotho Times. (2014). Tug Of War Over Letšeng-La-Letsie. Available from https://lestimes.com/tug-of-war-over-letseng-la-letsie/, accessed 9 June 2022.

Liu, Y., Chen, C. and Yang, S. (2019). Assessment of anthropogenic impact versus climate change on the succession of the diatom community in Lugu Lake (Yunnan-Guizhou plateau, China) using the sedimentary record of geochemical elements. *Water*, 11(665): 1-16, DOI: 10.3390/w11040655.

Mackay, A.W., Davidson, T., Wolski, P., Woodward, S., Mazebedi, R., Masamba, W.R.L., Todd, M. (2012). Diatom sensitivity to hydrological and nutrient variability in a subtropical, flood-pulse wetland. *Ecohydrology*, 5: 491-502.

Mandela, N.Z. (2019). Drought update; Provinces'state of readiness for 2019/20 planting season. Available from https://pmg.org.za/committee-meeting/29261/, accessed 12 June 2022.

Mangadze, T., Dalu, T. and Froneman, P.W. (2019). Biological monitoring in southern Africa: A review of the current status, challenges and future prospects. *Science of the Total environment*, 648: 1492-1499.

Mangadze, T., Wasserman, R.J. and Dalu, T. (2017). Use of diatom communities as indicators of conductivity and ionic composition in a small austral temperate river system. *Water, Air and Soil Pollution*, 228(11): 428, DOI: 10.1007/s11270-017-3610-3.

Mapcarta. (2022). Lake Chrissie. Available from https://mapcarta.com/14372806, accessed on 19 April 2022.

Maponya, P., Mpandeli, S. and Oduniyi, S. (2013). Climate change awareness in Mpumalanga Province, South Africa. *Journal of Agricultural Science*, 5(10): 273-282.

Marais, E.A. and Wiedinmyer, C. (2016). Air quality impact of diffuse and inefficient combustion emissions in Africa (DICE-Africa). *Environmental Science and Technology*, 50(19): 10739-10745.

Marais, E.A., Silvern, R.F., Vodonos, A., Dupin, E., Bockarie, A.S., Mickley, L.J. and Schwartz, J. (2019). Air quality and health impact of future fossil fuel use for electricity generation and transport in Africa. *Environmental Science and Technology*, 53(22): 13524-13534.

Matlala, M.D., Taylor, J.C. and Harding, W.R. (2011). Development of diatom index for Wetland Health Water Research Commission Report No. KV 270/11, *WRC*: Geniza.

Matlakala, M.E. and Von Kallon, D.V. (2021). Empirical modelling of the water supply crisis in the Mpumalanga Province of South Africa. *Proceedings of the International Conference on Industrial Engineering and Operations Management (IEOM),* Sao Paulo, Brazil.

McCarthy, T., Cairncross, B., Huizenga, J.M. and Batchelor, A. (2013). Choosing between coal or wetlands in Chrissiesmeer. Available from http://www.chrissiesmeer.co.za/cp/19247/mining, accessed 30 October 2021.

Minaoui, F., Hakkoum, Z., Douma, M., Mouhri, K. and Loudiki, M. (2021). Diatom communities as bioindicators of human disturbances on Suburban soil quality in arid Marrakesh area (Morocco). *Water, Air and Soil Pollution*, 232(146): 1-19, DOI: 10.1007/s11270-021-05094-3.

Municipalities. (2021). Municipalities of South Africa: Mpumalanga Municipalities. Available from https://municipalities.co.za/Provinces/view/6/mpumalanga, accessed 18 September 2021.

Musa, R. and Greenfield, R. (2018). Use of diatom indices to categorise impacts on and recovery of a floodplain system in South Africa. *African Journal of Aquatic Science*, 43(1): 59-69.

Ndiritu, G.G., Gichuki, N.N., Kaur, P. and Triest, L. (2003). Characterization of environmental gradients using physico-chemical measurements and diatom densities in Nairobi River, Kenya. *Aquatic Ecosystem Health and Management*, 6: 343-354.

Netshakhuma, N.S. (2021). The impact of climate change on Mpumalanga provincial archives and records management activities. *Records Management Journal*, 31(3): 1-15, DOI: 10.1108/RMJ-09-2020-0031.

Nguetsop, V.F., Bentaleb, I., Favier, C., Bietrix, S., Martin, C., Servant-Vildary, S. and Servant, M. (2013). A late Holocene palaeoenvironmental record from Lake Tizong, northern Cameroon using diatom and carbon stable isotope analyses. *Quaternary Science Reviews,* 72: 49-62.

Niyatbekov, T. and Barinova, S.S. (2018). Bioindication of aquatic habitats with diatom algae in the Pamir Mountains, Tajikistan. *Ecology and Environmental Sciences,* 3(3): 117-120.

Noome, K. and Fitchett, J.M. (2019). An assessment of the climatic suitability of Afriski Mountain Resort for outdoor tourism using the Tourism Climate Index (TCI). *Journal of Mountain Science*, 16(11): 2453-2469.

Nortröm, E., Bringensparr, C., Fitchett, J.M., Grab, S.W., Rydberg, J. and Kylander, M. (2018). Late-Holocene climate and vegetation dynamics in eastern Lesotho highlands. *The Holocene,* 28(9): 1483-1494.

Oberg, H., Andersen, T.J., Westerberg, L.O., Risberg, J. and Holmgren, K. (2012). A diatom record of recent environmental change in Lake Duluti, northern Tanzania. *Journal of Palaeolimnology*, 48: 401-416.

Oğuz, A., Kaleli, A., Akçaalan, R., Köker, L., Dorak, Z., Gaygusuz, O., Aydin, F., Çetin, T., Karaaslan, Y. and Albay, M. (2020). Composition and distribution of benthic diatoms in different habitats of Burdur River Basin, *Turkish Journal of Water Science and Management*, 4(1): 31-57.

Olaleye, A.O., Akinyemi, J.O. and Odusanya, O.A. (2021). Long term hydrochemical analysis and quality assessment of five dams in Lesotho, southern Africa. *International Conference on Energy and Sustainable Environment.* 665: 1-25 , DOI: 10.1088/1755-1315/665/1/012045.

Olodo, I.Y., Cocquyt, C., Abou, Y. and Kokou, K. (2020). Seasonal variations and distribution of diatom flora of Lake Ahémé (Benin, West Africa). *Botany Letters*, 161(1): 160-173.

Olufemi, A.C., Bello, P.O. and Mji, A. (2018). Conflict implications of coal mining and environmental pollution in South Africa: Lessons from Niger Delta, Nigeria. *African Journal on Conflict Resolution*, 18(1): 7-35.

Padhi, B.K., Rath, J. and Padhy, P.K. (2010). Diatoms for assessing the ecological condition of inland freshwater bodies. *World Review of Science, Technology and Sustainable Development,* 7(4): 352-359.

Pajunen, V., Kahlert, M. and Soininen, J. (2020). Stream diatom assemblages as environmental indicators: A cross-regional assessment. *Ecological Indicators*, 113: 1-10, DOI: 10.1016/j.ecolind.2020.106183.

Panichev, N., Mokgalaka, N. and Panicheva, S. (2019). Assessment of air pollution by mercury in South African Provinces using lichens *Parmelia caperata* as bioindicators. *Environmental Geochemical Health*, 41: 2239-2250.

Pelletier, N., Chetelat, J., Palmer, M.J. and Vermaire, J.C. (2021). Bog and lake sediment analysis reveal a lagged response of subarctic lakes to diminishing atmospheric Hg and Pb deposition. *Science of the Total Environment*, 775: 1-17, DOI: 10.1016/j.scitotenv.2021.145521.

Perez. L., Brugnoli, E., Muniz, P., Sunesen, I., Sar, E.A., Crisci, C., Cuna, C. and Garcia-Rodriguez, F. (2017). Diatom assemblages from surface sediments of the Rio de la Plata estuary, Uruguay. *New Zealand Journal of Marine and Freshwater Research*, DOI: 10.1080/00288330.2017.1417318.

Pretorius, I., Piketh, S., Burger, R. and Neomagus, H. (2015). A perspective on South African coal-fired power station emissions. *Journal of Energy in South Africa*, 26(3): 27-40.

Princeton Hydro. (2019). Deep vs. shallow lakes: Let's explore the differences. Available from https://princetonhydro.com/deep-vs-shallow-lakes/, accessed 11 June 2022.

Pullanikkatil, D. and Urama, K.C. (2011). The effects of industrialisation on water quality and livelihoods in Lesotho. *International Journal of Environmental Engineering,* 3(2): 175-191.

Raju, P. and Perumal, K. (2015). Application of diatom-base indices for monitoring environmental quality of riverine ecosystems: A review. *Environmental Management of River Basin Ecosystems*, 593-619.

Ramsar. (2022). Letséng-la Letsie. Available from https://rsis.ramsar.org/ris/1388, accessed on 10 May 2022.

Reid, M.A., Tibby., J.C., Penny, D. and Gell, P.A. (1995). The use of diatoms to assess past and present water quality. *Australian Journal of Ecology,* 20: 57-64.

Rhodes, C., Bingham, A., Heard, A.M., Hewitt, J., Lynch, J., Waite, R. and Bell, M.D. (2017). Diatoms to human uses: linking nitrogen deposition, aquatic eutrophication, and ecosystem services. *Ecophere*, 8(7): 1-18, DOI:

Riato, L. and Leira, M. (2020). Heterogeneity of epiphytic diatoms in shallow lakes: Implications for lake monitoring. *Biological Indicators*, 111: 1-11, DOI: 10.1016/j.ecolind.2019.105988.

Riato, L., Leira, M., Della Bella, V. and Oberholster, P.J. (2017). Diatom-based models for inferring water quality chemistry and hydrology in temporary depressional wetlands. *Hydrobiologia*, 797: 127-143.

Rivera-Rondón, C.A. and Catalan, J. (2019). Diatoms as indicators of the multivariate environment of mountain lakes. *Science of the Total Environment*, 703: 1-13, DOI: 10.1016/j.scitotenv.2019.135517.

Roffe, S.J., Fitchett, J.M. and Curtis, C. (2020). Investigating changes in rainfall seasonality across South Africa: 1987-2016. *International Journal of Climatology*, DOI: 10.1002/joc.6830.

Rose, N.L. (2008). Quality control in the analysis of lake sediments for spheroidal carbonaceous particles. *Limnology and Oceanography: Methods*, 6: 172-179.

Rose, N.L., Jones, V.J., Noon, P.E., Hodgson, D.A., Flower, R.J. and Appleby, P.G. (2012). Long-range transport of pollutants to the Falkland Islands and Antarctica: Evidence from lake sediment fly ash particle records. *Environmental Science and Technology*, 46(18): 9881-9889.

Rose, N. L., Milner, A., Fitchett, J.M., Curtis., C.J., Langerman, K., Yang, H., Turner, S., Jourdan, A., Shilland, J., de Castro, Martins, C.C., and Camara, A. (2020). Natural archives for long-range transported contamination at the remote lake Letšeng-la Letsie, Maloti Mountains, Lesotho. *Science of the Total Environment*, DOI: 10.1016/j.scitotenv.2020.139642.

Rose, N.L., Turner, S.D., Yang, H., Yang, C., Hall., C. and Harrad, S. (2018). Palaeotoxicity: Reconstructing the risk of multiple sedimentary pollutants to freshwater organisms. *Environmental Geochemistry and Health*, 40: 1667-1682.

Russell, J.L. (2008). The inorganic chemistry and geochemical evolution of pans in the Mpumalanga Lakes District, South Africa. MSc Geology [Unpublished], University of Johannesburg.

Salomoni, S.E., Rocha, O., Hermany, G., Lobo, E.A. (2011). Application of water quality biological indices using diatoms as bioindicators in the Gravatai river, RS, Brazil. *Brazilian Journal of Biology*, 71(4): 949-959.

Schneck, F., Torgan, L.C. and Schwarzbold, A. (2007). Epilithic diatom community in a high-altitude stream impacted by fish farming in southern Brazil. *Acta Limnology Brasil*, 19(3): 341-355.

Schoeman, F.R. (1970). Diatoms from the Orange Free-State (South Africa) and Lesotho-No.3. *Botanica Marina*, 13(1): 49-70.

Schoeman, F.R. (1973). A Systematical and Ecological Study of the Diatom Flora of Lesotho with Special Reference to the Water Quality. V & R Printers, Pretoria.

Schoeman, F.R. (1976). Diatom indicator groups in the assessment of water quality in the Jukskei-Crocodile River system (Transvaal, Republic of South Africa). *Journal of the Limnological Society of southern Africa*, 5: 73-78.

Schoeman, F.R. (1979). Diatoms as indicators of water quality in the upper Hennops River *Journal of the Limnological Society of southern Africa*, 5: 73–78.

Schoeman, F.R. (1982). The diatoms of the Jukskei-Crocodile River system (Transvaal, Republic of South Africa): A preliminary check-list. *Journal of South African Botany*, 48: 295-310.

Selin, H., Keane, S.E., Wang, S., Selin, N.E., Davis, K. and Bally, D. (2018). Linking science and policy to support the implementation of the Minamata Convention on mercury. *Ambio*, 47: 198-215.

Simpson, G.B., Badenhorst, J., Jewitt, G.P.W., Berchner, M. and Davies, E. (2019). Competition for land: The water-energy-food nexus and coal mining in Mpumalanga Province, South Africa. *Frontiers in Environmental Science,* 7(86), DOI: 10.3389/fenvs.2019.00086.

Sitoe, S.R., Risberg, J., Norstrom, E. and Westerberg, L.O. (2017). Late Holocene sea-level changes and palaeoclimate recorded in Lake Lungue, southern Mozambique. *Palaeogeography, Palaeoclimatology, Palaeoecology,* 485: 305-315.

Sivarajah, B., Paterson, A.M., Ruhland, K.M., Koster, D., Karst-Riddoch, T. and Smol, J.P. (2018). Diatom response to 20th century shoreline development and climate warming in the three embaymenrs of Georgian Bay, Lake Huron. *Journal of Great Lakes*, DOI: 10.1016/j.jglr.2018.09.004.

Smit, G.N. and van Rensburg, J. (2021). Phytomass and ecological significance of Chrysocoma ciliate L. within the Letšeng-la Letsie catchment area of Lesotho, southern Africa. *African Journal of Range and Forage Science,* 38(1): 102-109.

Solovieva, N., Jones, V., Birks, J.H.B., Appleby, P. and Nazarova, L. (2008). Diatom responses to 20th century climate warming in lakes from the northern Urals, Russia. *Palaeogeography, Palaeoclimatology, Palaeoecology,* 259: 96-106.

Sousa, P.M., Blamey, R.C., Reason, C.J.C., Ramos, A.M. and Trigo, R.M. (2018). The "Day Zero" Cape Town drought and the poleward migration of moisture corridors. *Environmental Research Letters*, 13: 1-12, DOI: 10.1088/1748-9326/aaebc7.

Stager, J.C. and Johnson, T.C. (2000). A 12,400 ^{14}C yr offshore diatom record from east central Lake Victoria, East Africa. *Journal of Paleolimnology*, 23: 373-383.

Stager, J.C., Ryves, D.B., King, C., Madson, J., Hazzard, M., Neuman, F.H. and Maud, R. (2013). Late Holocene precipitation variability in the summer rainfall region of South Africa. *Quaternary Science Reviews*, 67: 105-120.

Stevenson, J. (2014). Ecological assessments with algae: a review and synthesis. *Journal of Phycology.* 50: 437–461.

Tan, X., Liu, Y., Burford, M.A., Zhang, Q. (2020). The performance of diatom indices in assessing temporal changes in water quality in a large lowand river ecosystem. *River Research and Applications,* 1-10, DOI: 10.1002/rra.3754

Tang, T., Tang, T., Tan, L., Gu, Y., Jiang, W. and Cai, Q. (2017). Identifying community thresholds for lotic benthic diatoms in response to human disturbance. *Scientific Reports*, 7: 4134-4144.

Taylor, J.C., Harding, W.R. and Archibald, C.G.M. (2007a). An illustrated guide to some common diatom species from South Africa. WRC Report TT 282/07, *Water Research Commission,* Pretoria.

Taylor, J.C., Janse van Vuuren, M.S. and Pieterse, A.J.H. (2007b). The application and testing of diatom-based indices in the Vaal and Wilge rivers, South Africa. *Water South Africa*., 33: 51-60.

Taylor, J.C. and Cocquyt, C. (2016). Methodologies and identification of genera. In Samyn, Y., Vanden-Spiegel, D. and Degreef, J. (Eds.) *ABC Taxa, Volume 16: Diatoms from the Congo and Zambezi Basins, Belgium*: 1-355.

Terblanche, S. (2022). Losing yourself in South Africa's enchanting lake districts. Available from https://mzanzitravel.co.za/losing-yourself-in-south-africas-enchanting-lake-districts/, accessed on 1 June 2022.

Tolotti, R., Consani, S., Carbone, C., Vagge, G., Capello, M. and Cutroneo, L. (2018). Benthic diatom community response to metal contamination from an abandoned Cu mine: Case study of the Gromolo Torrent (Italy). *Journal of Environmental Sciences*, 75: 233-246.

Tuturí, A., Becona, L.P., Venturini, N., Rodriguez-Gallego, L., Gaecia-Rodriguez, F., Gonzalez, L., Lescano, C., Costa, S., del Puerto, L. and Bergamino, L. (2021). Trophic assessment in South American Atlantic coastal lagoons: Linking water, sediment and diatom indicators. *Marine Pollution Bulletin*, 165: 112-119.

Van Deventer, H. (2021). Monitoring changes in South Africa's surface water extent for reporting sustainable development goal sub-indicator 6.6.1.a. *South Africa Journal of Science*, 117(5/6): 1-5, DOI: 10.17159/sajs.2021/8806.

Van Tienhoven, A., Olbrich, K., Skoroszewski, R., Taljaard, J., Zunckel, M. (1995). Application of the critical loads approach in South Africa. *Water, Air, and Soil Pollution* 85: 2577–2582.

Vander Zanden, M. J. and Vadeboncoeur, Y. (2020). Putting the lake back together 20 years later: What the benthos have we learned about habitat linkages in lakes? *Inland Waters*, 10(3): 305-321.

Varona-Cordero, F., Rez-Mendieta, F.J. and Del Castillo, M.E.M. (2010). Phytoplankton assemblages in two compartmentalized coastal tropical lagoons (Carretas-Pereyra and Chantuto-Panzacola, Mexico). *Journal of Planktonic Research*, 32(9): 1283-1299.

Venter, A., Barnard, S., Dickinson, M.A., can Vuuren, S.J., Levanets, A. and Taylor, J.C. (2013). Planktonic algae and cyanoprokaryotes as indicators of ecosystem quality in the Mooi River system in the North-West Province, South Africa. *Water South Africa*, 39(5): 707-719.

Wellinton, J.H. (1943). The Lake Chrissie problem. *South African Geographical Journal*, 25(1): 50-64.

Westover, K.S., Stone, J.R., Yost, C.I., Scott, J.J., Cohen, A.S., Rabideaux, N., Stockhecke, M. and Kingston, J.D. (2019). Diatom paleolimnology of late Pliocene Baringo Basin (Kenya) paleolakes. *Palaeogeography, Palaeoclimatology, Palaeoecology,* 570, DOI: 10.1016/j.palaeo.2019.109382.

Williamson, C.E., Dodds, W., Kratz, T.K. and Palmer, M.A. (2008). Lakes and streams as sentinels of environmental change in terrestrial and atmospheric processes. *Frontiers in Ecology and* Environment, 6(5): 247-254.

Wolin, J.A. and Stone, J.R. (2010). Diatoms as indicators of water-level change in freshwater lakes. In: The diatoms applications to the environmental and Erath sciences, E.F. Stoermer and J.P. Smol (eds.)., Cambridge University Press, pp: 174-185.

Wu, H., Liso, M., Guo, J., Zhang, Y. and Li, Y. (2022). Diatom assemblage responses to multiple environmental stressors in a deep brackish plateau lake, SW China. *Environmental Science and Pollution*, 1-13, DOI: 10.1007/s11356-021-17853-0.

Yang, J., Ji, Y., Yan, R., Liu, X., Zhang, J., Wu, N. and Wang, K. (2020). Applicability of benthic diatom indices combined with water quality valuation for Dish Lake from Nanjishan Nature Reserve, Lake Poyang. Water, 12: 27-32.

Zaky A.S., Kashima, K., Frontalini, F., Ibrahim, M.I.A., Khalifa, M.M., Fukumoto, Y., Gad, D. and Behling, H. (2020). Mid-to Late Holocene paleoclimate changes and paleoenvironmental shifts inferred from pollen and diatom assemblages at Lake Hamra, Wadi El Natrun (Western Nile Delta, North Western Desert, Egypt. *Quaternary International*, 542: 109-120.

Zohary, T. and Ostrovsky, I. (2011). Ecological impacts of excessive water level fluctuations in stratified freshwater lakes. *Inland Waters*, 1(1): 49-57.

Zou, Y., Wang, L., Xu, H., Yan, Y., Zhang, J., Liu, Y., Li, P., Peng, Z, Gu, Z. and Lu, H. (2020). Do changes in water depth and water level influence the diatom diversity of Yunlong Lake, in Yunnan Province, Southwest China? *Journal of Palaeolimnology*, 63: 273-291.

Appendix A: Additional Information

A.1. Methods Flow Charts

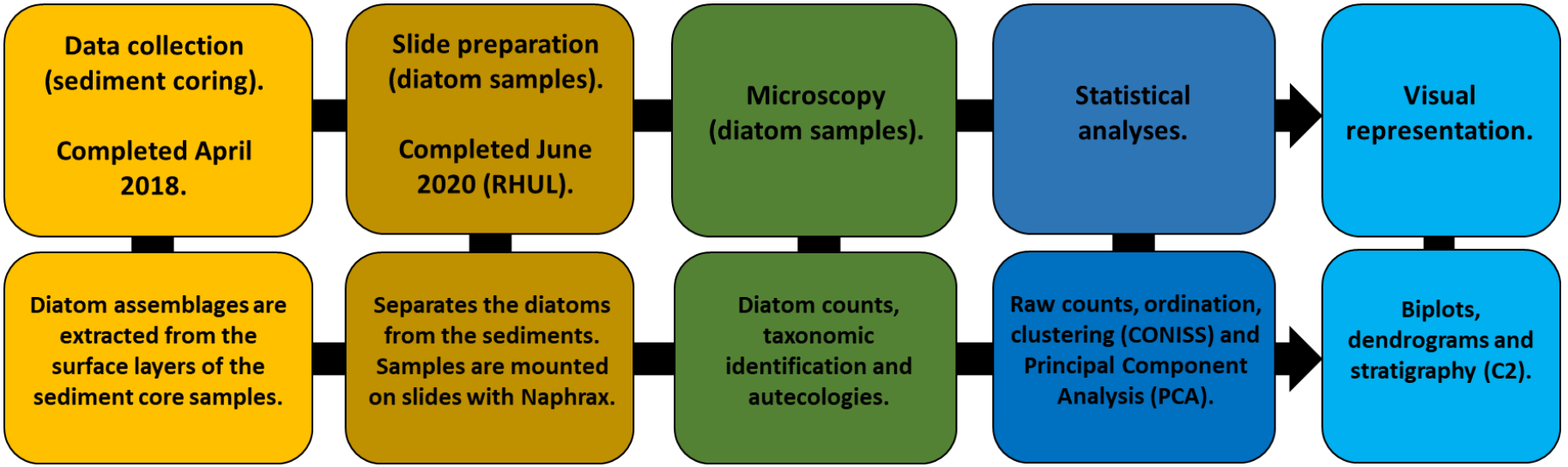

Figure A.1. The summarised methodological process.

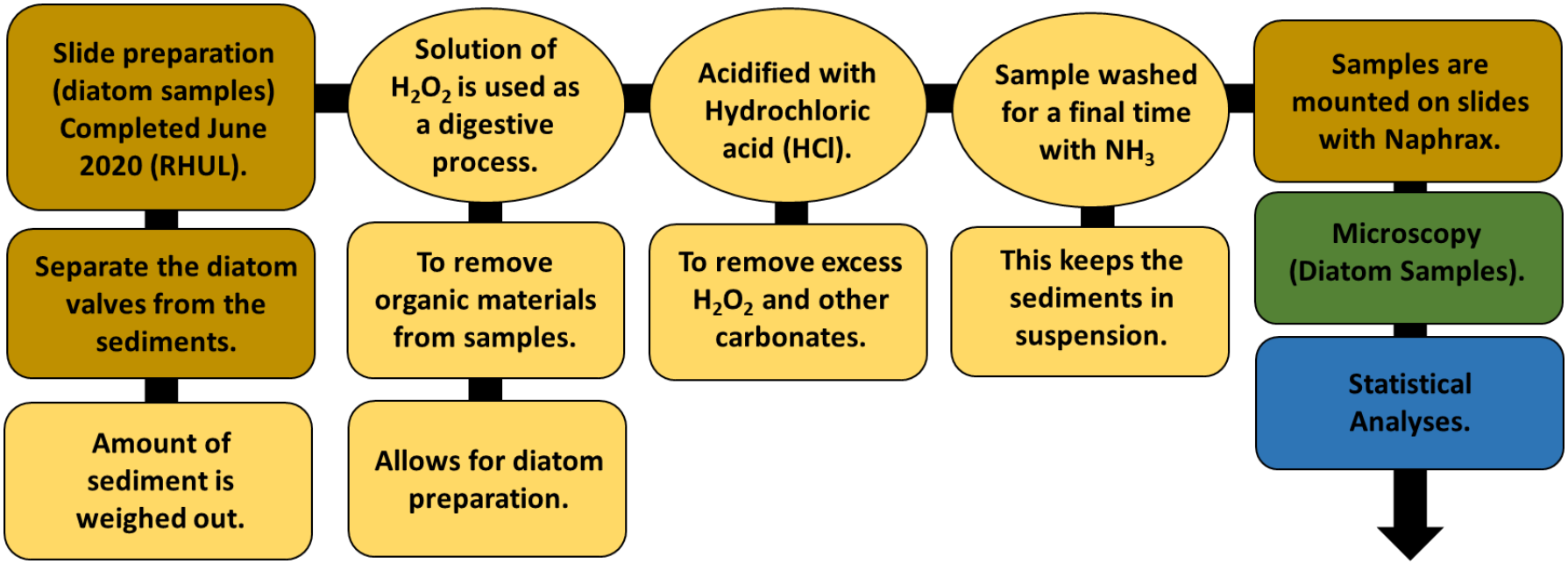

Figure A.2. The summarised methodological process of sample preparations.

Appendix B: Additional Data Analysis

B.1 Principal Component Analysis Output

B.1.1. Lake Chrissie Diatom PCA

Table B.1. Importance of Lake Chrissie PCA components

Importance of components:							
	PC1	PC2	PC3	PC4	PC5	PC6	PC7
Eigenvalue	7.4587	6.4302	3.4827	2.50289	1.70109	1.26496	1.03386
Proportion	0.2515	0.2169	0.1174	0.08441	0.05737	0.04266	0.03487
Cumulative	0.2515	0.4684	0.5858	0.67024	0.72761	0.77027	0.80514

Table B.2 Lake Chrissie species PCA scores

Species scores					
	PC1	PC2	PC3	PC4	PC5
Eupodiscus radiatus	2.331957	0.333465	0.0875757	-0.023300	0.422224
Aulacoseira sp.	0.086319	-2.666183	0.5300986	-0.278070	-0.087345
Nitzschia sp.	-1.210897	-0.015589	-0.5533752	-0.191880	-0.132636
Cyclotella meneghiniana	-0.300435	-0.460267	-1.3328309	0.846104	-0.180041
Gomphonema minutum	-0.028817	0.004536	-0.0451757	0.153197	0.010017
Amphora ovalis	-0.569385	0.262603	-0.0745132	0.331063	0.868923
Fragilaria pinnata	-0.320821	-0.413854	0.0968944	-0.007728	0.389666
Pinnularia divergens	-0.241915	-0.079193	-0.0520264	0.181530	0.375060
Fragilaria famelica	-0.880744	0.478330	1.3861573	0.907294	-0.041877
Gomphonema sp	-0.010887	-0.001750	-0.0007727	-0.111746	-0.030958
Navicula sp.	-0.113606	0.035466	0.0519987	-0.088153	-0.058845
Navicula trivialis	-0.096366	-0.089623	0.0098250	0.078665	0.126430
Aulacoseira granulata	0.008673	0.069597	0.0785440	0.054876	-0.072419
Pinnularia borealis	-0.540605	0.180218	0.0515614	-0.521981	0.112655
Fragilaria fasciculata	-0.117686	-0.064384	-0.1748745	-0.213484	0.577352

Nitzschia acidoclinata	-0.145919	-0.107623	0.0042935	0.134151	0.259988
Fragilaria construens	-0.253834	0.027401	-0.1100990	-0.266392	0.414780
Gomphonema parvulum	-0.064848	-0.114282	0.0248294	-0.027879	0.045367
Navicula veneta	-0.147151	0.070259	-0.0175539	-0.117584	0.039387
Anomoeneis sphaerophora	-0.252354	0.019936	0.0169949	-0.222733	0.083187
Achnanthes minutissima	-0.111228	0.089359	0.0875966	-0.084508	0.032842
Surirella ovalis	-0.235513	0.354679	0.0628798	-0.348824	0.175955
Stauroneis phoenicentron	-0.344187	0.083252	0.1303459	-0.169057	0.011929
Navicula antonii	-0.488666	0.058619	0.1048068	-0.158225	-0.070338
Hantzschia amphioxys	-0.488666	0.275304	-0.2293834	-0.384556	0.119042
Cymbella cistula	-0.055379	0.090419	0.1279301	0.013033	0.029650
Eunotia minor	-0.256814	0.168283	0.0989174	-0.325821	-0.022475
Fragilaria ulna	-0.198624	0.074939	-0.0695145	-0.124843	0.284147
Nitzschia amphibia	-0.333739	-0.053233	0.0389958	0.270242	0.377960
Navicula goeppertiana	-0.274355	0.255139	0.0532365	-0.562388	-0.167904
Pinnularia viridis	-0.156866	0.003781	0.0386098	-0.004241	0.002319
Achnanthes exigua	0.008673	0.069597	0.0785440	0.054876	-0.072419
Eunotia eruca	0.012265	0.098425	0.1110779	0.077606	-0.102416
Diploneis sp.	-0.275010	0.170085	0.1368510	-0.211316	-0.055774
Eunotia bilunaris	0.046225	0.142488	-0.0213713	-0.015199	0.014577
Rhapolodia gibba	-0.322957	0.224865	0.1805267	-0.257762	0.015454

B.1.2. Letšeng-la Letsie Diatom PCA

Table B.3. Importance of Lake Letšeng-la Letsie PCA components

Importance of components:							
	PC1	PC2	PC3	PC4	PC5	PC6	PC7
Eigenvalue	4.9639	2.9171	1.27677	1.01729	0.83108	0.57664	0.50951
Proportion	0.3023	0.1777	0.07777	0.06196	0.05062	0.03512	0.03103
Cumulative	0.3023	0.4800	0.55780	0.61976	0.67038	0.70550	0.73653

Table B.4 Lake Letšeng-la Letsie species PCA scores

Species scores	PC1	PC2	PC3	PC4	PC5
Gomphonema minutum	-0.222274	-0.093168	0.1214878	-0.31416	0.147020
Achnanthes minutissima	-0.192218	0.415308	0.0430427	-0.15374	0.078156
Fragilaria construens	-0.248575	-0.404227	0.3257018	-0.29354	-0.669142
Aulacoseira granulata	1.970779	0.341642	-0.1745440	0.21303	0.001087
Nitzschia sp.	-1.185271	0.563126	0.4472385	0.20010	0.257179
Navicula trivialis	-0.447754	0.558546	0.1930122	-0.03583	0.250903
Fragilaria famelica	-0.644281	-0.342233	-0.0063106	0.13189	0.108244
Melosira varians	-0.160725	-0.282893	-0.1243658	0.02451	-0.111614
Gomphonema parvulum	-0.360079	-0.161786	0.1743203	-0.26044	-0.036617
Cymbella cistula	-0.814612	-0.800529	-0.5373883	0.19723	-0.145922
Pinnularia divergens	-0.242333	-0.007185	0.1906625	0.08604	0.108087
Navicula veneta	-0.722033	0.496528	-0.3597980	-0.30001	-0.329747
Nitzschia palea	-0.375685	0.537603	-0.1278098	-0.17486	-0.013241
Cocconeis placentula	-0.069139	0.208925	0.5352109	0.27661	0.018828
Cyclostephanos dubius	-0.011759	0.084012	-0.0751552	-0.05529	-0.027332
Fragilaria capucina	-0.134433	0.181487	0.3343483	-0.28298	0.142978
Cymatopleura solea	-0.232916	-0.669421	0.0006303	-0.33647	0.408624
Pinnularia borealis	-0.131767	-0.147863	-0.1466624	0.11210	-0.026887
Fragilaria biceps	0.044113	0.008082	0.0454857	-0.02476	-0.052681

Eunotia minor	-0.070785	-0.233996	-0.1425767	-0.06024	0.220672
Caloneis schumanniana	-0.435322	-0.274723	-0.0530005	0.40426	0.128067
Cymbella tumida	0.214304	-0.534416	0.5111695	-0.21865	-0.158324
Fragilaria pinnata	0.083443	0.092639	0.4032477	0.12268	-0.421672
Gyrosigma acuminatum	-0.714424	0.126121	0.0138734	0.70228	-0.058058
Aulacoseira ambigua	0.177257	0.017792	0.2179895	-0.36931	0.233409
Diploneis subovalis	-0.035274	-0.630034	0.4280467	0.10651	0.061125
Gomphonema clavatum	-0.097519	-0.249215	0.1262490	-0.07048	0.175892
Fragilaria ulna	-0.086435	-0.595411	-0.2337874	-0.12112	0.198249
Gyrosigma sp.	0.048919	0.064015	0.0553399	0.01716	0.004996
Navicula antonii	-0.349775	0.132499	-0.2377213	-0.17334	-0.086293
Navicula erifuga	-0.478699	0.454168	-0.1286357	-0.07709	-0.167120
Rhopalodia gibba	0.015049	-0.236359	0.2524388	0.06537	-0.144704
Cyclotella pseudostelligera	-0.278725	0.442352	-0.0776185	-0.16807	-0.022830
Hantzschia amphioxys	-0.004444	-0.390848	-0.0702622	-0.15733	0.089050
Cyclotella sp	-0.259598	0.462893	-0.1413828	-0.18277	-0.112130
Cyclotella meneghiniana	-0.203475	0.038862	-0.3046793	-0.04800	0.145818
Pinnularia viridis	-0.327103	-0.354222	0.0169292	0.06472	-0.232148
Fragilaria sp.	-0.133020	0.126051	-0.0329065	-0.11621	-0.068322
Fragilaria fasciculata	-0.074818	-0.316359	-0.0986783	-0.08608	-0.118024